



**Aerospace
Systems Division**

ASE REDESIGN EVALUATION

NO.	REV. NO.
ATM-1064	
PAGE 1	OF 212
DATE 11/24/71	

This ATM summarizes the Bendix evaluation of the ASE pallet design and subsequent results of the test program conducted at Langley Research Center to verify the adequacy of the ASE design and deployment modifications during a series of live grenade firings in a vacuum environment. The verification includes an evaluation of (1) the Mortar Package/Pallet Assembly stability and structural integrity, (2) dust accumulation and pressure wave impingement effects on ALSEP, (3) performance and effects of launch tube covers and (4) the overall effects of firing grenades in an off-loaded configuration.

In summary, all test objectives were met and all redesign goals achieved.

With the successful demonstration of the design, concept, analysis and evaluation of test data in terms of the lunar environment, it is concluded that the addition of the ASE pallet will provide a stable launch platform for the Array D ASE on Apollo 16 so that its scientific goals can be successfully achieved.

Prepared by:

J. H. Griffin, Jr.
J. Griffin
Thermal Design Project Engineer

J. M. S. Dowell
J. McDowell
ASE Project Engineer

J. Maszatics
J. Maszatics, Staff Engineer/
Stress-Dynamics Supervisor

R. G. Thomas
R. Thomas
Senior Engineer/Stress Analyst

H. Wiger
H. Wiger
Staff Engineer/Stress Analyst

Approved by:

J. McNaughton
J. McNaughton, Group Supervisor
Structural/Thermal/Crew Engineering

W. Tosh
W. Tosh
ALSEP Experiments Manager



**Aerospace
Systems Division**

ASE REDESIGN EVALUATION

NO.	REV. NO.
ATM-1064	
PAGE	2 OF 212
DATE	11/24/71

TABLE OF CONTENTS

	<u>Page</u>
I. Introduction	8
A. Initial LRC Test	8
1. Objectives	8-9
2. Problem Identification	9
B. ASE Modification Program	9-10
C. LRC Retest Program	10
1. Objectives	10-15
2. Test Configuration Comparisons	15
3. LRC/Flight Hardware Comparisons	18
4. Brief Test Results	22-28
II. Discussion	29
A. Test Hardware	29
1. Analysis of Launch Tube Cover Effects	29-31
2. Evaluation of Strain Gauge Data	32
3. Platform Evaluation - Structural Integrity	33-34
4. Mortar Box Structural Evaluation	35-37
5. Mortar Box/Pallet Structural Attachment Analysis	38
6. Misfire Analysis	39-41
B. Pressure/Dust	42
1. Analysis of Pressure Impingement Effects	42-43
2. Evaluation of Pressure Transducer Data	44
3. Analysis of Dust Accumulation Effects	45-47



**Aerospace
Systems Division**

ASE REDESIGN EVALUATION

NO.	REV. NO.
ATM-1064	
PAGE 3	OF 212
DATE 11/24/71	

TABLE OF CONTENTS (CONT)

	<u>Page</u>
C. Stability	48
1. MBA/Pallet Stability (Normal Firing Order)	48
a. Film Data	48-50
b. Accelerometer Data	51
c. MBA/Pallet Dynamic Analysis	52-54
d. Analysis of Soil Effects	55-62
e. Predicted MBA/Pallet Stability on the Lunar Surface	63-66
2. MBA/Pallet Stability (Off-loaded Configuration)	67
3. (-4) Grenade Movement Analysis	68
D. Comparison of Two LRC Test Program Results	69-72
III. Conclusions	73-75
IV. Recommendations	76
Appendices	
A. MBA/Pallet Dynamic Analysis	77-98
B. (-4) Grenade Movement Dynamic Analysis	99-106
C. Structural Analysis	107-130
D. LRC Data	131-171
E. (-2), (-4), (-3), (-1) Grenade Launch Sequences	172-212



**Aerospace
Systems Division**

ASE REDESIGN EVALUATION

NO.	REV. NO.
ATM-1064	
PAGE 4	OF 212
DATE 11/24/71	

LIST OF FIGURES

<u>Figure Number</u>	<u>Title</u>	<u>Page</u>
1.	Array D ASE Mortar Box Deployed on Subpallet	11
2.	Array D ASE Subpallet Underside	12
3.	Launch Tube Protective Covers	13
4.	Apollo 16 ALSEP Deployment	14
5.	LRC Chamber Platform Configuration	16
6.	LRC MBA/Pallet Deployed in Soil Bed	17
7.	LRC C/S and PSE Deployed	18
8.	MBA/Pallet Displacement	24
9.	Accumulative Dust Effects	25
10.	MBA/Pallet After Four Firings	26
11.	MBA/Pallet After Four Firings	27
12.	MBA/Pallet After Four Firings	28
13.	Modified Launch Tube Covers	31
14.	Launch Platform After Eight Grenade Firings	34
15.	Qual C Mortar Box After Four Firings	36
16.	Qual C Mortar Box After Four Firings	37
17.	Dust Coverage Aft of Launch Platform	46
18.	Coordinate System Used in Film Analysis	49
19.	Assumed Pallet Pressure Distribution for (-1) Grenade	56
A-1	Mortar Box/Pallet Configuration	79
A-2	MBA Sequence of Motion for -1, -2, -3, -4 Grenades	80
A-3	Free Body Diagram of Pallet	82
A-4	Impact of Two Bodies	87
A-5	Skin Deformation	88
A-6	(-1) Firing Dynamic Analysis	89
A-7	Pivotal Action About Anchor Bracket	91
A-8	(-1) Firing - Pallet Velocity Profile	91
A-9	(-) Firing - Pallet Velocity Profile After Rebound	92
A-10	Velocity Profile of Pallet for $\epsilon = 2\%$	93
A-11	Displacement Profile of Pallet for $\epsilon = 2\%$	93
A-12	(-3) Firing Dynamic Analysis	94
A-13	(-3) Firing - Pallet Velocity Profile	95
A-14	(-3) Pivotal Action About Anchor Bracket	95
A-15	(-3) Firing - Pallet Velocity Profiles	96



**Aerospace
Systems Division**

ASE REDESIGN EVALUATION

NO.	REV. NO.
ATM-1064	
PAGE 5	OF 212
DATE 11/24/71	

LIST OF FIGURES (CONT.)

<u>Figure Number</u>	<u>Title</u>	<u>Page</u>
A-16	(-3) Firing Displacements of Pallet for $\epsilon = 5\%$	96
A-17	(-4) Firing Dynamic Analysis	97
B-1	Free Body Diagram of (-4) Grenade	100
B-2	Motion Diagram for (-4) Grenade	101
B-3	Lunar vs. Earth Displacement of (-4) Grenade	104
B-4	Lunar/Earth Motion vs. Coefficient of Friction	105
C-1	Mortar Box/Pallet Attachment	108
C-2	Mortar Box/Pallet Attachment Drawings	109
C-3	Plunger Drawing	110
C-4	Latch Assembly - Rear Mortar Box	111
C-5	Pedestal Drawing	117
C-6	Stress Model of Pedestal Base	120
C-7	Locking Mechanism - MBA Lug	127
C-8	Slide Bolt - Locking Mechanism	127
C-9	Lug Carrier Frame	128
D-1	LRC Pressure Transducer Locations	132
D-2	MBA/Pallet Accelerometer Locations	133
D-3	Strain Gauge Locations	134
D-4	D-27 Grenade Accelerometer Output (#3)	135
D-5	(-2) Grenade Accelerometer Output (#3 Test)	136
D-6	(-4) Accelerometer Output (#4 Test)	137
D-7	(-3) Accelerometer Output (#5 Test)	138
D-8	(-1) Accelerometer Output (#6 Test)	139
D-9	(-2) Accelerometer Output (#7 Test)	140
D-10	(-1) Accelerometer Output (#8 Test)	141
D-11	(-4) Accelerometer Output (#9 Test)	142
D-12	(-3) Accelerometer Output (#10 Test)	143
D-13	(-2) Vertical Accelerations (#3 Test)	144
D-14	(-1) Vertical Accelerations (#6 Test)	145
D-15	(-2) Strain Gauge Output (#3 Test)	146
D-16	(-2) Strain Gauge Output (#3 Test)	147
D-17	(-2) Strain Gauge Output (#3 Test)	148



**Aerospace
Systems Division**

ASE REDESIGN EVALUATION

NO.	REV. NO.
ATM-1064	
PAGE <u>6</u>	OF <u>212</u>
DATE	11/24/71

LIST OF FIGURES (CONT.)

<u>Figure Number</u>	<u>Title</u>	<u>Page</u>
D-18	(-2) Strain Gauge Output (#3 Test)	149
D-19	(-4) Strain Gauge Output (#4 Test)	150
D-20	(-4) Strain Gauge Output (#4 Test)	151
D-21	(-3) Strain Gauge Output (#5 Test)	152
D-22	(-3) Strain Gauge Output (#5 Test)	153
D-23	(-1) Strain Gauge Output (#6 Test)	154
D-24	(-1) Strain Gauge Output (#6 Test)	155
D-25	Composite Strain Gauge, Pressure Data	156
D-26	FILTERED DATA - Accelerometer Locations	157
D-27	(-2) Accelerometer Output Filtered (#3 Test)	158
D-28	(-2) Accelerometer Output Filtered (#3 Test)	159
D-29	(-4) Accelerometer Output Filtered (#4 Test)	160
D-30	(-3) Accelerometer Output Filtered (#5 Test)	161
D-31	(-1) Accelerometer Output Filtered (#6 Test)	162
D-32	(-2) Accelerometer Output Filtered (#7 Test)	163
D-33	(-4) Accelerometer Output Filtered (#8 Test)	164
D-34	(-4) Accelerometer Output Filtered (#8 Test)	165
D-35	(-4) Accelerometer Output Filtered (#9 Test)	166
D-36	(-3) Accelerometer Output Filtered (#10 Test)	167
D-37	(-2, -4) Pressure Transducer Output (#3 Test)	168
D-38	(-2) Pressure Transducer Output (#3 Test)	169
D-39	(-3) Pressure Transducer Output (#5 Test)	170
D-40	(-1) Pressure Transducer Output (#6 Test)	171
E-1	(-2) Sequence of Motion	173-184
E-2	(-4) Sequence of Motion	185-197
E-3	(-3) Sequence of Motion	198-205
E-4	(-1) Sequence of Motion	206-212



**Aerospace
Systems Division**

ASE REDESIGN EVALUATION

NO.	REV. NO.
ATM-1064	
PAGE <u>7</u>	OF <u>212</u>
DATE	11/24/71

LIST OF TABLES

<u>Table Number</u>		<u>Page</u>
1.	Comparison of First and Second Series of ASE Test Configurations	19-21
2.	Maximum Dynamic Displacements of the MPA/ Platform Assembly During Grenade Launchings	50
3.	First LRC Test Summary of Grenade Firing vs Effects/Damage	70
4.	Second LRC Test Summary of Grenade Firing vs Effects/Damage - MBA #1	71
5.	Second LRC Test Summary of Grenade Firing vs Effects/Damage - MBA #2	72



**Aerospace
Systems Division**

ASE REDESIGN EVALUATION

NO.	REV. NO.
ATM-1064	
PAGE 8	OF 212
DATE	11/24/71

I. INTRODUCTION

A series of vacuum firings of the Active Seismic Experiment (ASE) grenades from a Mortar Box were conducted at the Langley Research Center (LRC) in March, 1971. Results of those tests identified undesirable pressure and dust effects associated with a grenade rocket motor firing. In addition, the results indicated instability of the mortar box during a firing. An investigation of the tests and evaluation of the test data verified the validity of the test results and substantiated that the pressure and dust effects were representative of lunar effects. It was further established that the mortar box instability would be greater in the lunar environment. A NASA/MSC test report (EH3/4-15/A165) dated April 1971, documents that test program.

Subsequent to the LRC tests, ASE design and deployment changes were implemented per CCP #308 to eliminate the pressure and dust effects and to correct the mortar box instability problem. A second series of grenade vacuum firings was conducted at LRC during August-September 1971, to verify the adequacy of the design and deployment changes. A NASA/MSC test report (EH3/9-28/A335) dated September 1971, documents the LRC retest. This ATM documents the analysis of the test results and the evaluation of the adequacy of the ASE design and deployment changes.

A. Initial LRC Test (March, 1971)

1. Objective

The original development plans for the ASE called for activation of the Mortar Box mode and firing of grenades at the end of the planned one year operation of ALSEP. The secondary effects of the grenade firings on ALSEP, after the one year of operation, were not considered to be reasons for concern. However, the demonstrated extended life of ALSEP beyond one year's operation and the desire to fire the ASE grenades on Apollo 14 as early as three months after deployment led to the initiation of vacuum firings at LRC. The primary objective of the first LRC test program was to determine the grenade firing secondary effects under simulated lunar surface conditions by evaluating the pressure,



**Aerospace
Systems Division**

ASE REDESIGN EVALUATION

ATM-1064

PAGE 9 OF 212

DATE 11/24/71

dust and debris effects on 1/6 g models of the ALSEP Central Station (C/S) and Passive Seismic Experiment (PSE).

2. Problems Identified

The tests were performed in a 41' diameter sphere vacuum chamber at LRC. A test platform was erected at the 34' level which permitted deployment of the full earth weight mortar box and the ALSEP C/S and PSE models. The relative positions and separation distances between those units were derived from the actual Apollo 14 lunar deployment. The mortar box was deployed in a soil pan filled to a depth of five inches with simulated lunar soil (ground basalt) compacted to approximately 100 pounds per cubic foot.

A total of four flight configuration grenades were fired, in vacuum, from the mortar box. Significant pressure and dust effects on the C/S and PSE were experienced on each grenade firing. Structural damage occurred on the C/S side curtains and specular reflector and dust accumulations were seen on the C/S and PSE. The PSE shroud was lifted and/or folded back and small displacements of the sensor can were seen. Overall, it was evaluated that these effects on the lunar surface would cause severe thermal performance degradation of the C/S and PSE and would result in an ALSEP failure.

In addition, all grenade firings except the -2 grenade resulted in significant mortar box displacements (vertical, forward, backward and rotational). Extrapolation of the mortar box motion to the lunar environment would predictably cause overturning of the box and loss of the experiment data. It was also speculated that, in addition to the instability problem, the pressure forces from a grenade firing could cause an adjacent grenade to move in its launch tube.

B. ASE Modification Program

Modifications to the design and deployment of the ASE have been implemented to resolve the problems identified during the initial LRC test. A new subpallet has been designed as the mortar box launch platform to resolve the instability problem. Structural modifications have been



**Aerospace
Systems Division**

ASE REDESIGN EVALUATION

NO.	REV. NO.
ATM-1064	
PAGE 10	OF 212
DATE	11/24/71

made to the mortar box frame so that the mortar box can be mounted firmly, at a 45° launch angle, to the pallet by the astronaut during final lunar deployment. The mounting of the mortar box to the 24" x 25" pallet provides a flat plate so that the grenade rocket motor exhaust plume pressures create a downward vertical force to the entire mortar box/pallet assembly to eliminate vertical motion. The pallet design includes four 7" stakes to prevent translation and rotation in the horizontal plane. See Figures 1 and 2.

Plastic protective covers have been designed to be installed in the ends of the #1 and #3 launch tubes of the Grenade Launch Assy (GLA). (See Fig. 3) Thus installed these launch tube caps will provide back pressure protection to the -1 grenade as a result of the -2 grenade firing and protection to the -3 grenade when the -4 grenade is fired. This protection is intended, therefore, to prevent any motion of those grenades from an adjacent grenade firing as was speculated from the LRC tests. The cap design is such that the grenade rocket motor blast in the tube in which the cap is installed will readily shatter the cap.

The secondary effects of dust accumulation and pressure wave impingement on ALSEP due to a grenade firing have been resolved by the planned deployment of the mortar box/pallet at a minimum distance of 40 feet from the C/S. Also, the firing line of the mortar box will be perpendicular to a line from the C/S. See Figure 4. This deployment change necessitated replacing the mortar box RF coax and flat ribbon cables with 58' cables.

C. LRC Retest (August - September 1971)

The ASE Modification Program included a retest program at LRC to verify the design modifications and the new deployment configuration.

1. Test Objective

The primary objective of the second LRC vacuum tests was to verify the adequacy of design and deployment modifications to the ASE during live grenade firings in a vacuum environment. The verification was to include an evaluation of:

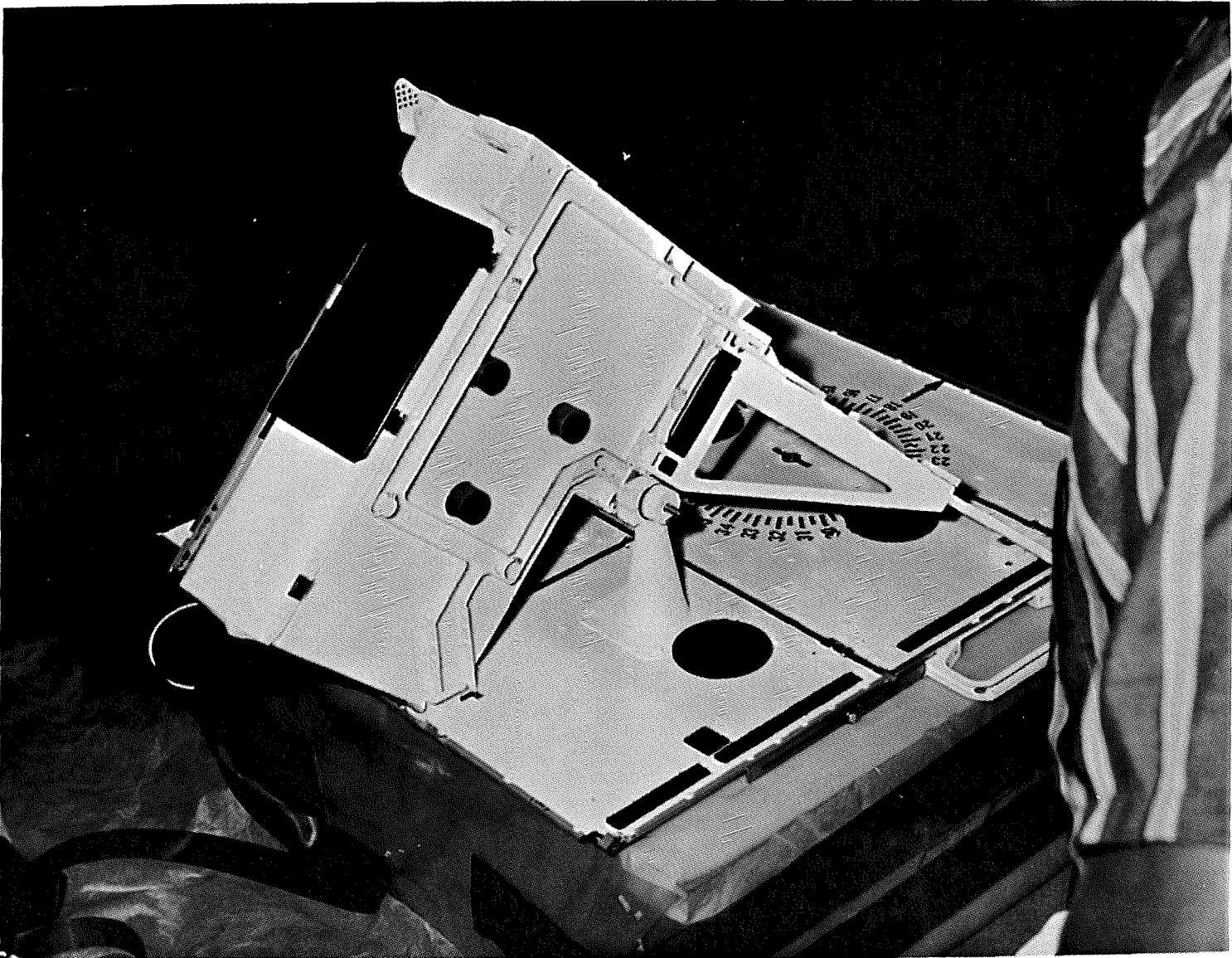


Figure 1. Array D ASE Mortar Package Deployed on Subpallet

ASE REDESIGN EVALUATION

NO.	REV. NO.
ATM-1064	
PAGE 11 OF 212	
DATE 11/24/71	



**Aerospace
Systems Division**

ASE REDESIGN EVALUATION

NO.	REV. NO.
ATM-1064	
PAGE <u>12</u>	OF <u>212</u>
DATE	11/24/71

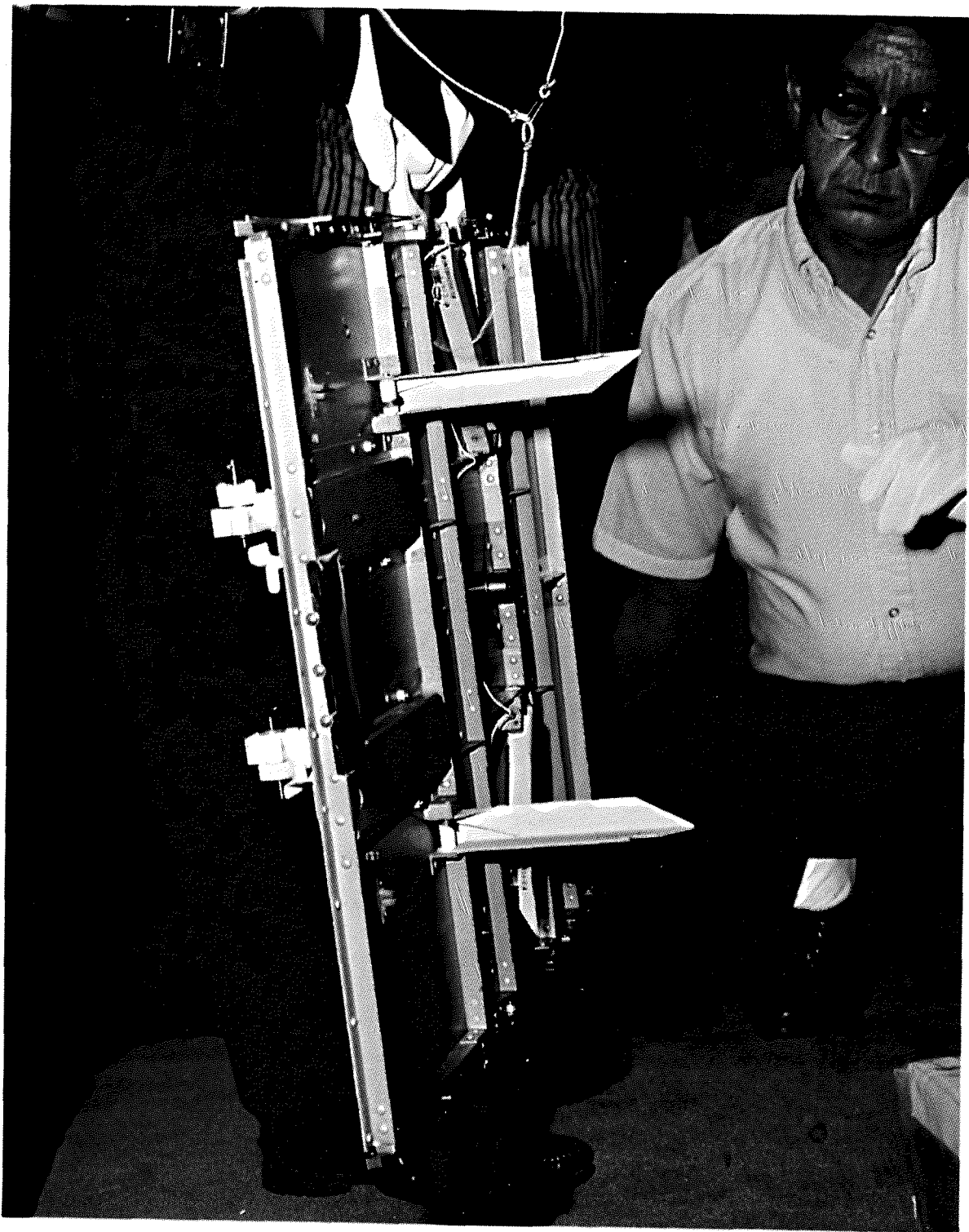


Figure 2. Array D ASE Subpallet Underside

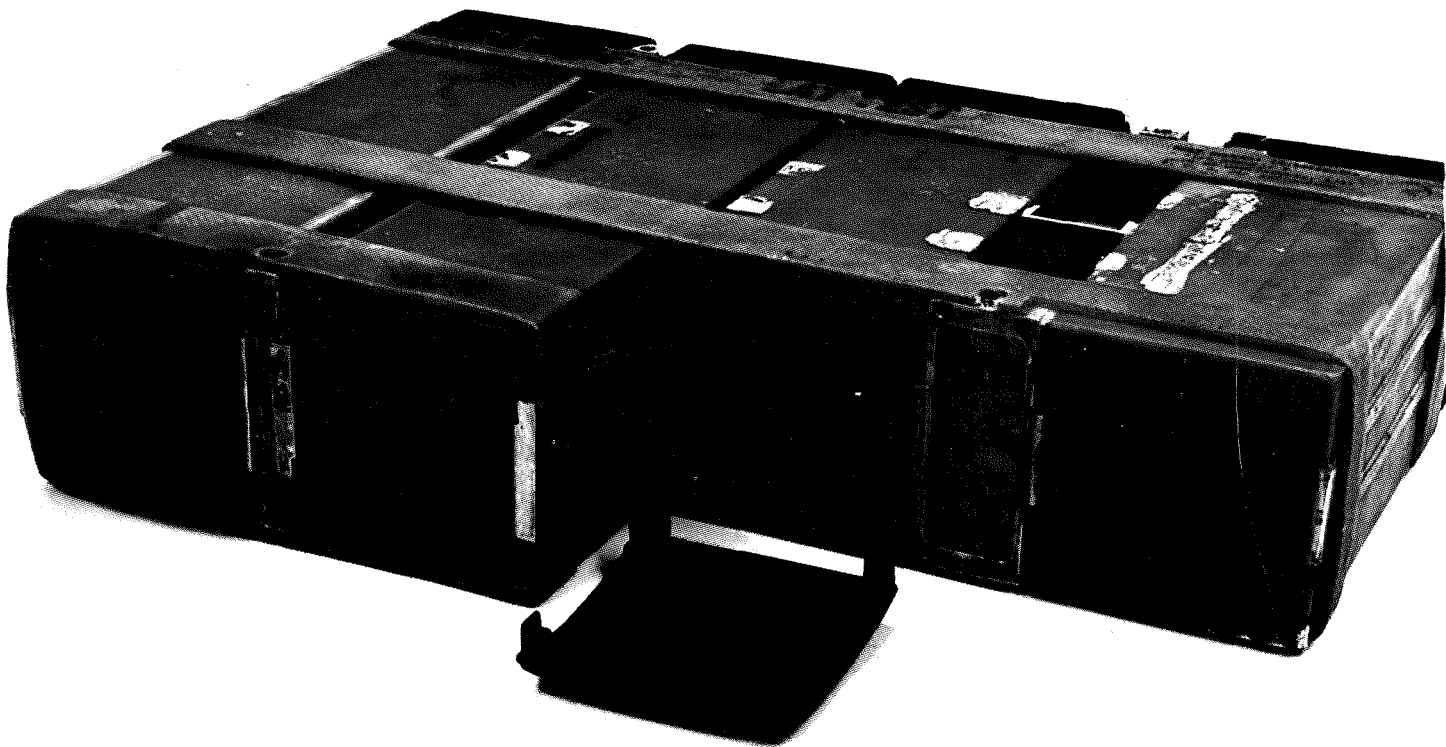
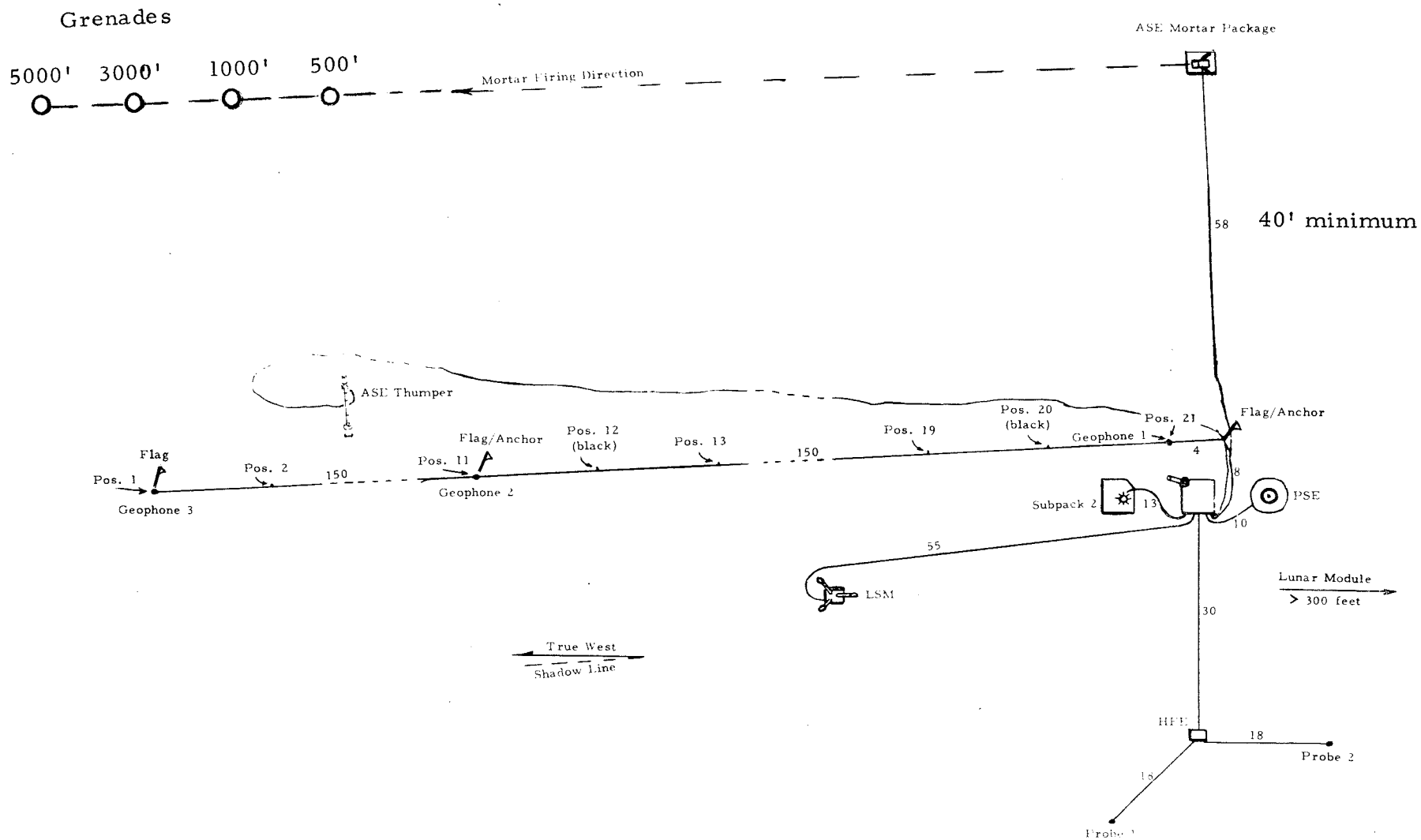


Figure 3. Launch Tube Protective Covers

ASE REDESIGN EVALUATION

NO.	ATM-1064	REV. NO.
PAGE	13	OF 212
DATE	11/24/71	



Descartes
 Latitude 8.9° South
 Longitude 15.5° East

Array D General Deployment Configuration

Figure 4



**Aerospace
Systems Division**

ASE REDESIGN EVALUATION

NO.	REV. NO.
ATM-1064	
PAGE 15	OF 212
DATE 11/24/71	

- (a) The Mortar Package/Pallet Assembly stability and structural integrity.
- (b) The dust accumulation and pressure wave impingement on deployed models of the ALSEP Central Station, PSE and CPLEE.
- (c) Protective covers installed on the ends of launch tubes to prevent grenade movement in a launch tube as a result of pressure from an adjacent grenade firing.
- (d) The overall effect of firing a -2 and a -1 grenade with the #3 and #4 launch tubes empty and the effect of firing a -4 and -3 grenade with the #1 and #2 tubes empty.

2. Test Configuration

The test setup for the LRC retest was similar to the first test program. The major difference was the use of the 60' sphere instead of the 41' sphere. The larger vacuum chamber permitted the installation of a 43' diameter working platform which allowed the ALSEP C/S and PSE 1/6 g models to be deployed at a distance of 25' from the mortar box/pallet. A simulated lunar soil bed 12" deep was used for the pallet deployment with the 7" stakes embedded in the soil. The soil (ground basalt) was again compacted to 100 pounds per cubic foot. The chamber configuration is shown in Figure 5. The MBA/Pallet assembly, deployed in the soil bed, is shown in Figure 6 and the C/S and PSE deployment is shown in Figure 7.

3. LRC/Flight Hardware Comparison

Two mortar boxes and GLAs were used in the test. All ASE hardware was flight weight and the mortar boxes had been modified as required to attach to the pallet. The pallet was functionally and structurally identical to the flight model. Missing from the model were its astronaut and ALSEP subpackage stowage interfaces. Those items which had not been included (handle, stowage bracket, bubble level, UHT socket, etc) did in no way compromise the pallet's launch platform function nor its structural integrity. A summary is presented in Table 1 comparing the test configuration and hardware of the initial LRC test program to the LRC retest program.

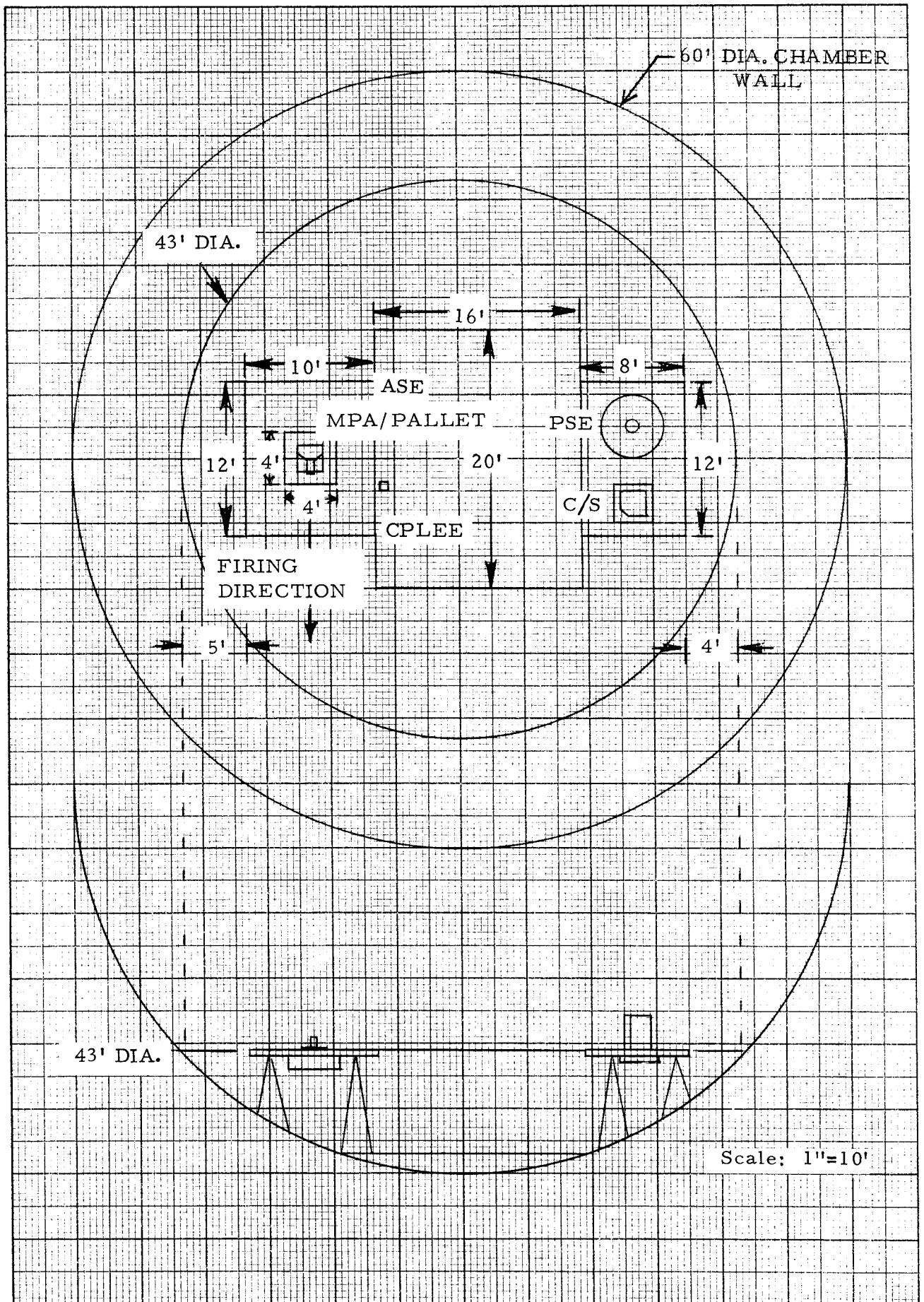


Figure 5 Chamber Platform Configuration

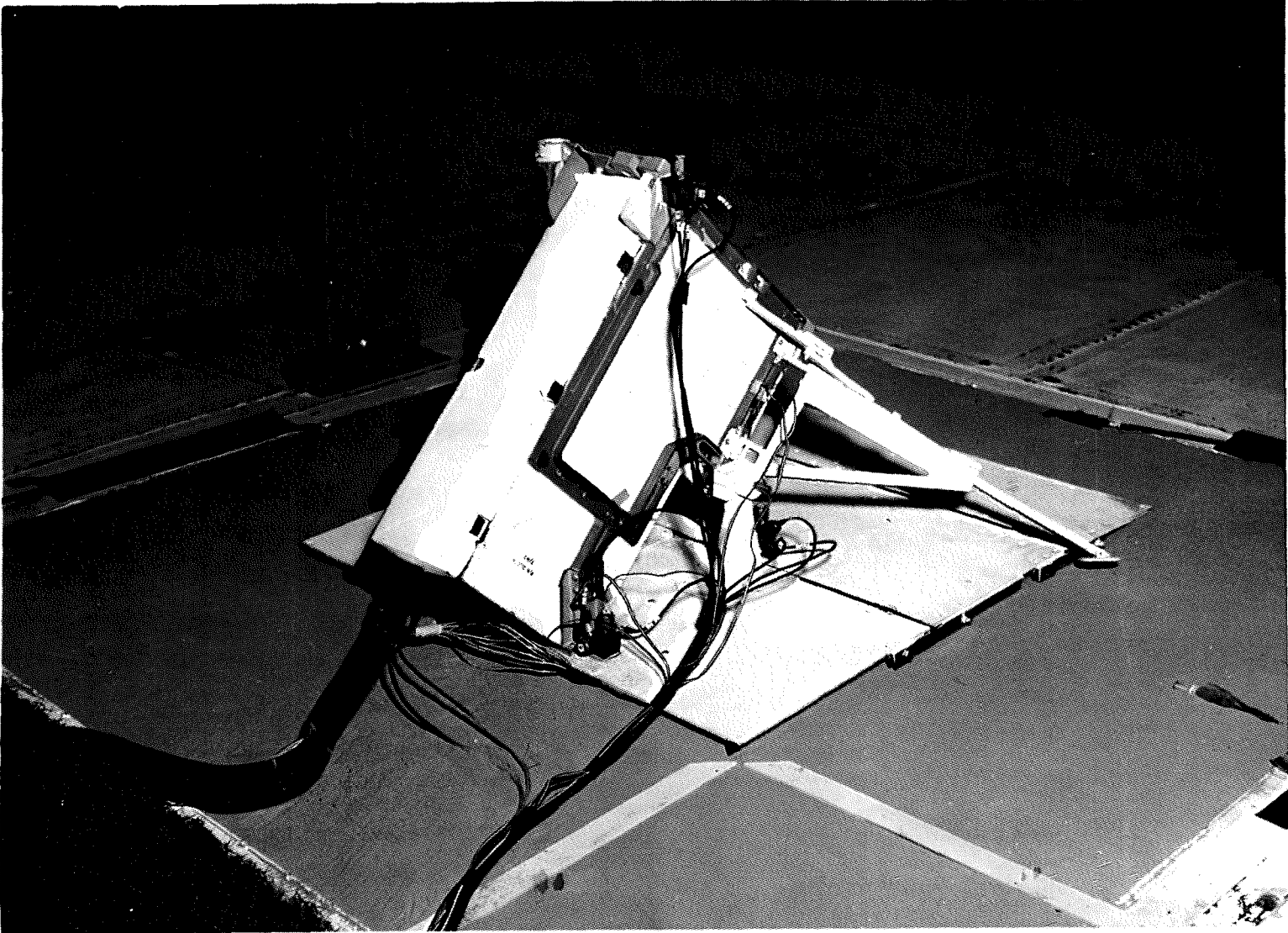


Figure 6. LRC MBA/Pallet Deployed in Soil Bed

ASE REDESIGN EVALUATION

NO.	REV. NO.
ATM-1064	
PAGE 17 OF 212	
DATE 11/24/71	

ASE REDESIGN EVALUATION

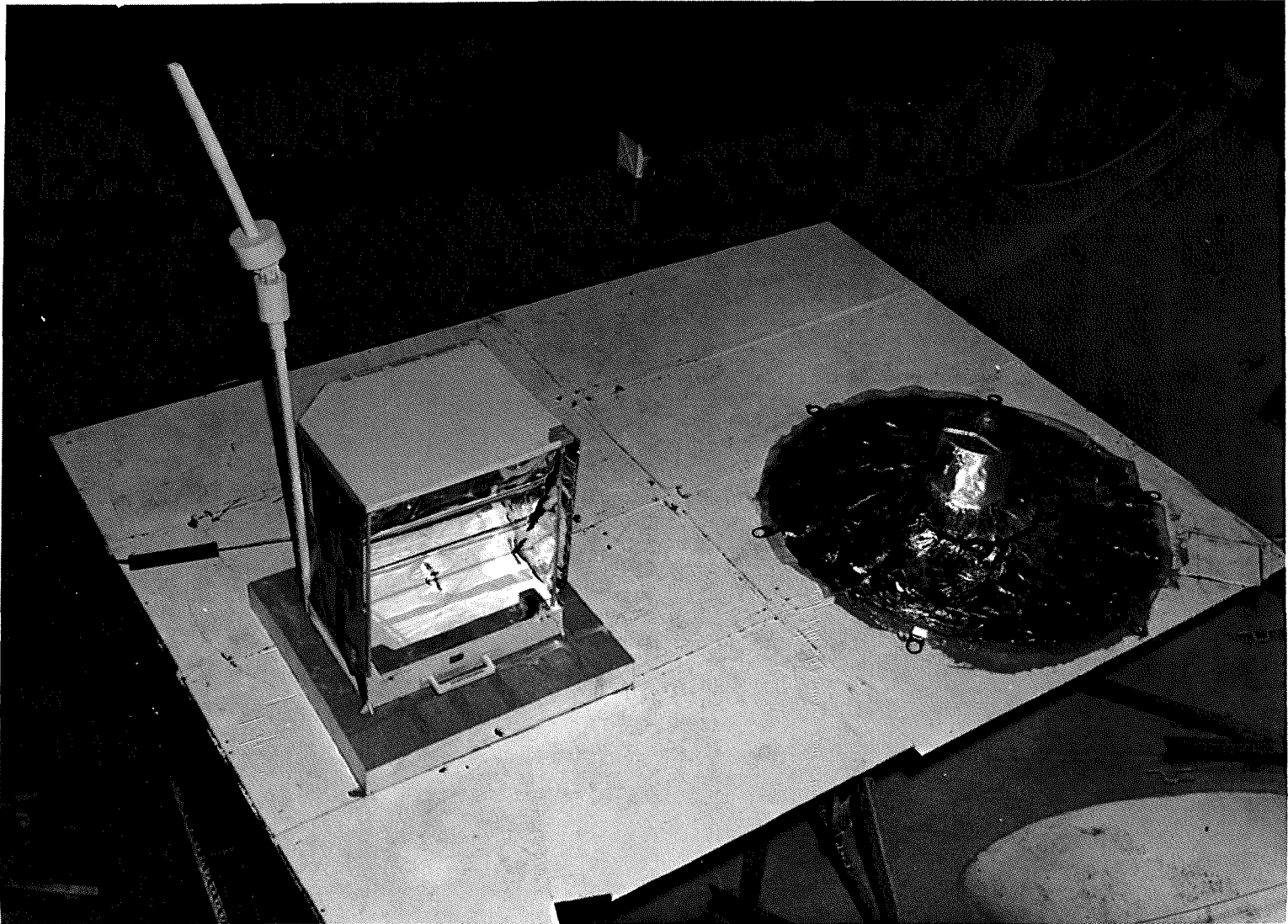


Figure 7. LRC C/S and PSE Deployed

NO.	REV. NO.
ATM-1064	
PAGE 18 OF 212	
DATE 11/24/71	



**Aerospace
Systems Division**

NO. REV. NO.

ATM-1064

PAGE 19 OF 212

DATE 11/24/71

ASE REDESIGN EVALUATION

TABLE I

Comparison of First & Second Series of
ASE Test Configurations

Item to be Compared	First Test Series (March 4-18, 1971)	Second Test Series (August 10-Sept 9, 1971)	
	Nominal Firing Configuration	Nominal Firing Configuration	Off-Loaded Configuration
Vacuum Chamber	41' dia. sphere	60' dia. sphere	60' dia. sphere
Platform Size	34' dia.	43' dia.	43' dia.
Vacuum	1×10^{-4} Torr	1×10^{-4} Torr	1×10^{-4} Torr
ASE Test Platform	A portion of the elevated platform	10' x 12' isolated platform	10' x 12' isolated platform
C/S, PSE Test Platform	A portion of the elevated platform	8' x 12' isolated platform	8' x 12' isolated platform
Separation Floor	None	16' x 20' isolated platform	16' x 20' isolated platform
ASE Soil Bed	3' x 3' x 4" soil pan shock mounted to floor	4' x 4' x 1' soil pan mounted to floor	4' x 4' x 1' soil pan mounted to floor
C/S Soil Bed	2' x 2' x 4" soil pan	2' x 2' x 4" soil pan	2' x 2' x 4" soil pan
1g ASE Mortar Box	Qual C	Qual C (modified for pallet mounting)	Proto C (modified for pallet mounting)
1 g ASE GLA	DVT	Eng. Model	DVT
Central Station	1/6 g Mockup	1/6 g Mockup	1/6 g Mockup
PSE	Proto 1	Proto 1	Proto 1
CPLEE	None	E 2B Trainer (1/3 g)	E 2B Trainer (1/3 g)



**Aerospace
Systems Division**

ASE REDESIGN EVALUATION

NO. ATM-1064	REV. NO.
PAGE 20	OF 212
DATE 11/24/71	

TABLE 1 (contd)

Item to be Compared	First Test Series (March 4-18, 1971)	Second Test Series (August 10 - Sept 9, 1971)	
	Nominal Firing Configuration	Nominal Firing Configuration	Off-Loaded Configuration
PSE Skirt	1 g and 1/6 g	1/6 g	1/6 g
Soil Simulant	Ground Basalt compacted to 100 lb/ft ³	Ground Basalt compacted to 100 lb/ft ³	Ground Basalt compacted to 100 lb/ft ³
Pressure Gauge Instrumentation	10 Hydyne 5 Microphones	5 Kistler Piezotrons	5 Kistler Piezotrons
Strain Gauge Instrumentation	None	18	None
Accelerometers	None	10	10
Cameras	2- 400 f/s Milligen 4- 2000 f/s Fairchild Still	10 - 400 f/s Milligen Still	10 - 400 f/s Milligen Still
Timer	1003 rpm	1000 rpm	1000 rpm
GLA Safe Slides	Yes	No	Yes
Mortar Package Pallet Assembly	No	Yes	Yes
Launch Sequence	(-2, -4, -3, -1)	(-2, -4, -3, -1)	(-2, -1) (-4, -3)
Launch Tube Covers	No	Yes	Yes
Modified Launch Tube Covers	No	No	Yes



**Aerospace
Systems Division**

NO. ATM-1064	REV. NO.
PAGE <u>21</u>	OF <u>212</u>
DATE <u>11/24/71</u>	

ASE REDESIGN EVALUATION

TABLE 1 (cont'd)

Item to be Compared	First Test Series (March 4-18, 1971)	Second Test Series (August 10 - Sept. 9, 1971)	
	Nominal Firing Configuration	Nominal Firing Configuration	Off-Loaded Configuration
PSE Distance from MPA	5 ft forward at 45° angle	25 ft and 90° from firing line	25 ft and 90° from firing line
C/S Distance from MPA	8 ft back at 45° angle	25 ft and 90° from firing line	25 ft and 90° from firing line
CPLEE Distance from MPA	N/A	10 ft	10 ft



**Aerospace
Systems Division**

ASE REDESIGN EVALUATION

NO.	REV. NO.
ATM-1064	
PAGE 22	OF 212
DATE	11/24/71

4. Results

A total of eight grenades were fired from the two mortar boxes. The results from each set of four grenades from each mortar box were similar. The accumulative movement of the MBA/Pallet assembly after four grenade firings was negligible. Actual pallet movement was 1/8" to the left and 1/8" back, measured from the forward left corner. See Figure 8. The mortar box bubble level indicated an approximate 1° change in mortar box levelness. Some vertical motion was observed from the -1, -2, and -3 grenade firings. An evaluation of the mortar box/pallet assembly stability through analyses of the high speed film and accelerometer data is included in Section II C and Appendix A.

Little or no effects were seen from dust, debris and pressure wave impingement as evidenced by Figure 9. The analysis of the dust accumulation and pressure impingement effects are included in Section II B. An evaluation of the launch tube protective covers and their effect on the overall MBA/Pallet stability is included in Section II A.

Figures 10, 11 and 12 show the condition of the mortar box and pallet after the first four grenade firings. Damage to the mortar box was essentially the same or less from that previously incurred from earth firings of grenades from similar mortar boxes. The mortar box was still held firmly in place attached to the pallet with no frame or attachment point damage. The pallet withstood the firings very well. An area on the second panel, beneath the -1 and -2 grenades, was deformed, but not penetrated. It was also noted that the dimension between the mounting faces of the two pedestals had increased by approximately 1/4". The pedestals had in effect spread at the top due to a slight bowing at the inside edge of each base. An evaluation of the structural integrity of the pallet, and mortar box and the attachment points is included in Section II A and Appendix C.

Two misfires occurred during the LRC tests. In each case the cause was conclusively identified and shown to be unrelated to the modifications under test. Section II A. 6 summarizes the analysis of the two misfires.



**Aerospace
Systems Division**

ASE REDESIGN EVALUATION

NO.	REV. NO.
ATM-1064	
PAGE 23	OF 212
DATE	11/24/71

High speed film review subsequent to the first set of four grenade firings identified an apparent movement of the -4 grenade within its launch tube as a result of the -2 grenade firing. An evaluation of that observation has been included in Section II C 3. Still photos showing the grenade launch sequences are included in Appendix E.

The LRC retest program is considered to have met all of its test objectives and to have provided results satisfactorily resolving the problems identified during the initial LRC tests. A detailed comparison of the results of the two series of tests is included in Section II D.



**Aerospace
Systems Division**

ASE REDESIGN EVALUATION

NO.	REV. NO.
ATM-1064	
PAGE <u>24</u>	OF <u>212</u>
DATE	11/24/71

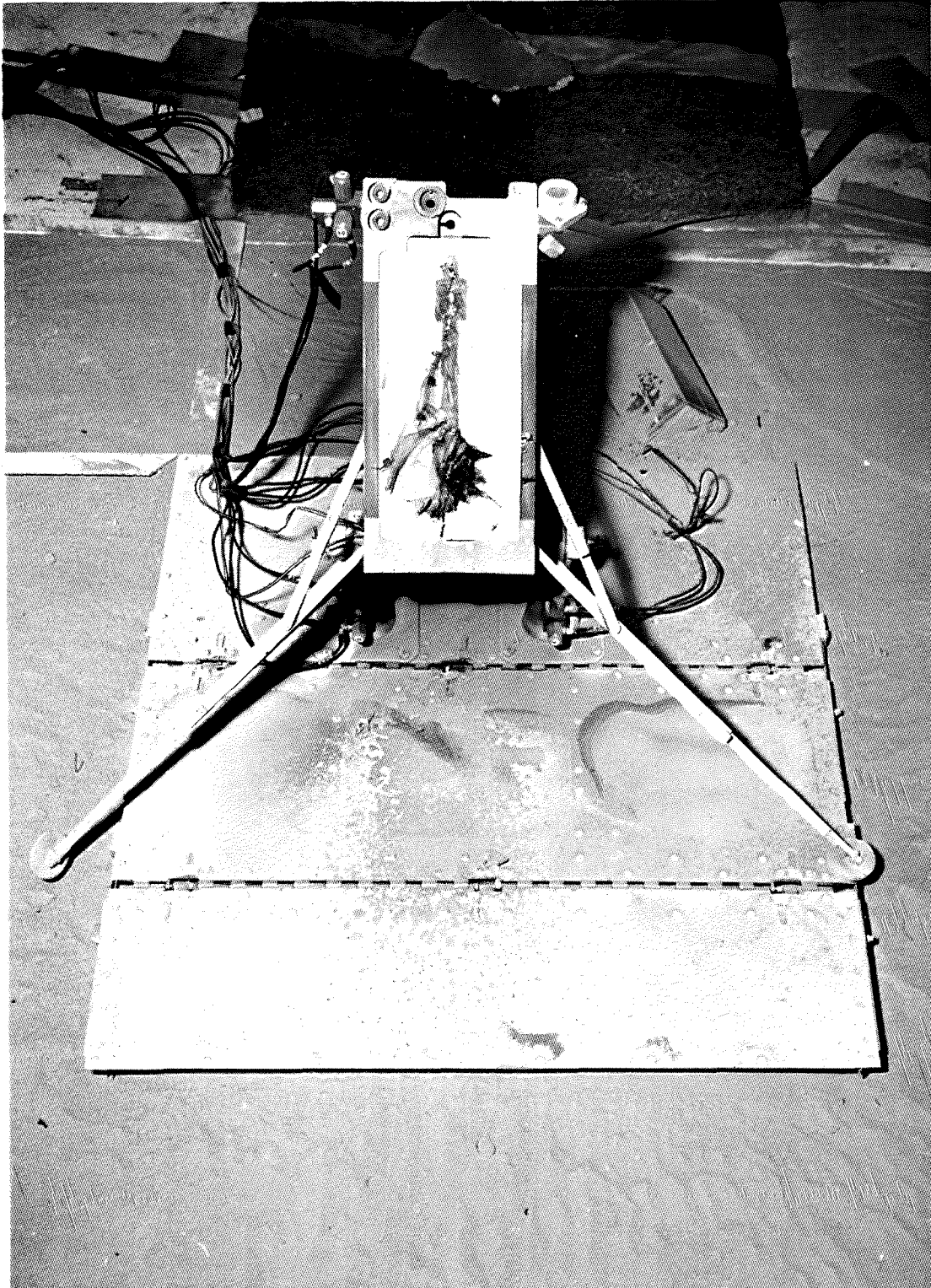


Figure 8. MBA/Pallet Displacement



**ospace
Systems Division**

ASE REDESIGN EVALUATION

NO.	REV. NO.
ATM-1064	
PAGE <u>25</u>	OF <u>212</u>
DATE	11/24/71

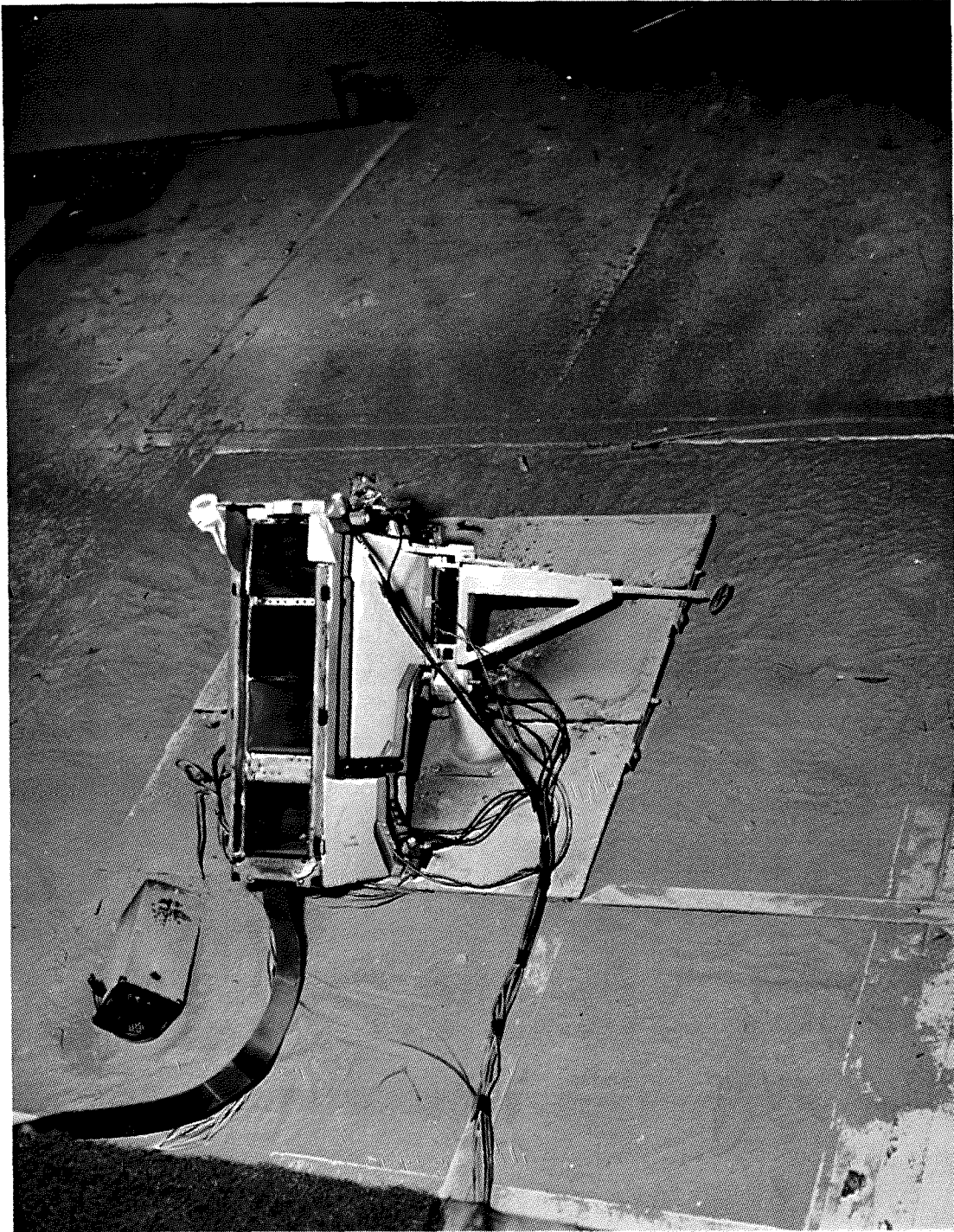


Figure 9. Accumulative Dust Effects



**Aerospace
Systems Division**

ASE REDESIGN EVALUATION

NO.

REV. NO.

ATM-1064

PAGE 26 OF 212

DATE 11/24/71

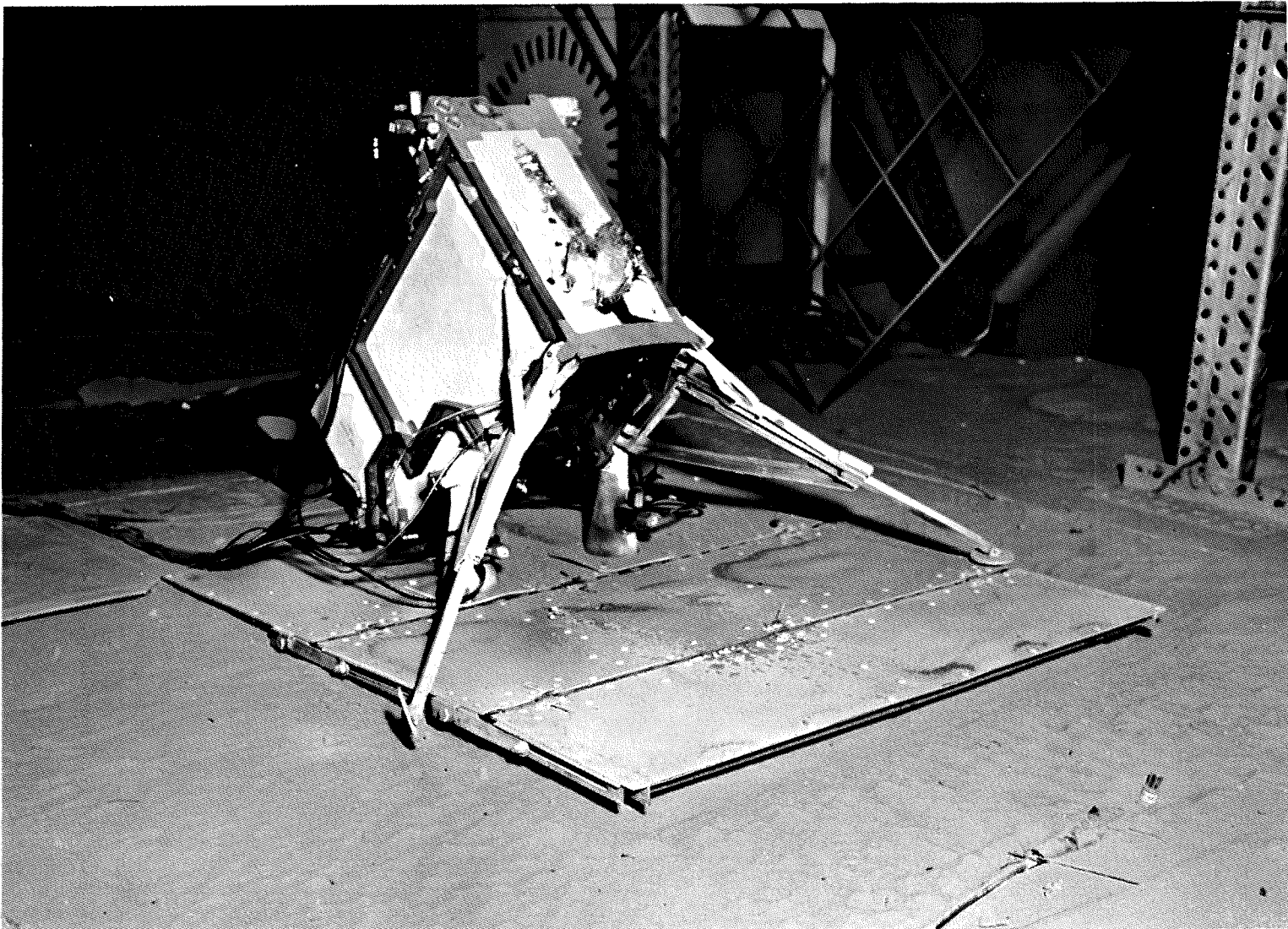


Figure 10. MBA/Pallet After Four Firings



Figure 11. MBA/Pallet After Four Firings

NO.	ATM-1064	REV. NO.
PAGE	27	OF 212
DATE	11/24/71	



broSPACE
systems Division

ASE REDESIGN EVALUATION

NO.

ATM-1064

REV. NO.

PAGE 28 OF 212

DATE 11/24/71

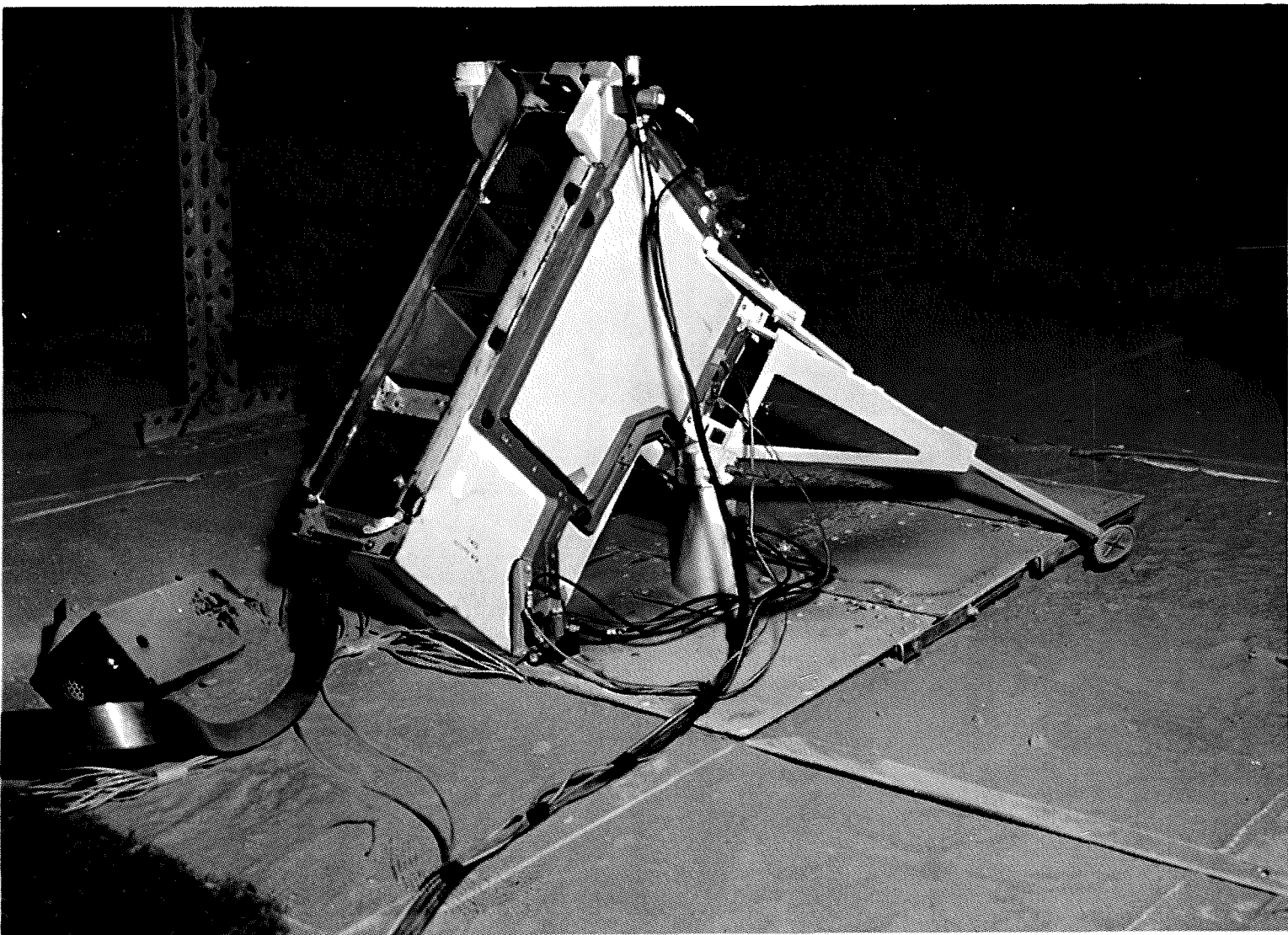


Figure 12. MBA/Pallet After Four Firings



**Aerospace
Systems Division**

ASE REDESIGN EVALUATION

NO.	REV. NO.
ATM-1064	
PAGE 29	OF 212
DATE	11/24/71

II. DISCUSSION

A. Test Hardware

1. ANALYSIS OF LAUNCH TUBE COVER EFFECTS

Under MSC direction, BxA designed and fabricated protective covers for the grenade launch assembly. The primary purpose of the covers was to provide a means by which a grenade could be protected from moving in a launch tube due to pressures from an adjacent motor firing.

One of the objectives of the second Langley test was to evaluate the presence of the launch tube covers in terms of their design, effectiveness in preventing grenade motion and their influence in the overall stability of the ASE Mortar Package/Pallet Assembly.

From previous analysis, it had been shown that grenades most susceptible to being expelled during another firing would be the (-1) grenade when the adjacent (-2) grenade was launched and the (-3) grenade when the adjacent (-4) was launched. Since the nominal firing sequence of (-2, -4, -3, -1) was to be followed it was agreed that only the (-1) and (-3) tubes needed to be covered with the protective caps. A fiberglass blow out panel and multilayer thermal bag remain in place beneath the -3 and -4 grenades thus providing pressure protection for the -4 grenade when the -2 fires. Furthermore, only these tubes could be covered due to the expressed concern of a cap imparting momentum to the mortar box if the multilayer insulation thermal bag had not been ruptured during a previous grenade firing. Since the (-2) grenade firing shreds the upper half of the thermal bag, only the (-1) needed to be protected. Similarly, the (-4) grenade firing ruptures the lower portion of the thermal bag so that a launch tube cover could be safely placed over the (-3) launch tube.

Rupture tests of the protective covers were conducted by Bendix using a nitrogen fed shock tube. The purpose of the tests was to verify that the thermosetting plastic covers would shatter at pressures below 1200 psi on their concave sides and to investigate minimum rupture pressures on their outer or convex side. The tests showed that the covers burst under back pressures of 142 psi. The covers were either blown off or shattered when a simulated motor pressure of at least 6 psi was applied internally.



**Aerospace
Systems Division**

ASE REDESIGN EVALUATION

NO.	REV. NO.
ATM-1064	
PAGE 30	OF 212
DATE	11/24/71

Results of two calibration motor firings at LRC showed that peak pressures of 200 to 300 psi may exist on the external surface of the launch tube cover.

Indeed, when the (-2) grenade was fired the (-1) protective cover shattered, verifying the pressure must have exceeded 142 psi. Similarly the launch tube cover over the (-3) tube cracked when the (-4) motor was fired. As a result of these firings the cover design was re-evaluated and the 0.020" failure troughs filled with Eccobond 26 epoxy to bring the reduced sections up to the 0.060" major cap thickness. See Figure 13. Tests using these modified engineering caps were made at Langley under similar conditions. Both covers survived the launch of an adjacent grenade, which verified the cap redesign. Furthermore, both the caps shattered successfully when the grenades were fired in the tubes which they covered. No real significant effect of the launch tube covers was apparent. The first set of mortar box firings was conducted with essentially no caps in place, whereas the second set of firings took place with the (-1) and (-3) covers in position. The (-1) provided the only real comparison since the only differences between the two (-1) firings was the presence of the covers. The effects of the cover on the (-3) grenade launching cannot be directly attributable to the presence of the cover because of the changes in center of gravity location in the off-loaded configuration. In summary, the presence of the launch tube covers have apparently no dramatic influence on Mortar Package/Pallet Assembly stability as tested and do provide adequate back pressure protection in the tubes in which they are installed.



broSPACE
systems Division

ASE REDESIGN EVALUATION

NO.

REV. NO.

ATM-1064

PAGE 31 OF 212

DATE 11/24/71

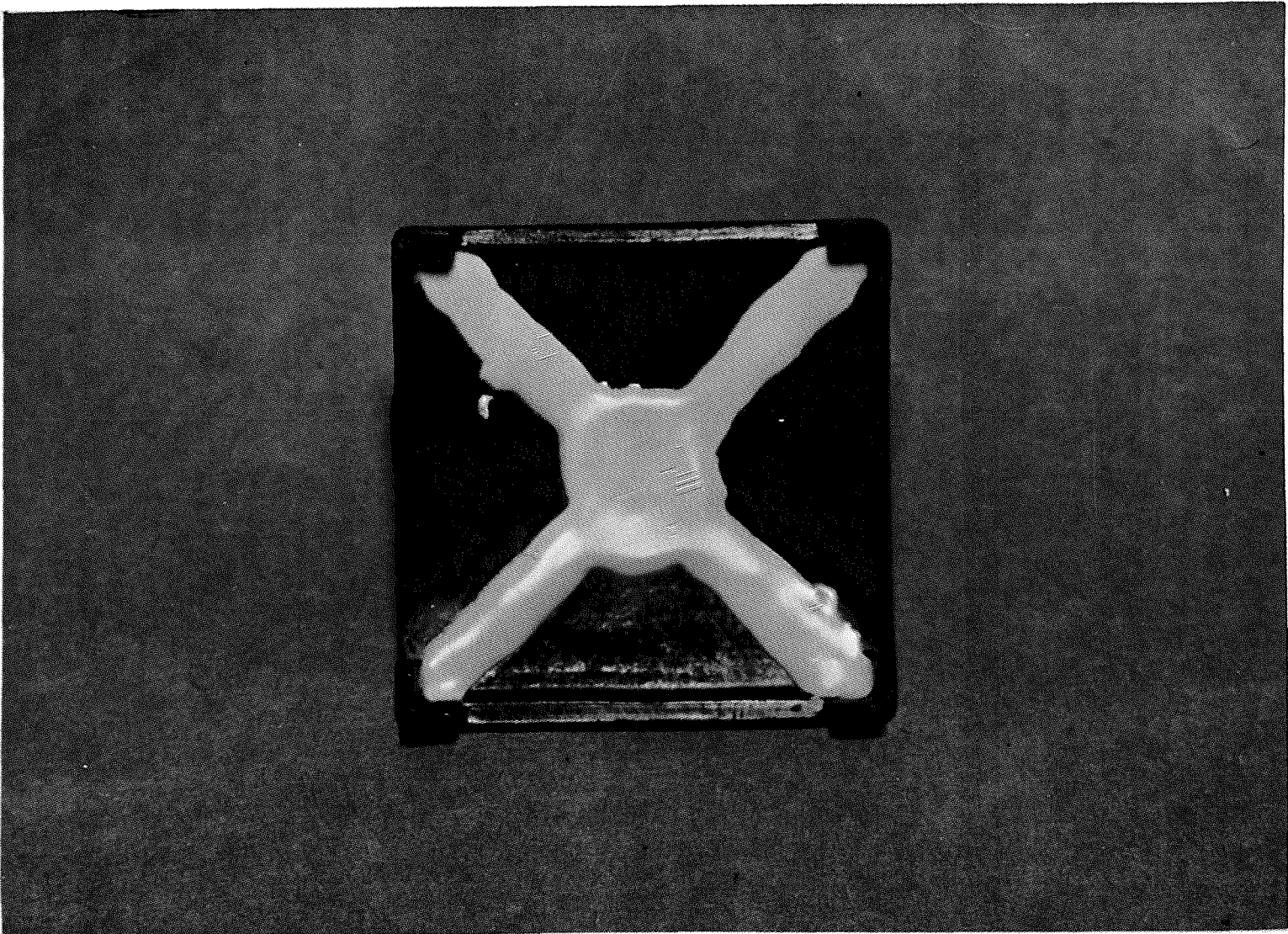


Figure 13. Modified Launch Tube Covers



**Aerospace
Systems Division**

ASE REDESIGN EVALUATION

NO.	REV. NO.
ATM-1064	
PAGE 32	OF 212
DATE	11/24/71

2. EVALUATION OF STRAIN GAUGE DATA

After careful scrutiny of the visacorder traces the strain gauge data does not yield useful information. A meaningful interpretation of the traces is lacking, especially, when the data is compared with the motion of the mortar box as displayed on film during the launching of the grenades.

The salient enigma in most of the traces is the occurrence of two large strain spikes that appear 12 to 21 milliseconds apart. The first pulse occurs approximately 8 milliseconds after initiation of grenade firing. This double pulse event is particularly evident when the -1 and -2 grenades are launched. However, when the -3 grenade was launched the double spike was recorded by the gauges located on the platform; but only the second spike was recorded by gauges mounted on the mortar box. The firing of the -4 grenade resulted in a single spike occurring at 27 milliseconds into the launch.

The order of magnitude of these spikes would seem to be much greater than would reasonably be anticipated - perhaps as high as 20,000 μ inches. The exact magnitude is not known since all gauges saturated.

The strain gauge pulses correlate exactly with the recorded pressure pulses. The only plausible conclusion that seems to be evident is that the strain gauge spikes do not arise as a result of a structural dynamic response. The simultaneity of strain and pressure events is an indication of a phenomenon affined to gas dynamics.

No attempt will be made to speculate, in this report, as to why or how two pressure pulses could be generated in such a small increment of time. Further evaluation will be required before a rational conclusion can be stated.

The strain gauge and pressure data are included in Appendix D of this report.



**Aerospace
Systems Division**

ASE REDESIGN EVALUATION

ATM-1064

PAGE 33 OF 212

DATE 11/24/71

3. PLATFORM EVALUATION - STRUCTURAL INTEGRITY

Inspection of the LRC test mortar platform after the grenade launchings, (see Figure 14), revealed the following structural discrepancies:

(a) Both pedestals were deformed at the base resulting in an increase in distance between the pedestals such that the MBA would not interface properly with the mounting pins.

(b) The skin at the mid-section of the center panel was permanently deformed indicating the yield load had been applied.

(c) Some of the anchor brackets showed evidence of yielding due to loads applied to the brackets (the worst case allowed the anchor to swing about 20 deg beyond the vertical position).

(d) A MBA support pin at the top of one of the pedestals was slightly bent indicating that the yield load had been experienced or that the point of load application had shifted toward the end of the pin (the latter is very probable due to the above mentioned pedestal deformation).

(e) The skin showed several small puncture holes in the vicinity of maximum exhaust impingement.

All but the first item have no effect upon the platform structural integrity. The pedestals have undergone a design change sufficient to provide a positive margin of safety relative to the yield load. A one-eighth inch thick doubler has been added to the bottom flange of the pedestals. The analysis is included in the following pages.

Other structural analysis are included herein (see Appendix C) which consider the estimated test loads and resulting stress levels at critical points in the platform design.

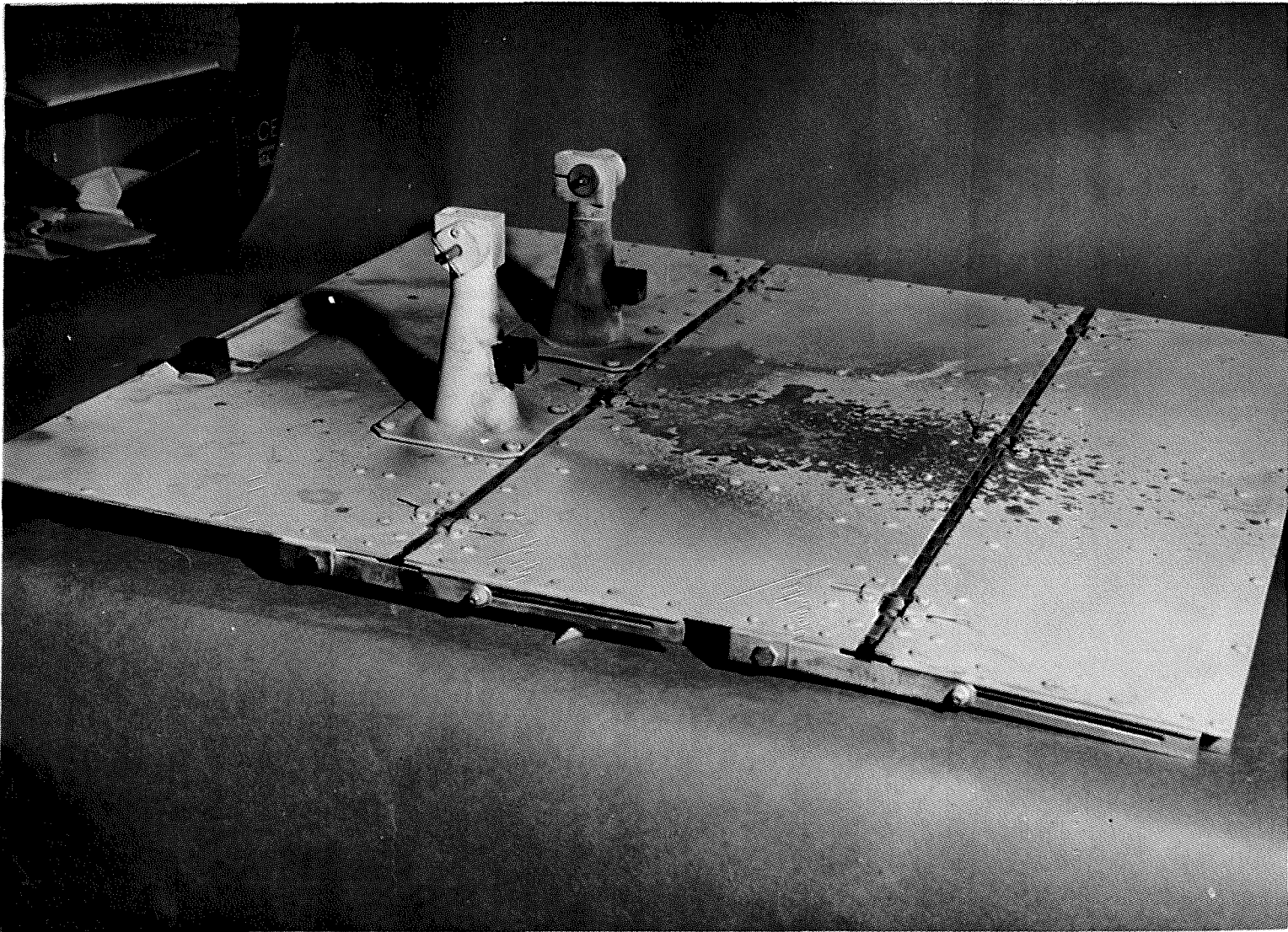


Figure 14. Launch Platform After Eight Grenade Firings

ASE REDESIGN EVALUATION

NO.	ATM-1064	REV. NO.
PAGE	34	OF 212
DATE	11/24/71	



**Aerospace
Systems Division**

ASE REDESIGN EVALUATION

NO.	REV. NO.
ATM-1064	
PAGE <u>35</u>	OF <u>212</u>
DATE 11/24/71	

4. MORTAR BOX STRUCTURAL EVALUATION

The structural integrity of the mortar box was adequately demonstrated by showing only secondary failures after the Langley Launch tests. (Ref. following 2 figures).

The only structural member experiencing cracks was the lower aft magnesium alloy strap connecting the two sides of the mortar box primary structure. However, it has been determined prior to the theoretical structural analysis of the frame assembly that this strap could not be considered as a primary structural member. Therefore, the strap was not included in the analysis as a load carrying member.

The torn fiberglass is of no consequence. Again, it was recognized that the fiberglass is a part of the mortar box that serves as secondary structure. Its only function is to constrain the insulation between the launch tube structure and the outer frame assembly.

The primary structure did not deform or show evidence of failure in any part of the assembly. Therefore, it can be concluded that the structural integrity of the mortar box is satisfactory.



**aerospace
systems Division**

ASE REDESIGN EVALUATION

NO.

REV. NO.

ATM-1064

PAGE 36 OF 212

DATE 11/24/71

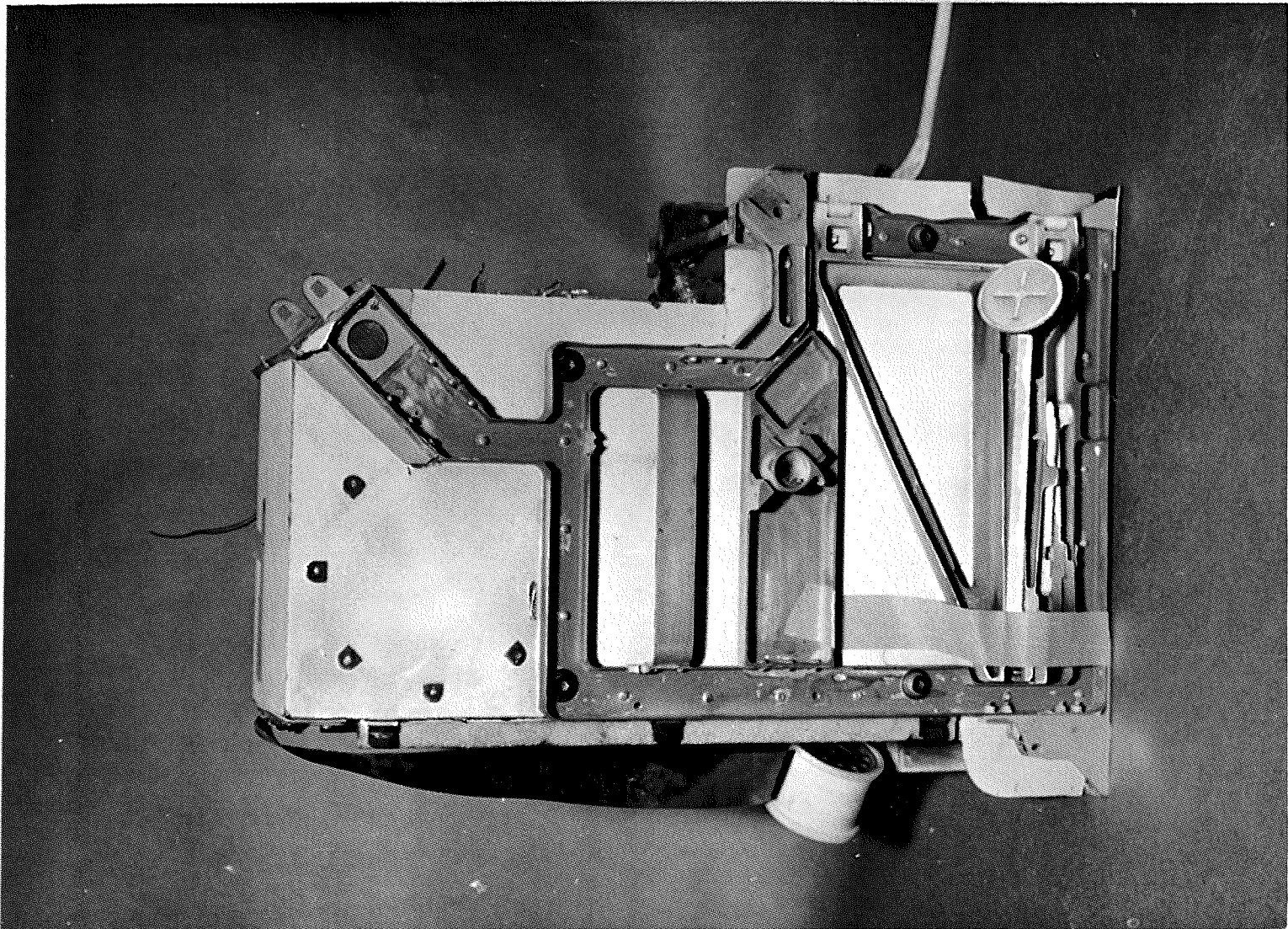


Figure 15. Qual C Mortar Box After Four Firings

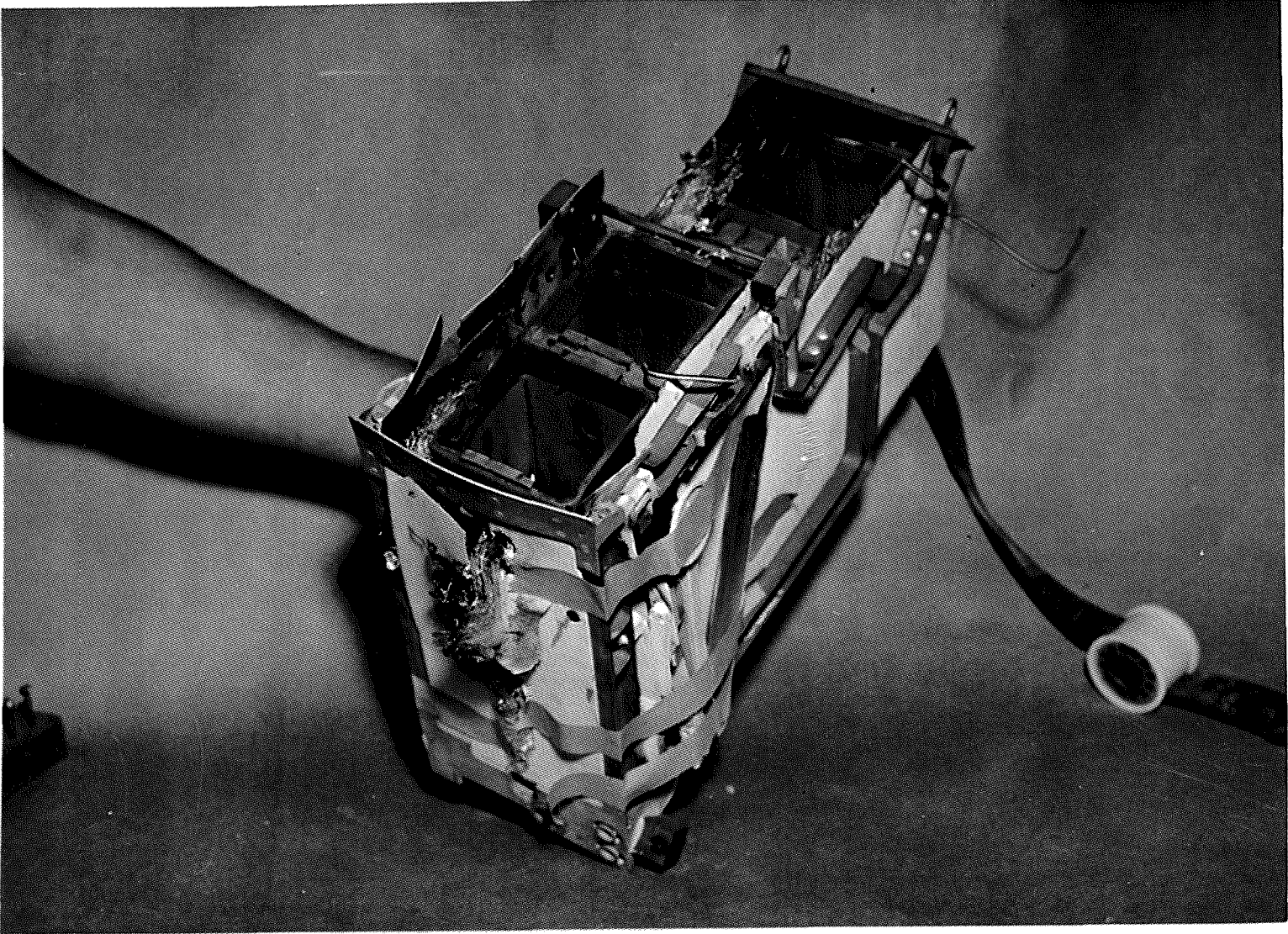


Figure 16. Qual C Mortar Box After Four Firings

ASE REDESIGN EVALUATION

NO.	REV. NO.
ATM-1064	
PAGE 37	OF 212
DATE 11/24/71	



**Aerospace
Systems Division**

ASE REDESIGN EVALUATION

NO. ATM-1064

REV. NO.

PAGE 38 OF 212

DATE 11/24/71

5. MORTAR BOX/PALLET STRUCTURAL ATTACHMENT ANALYSIS

The following items were analyzed for structural integrity:

1. Latch Assembly, Rear Mortar Box (2369286)
2. Locking Mechanism, Fwd. Mortar Box (2369289)
3. Lug Carrier Frame, ASE (2339034)
4. Pedestal (2369290)

The plunger (2369282), which makes up a part of the latch assembly - rear mortar box, is the critical item of the assembly. Allowable eccentric loads, acting transversely on the plunger, were calculated and compared with the loads applied during grenade launching. The minimum margin of safety was found to be 0.08. This margin of safety was referenced to loads determined from the LRC test firings.

The locking mechanism, forward mortar box lug was found to be much stronger than the mating lug carrier frame. Therefore, only the analysis of the latter is shown in Appendix C. A lug analysis was performed on this frame. Since loads were applied to the lug in two mutually perpendicular directions, an oblique loading correction was made to the lug. The minimum margin of safety was found to be 0.72. Thus, the forward attachment is structurally adequate.

The last item stress checked was the pedestal. The pedestal analysis was performed twice. The first check was based on an 0.06 inch base thickness, and the second check was based on the same base thickness plus a .12 inch doubler added to the base.

Test results showed that the base had physically deformed during the first series of four grenade launchings. The results of the analysis of the pedestal with the 0.06 inch base were in agreement with the observed deformations after test. Theoretically, the material was stressed to its ultimate strength. Hence, a doubler has been added to the flight pallet design.

The base was re-analyzed with the 0.12 inch thick doubler added. The results indicated that a positive margin of safety was attained. Therefore, there should be no tendency of the pedestals to rotate out of engagement with the latch assembly.

Detailed structural analysis are presented in Appendix C.



**Aerospace
Systems Division**

ASE REDESIGN EVALUATION

NO.	REV. NO.
ATM-1064	
PAGE 39	OF 212
DATE	11/24/71

6. MISFIRE SUMMARY

Two misfires occurred during the LRC vacuum tests. The first misfire occurred in the initial attempt to conduct Test Firing #4 and the second misfire occurred prior to firing Test Firing #7.

Misfire (Test Firing #4)

This misfire occurred subsequent to two grenade firings (a -2 and a -4 grenade) from the first mortar box to be tested. Since the first two grenades had fired correctly and test results appeared satisfactory an attempt was being made to complete all four grenade firings with the chamber remaining at the required vacuum. The actual misfire occurred in the attempt to fire grenade 3. This dictated the venting of the chamber and opening the door.

Troubleshooting and corrective action was constrained by a desire to maintain the hardware configuration under test so as to not compromise the launch stability and structural integrity evaluation objectives. Specifically this meant that to troubleshoot the GLA or mortar box would have necessitated removing the mortar box from the pallet, which in turn required lifting the pallet out of the soil bed. Therefore, the troubleshooting undertaken avoided these steps.

A series of troubleshooting steps verified proper arming voltages and firing commands (+15 vdc, 20 milliseconds) up to the chamber terminal board which interfaces with the mortar box flat ribbon cable. Additionally, continuity measurements verified continuity of those same circuits through the remaining cable and up to the mortar box electronic board. During the firing attempt the procedure of shorting out of the arming circuit at the chamber control panel after a firing had resulted in a definite discharge indication which verified that the mortar box firing capacitor had charged properly, as a result of the ARM command, but did not discharge. Failure to discharge upon a "fire" command could only be caused by (1) an open motor initiator circuit (from the capacitor in the mortar box electronic board, through this initiator to ground), (2) lack of a firing pulse from the chamber control panel, or (3) by a failure of the #3 firing circuit in the mortar box electronics.



**Aerospace
Systems Division**

ASE REDESIGN EVALUATION

NO.	REV. NO.
ATM-1064	
PAGE 40	OF 212
DATE	11/24/71

Verification of the chamber firing command to the mortar box had already eliminated cause #2. Visual examination of the firing leads and frangible circuit board on the -3 grenade motor indicated no breakage. This examination could not verify wiring back into the GLA after the wires pass the launch tube wall. An ALINCO check verified electrical continuity of the frangible circuit board and proper resistance of the initiator bridgewire. The end result of the troubleshooting had reasonably isolated the failure cause to the mortar box firing circuit, wiring in the GLA, or the 30 pin connector between the two. Further failure isolation would have necessitated the removal of the pallet, mortar box and GLA from their test configuration. Therefore, further troubleshooting was suspended.

A decision was made to by-pass the two suspected fault areas by wiring directly to the #3 initiator from the chamber terminal board. The firing command was changed to a +29vdc voltage. It was also decided to wire the remaining -1 grenade motor initiator in the same manner. Motor initiator leads were cut and jumper wires were spliced (using a crimp ferrule) to the chamber terminal board. This method of firing permitted the successful firing of the -3 and -1 grenades although one of the spliced wires, hanging down from the -1 motor, was blown off from the -3 motor blast. This had to be replaced prior to the -1 grenade firing.

After the -1 grenade firing the mortar box was removed from the pallet and chamber and a continuity check was made to verify that the 30 pin connector was mated. With the mortar box ARM-SAFE switches in the "SAFE" positions, continuity to ground was properly verified from each motor firing lead to the mortar box electronic board ground. The ground return leads on motors #2 and #4 also showed a proper ground. The ground return leads on motors #3 and #1 did not. When the GLA was removed from the mortar box the cause for this, and the misfire, was discovered. Both ground return wires had broken loose from a ground terminal in the GLA.

During the rework of the GLA at SOS, prior to delivery to LRC, the ground return wires had been rewired to a ground terminal to bypass the sequential microswitches which were inoperative on that GLA. The terminal is located between launch tubes #3 and #4 and is recessed back and down from a fiberglass band around all the tubes. This made the terminal difficult to solder and resulted in the cold solder joint which failed during the LRC test. It should be noted that this terminal strip or block in the GLA is normally wired as a subassembly prior to its installation in a GLA so that proper soldering is assured. This then is not considered to be a flight applicable failure. It should also be noted that no other solder joint on the GLA failed and that the second mortar box and GLA successfully survived the second set of grenade firings from the pallet. Historically, no



**Aerospace
Systems Division**

ASE REDESIGN EVALUATION

NO.	REV. NO.
ATM-1064	
PAGE 41	OF 212
DATE 11/24/71	

such failure has ever occurred during the extensive earth atmosphere test firings of the GLA.

After the mortar box was returned to Bendix, at the completion of the LRC tests, the mortar box was subjected to a functional PIA test per TP 2346326 on 19 September. This test re-verified proper operation of the arming circuitry, all firing circuitry and the ARM-SAFE switches subsequent to the firing of four grenades.

Misfire (Test Firing #7)

This misfire occurred with the second mortar box and GLA prior to any grenade firings. The same symptoms associated with the first misfire were seen including indications that the mortar box firing capacitor had charged but did not discharge until the shorting plug had been installed after the firing. Troubleshooting similar to that done earlier on the first misfire again isolated the problem to the mortar box, GLA or the interface 30 pin connector. Since no firings had been conducted from this mortar box/pallet there was less reluctance to disassemble the test hardware. As the GLA was being removed from the mortar box the cause for failure was identified. The 30 pin connector was separated by approximately 1/8" with a greater spread at the pin #30 end. The connector separation occurred during the GLA installation and was a result of the connector not being lock wired at that end. The lock wiring had not been accomplished during the installation because of the difficulty presented by the short wiring harness to the connector on that particular mortar box (Proto C model). Flight models have a longer cable harness which permits lock wiring both ends of the connector, which is a flight GLA installation procedure mandatory requirement. The flight mortar box, after GLA installation, is X-rayed to verify connector mating. The failure cause then was conclusively shown to be an installation error, not associated with the ASE modifications nor test environment and not applicable to a flight failure. The separated connector was, after much difficulty, adequately lock wired and, as such, survived four firings.



**Aerospace
Systems Division**

ASE REDESIGN EVALUATION

NO.	REV. NO.
ATM-1064	
PAGE 42	OF 212
DATE 11/24/71	

B. PRESSURE/DUST

1. ANALYSIS OF PRESSURE IMPINGEMENT EFFECTS

Another major test objective of the Langley retest program was to insure that the minimal fifty foot separation distance between the ASE and ALSEP would be sufficient to allow rocket motor exhaust gasses to be expanded enough so that the pressures would not influence the other experiments.

As a result of the 10 foot ASE cable lengths and deployment configuration used on Apollo 14 it was shown in the previous Langley tests that considerable damage could be wrought on both the Central Station and Passive Seismic Experiment due to the intensity of the advancing pressure wavefront resulting from a rocket motor. In that test the Central Station side curtains were thrown back and the reflector torn and mutilated. The Passive Seismic Experiment performance would have been degraded to a point beyond usefulness since an important part of its thermal control system might possibly have been removed. Some of the tests had shown the thermal skirt to be folded back which would have seriously influenced the experimental data.

In the Langley retest program one-sixth gravity models of both the Central Station and Passive Seismic experiment were located twenty five feet from the ASE; less than half the separation distance planned for Apollo 16. This test would also provide data under conditions more severe than to be expected on the Lunar surface.

To investigate pressure effects, pointers were placed at one edge of the Central Station to provide references for any translational motion. A 1° bubble level on the Passive Seismic Experiment would record any change in its levelness.

Checking the bubble level from outside the chamber with the aid of a telescope and later re-entering the chamber showed no change in PSE levelness after any of the firings. Investigation of the Central Station reference markers showed no displacements. Later analysis of the high speed photography coverage showed a very slight movement of the Central Station side and rear curtains, as the pressure wave passed. The light



**Aerospace
Systems Division**

ASE REDESIGN EVALUATION

NO.	REV. NO.
ATM-1064	
PAGE 43	OF 212
DATE	11/24/71

multilayer insulation of the Passive Seismic Experiment was unruffled and not influenced by the exhaust pressures at these distances. Finally, two pressure transducers provided numerical values of the pressure peaks. One transducer was located between the Central Station and ASE (12 feet) and another at the edge of Central Station (25 feet). The transducers were calibrated to 0.1 psi full scale. Throughout the grenade firing sequence, none of the transducers recorded peak pressures in excess of 0.03 psi. The time duration was on the order of 6-8 milliseconds. Another important objective of the retest program had been met. With very low pressure levels, no damage and no motion of the Central Station, Passive Seismic Experiment or Charged Particle Lunar Environment Experiment being observed, it was verified that when deployed on the Lunar surface all pressure effects due to ASE rocket motor exhaust gases will not cause physical damage to any of these experiments.



**Aerospace
Systems Division**

ASE REDESIGN EVALUATION

NO.	REV. NO
ATM-1064	
PAGE <u>44</u>	OF <u>212</u>
DATE	11/24/71

2. EVALUATION OF PRESSURE TRANSDUCER DATA

Analysis of the pressure transducer data has produced results of very limited usefulness. The interpretations of the data to date neither provide a qualitative nor a quantitative description of the flow phenomena at the edges of the launch platform or in the vacuum chamber itself.

Comparisons of the test data for all firings have revealed that pressure and strain gauges reach a peak typically between 25 to 30 milliseconds after initiation of the rocket motor ignition pulse. Only one such pulse occurs for the smaller (-3) and (-4) grenades. However, for the (-1) and (-2) grenades a second pulse of this type occurs at about 10 milliseconds after the indicated initiation firing pulse is sent. Pressure transducers 2, 3 and 4 were located at the edge of the launch platform and were to provide a minimum pressure distribution over the pallet surface as a function of time. The pressure transducer number 5 was located midway between the ASE and Central Station - a distance of about 12 feet. The number 6 pressure transducer was located at the Central Station - a distance of 25 feet. The very large strains and pressure pulses on the pallet should have been reflected in the accelerometer traces, but none were observed. The absence of the pulse in accelerometer traces would lead one to believe that glitches had occurred in the electronics conditioning or recording equipment, however the strain gauge and pressure data were recorded independently.

The simultaneity of these events led to close visual inspection of all photographic films during this time interval, but no motion was observed or possible cause suggested. Many causes were theorized, investigated and shown to be inconsistent with other data in one way or another. To date it has not been possible to organize a meaningful interpretation of the data.



**Aerospace
Systems Division**

ASE REDESIGN EVALUATION

NO.	REV. NO.
ATM-1064	
PAGE 45	OF 212
DATE 11/24/71	

3. ANALYSIS OF DUST ACCUMULATION EFFECTS

The evaluation of the accumulation of dust on ALSEP due to ASE grenade firings was one of the primary objectives of the Langley test. The mortar box RF and power cables have been increased in length from ten (10) to fifty eight (58) feet to allow ASE deployment at a distance sufficient to escape the lunar dust spray kicked up by the rocket motor firings. Previous estimates of the lunar dust accumulation footprint showed the pattern to be elliptical with major and minor axes of 50 and 25 foot, respectively.

To minimize the possibility of dust accumulation the general ALSEP deployment configuration as shown in Figure 4 was suggested for Array D. Most of the dust kicked up falls behind the ASE; a reduced amount falls to the side. To test this deployment configuration, the Central Station and Passive Seismic Experiment were located a distance of twenty five (25) feet from the ASE and 90° from the mortar box firing line in the sixty (60) foot Langley vacuum chamber. This was the maximum allowable due to chamber floor configuration.

The results of the test confirmed the separation distance selection in the Earth's gravitational field. The (-3) and (-4) grenade firings created only a slight amount of dust since the launch platform deflected most of the gases, hence preventing them from impinging on the lunar soil.

The first Langley test revealed that these same rocket motors created the most dust; in fact, a small crater had been dug by the impinging gases. The presence of the launch platform prevented this phenomena from occurring and reduced the volume of dust particles by many orders of magnitude.

Similar results were observed upon firing the (-1) and (-2) grenades. Although no craters were formed in the first Langley test, some dust had been stirred up. The presence of the launch pallet significantly reduced dust volume. Most of the dust which was set in motion resulted from forcing dust out from under the pallet and through the two hinge lines. The dust forced out from under the pallet along the edges had low velocity and small launch angles with the result that it did not travel far. See Fig. 17.



**Aerospace
Systems Division**

ASE REDESIGN EVALUATION

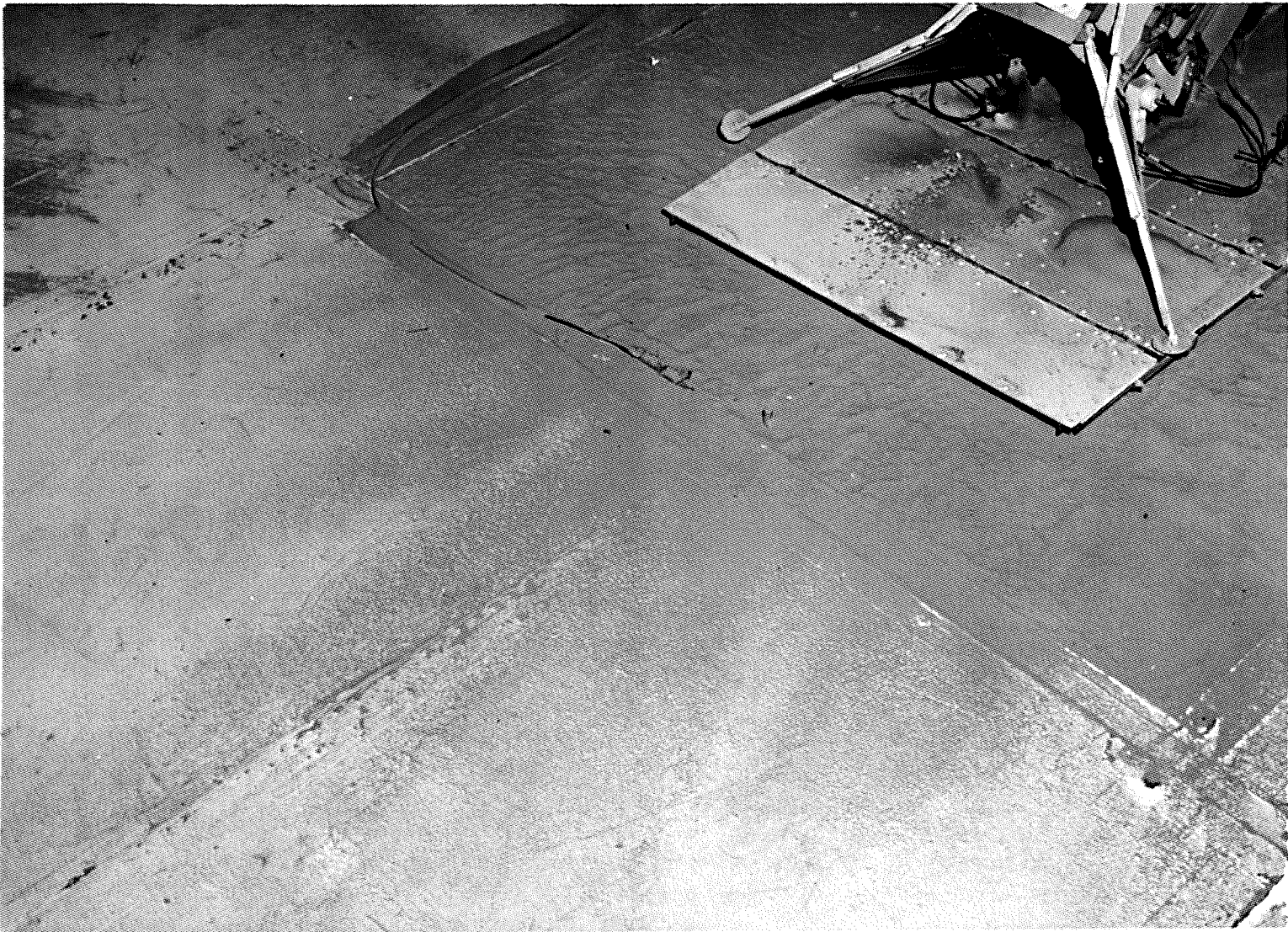


Figure 17. Dust Coverage Aft of Launch Platform

NO.

REV. NO.

ATM-1064

PAGE 46 OF 212

DATE 11/24/71



**Aerospace
Systems Division**

ASE REDESIGN EVALUATION

NO.	REV. NO.
ATM-1064	
PAGE 47	OF 212
DATE 11/24/71	

The dusting effect and influence of the rocket motor exhaust gases was investigated during a set of (-1) and (-2) firings by spreading a six inch band of soil in an arc approximately five feet from the exit plane of the grenades. Upon examination after firing it was observed that very little of the dust had been moved. Also, little of the soil at the edges of the soil bed was influenced. The dust volume expelled through the hinge lines as the launch platform was forced into the soil was small. Most of the dust remained on the pallet and was blown away in subsequent firings.

It was estimated that, at most, the extent of this dust reached 7.5 feet behind the mortar box. Examination of the (-1) films showed that all the dust had settled in about 12 revolutions of the timing clock which corresponds to 0.72 seconds. If it is assumed that this dust originated with a velocity such that its launch angle is 45° to the horizontal, hence giving maximum range, then an estimation of the maximum range under the Lunar gravitational field can be determined using simple kinematical relationships:

$$x = V_{ox}t$$

$$y = V_{oy}t - 1/2 gt^2$$

With $x_f = 7.5$ ft and $t_f = 0.72$ seconds then the horizontal initial velocity component is 10.4 ft/sec. If it is assumed that soil particles are given the same initial velocity in the Lunar environment the range will be increased due to the reduced gravitational acceleration. Performing these calculations it can be shown that the time of flight corresponding to a launch angle of 45° is 3.87 seconds and the maximum range achieved is 40.25 feet behind the ASE. Since the closest ALSEP equipment is 58 feet and the launch direction is such that these dust particles are accelerated in the opposite direction, no dust would be able to reach ALSEP and cause damage or influence the thermal control surfaces of the other experiments.

Hence, an important objective of the test has been investigated with the results confirming the pre-test minimum separation requirement between ASE and ALSEP of at least 40 feet. The absence of dust accumulation on ALSEP can be assured.



**Aerospace
Systems Division**

ASE REDESIGN EVALUATION

NO.	REV. NO.
ATM-1064	
PAGE 48	OF 212
DATE 11/24/71	

C. STABILITY

1. MBA/Pallet Stability (Normal Firing Order)

a. Film Data

The high speed motion picture film was used to determine the maximum excursions of various points on the MBA/Pallet assembly during each test. The three points which were observed are:

- A. The top of left (looking towards the launch direction) MBA support pedestal.
- B. The left forward corner of the pallet.
- C. The top of the MBA.

The coordinate system and points A, B, and C are shown in Figure 18.

The results are tabulated in Table 2. It should be noted that the measured displacements are peak dynamic values which occurred during each test and are not permanent displacements. In all cases the MBA/Pallet assembly returned to nearly its original position with very little accumulated movement through launching of all four (4) grenades.



**Aerospace
Systems Division**

ASE REDESIGN EVALUATION

NO.	REV. NO.
ATM-1064	
PAGE 50 OF 212	
DATE 11/24/71	

TABLE 2

Maximum Dynamic Displacements of the MPA/Pallet Assembly During Grenade Launchings

MAXIMUM DISPLACEMENTS^a (in)

Location ^b		A			B			C		
Test	Grenade	x	y	z	x	y	z	x	y	z
#3	-2	---	---	---	0.4	0.4	0.8	0.6	0.3	0.5
#4	-4	0.0	0.0	0.0	0.0	0.0	0.0	0.0	0.0	0.0
#5	-3	---	---	---	0.5	0.2	1.0	1.8	0.1	1.0
#6	-1	---	---	2.1	0.6	0.8	2.1	1.6	0.3	2.1
#7	-2	---	0.2	0.5	0.6	0.3	0.9	1.0	0.5	0.7
#8	-1	---	0.2	1.1	0.4	0.6	0.8	1.7	0.4	1.1
#9	-4	0.0	0.0	0.0	0.0	0.0	0.0	0.0	0.0	0.0 ^c
#10	-3	---	0.8	0.7	1.1	0.3	1.6	0.7	1.4	1.2

- a. measurements obtained, as accurately as possible, from the high speed film data
- b. see Figure 18 for location of points A, B, and C
- c. a slight downward motion is observable from the film.
- d. Tests #1 and #2 were calibration motor firings.



**Aerospace
Systems Division**

ASE REDESIGN EVALUATION

NO.	REV. NO.
ATM-1064	
PAGE 51	OF 212
DATE 11/24/71	

b. Accelerometer Data

The LRC accelerometer data (see Appendix D), in its present form, is of little value for purposes of determining the degree of stability the ASE will possess on the lunar surface. The data illustrates that a high intensity, non-stationary, random environment exists for a few milliseconds after each grenade launching. The impulses which cause the motions recorded on movie film are obscured by the vibration data.

Filtering techniques were applied to the data without success. The filtered data appears to be high level non-stationary random vibration over a low frequency bandwidth. Shock spectrum analysis of the accelerometer data could prove to be of value. However, the expense of such analysis is not warranted at the present time.

Aside from the random vibration difficulty with the accelerometer data, many of the accelerometers displayed a serious "drift". Several hundreds of milliseconds after ignition when the vibrations had been damped completely, some accelerometers recorded hundreds of g's acceleration over relatively long time periods. Such acceleration - time histories were obviously in error. This type of behavior of a large percentage of the data, tends to cast serious doubts on all the accelerometer data.



**Aerospace
Systems Division**

ASE REDESIGN EVALUATION

NO.	REV. NO.
ATM-1064	
PAGE 52	OF 212
DATE	11/24/71

c. MBA/Pallet Dynamic Analysis

INTRODUCTION

During the first LRC test series it was observed that the mortar box was displaced several inches during each grenade launch. Such motion was attributed primarily to grenade rocket motor exhaust gas pressure acting on the rear of the mortar box.

The launch pallet was added to the system to overcome the exhaust gas effects and maintain a stable mortar box throughout the grenade launchings. With respect to the pallet concept the basic hypothesis is that gases acting on the pallet would result in forces sufficient to overcome the forces acting on the MBA. That is, the downward force acting on the pallet would exceed the upward force acting on the MBA, and the lateral forces due to reaction of the soil on the pallet would be sufficient to balance lateral forces acting on the MBA. By attaching the MBA to the pallet, stability will be maintained throughout the launching period of the four grenades.

Using the pallet, the second LRC test series resulted in small but unexpected MBA displacements. By careful high speed test film observation, it was concluded that the motion was caused by the bulk of the rocket motor exhaust gases, which impact the pallet in a relatively small area, resulting in a pivoting (seesaw) type motion of the pallet about the hinges and the anchor brackets. Examination of the still photographs of the LRC pre-test deployment configuration (see Figure 6) shows that the pallet, as deployed in the compacted soil bed, is not making complete pallet-soil contact. Thus deployed, even with the 7" anchor stakes fully embedded, the soil did not provide adequate support of the pallet panel hinge lines and skin areas. By applying loads to the pallet at the center of the motor exhaust gas impact areas for the four grenades, it can be demonstrated that the pallet, deployed as it was at LRC, will pivot and deflect into positions corresponding to the LRC results.

To further substantiate the above explanation of the MBA motion during the second LRC tests, an impulse-momentum analysis was conducted (the details are presented in Appendix A.) The intent of the analysis was analytically to demonstrate the MBA/Pallet motions observed during the LRC tests.



**Aerospace
Systems Division**

ASE REDESIGN EVALUATION

NO.	REV. NO.
ATM-1064	
PAGE 53	OF 212
DATE 11/24/71	

ASSUMPTIONS

The analysis assumes that the panels have no initial resistance to rotation (corresponding physically to about $\pm 5^{\circ}$ of free play) and that the platform is placed on the soil such that an impulsive force can induce an initial translational and rotational velocity to each of the three individual panel segments. That is, pallet-soil contact is not complete whereby forces applied to the pallet would be transferred directly through the pallet to the soil. The coefficient of restitution takes into account the relationship between the soil and platform.

An impulsive load of 3 lb-sec is assumed. This value is based upon calculated forces required to cause the permanent deformation experienced by the center panel of the pallet during the LRC tests (see Appendix A for details).

RESULTS

By applying an impulsive load of about 3.0 lb-sec at the second hinge due to the -1 grenade firing, a uniform vertical rise of the platform of about 2 in. results. Similarly by applying the same impulse at the first hinge due to the -3 grenade firing, an upward motion of the front panel of about 1 in. results.

The analysis further shows that by varying the coefficient of restitution between the platform and soil, different displacement profiles can be generated. Depending on the soil properties, the motion can range from a perfectly "elastic" impact causing large motions to a perfectly "plastic" collision causing nearly negligible motion with only slight rotation about the hinge points.

For the case of the -4 grenade launch, the observed dynamic motion was negligible. This is explained by the fact that directly below the -4 grenade pressure pulse area are two hat section stiffeners which come in direct contact with the soil surface. A vertical force or impulse applied at this point on the pallet is directly transmitted to the soil resulting in no induced motion.



**Aerospace
Systems Division**

ASE REDESIGN EVALUATION

NO.	REV. NO.
ATM-1064	
PAGE 54	OF 212
DATE 11/24/71	

CONCLUSION

A relatively simple, but adequate, mathematical model of the MBA/pallet demonstrates that application of impulsive loads at or between the pallet hinge lines results in motions similar to those observed during the second LRC tests. Hence, the causative factor relative to MBA/pallet motion has been verified.

The motion can be eliminated by preventing the pivotal action. This can be accomplished either by firmly implanting the pallet into the soil such that all loads are transferred through the pallet to the soil (i. e., the fulcrum for the "seesaw" will be eliminated), or by a hardware modification which mechanically supports the hinges.



**Aerospace
Systems Division**

ASE REDESIGN EVALUATION

NO.	REV. NO.
ATM 1064	
PAGE 55	OF 212
DATE 11/24/71	

d. ANALYSIS OF SOIL EFFECTS

During preliminary discussions with NASA/MSC, Bendix was directed to "evaluate the forces exerted by the platform during each firing (all 8 LRC) on the lunar soil and the expected reactions on the lunar surface. This analysis should include comparisons using various soil types." The "various soil types" have been defined by NASA/MSC by the following soil parameter ranges.

Density (gm/cc):	$1.3 \leq \rho \leq 2.0$
Cohesion (psi):	$0.004 \leq c \leq 0.159$
Internal friction (deg):	$35 \leq \phi \leq 51.5$
Pressure gradient (psi/in):	$3 \leq \frac{d\sigma}{dZ} \leq 16$
Coefficient of friction:	$0.27 \leq \mu \leq 0.50$

It should be noted that (1) the above minimum and maximum soil conditions are contrary to the Apollo 16 soil defined by NASA/MSC letter no. EH3/6-7/L226/B275(PDG), and (2) the LRC soil density was 100 lb/cu. ft. (1.6 gm/cc) which is a mid-range value.

The purpose of this analysis is to evaluate horizontal stability of the pallet and to substantiate that seven inch long anchors can be driven into the lunar soil.

Horizontal Stability

The rather poor quality accelerometer, strain gage, and pressure transducer data, obtained from the LRC test, made it impossible to determine exact mortar pallet loads. However, permanent deformations of portions of the pallet have made it possible to estimate these loads.

Paragraph 3.3 of Appendix A discusses the deformation of the mid-section of the pallet center panel. It was calculated that a uniform pressure distribution of 48.8 psi over the deformed area (48 in²) would have been required to cause such damage. Since the centerline of the -2 grenade intersects the pallet at about the center of the deformed area, it can be assumed that such deformation was caused primarily by the launching of that grenade.



**Aerospace
Systems Division**

ASE REDESIGN EVALUATION

NO.	ATM 1064	REV. NO.
PAGE	56	OF 212
DATE	11/24/71	

Paragraph 2.1.3 of Appendix C considers the deformation of the cantilever pins which are a part of the MBA latching mechanism on each pedestal. The pins experienced an excessive bending moment due to deformations of the pedestals. As the pedestals rotated the MBA beared against the pins at points nearer the ends thereby increasing the resulting moment even though the applied force was not necessarily higher than expected.

The exact point of load application on the pins is not known, but a conservative estimate can be obtained. Inspection of a deformed pin revealed the deformation to be primarily due to bending. For such short pins (relative to diameter), shear deformation would also be evident. It will be conservatively assumed that the deflection of the end of the pin was 50% bending and 50% shear. From the data in Appendix C the corresponding moment arm (e) is 0.20 in. and the required ultimate load (P) is 246 lb.

Figure 19 defines the assumed pallet loading configuration. Exhaust gases from the grenade rocket imparts a local high uniform pressure distribution (P_1) over air area ($\Delta A=48 \text{ in.}^2$) and a low uniform pressure distribution (P_p) over the remainder of the pallet area (i. e., $A - \Delta A= 576 \text{ in.}^2$). The horizontal and vertical reactions forces (H_1 , V_1 , H_2 , and V_2) act at the forward and aft MBA attachments points and restrain the MBA which is being subjected to exhaust gas pressure tending lift it from the pallet. The reaction of the soil against the pallet is shown by the friction force (H_f), the anchor restraining force (H_a), and the unknown normal soil pressure distribution (P_s).

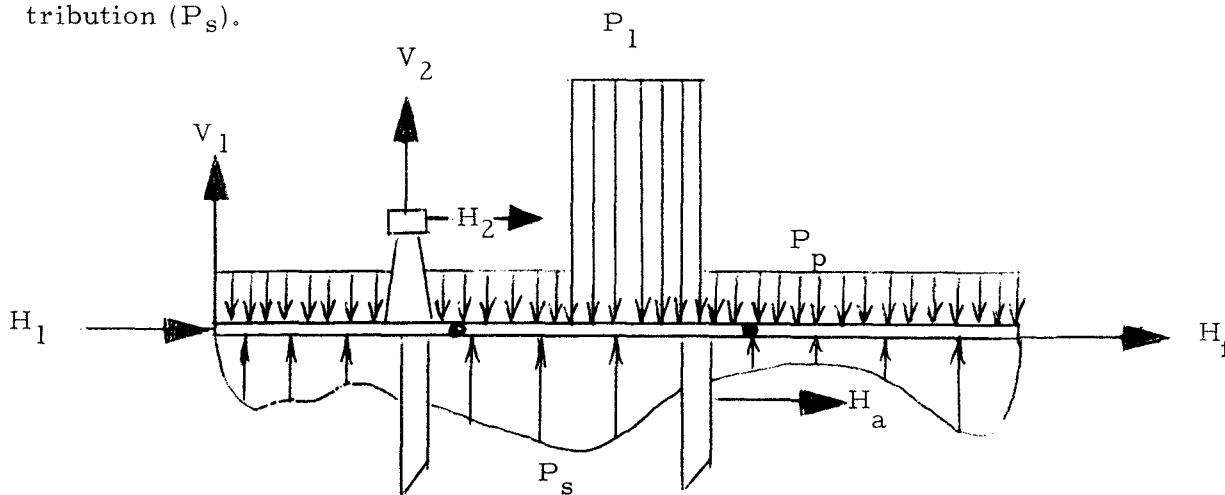


Figure 19 Assumed Pallet Loading



**Aerospace
Systems Division**

ASE REDESIGN EVALUATION

NO.	REV. NO.
ATM 1064	
PAGE 57	OF 212
DATE 11/24/71	

The total horizontal and vertical forces acting on the pallet as a result of the exhaust gases are given by:

$$(1) \quad H_p = H_1 + H_2$$

$$(2) \quad V_1 = P_1 \Delta A + P_p (A_p - \Delta A) + V_1 + V_2$$

The total horizontal reaction force of the soil on the pallet is,

$$(3) \quad H_s = H_f + H_a$$

where

$$(4) \quad H_f \leq \mu V_p$$

$$(5)* \quad H_a = \frac{1}{2} \gamma A_a l_a \tan^2 (45 + \frac{\phi}{2}) + 2 c A_a \tan (45 + \frac{\phi}{2})$$

and A_a and l_a are the horizontal area and length, respectively, of the anchors. From design geometry,

$$A_a = 28 \text{ in.}^2$$

$$l_a = 7 \text{ in.}$$

Under actual conditions H_f will be just sufficient to achieve equilibrium within the limitation given by equation (4). However, for the remainder of this analysis the inequality sign will be replaced by an equality sign. In this way a factor of safety (SF) can be calculated. For stability it is required that,

$$(6) \quad H_s > H_p$$

Hence,

$$(7) \quad SF = \frac{H_s}{H_p}$$

*Terzaghi & Peck, "Soil Mechanics in Engineering Practice", Wiley & Sons, 1948.



**Aerospace
Systems Division**

ASE REDESIGN EVALUATION

NO.	REV. NO.
ATM 1064	
PAGE 58	OF 212
DATE 11/24/71	

It was previously determined that for the -2 grenade launch $P_1 = 48.8$ psi. It will be assumed that P_1 is proportional to peak chamber pressure, allowing one to calculate P_1 for the other three grenade launches. The results are listed in Table I together with values for P_p which were previously estimated from the first LRC test data and gas dynamic analysis.

TABLE I - PRESSURES

Grenade	P_c	r_1	r_2	P_p	P_1
-2	4135 psi	0.671	1.000	3.21 psi	48.8 psi
-4	2542	0.413	0.612	1.97	30.0
-3	3170	0.516	0.767	2.46	37.4
-1	6150	1.000	1.49	4.66	72.7

Notes

- (1) P_c = average peak chamber pressure, see Letter No. 9712-353, "Rationale for Selection of ASE Mounting Plate Dimensions", 21 May 1971
- (2) $r_1 = (P_c)_i / (P_c)_1$, (i = 1, 2, 3, 4 corresponding to grenade numbers)
- (3) $r_2 = (P_c)_i / (P_c)_2$, (i = 1, 2, 3, 4)
- (4) P_p , see Letter No. 9712-399, "ASE Mortar Box - Platform Stability", 16 June 1971.
- (5) $P_1 = r_2 P_c$

The MBA/pallet structural analysis* reveals that the pins experience maximum loads during the -1 grenade launch. Analytically determined values for the reaction forces (denoted by H'_1 , V'_1 , H'_2 , and V'_2) are listed in Table II. It will be assumed that the vector relationship determined by analysis is accurate. However, a scale factor (η) will be applied to the magnitude of the force vectors such that

*BSR 3237 "Final Report - ALSEP Array-D MBA/Pallet Structural Analysis," Nov. 30, 1971.



**Aerospace
Systems Division**

ASE REDESIGN EVALUATION

ATM 1064

PAGE 59 OF 212

DATE 11/24/71

$$(8) \left\{ \begin{array}{l} H_1 = \eta H'_1 \\ V_1 = \eta V'_1 \\ H_2 = \eta H'_2 \\ V_2 = \eta V'_2 \end{array} \right.$$

Equating twice (since there are two pins) the value of the calculated pin load (P) to the vector sum of H_2 and V_2 , substituting from equations (8), and solving for η , yields,

$$(9) \quad \eta_1 = 2P \left[(H'_2)^2 + (V'_2)^2 \right]^{-\frac{1}{2}} \\ = 0.935$$

TABLE II - ANALYTICALLY DETERMINED PEAK REACTION FORCES

Grenade	H'_1	V'_1	H'_2	V'_2
-2	-172 lb	-325 lb	-144 lb	-278 lb
-4	-158	+284	-139	+245
-3	-138	+254	-105	+257
-1	-223	-439	-137	+511

Equation (9) applies only to the -1 grenade launch since it was assumed that the pin deformation occurred at that time. In order to determine scale factors for the other three cases it will again be assumed that loads are proportional to chamber pressure, Hence,

$$(10) \quad \eta = r_1 \eta_1$$

where r_1 is chamber pressure ratio (see Table I).



**Aerospace
Systems Division**

ASE REDESIGN EVALUATION

NO.	REV. NO.
ATM 1064	
PAGE 60	OF 212
DATE	11/24/71

Using equations (1) through (9), the forces and pressures listed in Tables I and II, and various other parameter values given in the text of this report; yields the results given in Table III. The maximum and minimum values are relative to soil parameters.

The soil pressure distribution (p_s) could be determined by assuming a reasonable approximate shape and solving the free body moment equation. However, this information is not required for purposes of the present analysis.

Appendix C calculates the ultimate load per anchor to be 17.4 lb assuming a load distribution which increases linearly with depth of penetration. Hence H_a cannot exceed 69 lb. Although equation (5) calculates a maximum value of 187 lb., Table III lists the limiting value of 69 lb.

TABLE III - RESULTS

Grenade	-2	-4	-3	-1
H_1	-108	-61	-67	-208 lb
H_2	-91	-54	-51	-128 lb
V_1	-205	+110	+123	-410 lb
V_2	-175	+95	+125	+480 lb
H_p	-199	-115	-118	-336 lb
V_p	-4550	-2345	-2942	-6110 lb
$(H_f)_{max}$	2775	1172	1471	3055 lb
$(H_f)_{min}$	1230	630	790	1650 lb
$(H_a)_{max}$	69	69	69	69 lb
$(H_a)_{min}$	13	13	13	13 lb
$(H_s)_{max}$	2844	1241	1540	3124 lb
$(H_s)_{min}$	1243	643	803	1663 lb
$(SF)_{max}$	14.2	10.8	13.0	9.3
$(SF)_{min}$	6.1	5.6	6.8	4.95



**Aerospace
Systems Division**

ASE REDESIGN EVALUATION

NO.	REV. NO.
ATM 1064	
PAGE 61	OF 212
DATE 11/24/71	

It should be noted that a somewhat controversial term has been deleted from the equation for the force of the soil on the anchors. It is BxA's contention that the force applied to the anchor by the soil is a function of the pressure (P_p) acting on the platform in the general vicinity of the anchor. To be specific,

$$(11) * \Delta H_a = \frac{1}{2} P_p A_a \tan^2 (45 + \frac{\phi}{2}).$$

For the worst case (-1 grenade and minimum soil strength parameters),

$$\Delta H_a = 240 \text{ lb}$$

The significance of ΔH_a is that it raises the minimum load capability of the four anchors from 13 lb (limitation due to soil strength) to 69 lb (limitation due to structural strength of the anchors).

Soil Penetration

The force required to penetrate the soil with an anchor is,

$$(12) **F = \left(\frac{d\sigma}{dZ}\right) l_a A_c + \frac{1}{4} \gamma \mu l_a A_s$$

where A_c is the cross-sectional area of an anchor (0.1 in.²) and A_s is the total surface area of an anchor (25 in.²). Hence,

$$\left. \begin{aligned} F &= 2.2 \text{ lb (min)} \\ &= 11.5 \text{ lb (max)} \end{aligned} \right\} \text{ per anchor}$$

If the worst conditions are encountered all four anchors could be driven into the lunar soil by a total of 46 lb. Since an astronaut's lunar weight is about 60 lbs., no difficulties would be encountered on the lunar surface.

*Terzaghi & Peck, "Soil Mechanics in Engineering Practice," Wiley & Sons, 1948.

**Source: Apollo 15 - Preliminary Analysis of Soil Behavior.



**Aerospace
Systems Division**

ASE REDESIGN/EVALUATION

NO. ATM 1064	REV. NO.
PAGE <u>62</u>	OF <u>212</u>
DATE	11/24/71

Conclusions

From the preceding analysis the following conclusions can be drawn:

- (1) For all possible circumstances the horizontal stability of the MBA/pallet is assured since the soil/pallet interface is capable of generating reaction forces five times (or better) greater than that required to overcome applied loads as determined from the LRC test.
- (2) The strongest soil conditions expected will not offer more resistance (46 lb) to anchor penetration than an astronaut is capable of providing (60 lb).



**Aerospace
Systems Division**

ASE REDESIGN EVALUATION

NO.	REV. NO.
ATM-1064	
PAGE 63	OF 212
DATE 11/24/71	

e. Predicted MBA/Pallet Stability on the Lunar Surface

INTRODUCTION

If the LRC test set-up were duplicated on the lunar surface, it would be expected that any earth motion of the MBA/pallet would be amplified to some extent. The following analysis is performed to predict the motion of the MBA/pallet on the lunar surface assuming an earth motion of about 2 inches vertical due to the -1 grenade being fired. The analysis takes into account the soil resistance due to the friction forces at the leg supports.

ANALYSIS

The basic energy equation for the complete mortar box/platform can be written -

$$K. E. _E = (P. E. + WORK) _E = (P. E + WORK) _L$$

or $P. E. _L + WORK _L = P. E. _E + WORK _E$

$$y_L W_L + 4 \mu N Y_L = Y_E W_E + 4 \mu N Y_E$$

Where $N = \frac{1}{2} (X_1 Y_1 \theta_{11} \theta_{2} \theta_{3} K) =$ Avg normal force/stake, subscripts "E" & "L" refer to earth & lunar respectively, and angular displacements are assumed small. The above equation reduces to -

$$Y_L = \frac{Y_E (W_E + 4\mu N)}{(W_L + 4\mu N)}$$



**Aerospace
Systems Division**

ASE REDESIGN EVALUATION

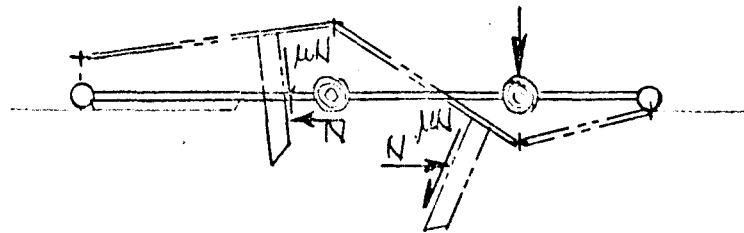
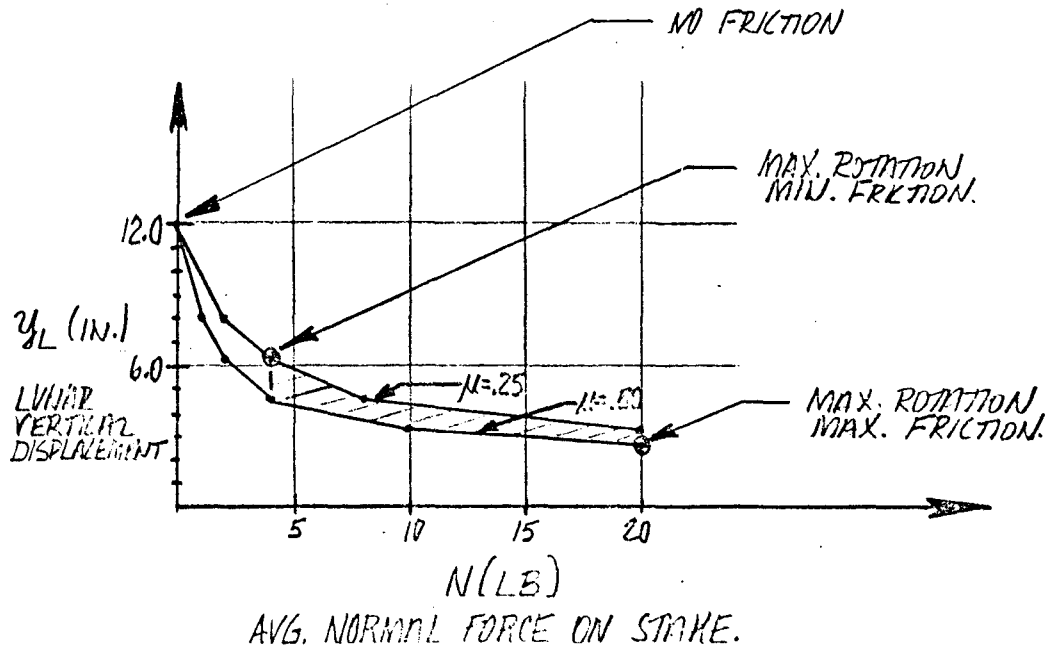
NO.	REV. NO.
ATM-1064	
PAGE 64	OF 212
DATE 11/24/71	

RESULTS

For the -1 grenade case the following values apply -

- $Y_E = 2.1$ in. (from II. C. 1. a)
- $W_E = 18.0$ lb
- $W_L = 3.0$ lb
- $U = 0.25$ to 0.50 from II. C. 1. d
- $N = 4.0$ to 21.0 lb

The equation for vertical lunar displacement can be plotted as follows:





**Aerospace
Systems Division**

ASE REDESIGN EVALUATION

NO.	REV. NO.
ATM-1064	
PAGE 65	OF 212
DATE 11/24/71	

The normal force (N) was calculated in the previous section to range from 4 to 21 lb per stake. Hence, for the -1 grenade launch the minimum vertical displacement will be 3.2 in. ($\mu = 0.50$, $N=21$) and the maximum will be 6.3 in. ($\mu = 0.25$, $N=4$).

The ratio of LRC vertical displacement to lunar surface vertical displacement ranges from 1.5 to 3.0. Apply this ratio to the other three grenade launch cases determines predicted displacements as listed in the following table.

Grenade Launched	LRC Vertical Displacement	Predicted Lunar Vertical Displacement* Minimum	Maximum
-2	0.7 in.	1.1 in.	2.1 in.
-4	0.0	0.0	0.0
-3	1.2	1.8	3.6
-1	2.1	3.2	6.3

*These displacements assume that the pallet deployment on the lunar surface exactly duplicates that employed at LRC.



**Aerospace
Systems Division**

ASE REDESIGN EVALUATION

NO.	REV. NO.
ATM-1064	
PAGE 66	OF 212
DATE 11/24/71	

CONCLUSION

If the LRC pallet deployment were duplicated on the lunar surface the stability of the MBA/pallet assembly during each grenade launch would be sufficient to allow successful operation of the ASE. At no time would vertical displacements be great enough to retract the 7 in. anchors (or stakes) from the lunar soil. Hence, it would be expected that MBA/pallet assembly would return to very nearly its original position after each grenade launch.

However, if the platform hinges are given support, either mechanically or by firmly implanting the platform into the lunar soil, no motion will occur for any of the four grenade launches.



**Aerospace
Systems Division**

ASE REDESIGN EVALUATION

NO.	REV. NO.
ATM-1064	
PAGE <u>67</u>	OF <u>212</u>
DATE 11/24/71	

2. MBA/PLATFORM STABILITY - OFF-LOAD CONFIGURATIONS

High speed motion pictures taken during the LRC tests were used to measure approximate maximum displacements of the MBA and platform during the eight grenade launchings. The results are given in Table 2.

No essential differences were observed between tests #3 - #6 and tests #7 - #10. It can be concluded therefore, that the off-load configurations were neither more nor less stable, regarding the MBA/platform assembly, than the normal four grenade configuration.



**Aerospace
Systems Division**

ASE REDESIGN EVALUATION

NO.	REV. NO.
ATM-1064	
PAGE <u>68</u>	OF <u>212</u>
DATE 11/24/71	

3. (-4) GRENADE MOVEMENT ANALYSIS

Some apparent motion of the (-4) grenade relative to the grenade launch assembly was observed during the firing of the (-2) grenade. It is unlikely that the motion was the result of pressure forces acting on the (-4) grenade since the thermal bag and blowout cover had remained intact over the end of the (-3) and (-4) launch tubes, hence offering some degree of protection to the (-4) grenade. It is more likely that the apparent motion was due to the inertial properties of the grenade itself. As the grenade and mortar box moved vertically both attained the same velocity. As the mortar box reached its peak vertical displacement the grenade inertial properties permitted it to maintain its velocity since the tube frictional forces were small. It should be noted that the grenades fired in the first mortar box test were not flight configuration in that they did not have safe slides which are spring loaded against the launch tube inner wall. Furthermore, with the absence of the safe slides, the tube frictional forces are much less than those in a GLA equipped with the spring loaded devices. An analysis (see Appendix B) was conducted to determine movement considering these possible causes. The results of the study indicate that in flight configuration the grenade should move no more than 1/2 inch. In summary, this apparent motion of the (-4) should not occur within the tube when deployed properly on the lunar surface (since the vertical mortar box stability will be much improved) and with flight installed safe slides (providing greater grenade/tube frictional forces).



**Aerospace
Systems Division**

ASE REDESIGN EVALUATION

NO.	REV. NO.
ATM-1064	
PAGE <u>69</u>	OF <u>212</u>
DATE 11/24/71	

D. Comparison of Two LRC Test Results

A detailed comparison is given in Tables 3, 4, and 5. It should be noted that the worst vertical motion during the first LRC test occurred during the -4 grenade launch. The MBA moved upward 4 in. and forward 4 in. The second LRC test -4 grenade launches resulted in no motion at all. This result is a strong indication that the basic design concept for the ASE modifications was sound. In addition, no motion was observed during the first test -2 grenade launch, but such was not the case for the second test. If the exhaust gases did not generate any appreciable impulses on the MBA the first time there is no reason to expect a change. The difference in MBA motion for the -2 grenades strongly indicates that the platform hinges and the lack of contact of the pallet skin with the soil were the cause of the motions observed.

FIRST LANGLEY TEST
SUMMARY OF GRENADE FIRING VERSUS EFFECTS/DAMAGE

Grenade Launch Effect/Damage	(-2) Grenade	(-4) Grenade	(-3) Grenade	(-1) Grenade
Mortar Box Stability	Stable	Forward (4"), 3-5° Rotation (Left) Azimuth, Vertical (4")	Backward (17-23"), 13° Rotation (Right) Azimuth, 45° Pitch Rotation (Forward)	Forward (9") 45° Rotation (Left) Azimuth, Some Pitch Motion
Dust Accumulation on PSE, C/S	Light	Heavy	Medium	Medium
PSE Skirt Fold	1-G, Lifted then Returned to Position	1/6 G, 6-8" Fold Back of Edge	1/6 G, 2' Fold Back to Cannister	1-G, Lifted then Returned to Position
PSE Cannister Motion	1° Tilt	None	None	None
C/S Motion	1/8" Backward	None	None	3/4" to Left 1/4" Backward 8" Tilt Up
C/S Far Side Curtain	Torn Loose @ Bottom Folded Back, Open	None	None	Top & Bottom Torn Loose, Wrapped on Antenna
C/S Near Side Curtain	Numerous Particle Punctures	Numerous Particle Punctures	Particle Punctures, Several 1/2" Tears	Torn Loose @ Bottom & Top
C/S Rear Curtain	**	**	**	**
C/S Specular Reflector	Pulled Loose @ Bottom	None	None	Torn @ Bottom & Top Wrinkled, Twisted 90°
C/S Reflectance Change	Optical Reflectance Degraded 70%			Reflectance Degraded 66%
CPLEE Motion	**	**	**	**
Launch Tube Covers	**	**	**	**
ASE Structure	Normal	Normal	Normal	Normal
Pallet Structure	**	**	**	**
Lunar Surface Beneath Grenade	Very Shallow Crater, 1/4" Dust Removed	3" Deep, 9" Diameter Crater Under ASE	Crater Enlarged to 12" Diameter	Shallow Crater After Repacking
Motion of Other Grenades	**But all Grenades Remained in Tubes	**But all Grenades Remained in Tubes	**But all Grenades Remained in Tubes	None

**Not Evaluated

SECOND LANGLEY TEST - MBA #1
SUMMARY OF GRENADE FIRING VERSUS EFFECTS/DAMAGE

Grenade Launch Effect/Damage	(-2) Grenade	(-4) Grenade	(-3) Grenade	(-1) Grenade
Mortar Box Stability (Maximum Dynamic Displacement of Top of MBA)	Vertical (1/2") Aft (0.6")	Stable	Vertical (1") Aft (1.8")	Vertical (2.1") Fwd. (1.6")
Dust Accumulation on PSE, C/S	None	None	None	None
PSE Skirt Fold	None	None	None	None
PSE Cannister Motion	None	None	None	None
C/S Motion	None	None	None	None
C/S Far Side Curtain	None	None	None	None
C/S Near Side Curtain	None	None	None	None
C/S Rear Curtain	None	None	None	None
C/S Specular Reflector	None	None	None	None
C/S Reflectance Change	None	None	None	None
CPLEE Motion	None	None	None	None
Launch Tube Covers	(-1) Cover Shattered	(-3) Cover Cracked	**	**
ASE Structure	None - Less than Normal	None - Less than Normal	None - Less than Normal	None - Less than Normal
Pallet Structure	1/8" Skin Deformation in Center Section	Negligible Skin Deformation	Slight Additional Deformation Front Section	Skin in Center Deformed Slightly More (a)
Lunar Surface Beneath Grenade	None	None	None	None
Motion of Other Grenades	Slight Apparent Motion of #4 (b)	None (b)	None (b)	None (b)

** Not Evaluated

(a) 1/4" Pedestal Separation (b) No Safe Slides

SECOND LANGLEY TEST - MBA #2
SUMMARY OF GRENADE FIRING VERSUS EFFECTS/DAMAGE

Grenade Launch Effect/Damage	(-2) Grenade	(-1) Grenade	(-4) Grenade	(-3) Grenade
Mortar Box Stability (Maximum Dynamic Displacement of Top of MBA)	Vertical (0.7") Aft (1.0")	Vertical (1.1") Fwd. (1.7")	Stable	Upward (2") Vertical (1.2") Aft (0.7")
Dust Accumulation on PSE, C/S	None	None	None	None
PSE Skirt Fold	None	None	None	None
PSE Cannister Motion	None	None	None	None
C/S Motion	None	None	None	None
C/S Far Side Curtain	None	None	None	None
C/S Near Side Curtain	None	None	None	None
C/S Rear Curtain	None	None	None	None
C/S Specular Reflector	None	None	None	None
C/S Reflectance Change	None	None	None	None
CPLLEE Motion	None	None	None	None
Launch Tube Covers	None	Cover Shattered as Designed	None	Cover Shattered as Designed
ASE Structure	None	None	None	None
Pallet Structure	Slight Deformation to 1/4"	Slight Deformation	Slight Deformation	Slight Deformation
Lunar Surface Beneath Grenade	None	None	None	None
Motion of Other Grenades	None	NA	None	NA

*Not Evaluated



**Aerospace
Systems Division**

ASE REDESIGN EVALUATION

NO.	REV. NO.
ATM-1064	
PAGE 73	OF 212
DATE 11/24/71	

III. CONCLUSIONS:

By meeting all test objectives and achieving all redesign goals, several specific conclusions can be drawn from the Langley test program, subsequent analysis, and reduction of test data.

The test verified the deployment distance between ASE and ALSEP in terms of pressure. The results are valid in a 1/6 g environment as well as the 1 g environment in which the test was conducted. It has been shown that the adverse pressure effects on Central Station and the Passive Seismic Experiment have been eliminated.

It has been demonstrated that in a 1 g environment dust accumulation on the other ALSEP experiments is eliminated by increasing the ASE deployment distance to 25 feet. Under 1/6 g conditions it has been shown that the dust particles could reach a maximum range of 40 feet. The increased cable length to 58 feet and planned deployment of 40 ft minimum will provide an adequate margin of safety to escape adverse dust effects.

It was shown that the launch tube covers have little impact on the stability of the mortar box. The structural design of the launch tube covers was verified and shown to provide adequate protection in preventing grenade motion that could possibly result from the firing of an adjacent grenade.

The apparent movement of the (-4) grenade relative to its launch tube was investigated. The grenade motion was due to mortar box motion and not from pressure forces acting on the grenade. The motion within the tube was permitted by lower than normal grenade/launch tube friction forces caused by the absence of flight configuration spring loaded safe slides in the first GLA being fired. Mortar box motion will not occur when the pallet is deployed properly on the lunar surface. Analysis shows that the flight configuration GLA which includes safe slides should not permit excessive grenade motion in the 1/6 g lunar environment.

The Langley tests revealed that there is little difference in the stability characteristics of the Mortar Box/Pallet Assembly in either of two off-loaded grenade configurations as compared to the nominal configuration which includes a full set of four grenades.



**Aerospace
Systems Division**

ASE REDESIGN EVALUATION

NO.	REV. NO.
ATM-1064	
PAGE <u>74</u>	OF <u>212</u>
DATE 11/24/71	

The structural integrity of the Mortar Box and Pallet, as well as the interface between them, was verified by subjecting the pallet assembly to twice the number of grenade firings that will occur during a typical launch sequence. The qualification of the system under a more numerous set of firings assures survival under a normal number of launchings.

The concept of achieving a more stable launch platform has been successfully demonstrated. By providing a pressure impingement plate for the rocket exhaust gases, the stability of the mortar box has been shown to be much improved. Upon comparison of the stability characteristics before and after the addition of the pallet, it is apparent that the measured motion of the mortar box when mounted to the pallet is due primarily to the multiple degrees of freedom of the pallet sections. The interaction of the sections due to local loading results in small vertical displacements of the mortar box if the hinge lines and pallet skins are not sufficiently supported. Either mechanical support of the hinge lines or proper emplacement of the pallet in lunar soil to provide the load bearing surfaces beneath the pallet skin is required to enable vertical load transmission to the lunar soil and not be accompanied by pallet section interactions due to induced moments. With proper emplacement or a simple add-on modification the system will be stable in the lunar gravitational environment.

Few conclusions can be drawn from the analysis of data obtained by instrumenting the Mortar Box/Pallet assembly with pressure transducers, accelerometers and strain gauges. The interpretation of the data and attempts to relate it to observed phenomena have not been successful to date. Upon finding that the sensing devices were sensitive to thermal as well as shock and vibration environments, the validity of the data is questionable although continuing efforts are being made to interpret it.

Analysis shows that no soil problems will be encountered either with pallet deployment nor grenade launchings. The weakest soil conditions anticipated will still provide sufficient resistance forces to prevent lateral motion of the MBA/pallet during all grenade launches. The most difficult to penetrate soil, as defined, will not offer more resistance to the pallet anchors than an astronaut can reasonably overcome during deployment.



**Aerospace
Systems Division**

ASE REDESIGN EVALUATION

NO.	REV. NO.
ATM-1064	
PAGE <u>75</u>	OF <u>212</u>
DATE 11/24/71	

Finally, the causes of the two misfires which occurred during the LRC retest program were conclusively shown to be unrelated to the ASE modifications under test and not applicable to a flight failure.

With the successful demonstration of the design concept it is concluded that the addition of the launch pallet will provide a stable launch platform for the four grenades.



**Aerospace
Systems Division**

ASE REDESIGN EVALUATION

NO.	REV. NO.
ATM-1064	
PAGE <u>76</u>	OF <u>212</u>
DATE	11/24/71

IV. RECOMMENDATIONS

1. There should be no constraints on firing all four grenades.
 - no performance degradation or undesirable secondary effects shown on any grenade firing.
2. The normal sequence of firing (-2, -4, -3, -1) is still recommended.
 - no reason for change has been identified.
 - all earth environment and vacuum testing have used normal sequence thus providing significant test confidence.
 - retention of normal sequence means retention of backup "sequential" firing capability in the design.
3. Fire grenades as soon after astronaut departure from lunar surface within mission safety requirements, ASE temperature constraints and scientific data goals.
 - no undesirable secondary effects shown from grenade firings.
 - maximum reliability will be achieved with early firings.
4. Deployment should include the following:
 - a) Mortar box should be a minimum of 40' from ALSEP C/S or experiments.
 - b) Maximum protection from secondary effects can be achieved with a mortar box firing line at right angle to C/S at 40' deployment distance.
 - c) Pallet should be deployed on soft lunar soil to achieve full soil to pallet skin coupling with 7" stakes fully embedded.
5. The LRC retest results have not provided any information regarding additional or changes to recommendations on the Apollo 14 ASE.



**Aerospace
Systems Division**

Appendix A - ASE MBA/Pallet
Dynamic Analysis

NO. ATM-1064	REV. NO.
PAGE <u>77</u> OF <u>212</u>	
DATE 11/24/71	

APPENDIX A

ASE MBA/Pallet
Dynamic Analysis



**Aerospace
Systems Division**

Appendix A - ASE MBA/Pallet
Dynamic Analysis

NO.	REV. NO.
ATM-1064	
PAGE <u>78</u>	OF <u>212</u>
DATE	11/24/71

ASE MORTAR BOX/PALLET DYNAMIC MOTION STUDY

1.0 PURPOSE

The purpose of this study is to explain the ASE Mortar Box motions observed during the Langley Research Center (LRC) tests, and to show how soil conditions affect these motions.

2.0 DISCUSSION

The basic arrangement of the Mortar Box/Pallet is shown in Figure A-1. The sequence of motion of each of the individual -1 through -4 grenade firings as observed from the LRC test high speed motion picture films is shown in Figure A-2. A tabulation of measured values of absolute displacements of different points of the Mortar Box/Pallet taken directly from film measurements can be found in Table 2, page 28.

The MBA/Pallet displacements were most severe during the -1 grenade launch. The entire assembly was lifted from the surface of the soil to a maximum height of 2.1 in. The -2 and -3 grenade launches resulted in rotation of the assembly about the rear edge of the platform. The forward platform edge was displaced vertically 0.8 and 1.0 in. for the -2 and -3 grenades, respectively. The -4 grenade caused no significant displacements whatsoever.

The observed motions can be briefly explained by considering where the impulsive pressure forces from the grenade rocket motor exhausts are applied to the Mortar Platform. Figure A-1 shows the points at which the center line of the exhausts gas plumes strike the platform. By applying the methods of momentum¹ and taking the vertical components of these impulsive forces, the sequence of observed motion can be duplicated by assuming a pivotal action at the anchor brackets and treating the platform as a system of hinged or linked panels. The motion is quite pronounced when the platform is placed on a hard surface. By varying the soil parameters it can be demonstrated that the motion of the Mortar Box/Platform can vary between significant motion (due to a perfectly elastic impact between platform and soil) and nearly negligible motion (due to a nearly plastic impact between platform and soil). This point will be discussed in the analytical section of this Appendix. The horizontal component of the applied impulsive force is resisted by the anchor legs and friction forces between platform and soil.

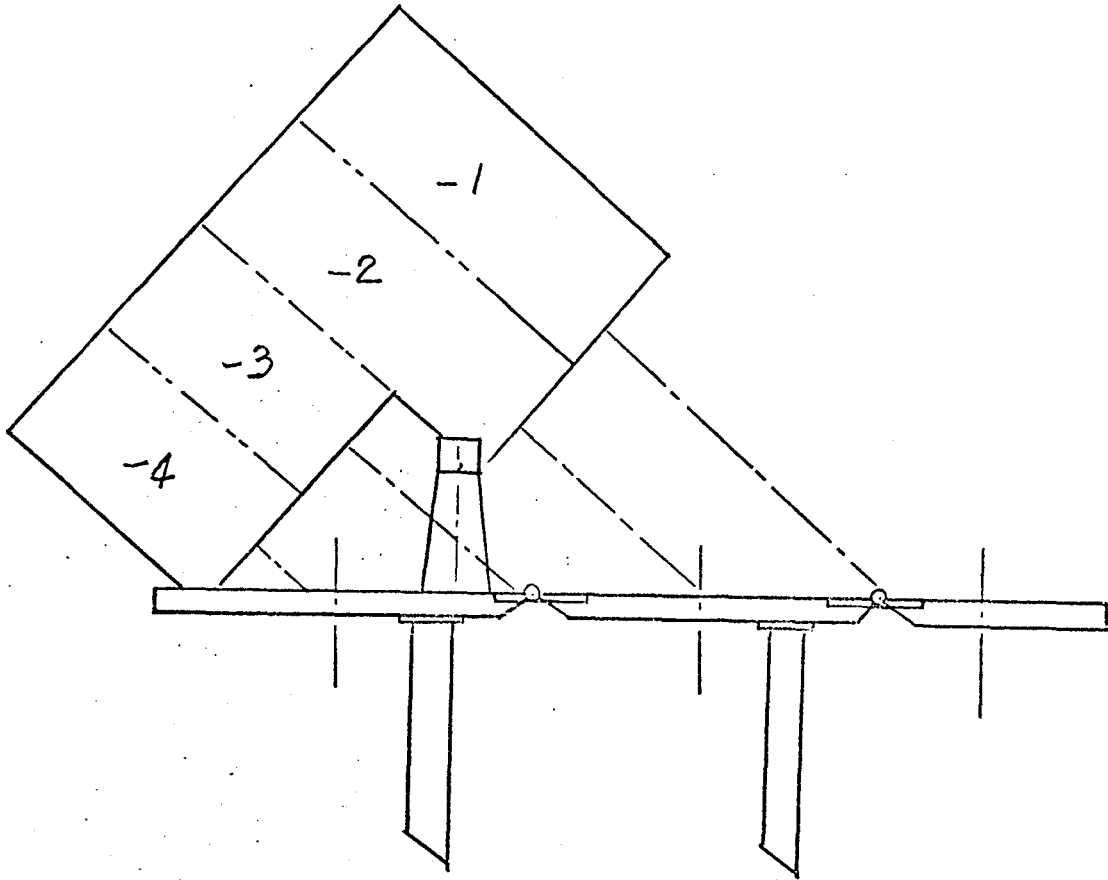
¹Engr. Mech. Statics & Dynamics, I.H. Shames.



**Aerospace
Systems Division**

Appendix A - ASE MBA/Platform
Dynamic Analysis

NO.	REV. NO.
ATM-1064	
PAGE 79	OF 212
DATE 11/24/71	



SCALE: 1/5 (APPROX.)

Figure A-1 - Mortar Box/Pallet Configuration



**Aerospace
Systems Division**

ASE REDESIGN EVALUATION

NO.	REV. NO.
ATM-1064	
PAGE 80	OF 212
DATE 11/24/71	

	Initiation of Impulse (\hat{P})	Conclusion of Impulse (\hat{P})	Maximum Vertical Displacement
-1 Grenade			2.1 IN.
-2 Grenade			0.9 IN.
-3 Grenade			1.6 IN.
-4 Grenade			NO MOTION.

Figure A-2

MBA Sequence of Motion for -1, -2, -3, and -4 Grenades



**Aerospace
Systems Division**

Appendix A - ASE MBA/Platform
Dynamic Analysis

NO.	REV. NO.
ATM-1064	
PAGE <u>81</u>	OF <u>212</u>
DATE	11/24/71

3.0 ANALYSIS

Following are the basic assumptions and derivation used to establish the translational and rotational velocities of the hinged three panel platform subjected to a vertical impulsive force applied at a hinge point. The analysis assumes that the panels have no initial resistance to rotation (corresponding physically to about $\pm 5^\circ$ of free play) and that the platform is loosely placed on the soil such that an impulsive force will induce an initial translational and rotational velocity to each of the three individual panel segments.

The motion of the MBA/Platform assembly is determined by using impulse-momentum analytical methods. The hardware model consists of three linked segments (two-dimensional). The rocket motor exhaust causes an impulse (\hat{P}) acting at the rear hinge point. Soil reaction is taken into account. A brief discussion of the momentum principle applied to impact problems is also presented, followed by calculations for the impulsive force \hat{P} based on observed deformations of the platform itself.

3.1 Hinged Panels²

Three hinged panels, "AB", "BC" and "CD" of mass M_1 , M_2 , and M_3 and length L_1 , L_2 , and L_3 are connected at "B" and "C" and lie in a straight line. A vertical impulsive force \hat{P} is applied at "C". The problem is to find the initial velocities generated.

The following notation will be used -

U_1, V_1 - Components of velocity of center of AB

U_2, V_2 - Components of velocity of center of BC

U_3, V_3 - Components of velocity of center of CD

² Derivation similar to Page 214 "Linked Rods" Principles of Mechanics, Synge and Griffith.



**Aerospace
Systems Division**

Appendix A - ASE MBA/Platform
Dynamic Analysis

NO.	REV. NO.
ATM-1064	
PAGE 82	OF 212
DATE 11/24/71	

W_1, W_2, W_3

- Angular velocity of "AB", "BC", and "CD"

\hat{X}_1, \hat{Y}_1

- Component of impulsive reaction on "BC" at "B"

\hat{X}_2, \hat{Y}_2

- Component of impulsive reaction on "CD" at "C"

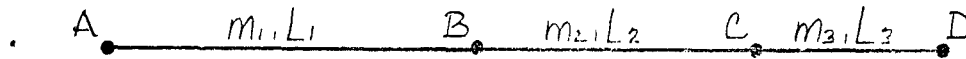


Figure A-3a

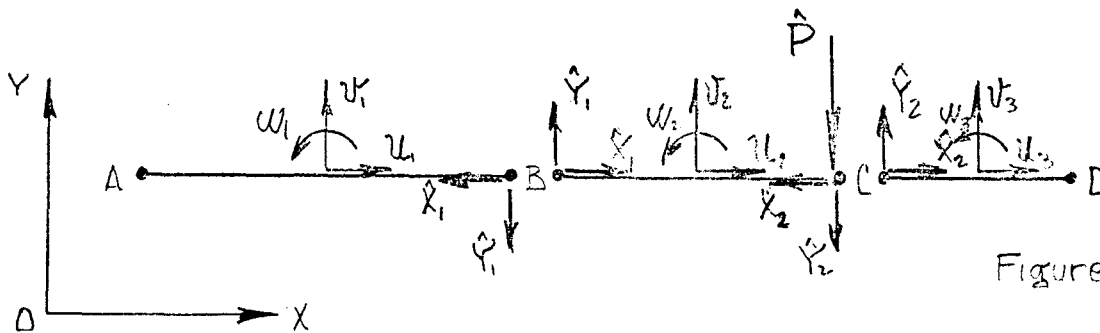


Figure A-3b

Since the panels are joined at "B" and "C", these points must have the same velocities for adjacent panels.

(1.) $U_1 = U_2$

(2.) $U_2 = U_3$

(3) $V_1 + \frac{L_1}{2} W_1 = V_2 - \frac{L_2}{2} W_2$

(4) $V_2 = \frac{L_2}{2} W_2 = V_3 - \frac{L_3}{2} W_3$



**Aerospace
Systems Division**

Appendix A - ASE MBA/Platform
Dynamic Analysis

NO.	REV. NO.
ATM-1064	
PAGE 83	OF 212
DATE	11/24/71

The principle of Linear Momentum applied to each segment -

$$(5.) \quad M_1 \dot{U}_1 = -\dot{X}_1$$

$$(6.) \quad M_1 \dot{U}_1 = -\dot{Y}_1$$

$$(7.) \quad M_2 \dot{U}_2 = \dot{X}_1 - \dot{X}_2$$

$$(8.) \quad M_2 \dot{V}_2 = \dot{Y}_1 - \dot{Y}_2 - \dot{P}$$

$$(9.) \quad M_3 \dot{U}_3 = \dot{X}_2$$

$$(10.) \quad M_3 \dot{V}_3 = \dot{Y}_2$$

The principle of Angular Momentum requires -

$$(11.) \quad M_1 k_1^2 \dot{W}_1 = -\frac{L_1}{2} \dot{Y}_1$$

$$(12.) \quad M_2 k_2^2 \dot{W}_2 = -\frac{L_2}{2} \dot{Y}_1 - \frac{L_2}{2} \dot{Y}_2 - \frac{L_2}{2} \dot{P}$$

$$(13.) \quad M_3 k_3^2 \dot{W}_3 = -\frac{L_3}{2} \dot{Y}_2$$

Where,

k_1 , k_2 , and k_3 are radius of gyration of M_1 , M_2 and M_3 about respective C.G. 's.

From (1.) and (2.)

$$(14.) \quad U_1 = U_2 = U_3 = U$$



**Aerospace
Systems Division**

From (5.), (7.), and (9.)

$$(15.) \quad M_2 U_2 = -M_1 U_1 - M_3 U_2$$

$$M_2 = -M_1 - M_3 \text{ or } U = 0$$

$$\hat{X}_1 = \hat{X}_2 = 0$$

Remaining are 8 unknowns - $V_1, V_2, V_3, W_1, W_2, W_3, \hat{Y}_1, \hat{Y}_2$ with eight equations.

From Equation (3.) -

$$(16.) \quad \hat{Y}_1 = \frac{\hat{Y}_2 (M_2^{-1} - \alpha_2) + P (M_2^{-1} - \alpha_2)}{(M_1^{-1} + M_2^{-1} + \alpha_1 + \alpha_2)}$$

From Equation (4.)

$$\hat{Y}_2 = P \left\{ \frac{-(M_2^{-1} - \alpha_2)(M_2^{-1} - \alpha_2) + (M_1^{-1} + M_2^{-1} + \alpha_1 + \alpha_2)(M_2^{-1} + \alpha_2)}{(M_2^{-1} - \alpha_2)(M_1^{-1} - \alpha_2) - (M_1^{-1} + M_2^{-1} + \alpha_1 + \alpha_2)(M_2^{-1} + M_3^{-1} + \alpha_2 + \alpha_3)} \right\}$$

where

$$\alpha_i = \frac{L_i^2}{4M_i k_i}$$

Now having values for Y_1 and Y_2 Equations (6.), (8.), (10.), (11.), (12.), and (13.) can be immediately solved for V_1, V_2, V_3, W_1, W_2 and W_3 .



**Aerospace
Systems Division**

NO.	REV. NO.
ATM-1064	
PAGE 85	OF 212
DATE 11/24/71	

3.2 Methods of Momentum/Impact

At this point a brief discussion of the momentum principle applied to impact problems and the coefficient of restitution is presented. The discussion will be completely general but of course can be carried over to the immediate problem of collision between platform and soil.³

Central Impact-

In the case of central impact one can consider the period of collision to be made up of two subintervals in time. The "period of deformation" refers to the duration of the collision, starting from the first initial contact of the bodies and ending with the time of maximum deformation. During this period, the impulse $\int D dt$ acts oppositely on each of the bodies. The second period, covering the time from maximum deformation to the condition when the bodies just separate, is called the "period of restitution." The impulse acting oppositely on each body during this period is $\int R dt$. If the bodies are perfectly elastic, they will resume their initial shapes during the period of restitution. When the bodies do not resume their initial shapes, plastic deformation has taken place. The ratio of the impulse during the restitution period $\int R dt$ to the impulse during the deformation period $\int D dt$ is a number e , which depends on the physical properties of the bodies in collision. This number is called the "coefficient of restitution" and is defined as -

$$(18) \quad e = \frac{\text{Impulse During Restitution}}{\text{Impulse During Deformation}} = \frac{\int R dt}{\int D dt}$$

It should be emphasized that the coefficient of restitution depends on size, shape, and velocities of the bodies before impact. These factors result from the fact that plastic deformation depends on the magnitude and nature of the stress distributions and also on the rate of loading.

A relationship between coefficient of restitution and initial and final velocities of bodies m_1 & m_2 undergoing impact can be formulated as follows -

³ "Shames" page 454-5



**Aerospace
Systems Division**

Appendix A - ASE MBA/Platform
Dynamic Analysis

NO.	REV. NO.
ATM-1064	
PAGE 86	OF 212
DATE 11/24/71	

Let $(V)_D$ = Velocity at max. deformation condition.

$$(19) \quad \int Ddt = (m_1 V_1)_i - (m_1 V_1)_D$$

$$(20) \quad \int Rdt = (m_1 V_1)_D - (m_1 V_1)_f$$

Dividing (20) by (19) canceling m_1 , and noting the definition (18) yields

$$(21) \quad e = \frac{(V_2)_D - (V_2)_f}{(V_2)_i - (V_2)_D} = \frac{(V_2)_t - (V_2)_D}{(V_2)_D - (V_2)_i}$$

A similar analysis for mass m_2 gives -

$$(22) \quad e = \frac{(V_2)_D - (V_2)_f}{(V_2)_i - (V_2)_D} = \frac{(V_2)_f - (V_2)_D}{(V_2)_D - (V_2)_i}$$

Since the quotients of Eqn. (21) & (22) are equal to each other, we can add numerators and denominators to form another equal quotient. Noting that $(V_1)_D = (V_2)_D$ one gets -

$$(23) \quad e = \frac{(V_2)_f - (V_1)_f}{(V_2)_i - (V_1)_i} = \frac{\text{Velocity of Separation}}{\text{Velocity of Approach}}$$

For a perfectly elastic impact $e = 1$, and $V_1 = V_1$
For a perfectly plastic impact $e = 0$, and $(V_2)_f = (V_1)_f$
and the bodies remain in contact.

Further analysis shows that there is a loss of kinetic energy in an inelastic collision despite the fact that the momentum of the system is conserved.



**Aerospace
Systems Division**

Appendix A - ASE MBA/Platform
Dynamic Analysis

NO.	REV. NO.
ATM-1064	
PAGE 87	OF 212
DATE 11/24/71	

The following schematic illustrates the concept of elastic, inelastic, and plastic collision between two bodies.

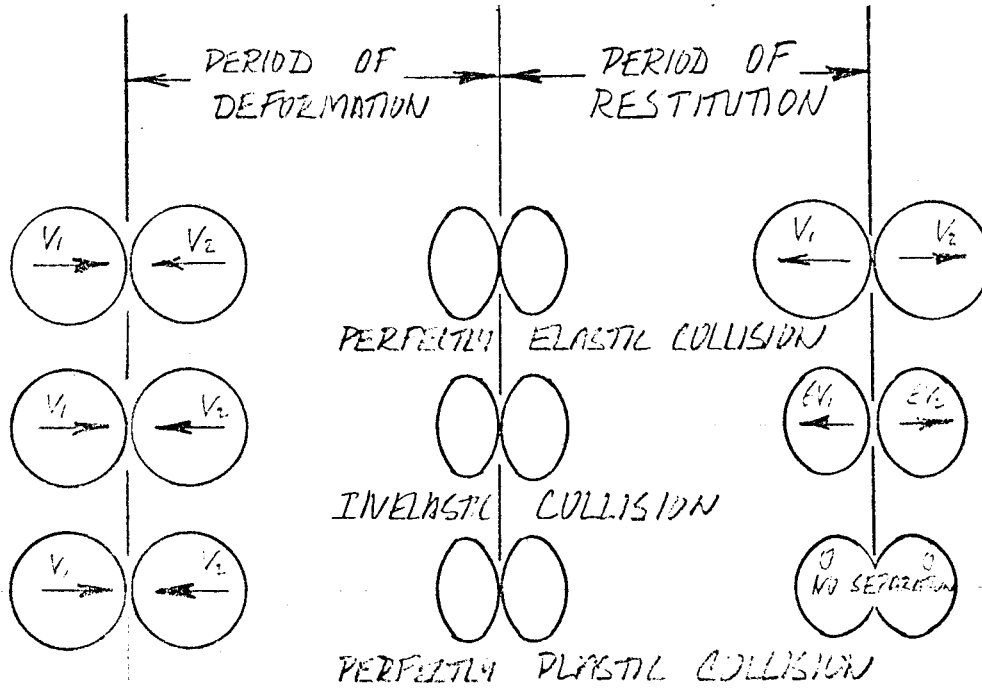


Figure A-4



**Aerospace
Systems Division**

Appendix A - ASE MBA/Platform
Dynamic Analysis

NO.	REV. NO.
ATM-1064	
PAGE 88	OF 212
DATE 11/24/71	

3.3 Determination of Impulsive Load

When the ASE mortar box/platform was received and inspected, it was noted that the skin in the center panel was deformed with a permanent deflection of about 0.25 in. at midspan. This deflection is assumed to be caused by the -2 grenade firing whose thrust vector is in direct line with the point of maximum deflection.

Simple plate theory ⁴ for large deflections ($\delta > 10t$) can be used to calculate the required normal force to produce the observed deflection.

$$\delta_{MAX.} = n_1 a \left(\frac{qa}{Et} \right)^{1/3}$$

or
$$\underline{q} = \frac{\delta_{MAX.}}{n_1^3 a^4} Et$$

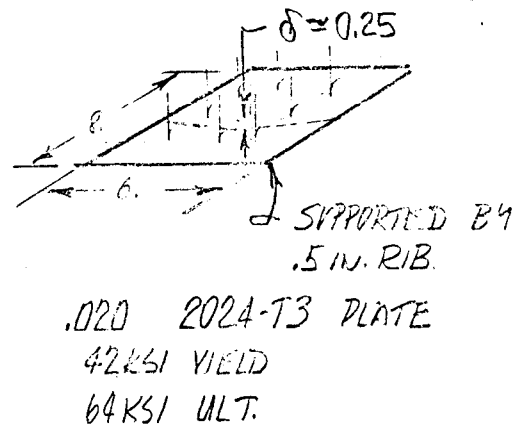


Figure A-5

For $\delta_{MAX.} = .25$, $E = 10^7$, $n_1 = .25$, $a = 8$, & $t = .020$

$$\underline{q} = 48.8 \text{ psi}$$

To calculate the total normal force required

For $\underline{q} = 48.8$ & $A = 48$

$$F = 2330 \text{ lb.}$$

⁴ Flight Vehicle Structures, Bruhn PA. 17.6 bending of plates

4.0 RESULTS

4.1 -1 Grenade

Using the equations derived in the previous section along with the typical values for the -1 Grenade firing, calculations can be performed to determine the dynamic motion of the mortar box/platform due to 2 3.0 lb-sec impulse applied at the rear hinge.

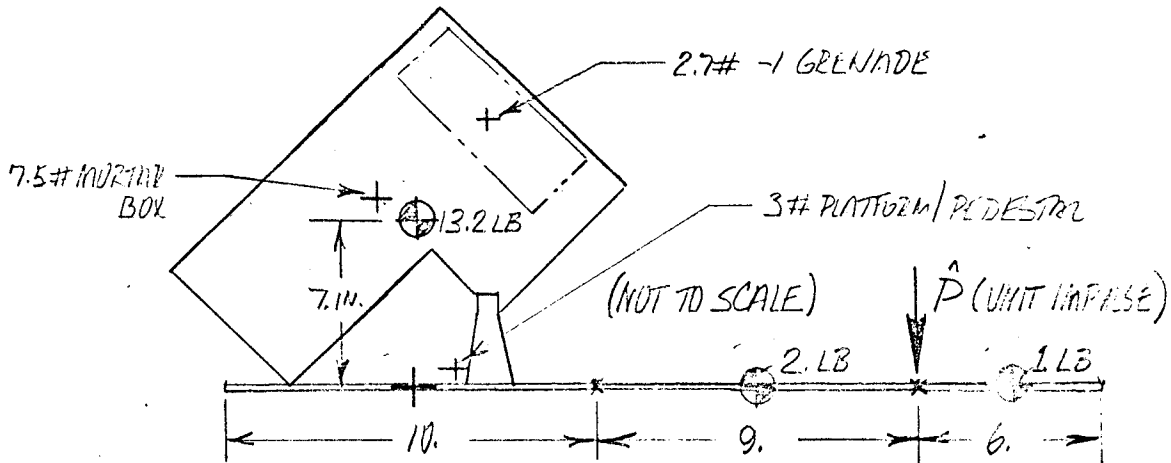


Figure A-6

-1 GRENADE FIRING

Typical Values

No	m (lb)	L (in)	k (in)	k^2 (in ²)	$\frac{m^{-1}}{ft}$ lb sec ²	$\frac{\alpha}{ft}$ lb sec ²
1.	13.2	10.0	7.0	49.0	2.42	1.25
2.	2.0	9.0	2.65	7.0	16.0	48.0
3.	1.0	6.0	1.73	3.0	32.0	96.0



**Aerospace
Systems Division**

Appendix A - ASE MBA/Platform
Dynamic Analysis

NO.	REV. NO.
ATM-1064	
PAGE 90	OF 212
DATE 11/24/71	

From EQN. (17)

$$\hat{Y}_2 = -0.275 \hat{P}$$

From EQN. (16)

$$\hat{Y}_1 = -0.343 \hat{P}$$

4.1.1 Linked Panels

From EQN. (6)

$$V_1 = 10.0 \hat{P} \text{ in/sec.}$$

From EQN. (8)

$$V_2 = -205. \hat{P} \text{ in/sec.}$$

From EQN. (10)

$$V_3 = -105.5 \hat{P} \text{ in/sec.}$$

From EQN. (11)

$$W_1 = +1.02 \hat{P} \text{ Rad/Sec.}$$

From EQN. (12)

$$W_2 = -52.3 \hat{P} \text{ Rad/Sec.}$$

From EQN. (13)

$$W_3 = +105.5 \hat{P} \text{ Rad/Sec.}$$



**Aerospace
Systems Division**

4.1.2 Pivotal Motion

Taking into account the pivotal action about the anchor bracket -

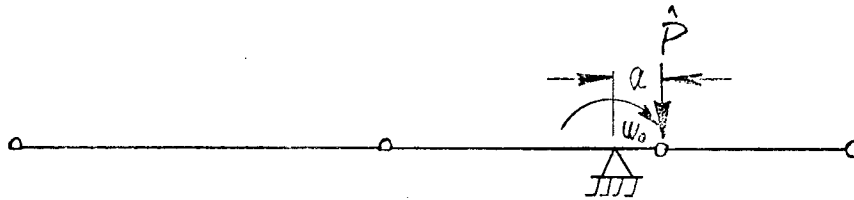


Figure A-7

$$mk^2 \hat{W}_0 = a \hat{P}$$

$$\hat{W}_0 = \frac{a \hat{P}}{mk^2}$$

For $a = 2.0$ in, $m = 16$. lb, & $k = 12$ in.

$$\hat{W}_0 = 0.33 \hat{P} \text{ Rad/Sec.} \quad \left(\text{This term is negligible compared to previous terms.} \right)$$

4.1.3 Superimposed Solutions

By super-imposing the angular & translational velocities of Section 1 and the angular velocity at the anchor bracket in Section 2, the Velocity Profile for the unit impulsive load case can be drawn -

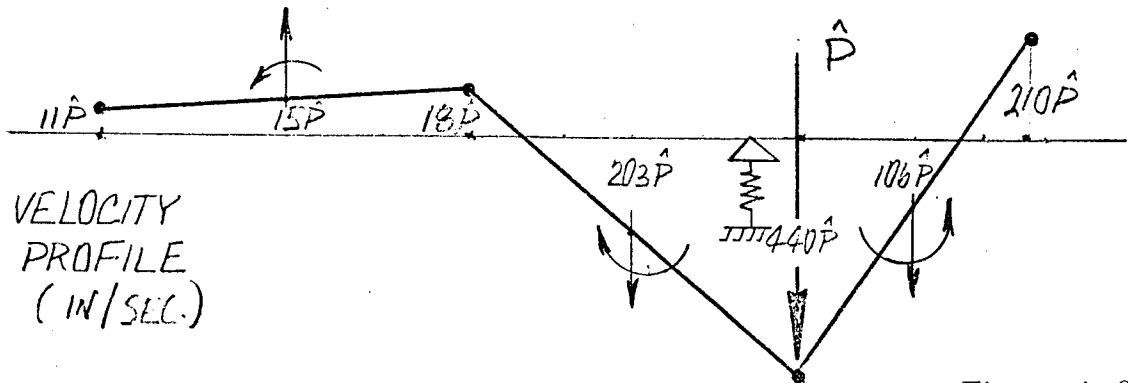


Figure A-8



**Aerospace
Systems Division**

NO.	REV. NO.
ATM-1064	
PAGE 92	OF 208
DATE 11/24/71	

4.1.4 Coefficient of Restitution

The momentum principle and coefficient of restitution will now be carried over to the platform/soil problem. As an impulse is applied at the second hinge, the pallet attempts to deflect into the soil at the point of load application while the front panel deflects upwards. The second hinge will impact the soil and attempt to rebound, the extent of which is dependent upon the coefficient of restitution between the soil and platform. Assuming that the soil impact occurs almost instantaneously, the previous velocity profile can be superimposed on a "rebound" velocity profile dependent only on the parameter ϵ .

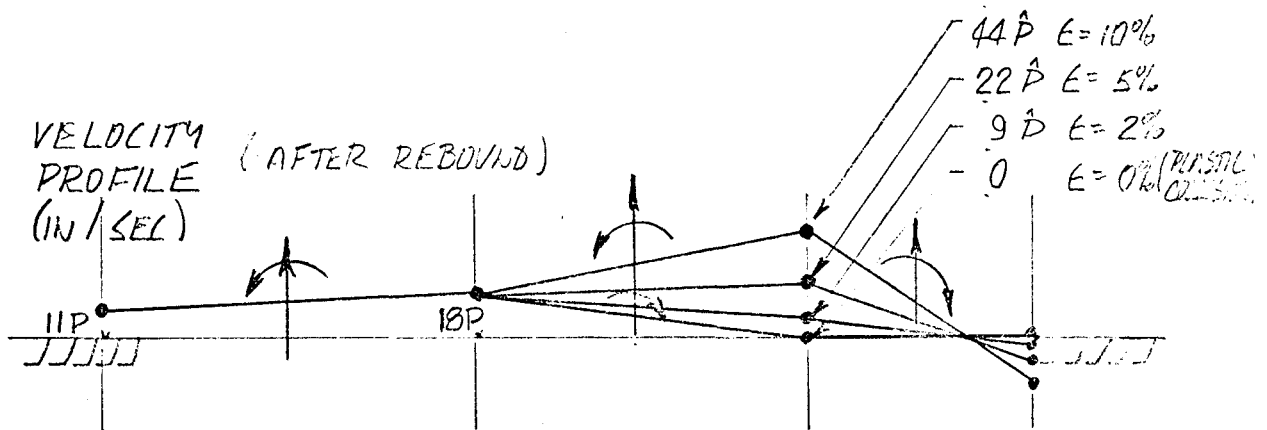


Figure A-9

It has been shown that a 2330 lb force could be generated from the -2 grenade firing. Assuming a 5 millisecc sawtooth pressure pulse, this corresponds to an impulse of

$$I = \int Fdt = \approx 6.0 \text{ lb. sec.}$$

Assuming part of this impulse is lost in deforming the pallet and taking about 50% of the calculated value, \hat{P} can be determined:

$$\hat{P} = 50\% I = 3.0 \text{ lb. sec.}$$

Applying this impulsive loading to the previous equations and assuming $\epsilon \approx 2\%$ gives the following velocity profile.

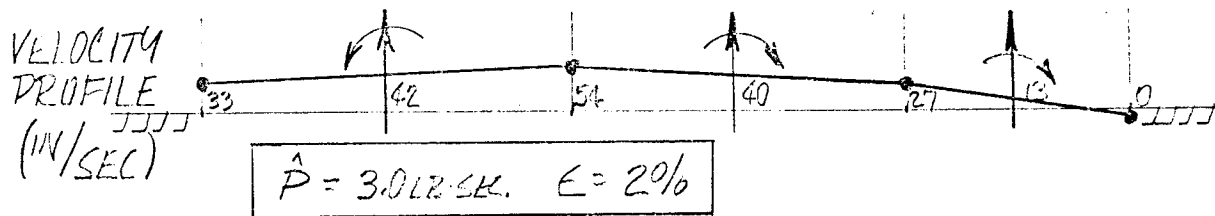


Figure A-10

Neglecting interaction of anchors and soil deformation, the upward travel of the mortar box/platform due to the initial velocities will be -

For M_1 :

$$d_1 = \frac{V_1^2}{28} = \frac{(42 \text{ in/sec})^2}{(2) (384 \text{ in/sec}^2)}$$

$$d_1 = 2.30 \text{ in.}$$

Similarly:

$$d_2 = 2.08$$

$$d_3 = 0.22$$

Hence for $\hat{P} = 3.0 \text{ lb-sec}$ and $\epsilon = 2\%$ the approximate deflection shape using earth gravity would be:

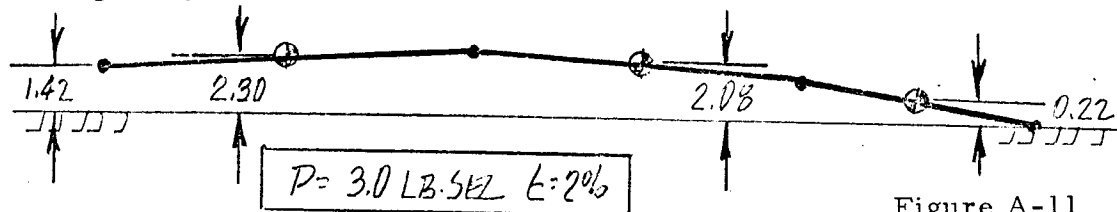


Figure A-11

$\epsilon = 2\%$ is in good agreement with LRC test results in which vertical deflections for the -1 grenade firing were observed.



**Aerospace
Systems Division**

Appendix A - ASE MBA/Platform
Dynamic Analysis

NO.	REV. NO.
ATM-1064	
PAGE 94	OF 212
DATE 11/24/71	

4.2 -3 Grenade

Similar to the previous -1 Grenade firing, calculations can be performed, using the appropriate equations, to determine the dynamic motion of the mortar box/platform due to 2 3.0 lb-sec impulse applied at the forward hinge from the -3 Grenade firing.

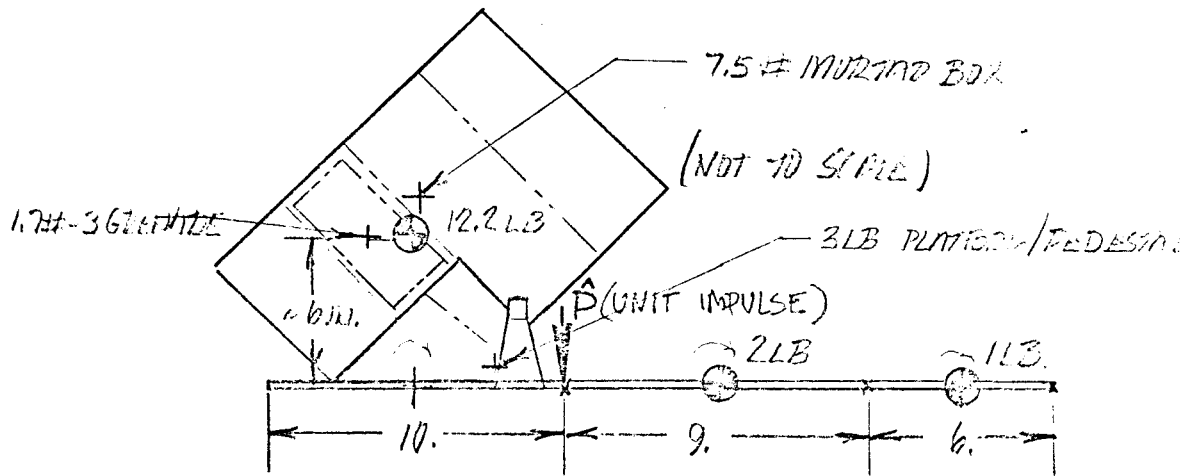


Figure A-12

-3 GRENADE FIRING

Typical Values

No.	m (lb)	L (in)	k (in)	k^2 (in ²)	$\frac{m}{ft^{-1}}$ lb. sec ²	$\frac{\alpha}{ft}$ lb. sec ²
1	1.0	6.0	1.73	3.0	32.0	96.0
2	2.0	9.0	2.65	7.0	16.0	48.0
3	12.0	10.0	6.0	36.0	2.62	1.48



**Aerospace
Systems Division**

Appendix A - ASE MBA/Platform
Dynamic Analysis

NO.	REV. NO.
ATM-1064	
PAGE 95	OF 212
DATE 11/24/71	

4.2.1 Linked Panels

The velocity profile for a unit impulsive load applied at the first hinge would thus be.

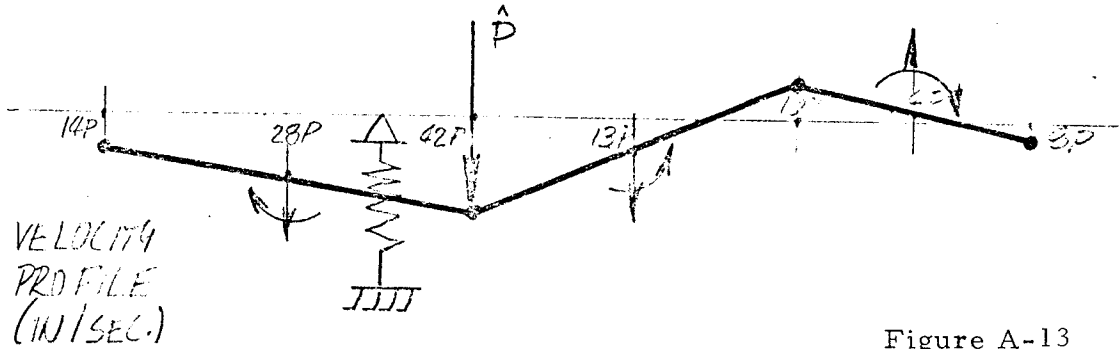


Figure A-13

4.2.2 Pivotal Motion

Taking into account the pivotal action about the anchor leg

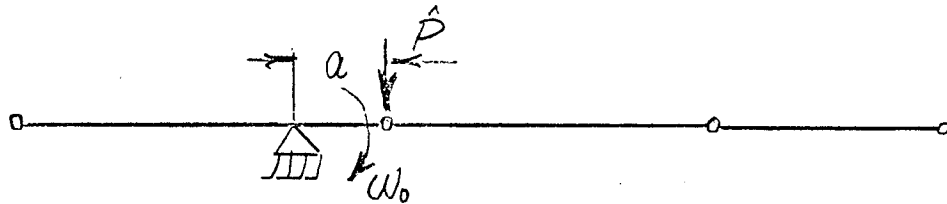


Figure A-14

$$\begin{aligned}
 mk^2 \omega_0 &= aP \\
 \omega_0 &= \frac{aP}{mk^2} \\
 \omega_0 &= 1.05 P \text{ Rad/Sec}
 \end{aligned}$$



**Aerospace
Systems Division**

Appendix A - ASE MBA/Platform
Dynamic Analysis

NO.	REV. NO.
ATM-1064	
PAGE 96	OF 212
DATE 11/24/71	

4. 2. 3 Superimposed Solutions

Superimposing the case of pivotal action about the anchor leg on the "rebound" case, a "rebound" velocity profile dependent only on the parameter ϵ is generated. Hence for a unit impulse applied at the first hinge.

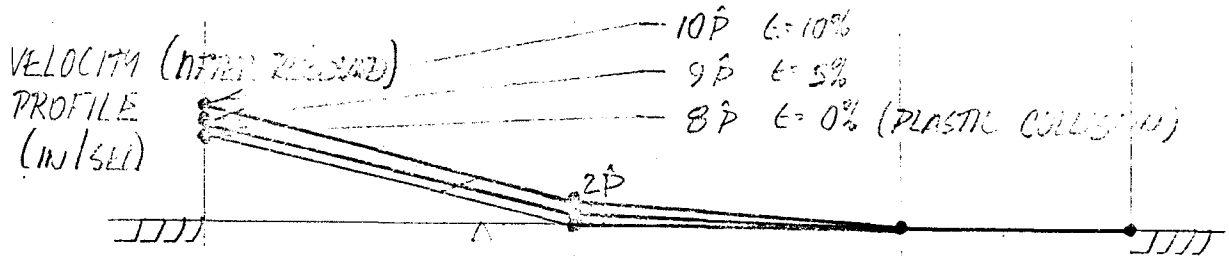


Figure A-15

The motion for this case is similar whether $\epsilon = 10\%$ or $\epsilon = 0\%$ (plastic collision). The front of the pallet will attempt to lift up and essentially be restrained by the torsional stiffness at the first hinge. The maximum deflection profile assuming $\hat{P} = 3.0$ lb-sec (such that the velocity at front panel is ≈ 25 in/sec) is thus -

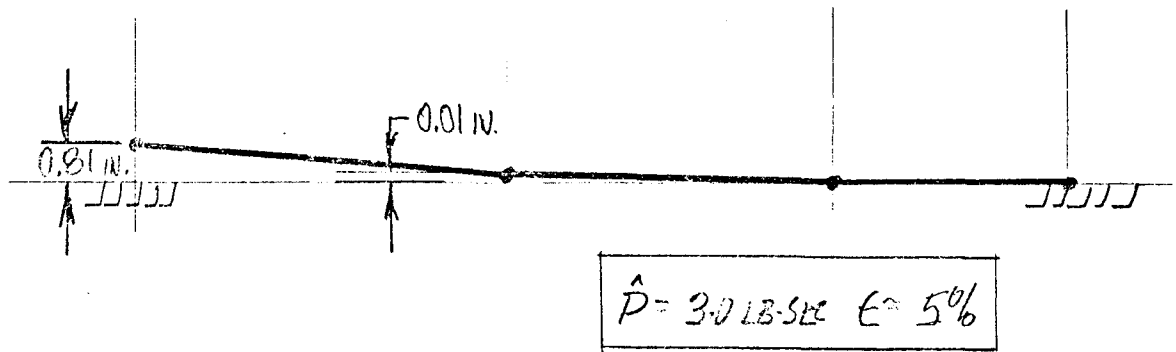


Figure A-16

This motion corresponds to that which was observed during the LRC Test firing of -3 Grenade.



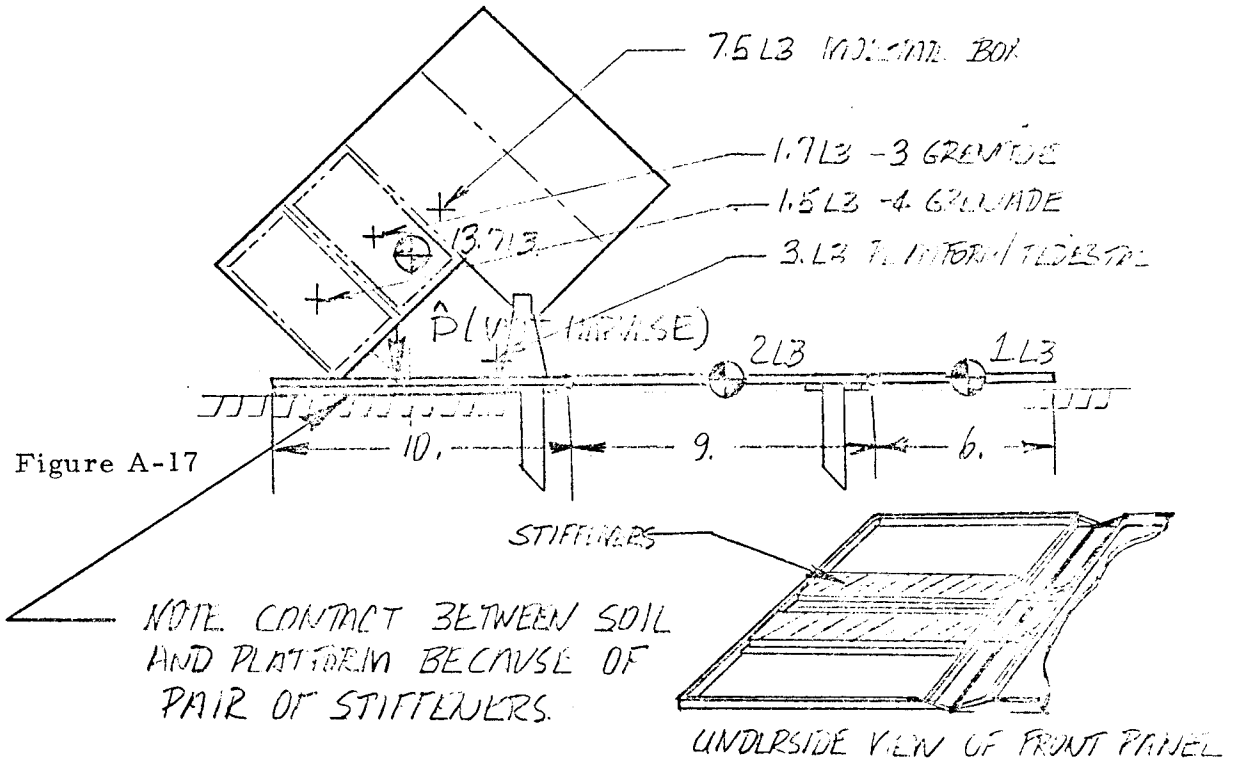
**Aerospace
Systems Division**

Appendix A - ASE MBA/Platform
Dynamic Analysis

NO.	REV. NO.
ATM-1064	
PAGE 97	OF 212
DATE 11/24/71	

4.3 -4 Grenade

The following schematic and explanation is presented to describe the dynamic motion of the mortar box/platform due to the -4 Grenade firing.



For the case of the -4 grenade firing, the dynamic motion study is treated slightly different from the previous -1 and -3 grenades. This is due to the fact that directly below the -4 grenade pressure pulse area are two hat section stiffeners which come in direct contact with the soil surface. Hence, the assumption of a "loose mount" as in the previous analysis is no longer valid. A vertical force or impulse applied at this point on the pallet is directly transmitted to the soil. The amount of the pallet rebound in this case is solely dependent on the coefficient of restitution, and there is no tendency to set up a pivotal action at the hinges.



**Aerospace
Systems Division**

Appendix A - ASE MBA/Platform
Dynamic Analysis

NO.	REV. NO.
ATM-1064	
PAGE 98	OF 212
DATE 11/24/71	

5.0 CONCLUSIONS

By applying the momentum principle to the impulse problem, it has been demonstrated that the motions observed during the LRC grenade firing tests can be analytically simulated. By applying an impulsive load of about 3.0 lb sec. at the second hinge due to the -1 grenade firing, a uniform vertical rise of the platform of about 2 in. can be calculated. Similarly, by applying the same impulse at the first hinge due to the -3 grenade firing, an upward motion of the front panel of about 1 in. results. The impulsive load of 3 lb-sec is based on forces required to deform the center panel during the -2 grenade firing.

The analysis further shows that by varying the coefficient of restitution between the platform and soil that different displacement profiles can be generated. Depending on the soil properties the motion can range from a perfectly "elastic" impact causing large motions to a perfectly "plastic" collision causing nearly negligible motion with only slight rotation about the hinge points.



**Aerospace
Systems Division**

Appendix B
(-4) Grenade Movement Dynamic Analysis

NO. ATM-1064	REV. NO.
PAGE <u>99</u>	OF <u>212</u>
DATE 11/24/71	

APPENDIX B

(-4) GRENADE MOVEMENT DYNAMIC ANALYSIS



**Aerospace
Systems Division**

Appendix B
(-4) Grenade Movement Dynamic Analysis

NO.	REV. NO.
ATM-1064	
PAGE 100	OF 212
DATE 11/24/71	

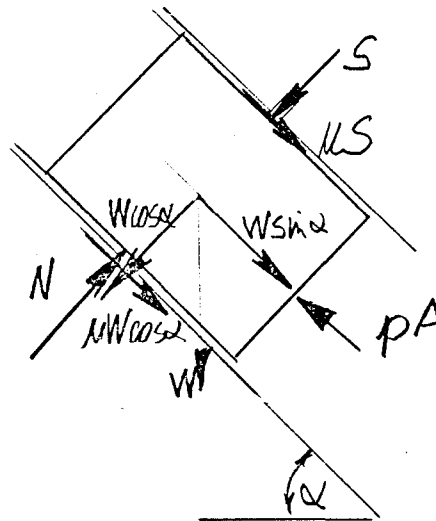
1.0 INTRODUCTION

During the LRC test the -4 grenade was detected to have moved approximately 0.25 inches in its launch tube as a result of the -2 grenade firing. During these tests the safe-arm slide mechanism was not used and of course the test was performed under earth gravity conditions.

2.0 ANALYSIS

The problem will be analyzed from two points of view. The first (Method-A) assumes the motion of the -4 grenade was caused by gas pressure acting impulsively on the rear of the same grenade. The source of the pressure was the exhaust gases from the -2 grenade launch.

The second (Method-B) assumes that the -4 grenade was protected from exhaust gases by the thermal bag and blowout cover and that the motion was caused by inertia effects. That is, initially the MBA (including -4 grenade) and platform were set in motion. The motion was restrained by reaction forces of the soil acting on the platform. Since only friction forces were available to retard the motion of the -4 grenade it continued in motion due to its inertia.



$$W-4 = 1.54 \text{ lb}$$
$$\alpha = 45^\circ$$

Figure B-1. Free Body Diagram of (-4) Grenade

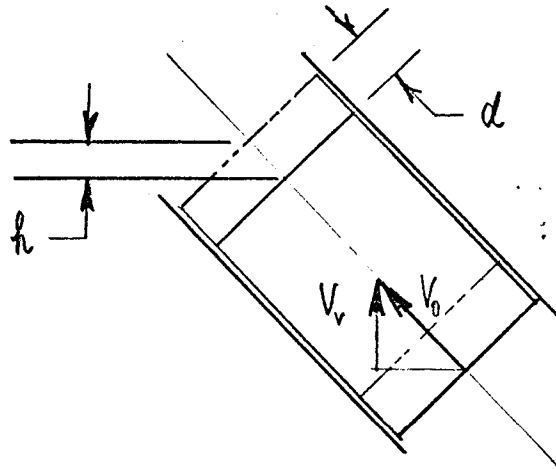


Figure B-2. Motion Diagram

2.1 Method-A

Basic Energy Equation -

$$\Delta K.E. = \Delta P.E. + \text{WORK (frictional forces)}$$

$$(1) \quad \frac{1}{2}mV_o^2 = mgh + \mu (W \cos \alpha + S) d + W \sin \alpha d$$

O*when safe-arm mechanism not used.

Solving for Vo -

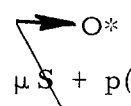
$$(2) \quad V_o = \left\{ \left[\mu (W \cos \alpha + S) + W \sin \alpha \right] \frac{2d}{M} \right\}^{1/2}$$

O*

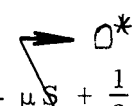
From mementum/impulse considerations -

$$I = \int_0^t F dt = mV_o$$

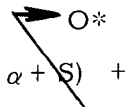
or

$$\frac{W}{g} V_o = \int_0^t (-\mu W \cos \alpha - W \sin \alpha - \mu S + p(t) A) dt$$


and assuming a simple sawtooth pressure pulse -

$$(4) \quad \frac{W}{g} V_o = (-\mu W \cos \alpha - W \sin \alpha - \mu S + \frac{1}{2} P_{max} A) \Delta t$$


and solving for Pmax

$$(5) \quad P_{max} = \frac{2}{A} \left[\frac{V_o}{\Delta t} \frac{W}{g} + \mu (W \cos \alpha + S) + W \sin \alpha \right]$$


Equation (5) corresponds to the pressure required during the Langley Tests to deflect the grenade a distance "d" (EQN 2). Taking into account the safe-arm slide mechanism as in the momentum EQN (4) we can now solve for the new volicty V_{o_s} -

$$(6) \quad V_{o_s} = \frac{\Delta t}{M} \left[-\mu (W \cos \alpha + S) - W \sin \alpha + 1/2 P_{max} A \right]$$

Again using the energy EQN (1), but this time solving for the displacement "d" due to the velocity V_{o_s} and taking into account the work energy lost due to overcomming the frictional forces of the safe-arm slide mechanism -

$$(7) \quad d_s = \frac{1/2 m V_{o_s}^2}{\mu (W \cos \alpha + S) + W \sin \alpha}$$



**Aerospace
Systems Division**

Appendix B
(-4) Grenade Movement Dynamic Analysis

NO. ATM-1064	REV. NO.
PAGE 103 OF 212	
DATE 11/24/71	

EQNS, (2) (5) (6) and (7) can be combined to give the single equation

$$(8) d_L = \frac{1}{2m} \left[\left\{ (\mu \cos \alpha + \sin \alpha) 2d_E g_E \right\}^{1/2} + \frac{\Delta t}{m} \left\{ (\mu \cos \alpha + \sin \alpha) (W_E - W_L) - \mu S \right\} \right]^2$$

$$W_L (\mu \cos \alpha + \sin \alpha) + \mu S$$

Where subscript "E" refers to earth, and subscript "L" to lunar.

2.2 Method-B

Assuming the motion of the -4 grenade to be caused by an induced inertial force due to the relative motion of the MBA, the following basic equation can be derived from basic energy considerations. It can be noted that it is similar in form to EQN. (8) with the omission of the Δt "pressure" term.

$$(9) d_L = \frac{W_E (\mu \cos \alpha + \sin \alpha) d_E}{W_L (\mu \cos \alpha + \sin \alpha) + \mu S}$$

Again where subscript "E" refers to earth, and subscript "L" to lunar.

3.0 RESULTS

Both equations (8) and (9) which relate LRC observed motions to expected lunar motions can be plotted as functions of the friction between the safe-arm slide mechanism and the MBA. The following values were used for computational purposes:

Earth Weight of -4 Grenade	1.54 lb
Lunar Weight of -4 Grenade	0.26 lb
Angle of inclination	45°
Safe-Arm Slide Spring Force	5.0 lb
Grenade Pressure Pulse Duration	6.7 milli-sec
Coefficient of Friction	0.0 - 1.0

Actual coefficient of friction measurements of a grenade sliding in a MBA launch tube varied between 0.1 and 0.3. Therefore using 0.1 should be conservative.

3.1 Method-A

The following plot of EQN (8) is obtained as a function of earth displacement "d_E" and coefficient of friction μ .

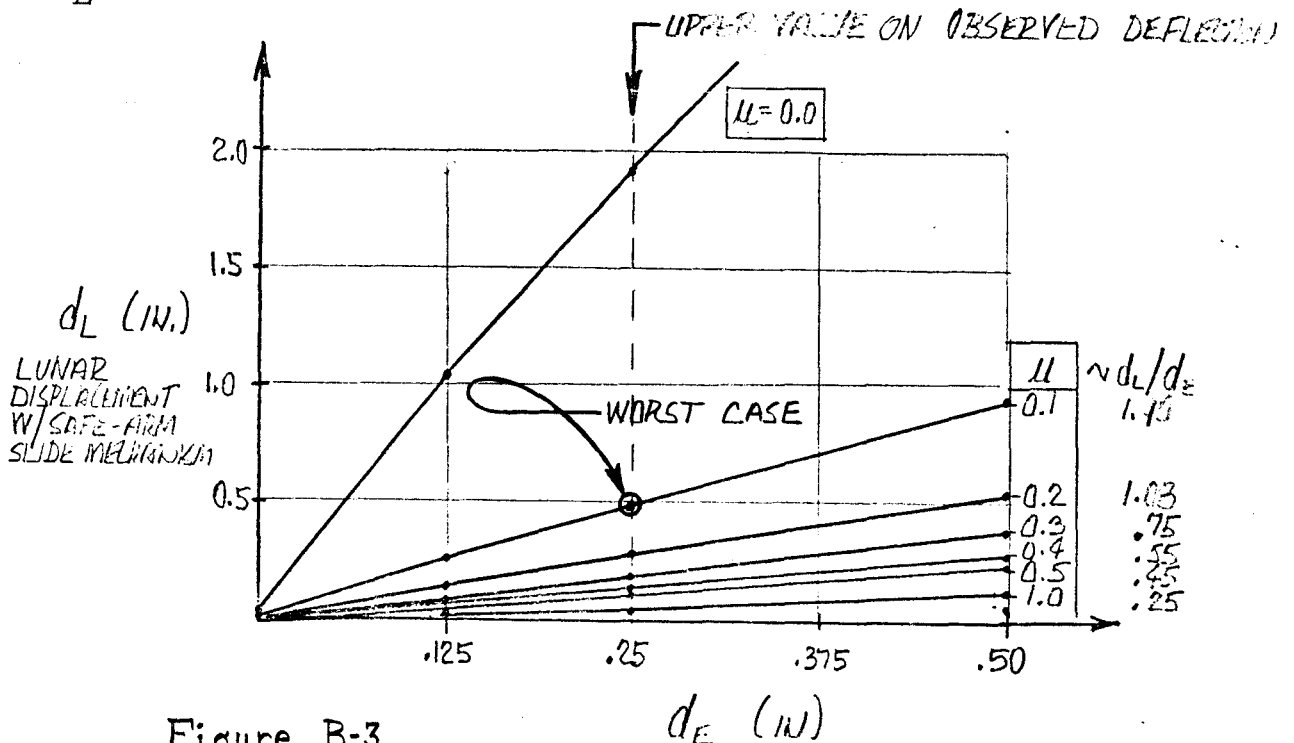


Figure B-3

d_E (IN)
 EARTH DISPLACEMENT
 W/O SAFE-ARM SLIDE MECH.



**Aerospace
Systems Division**

Appendix B
(-4) Grenade Movement Dynamic Analysis

NO.	REV. NO.
ATM-1064	
PAGE 105	OF 212
DATE 11/24/71	

3.2 Method-B

The following plot of d_L/d_E vs. μ is obtained using EQN. (9). It can be noted (by comparing the following plot with the previous plot) that in general the lunar displacements are less with the "inertial" assumption vs. the previous "pressure" assumption

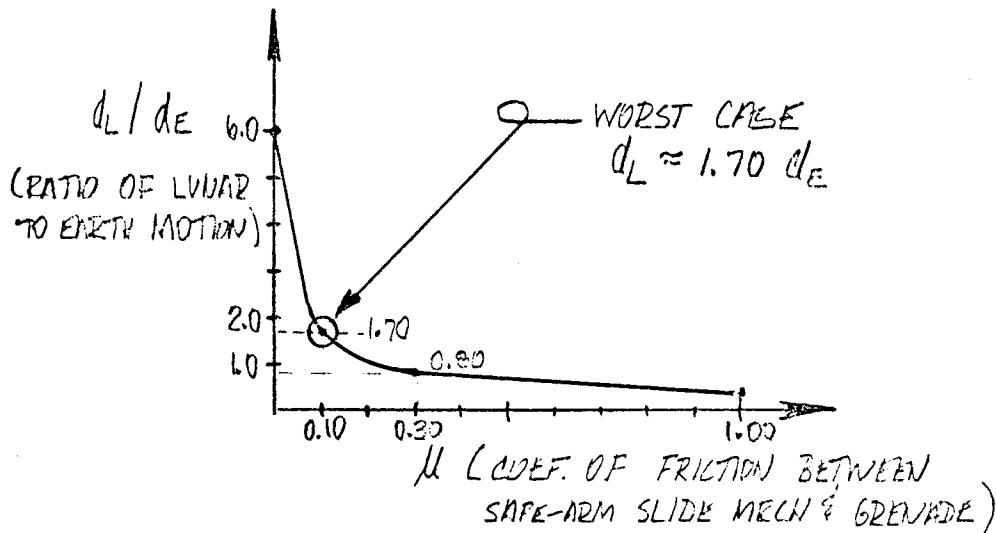


Figure B-4



**Aerospace
Systems Division**

Appendix B
(-4) Grenade Movement Dynamic Analysis

NO.	REV. NO.
ATM-1064	
PAGE 106	OF 212
DATE 11/24/71	

4.0 CONCLUSIONS

During the launch of the -2 grenade at LRC, it was observed that the -4 grenade moved forward relative to the MBA approximately 0.25 in. The problem of determining the amplification, if any, of such motion on the lunar surface was approached in two ways. The first assumed the relative motion to have been caused by exhaust gas pressure acting impulsively on the -4 grenade. The second assumed the motion to have been caused by inertia effects.

The results of the analyses showed that the worst case conditions yielded an amplification factor of 2. Hence the motion of the -4 grenade on the lunar surface would range between negligible and 0.50 in. depending upon the actual coefficient of friction in the launch tube, etc.

It is concluded that the motion of the -4 grenade due to launching the -2 grenade will not detract from the successful operation of the ASE on the lunar surface.



**Aerospace
Systems Division**

ASE REDESIGN EVALUATION

NO.	REV. NO.
ATM-1064	
PAGE <u>107</u>	OF <u>212</u>
DATE	11/24/71

APPENDIX C - STRUCTURAL ANALYSES

(MORTAR BOX/PALLET STRUCTURAL ATTACHMENT ANALYSIS)



**Aerospace
Systems Division**

Appendix C - Structural Analyses
(Mortar Box/Pallet Structural
Attachment Analysis)

NO.	ATM 1064	REV. NO.	
PAGE	108	OF	212
DATE	11/24/71		

Mortar Box/Pallet Structural Attachment Analysis

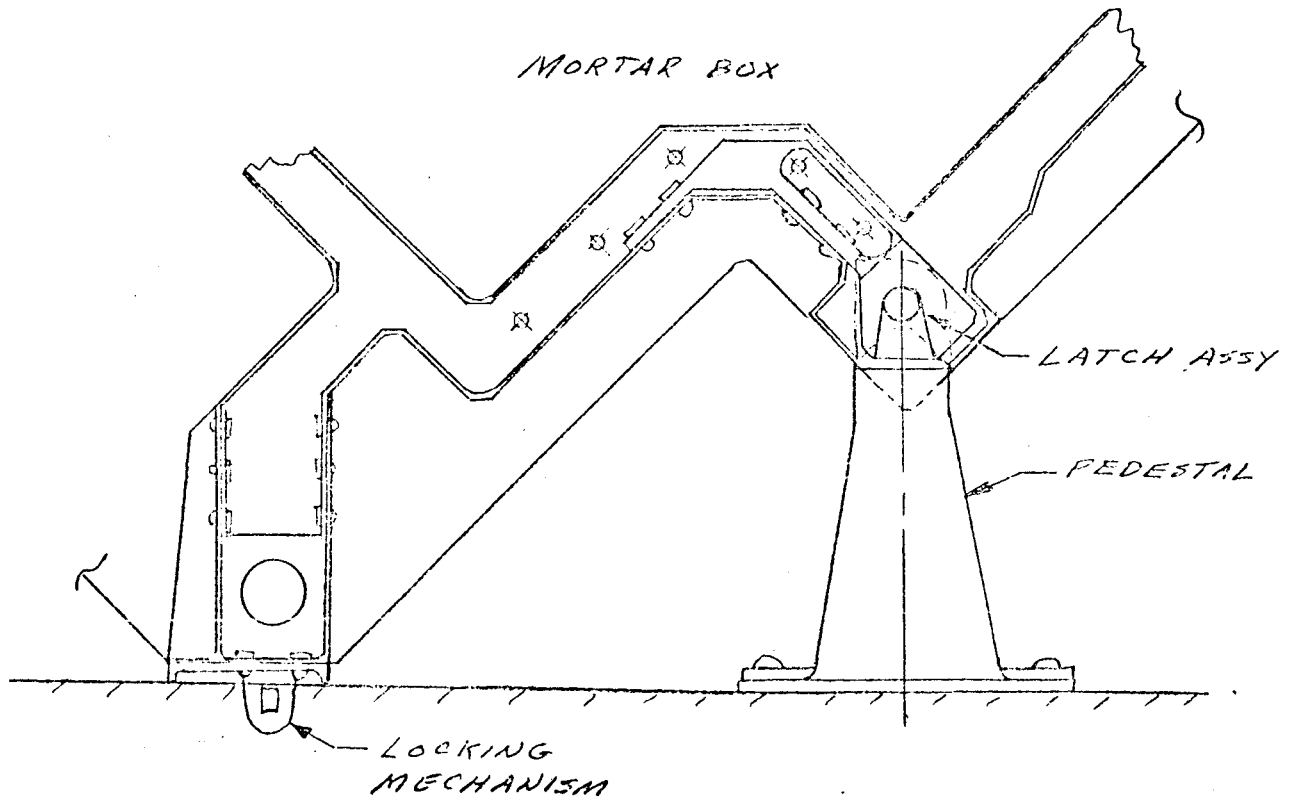


FIGURE C-1

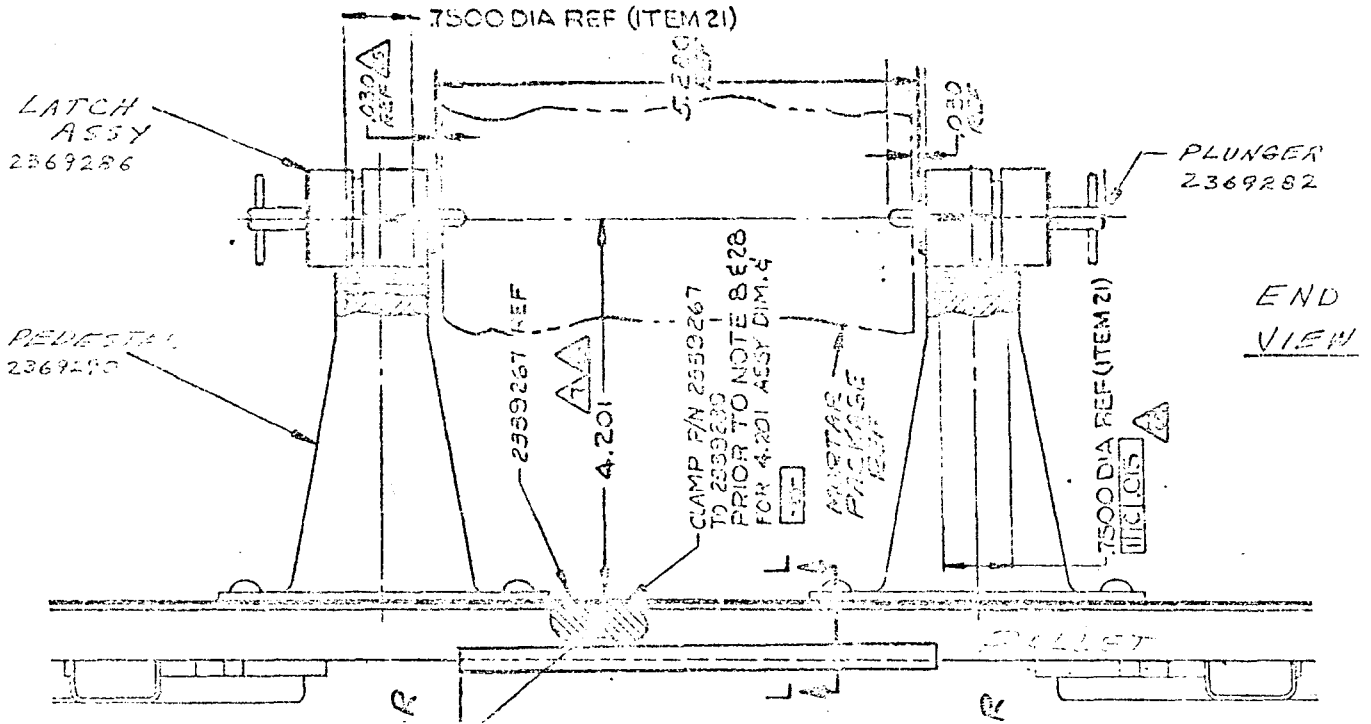
1. The report includes the analyses of the following fittings:
 1. Latch Assy., Rear Mortar Box
 2. Locking Mech., Fwd Mortar Box
 3. Pedestal



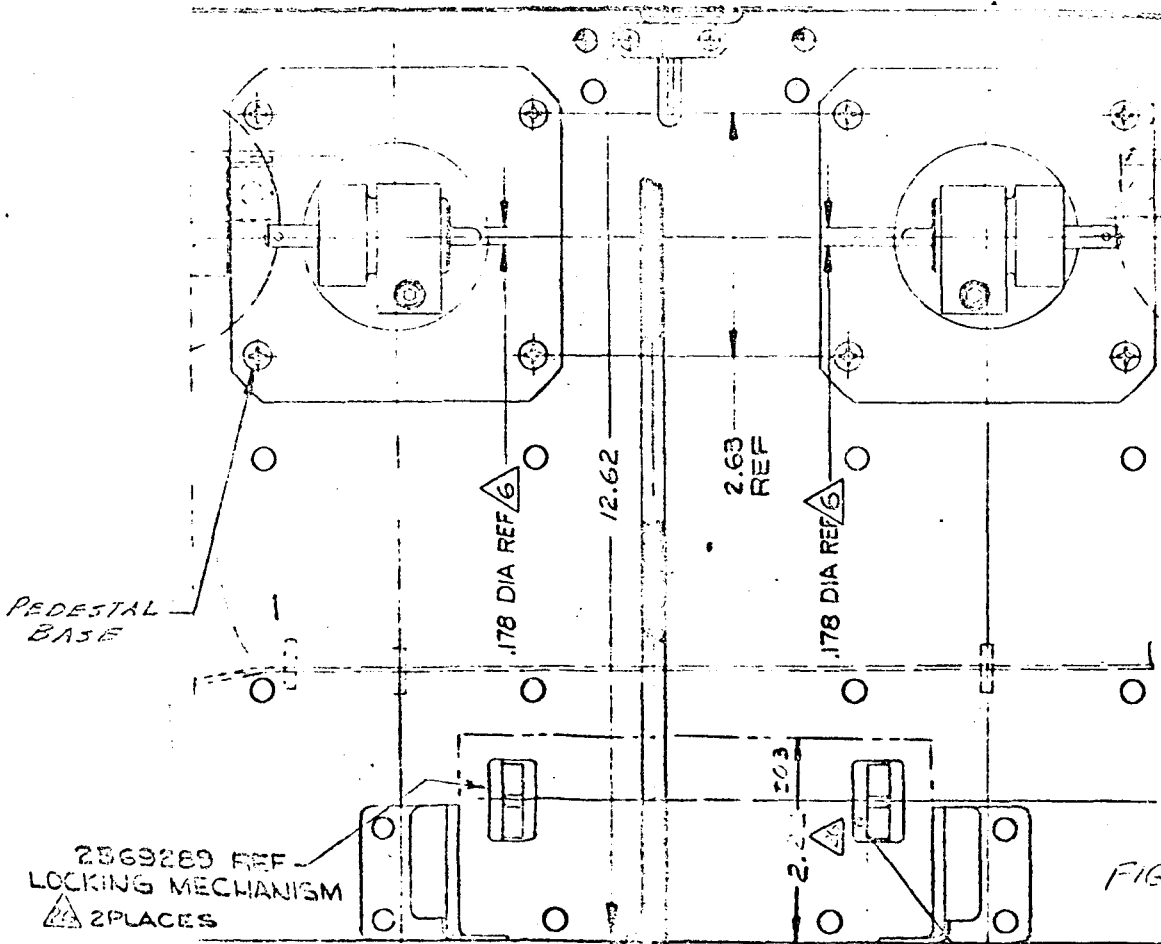
**Aerospace
Systems Division**

Appendix C - Structural Analyses
(Mortar Box/Pallet Structural
Attachment Analysis)

NO.	REV. NO.
ATM 1064	
PAGE 109	OF 212
DATE 11/24/71	



END
VIEW



PLAN
VIEW

FIGURE C-2



**Aerospace
Systems Division**

Appendix C - Structural Analyses
(Mortar Box/Pallet Structural
Attachment Analysis)

NO. ATM 1064	REV. NO.
PAGE 110	OF 212
DATE 11/24/71	

MATERIAL
303 ST. ST.
COND. A PER
QQ-5-764

MAT. PROPERTIES
 $F_{tu} = 75,000$ psi
 $F_{ty} = 30,000$ "
 $F_{cy} = 35,000$ "
 $F_{su} = 40,000$ "

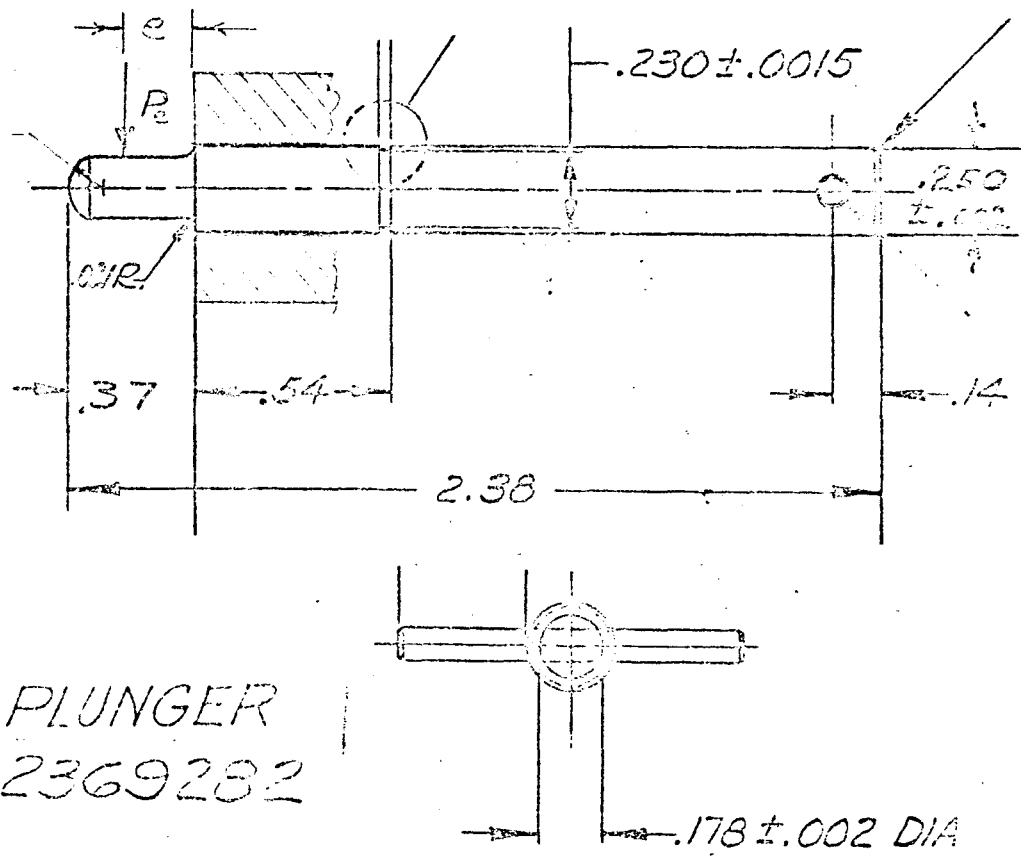


FIGURE C-3

2. ANALYSIS

2.1 Latch Assy., Rear Mortar Box ~ 2369286

The clamp assy. mount (2369284) and the plunger housing (2369283) are not critical. The plunger (2369282) mating with the mortar box structure is critical. Therefore, the analysis will be concerned with the plunger shown on this page.

The allowable eccentric load P_e will be determined for various eccentricities e . This load will then be compared with the applied load resulting from the launchings of grenades. Pages 2 and 4 illustrates the latch assemblies and their applications.



Aerospace Systems Division

Appendix C - Structural Analyses
(Mortar Box/Pallet Structural Attachment Analysis)

NO. REV. NO.

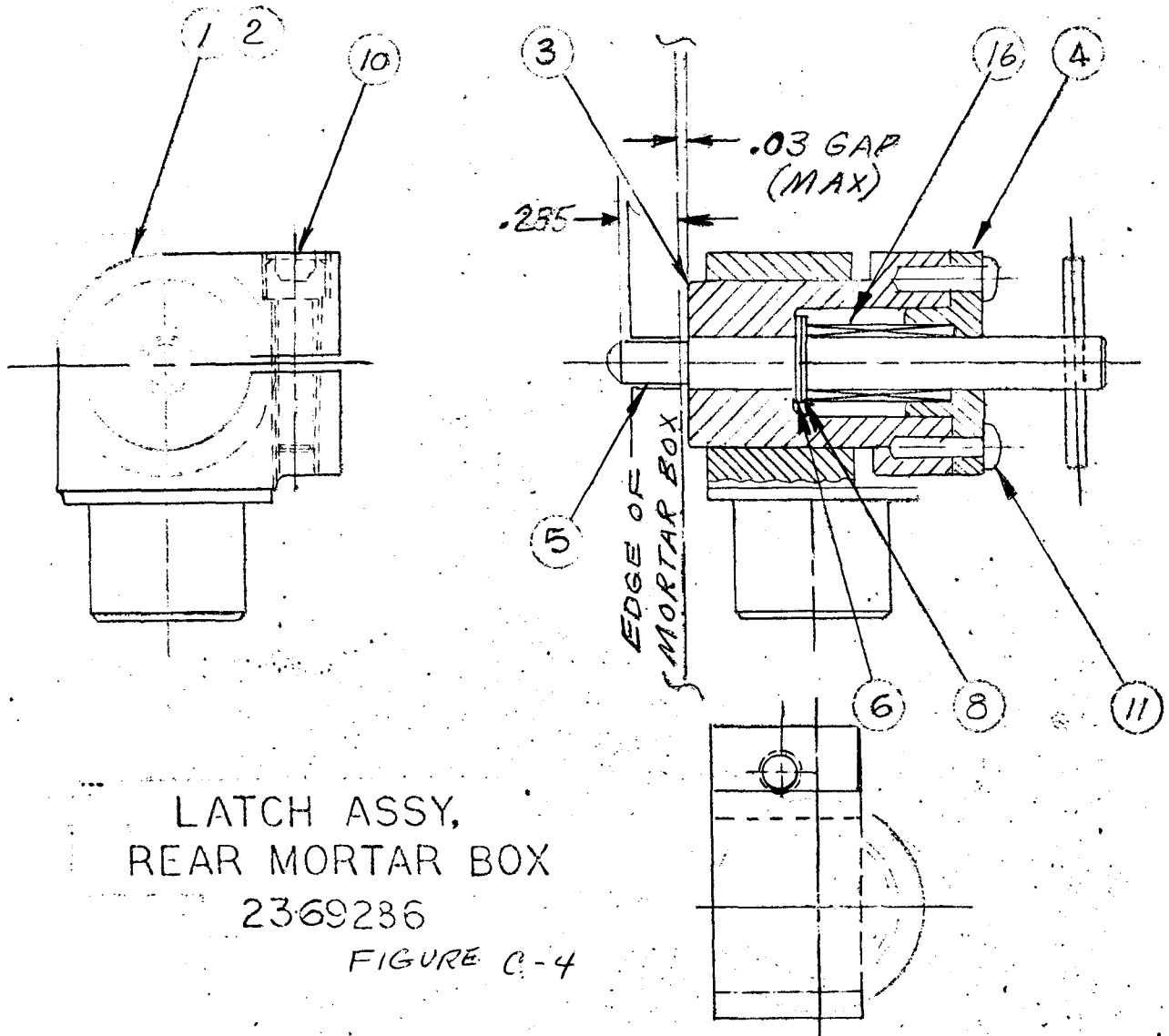
ATM 1064

PAGE 111 OF 212

DATE 11/24/71

QTY	UNIT	DESCRIPTION	CODE	PART OR SPECIFICATION NO.	FIGURE
1	1	SPRING, COMPRESSION	7047	CO260-052-09405	16
					15
					14
					13
					12
2	2	SCREW, PAN HD		MS51957-14	11
1	1	SCREW, CAP, SOC HD		MS16996-13	10
					9
1	1	RING, RETAINING		MS16624-4025	8
					7
1	1	WASHER, IMPACT		2369285	6
1	1	PLUNGER		2339282	5
1	1	END CAP, HOUSING		2369281	4
1	1	HOUSING, PLUNGER		2369283	3
1	-	CLAMP ASSY, L.H.		2369284-102	2
1	-	CLAMP ASSY, R.H.		2369284-101	1

LIST OF MATERIALS





**Aerospace
Systems Division**

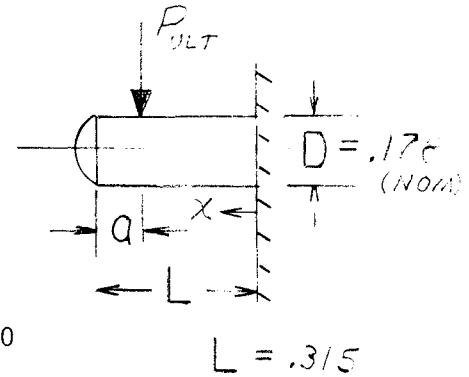
Appendix C - Structural Analyses
(Mortar Box/Pallet Structural
Attachment Analysis)

NO.	REV. NO.
ATM 1064	
PAGE 112	OF 212
DATE 11/24/71	

2.1.1 Pin Deflection Due to Shear and Bending

Assumptions

1. Pin deflects as a cantilever beam.
2. Shear stress distribution corresponding to rectangular bending stress distribution is not drastically altered. (Verification of this assumption will be shown later).
3. Limits of location of $P_{ULT} \sim .315 \leq \chi \leq 0$



The deflection of the pin at $\chi = L$ is:

$$\delta = \int_0^{L-a} M \frac{\partial M}{\partial P} \frac{dx}{EI} + \int_0^{L-a} V \frac{\partial V}{\partial P} \frac{dx}{GA} + a \int_0^{L-a} M \frac{\partial M}{\partial M_0} \frac{dx}{EI} + a \int_0^{L-a} V \frac{\partial V}{\partial M_0} \frac{dx}{GA}$$

$$M = Px$$

$$V = P$$

$$M = Px + M_0$$

$$V = P + \frac{M_0}{L-a}$$

$$\frac{\partial M}{\partial P} = x$$

$$\frac{\partial V}{\partial P} = 1$$

$$\frac{\partial M}{\partial M_0} = 1$$

$$\frac{\partial V}{\partial M_0} = \frac{1}{L-a}$$

or,

$$\delta = \int_0^{L-a} Px^2 \frac{dx}{EI} + \int_0^{L-a} P \frac{dx}{GA} + a \int_0^{L-a} (Px + M_0) \frac{dx}{EI} + a \int_0^{L-a} (P + \frac{M_0}{L-a}) \frac{1}{L-a} \frac{dx}{GA}$$

Note in the above integrals that $M_0 \equiv 0$. Hence, M_0 does not appear in the final result.

$$\delta = \frac{P}{6EI} \left[(L-a)^2 (2L+a) + 6L \left(\frac{EI}{GA} \right) \right] \quad (1)$$



**Aerospace
Systems Division**

Appendix C - Structural Analyses
(Mortar Box/Pallet Structural
Attachment Analysis)

NO.	REV. NO.
ATM 1064	
PAGE 113	OF 212
DATE 11/24/71	

The known parameters of Eq. (1) are:

$$I = \frac{\pi D^4}{64}$$

$$A = \frac{\pi D^2}{4}$$

$$E/G = 2.6$$

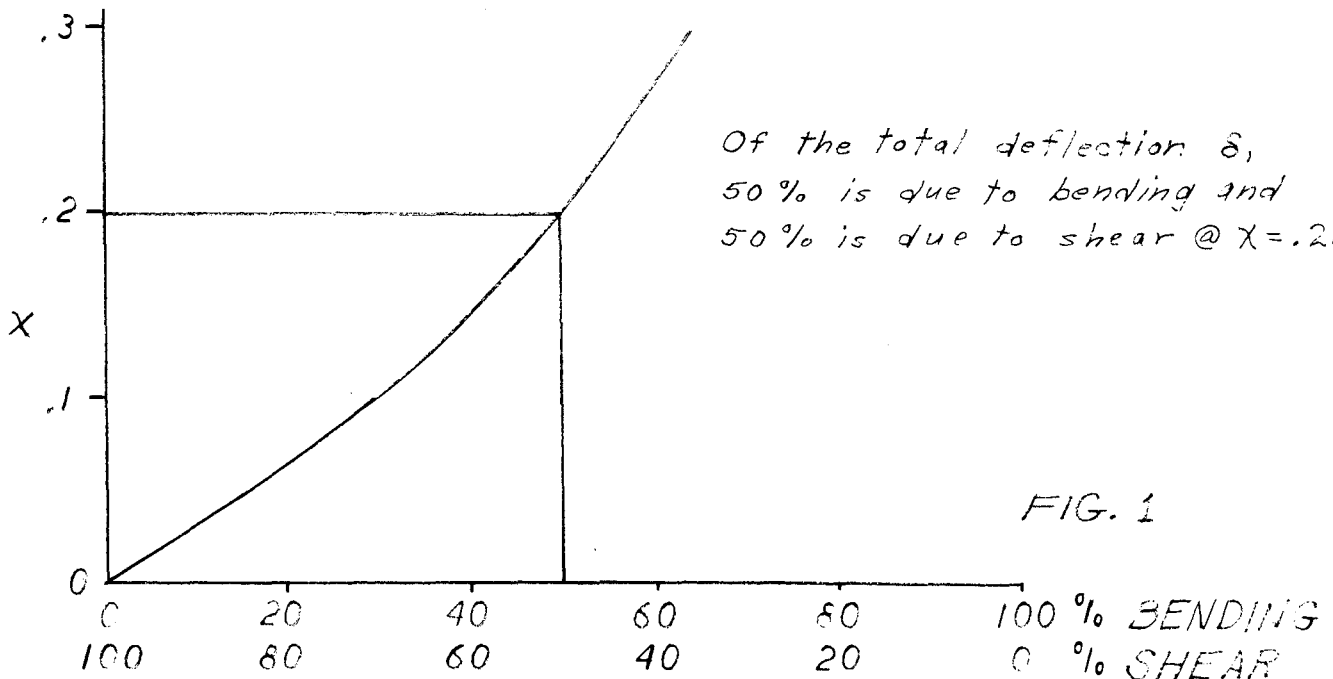
$$L = .315$$

$$D = .178$$

Thus, upon substitution of these values in Eq. (1) we have

$$\delta = \frac{P (L-a)^2 (2L+a)}{6 EI} \left[1 + \frac{.0309}{(.315 - a)^2 (.630 + a)} \right] \quad (2)$$

The first term (unity) in the bracket is the bending factor contributing to the total deflection. The second term is the relative factor contributing to the total deflection. Evaluation of Eq. (2) yields the following curve.





**Aerospace
Systems Division**

Appendix C - Structural Analyses
(Mortar Box/Pallet Structural
Attachment Analysis)

NO.	REV. NO.
ATM 1064	
PAGE 114	OF 212
DATE 11/24/71	

At this time the verification of assumption 2 will be explained.

The shear flow distribution for a triangular bending stress distribution is given by

$$q = \frac{VQ}{I} \quad (\text{lb/in}) \quad (3)$$

where V is the vertical shear, Q is the statical moment, and I is the moment of inertia.

The shear flow distribution for a trapezoidal bending stress is given by

$$q = \frac{VQ}{I} \left\{ \frac{1 + R [(AC/Q) - 1]}{1 + R (k - 1)} \right\} \quad (4)$$

where R is the rate of change of trapezoidal intercept stress f_o with respect to the maximum stress $= df_o/df_m$. C is distance from the principal axis to the extreme fiber, and k is the section factor $= 2Q/(I/C)$.

When the bending stress distribution is triangular, $f_o = 0$, and Eq. (4) is identical to Eq. (3).

The problem with a rectangular distribution of normal stress is simply that the normal stress is based on a reference stress which gives moment equality of internal stresses due to bending, but does not give the proper net force on the portion of the cross-section under tension.

The existence of shear in the beam section has an influence on the stress-strain curve of the beam material and causes a decrease in the value of F_{tu} and F_{ty} . Since R is a function of the stress-strain curve, and hence, F_{tu} and F_{ty} , it becomes virtually impossible to establish a reasonable value of R. When the shear is high the bending moment changes rapidly. This change of bending moment implies a change of normal stress distribution. Since the shear stress distribution is determined by the changes in normal stress along the length of the beam, it is clear that the rectangular distribution theory is inadequate for determining the shear stress distribution. However, there is light amidst the darkness. As the rectangular distribution



**Aerospace
Systems Division**

Appendix C - Structural Analyses
(Mortar Box/Pallet Structural
Attachment Analysis)

NO.	REV. NO.
ATM 1064	
PAGE 115	OF 212
DATE 11/24/71	

seems closer to actual test results than trapezoidal distribution, the latter cannot be used as a basis for shear distribution anyway. So, the aircraft industry, in general, has found that it is only necessary to calculate a fictitious average shear stress which can be combined with the bending stress by means of the conventional interaction equation.

For members of compact cross-section (rectangle, circle, etc.), the appropriate shear equation to be used in the interaction equation is

$$R_s = \text{shear stress ratio} = \frac{V}{AF_{su}} = \frac{V}{V_{ULT}}$$

similarly, $R_b = \text{bending moment ratio} = \frac{M}{M_{ULT}}$

The appropriate interaction equation is

$$R_b^2 + R_s^2 = 1. \quad (5)$$

For the present case,

$$\begin{aligned} M_{ULT} &= 2 F_{rb} Q_m = \frac{2 (54,000) (.178)^3}{12} \\ &= 50.76 \text{ in lb.} \end{aligned}$$

And, $V_{ULT} = (.02487) (40,000)$
 $= 995 \text{ lb}$

Thus, $R_b = M/M_{ULT} = P_{ULT} \chi / 50.76$

$$R_s = V/V_{ULT} = P_{ULT} / 995$$



**Aerospace
Systems Division**

Appendix C - Structural Analyses
(Mortar Box/Pallet Structural
Attachment Analysis)

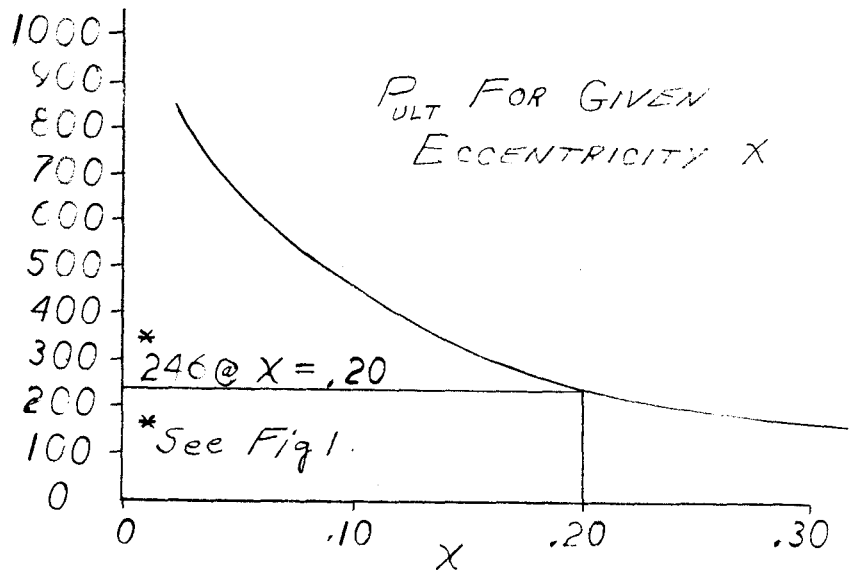
NO.	REV. NO.
ATM 1064	
PAGE 116	OF 212
DATE 11/24/71	

Substitution of these values in Eq. (5) yields

$$P_{ULT} = \frac{990,025}{384.24 x^2 + 1} \quad (6)$$

Eq. (6) is evaluated as follows:

γ	P_{ULT}
0	995
.03	854
.05	712
.10	452
.15	320
.20	246
.25	199
.30	167
.315	159





**Aerospace
Systems Division**

Appendix C - Structural Analyses
(Mortar Box/Pallet Structural
Attachment Analysis)

NO. ATM 1064	REV. NO.
PAGE <u>117</u> OF <u>212</u>	
DATE 11/24/71	

2.2 Pedestal Analysis

MATERIAL: AZ-31B Type 2, AMS 4375

$$F_{tu} = 32,000 \text{ psi}$$

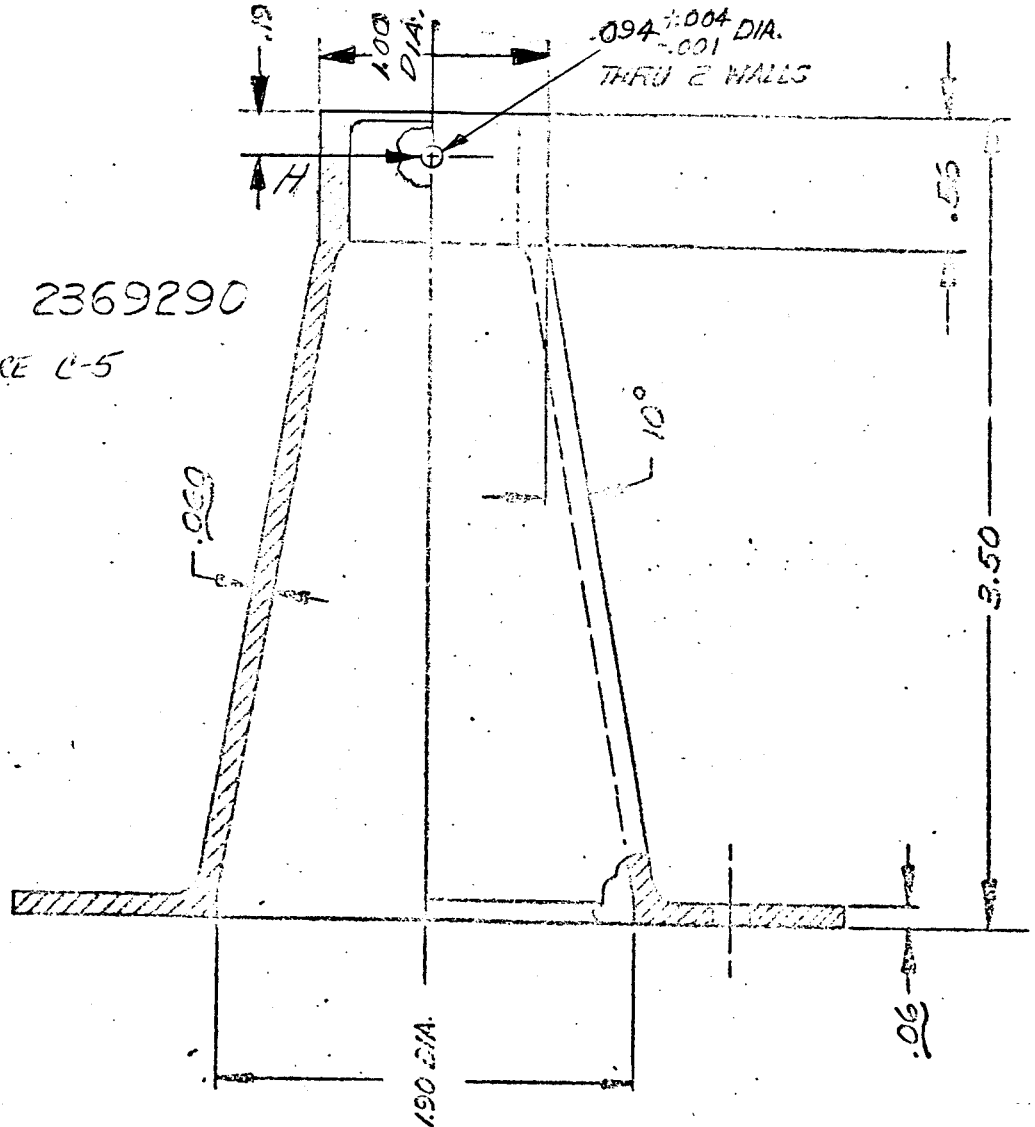
$$F_{ty} = 20,000 \text{ psi}$$

$$F_{cy} = 10,000 \text{ psi}$$

$$E = 6.5 \times 10^6$$

P = 296 lb
H = 162 lb

PEDESTAL 2369290
FIGURE U-5





**Aerospace
Systems Division**

NO.	REV. NO.
ATM 1064	
PAGE 118	OF 212
DATE 11/24/71	

Appendix C - Structural Analyses
(Mortar Box/Pallet Structural
Attachment Analysis)

2.2.1 Column Buckling Check

For short columns under a compressive loading condition, inelastic failure occurs at

$$F_c = \frac{K(F_{cy})^n}{(L'/\rho)^m}, \text{ Ref: Analysis \& Design of Flight Vehicle structures by Bruhn, p. 4.3}$$

Where $K = 3300$

$$n = 0.25$$

$$m = 1.5$$

$$L' = L'/\sqrt{c} = 3.5/\sqrt{2.05} = 2.45$$

$$= .466 \text{ (For 1.38 D-X-058 W, p. C.4.9)}$$

Therefore,

$$F_c = \frac{(3300)(20,000)^{.25}}{(2.45/.466)^{1.5}} = 2780 \text{ psi}$$

Applied Stress

$$f_c = \frac{P}{A}$$

where $P = 296 \text{ lb}$
 $A = .1885 \text{ in.}^2$

$$f_c = 1570 \text{ psi}$$

Hence,

$$R_c = \frac{1570}{3270} = 0.48$$



**Aerospace
Systems Division**

Appendix C - Structural Analyses
(Mortar Box/Pallet Structural
Attachment Analysis)

NO.	REV. NO.
ATM 1064	
PAGE 119	OF 212
DATE 11/24/71	

From Bruhn, p. C.4.16, using the bending modulus of rupture for magnesium and

$$\left. \begin{aligned} F_{cy} &= 10 \text{ KSI} \\ D/t &= 1.38/.060 = 23 \end{aligned} \right\} \Rightarrow F_b = 16,000 \text{ psi}$$

The applied bending stress is

$$f_b = \frac{162(3.5)}{.076} = 7500 \text{ psi}$$

Hence,

$$R_b = \frac{7500}{16,000} = 0.47$$

The MS is:

$$\begin{aligned} MS &= \frac{1}{R_e + R_b} - 1 \\ &= \frac{1}{0.48 + 0.47} - 1 \\ &= 0.05 \end{aligned}$$

2.2.2 Base Analysis

Assume a vertically upward load is applied at the top of the pedestal of 1000 lb. Displacements and stresses in the base will then be calculated. The results of this analysis are shown on the following computer print-out sheets.



**Aerospace
Systems Division**

NO.	REV. NO.
ATM 1064	
PAGE 120	OF 212
DATE 11/24/71	

Appendix C - Structural Analyses
(Mortar Box/Pallet Structural
Attachment Analysis)

MODEL OF QUARTER-SECTION OF BASE

1. ORIGINAL BASE - 0.06 in. thick

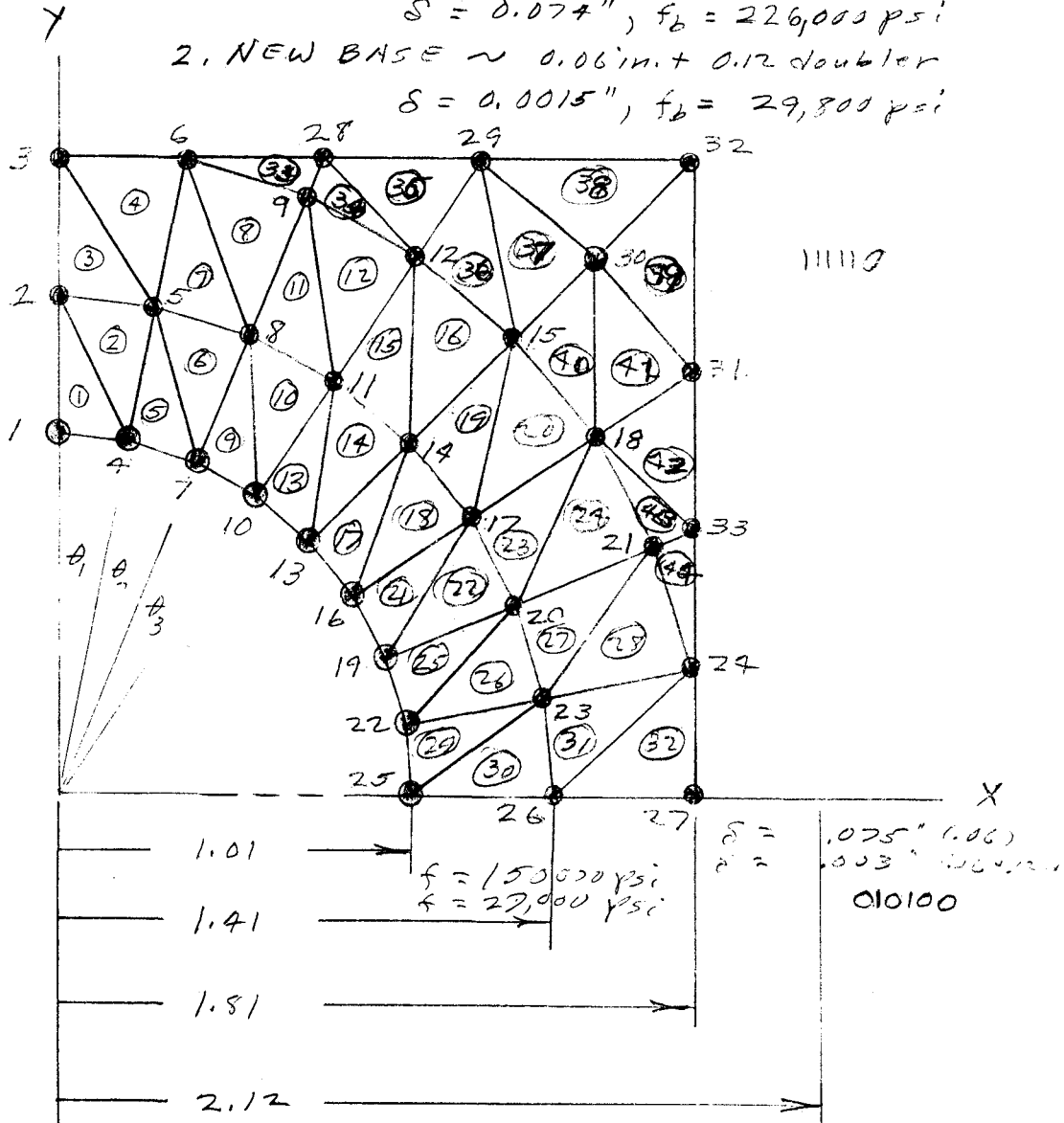
$S = 0.074"$, $f_b = 226,000 \text{ psi}$

2. NEW BASE ~ 0.06 in. + 0.12 doubler

$S = 0.0015"$, $f_b = 29,800 \text{ psi}$

100010

111110





**Aerospace
Systems Division**

LOAD CASE NUMBER... 1

LOAD CASE .06 PLATE THICKNESS

JOINT DISPLACEMENTS (GLOBAL REFERENCE SYSTEM)

JOINT NUMBER	X-DISPLACEMENT	Y-DISPLACEMENT	Z-DISPLACEMENT	X-ROTATION	Y-ROTATION	Z-ROTATION
1	0.	0.	7.41284E-02	-7.84580E-02	2.75665E-29	0.
2	0.	0.	4.46730E-02	-6.67429E-02	3.53217E-29	0.
3	0.	0.	2.01527E-02	-5.71068E-02	1.05142E-29	0.
4	0.	0.	7.34739E-02	-7.70641E-02	2.10118E-02	0.
5	0.	0.	4.37527E-02	-6.53856E-02	2.02369E-02	0.
6	0.	0.	1.86801E-02	-5.56232E-02	1.82012E-02	0.
7	0.	0.	7.20319E-02	-7.29101E-02	3.86135E-02	0.
8	0.	0.	4.11251E-02	-6.18967E-02	3.72421E-02	0.
9	0.	0.	1.55816E-02	-4.90625E-02	3.02643E-02	0.
10	0.	0.	7.05725E-02	-6.72317E-02	5.17376E-02	0.
11	0.	0.	3.83004E-02	-5.77867E-02	4.92241E-02	0.
12	0.	0.	1.22272E-02	-3.90224E-02	3.80740E-02	0.
13	0.	0.	6.96653E-02	-6.05115E-02	6.08821E-02	0.
14	0.	0.	3.68804E-02	-5.41925E-02	5.55507E-02	0.
15	0.	0.	9.71933E-03	-3.83991E-02	4.08544E-02	0.
16	0.	0.	7.02940E-02	-5.16103E-02	6.77523E-02	0.
17	0.	0.	3.79406E-02	-4.84128E-02	5.75389E-02	0.
18	0.	0.	1.16845E-02	-3.61159E-02	4.05358E-02	0.
19	0.	0.	7.15777E-02	-3.84999E-02	7.34213E-02	0.
20	0.	0.	4.04262E-02	-3.61493E-02	6.25206E-02	0.
21	0.	0.	1.44584E-02	-2.91485E-02	4.98791E-02	0.
22	0.	0.	7.28251E-02	-2.09761E-02	7.83151E-02	0.
23	0.	0.	4.25674E-02	-1.99556E-02	6.66405E-02	0.
24	0.	0.	1.66877E-02	-1.76687E-02	5.70726E-02	0.
25	0.	0.	7.33057E-02	-2.81602E-29	8.08558E-02	0.
26	0.	0.	4.33254E-02	-3.43400E-29	6.86401E-02	0.
27	0.	0.	1.77477E-02	-1.07739E-29	6.02490E-02	0.
28	0.	0.	7.17019E-03	-4.60963E-02	2.68086E-02	0.
29	0.	0.	-4.34465E-04	-2.51433E-02	1.43292E-02	0.
30	0.	0.	2.52008E-28	-1.46785E-28	1.46656E-28	0.
31	0.	0.	-6.36835E-04	-1.17738E-02	2.59537E-02	0.
32	0.	0.	-1.03303E-03	-7.63590E-04	-4.75384E-04	0.
33	0.	0.	6.06097E-03	-2.56213E-02	4.62492E-02	0.

Appendix C - Structural Analyses
(Mortar Box/Pallet Structural
Attachment Analysis)

NO.

ATM 1064

REV. NO.

PAGE 121 OF 212

DATE 11/24/71



Aerospace
Systems Division

TRIANGULAR ELEMENT STRESSES

LOAD CASE 1

- NOTE. 1. POSITIVE MEMBRANE RESULTANTS S(XX), S(YY) ARE TENSILE. THE UNITS ARE (F/L).
 2. POSITIVE BENDING RESULTANTS M(XX), M(YY) CAUSE COMPRESSION IN THE FIBERS OF THE POSITIVE FACE. THE UNITS ARE (FL/L).
 3. THE REFERENCE ANGLE IS THE ANGLE USED IN TRANSFORMING THE STRESS RESULTANTS TO THE COORDINATE SYSTEM DEFINED BY THE REFERENCE PLANE/TRIANGLE INTERSECTION.

ELEMENT NUMBER	MEMBRANE RESULTANTS			BENDING RESULTANTS			MAX/MIN STRESSES IN EXTREME FIBERS				REFERENCE ANGLE
	S(XX)	S(YY)	S(XY)	M(XX)	M(YY)	M(XY)	TX+	TX-	TY+	TY-	
1 0.	0.	0.	0.	-1.359E+02	-9.948E+00	3.337E+00	2.26E+05	-2.26E+05	1.66E+04	-1.66E+04	5.63
2 0.	0.	0.	0.	-7.787E+01	1.177E+01	1.084E+01	1.30E+05	-1.30E+05	-1.96E+04	1.96E+04	64.84
3 0.	0.	0.	0.	-9.063E+01	1.822E+00	3.077E+00	1.51E+05	-1.51E+05	-3.04E+03	3.04E+03	5.63
4 0.	0.	0.	0.	-5.250E+01	9.970E+00	9.164E+00	8.75E+04	-8.75E+04	-1.66E+04	1.66E+04	57.22
5 0.	0.	0.	0.	-1.136E+02	-8.482E+00	2.177E+01	1.89E+05	-1.89E+05	1.41E+04	-1.41E+04	16.88
6 0.	0.	0.	0.	-5.984E+01	9.427E+00	2.127E+01	9.94E+04	-9.94E+04	-1.57E+04	1.57E+04	76.09
7 0.	0.	0.	0.	-7.285E+01	5.210E+00	1.755E+01	1.21E+05	-1.21E+05	-8.69E+03	8.69E+03	16.88
8 0.	0.	0.	0.	-2.136E+01	1.979E+01	2.459E+01	3.58E+04	-3.58E+04	-3.30E+04	3.30E+04	68.47
9 0.	0.	0.	0.	-8.344E+01	-1.244E+01	3.170E+01	1.39E+05	-1.39E+05	2.07E+04	-2.07E+04	28.13
10 0.	0.	0.	0.	-3.411E+01	6.834E+00	2.477E+01	5.88E+04	-5.88E+04	-1.14E+04	1.14E+04	87.34
11 0.	0.	0.	0.	-3.523E+01	1.779E+01	2.863E+01	5.87E+04	-5.87E+04	-2.97E+04	2.97E+04	28.13
12 0.	0.	0.	0.	6.654E+00	3.244E+01	3.911E+01	-1.11E+04	1.11E+04	-5.41E+04	5.41E+04	79.72
13 0.	0.	0.	0.	-5.623E+01	-2.204E+01	3.473E+01	9.37E+04	-9.37E+04	3.67E+04	-3.67E+04	39.38
14 0.	0.	0.	0.	-5.425E+00	4.289E+00	2.178E+01	9.04E+03	-9.04E+03	-7.15E+03	7.15E+03	98.59
15 0.	0.	0.	0.	3.352E+00	3.351E+01	3.230E+01	-5.59E+03	5.59E+03	-5.59E+04	5.59E+04	39.38
16 0.	0.	0.	0.	4.490E+01	4.858E+01	2.736E+01	-7.48E+04	7.48E+04	-8.10E+04	8.10E+04	90.97
17 0.	0.	0.	0.	-3.574E+01	-4.055E+01	3.537E+01	5.98E+04	-5.98E+04	6.76E+04	-6.76E+04	50.63
18 0.	0.	0.	0.	2.004E+01	-7.532E+00	1.995E+01	-3.34E+04	3.34E+04	1.26E+04	-1.26E+04	109.84
19 0.	0.	0.	0.	2.851E+01	1.822E+01	3.040E+01	-4.75E+04	4.75E+04	-3.04E+04	3.04E+04	50.63
20 0.	0.	0.	0.	4.427E+01	2.726E+01	3.228E+01	-7.38E+04	7.38E+04	-4.54E+04	4.54E+04	102.22
21 0.	0.	0.	0.	-1.778E+01	-6.654E+01	3.403E+01	2.96E+04	-2.96E+04	1.11E+05	-1.11E+05	61.88
22 0.	0.	0.	0.	1.118E+01	-4.055E+01	2.470E+01	-1.85E+04	1.85E+04	6.77E+04	-6.77E+04	121.09
23 0.	0.	0.	0.	1.889E+01	-2.207E+01	3.684E+01	-2.81E+04	2.81E+04	3.68E+04	-3.68E+04	61.88
24 0.	0.	0.	0.	2.016E+01	-5.870E+00	2.990E+01	-3.38E+04	3.38E+04	9.45E+03	-9.45E+03	113.47
25 0.	0.	0.	0.	-1.631E+01	-1.012E+02	3.159E+01	2.72E+04	-2.72E+04	1.69E+05	-1.69E+05	73.13
26 0.	0.	0.	0.	1.410E+01	-6.027E+01	1.892E+01	-2.35E+04	2.35E+04	1.00E+05	-1.00E+05	132.34
27 0.	0.	0.	0.	7.381E+00	-5.881E+01	2.855E+01	-1.23E+04	1.23E+04	9.80E+04	-9.80E+04	73.13
28 0.	0.	0.	0.	1.184E+01	-3.892E+01	1.828E+01	-1.97E+04	1.97E+04	5.15E+04	-5.15E+04	124.72
29 0.	0.	0.	0.	-1.128E+01	-1.288E+02	1.803E+01	1.88E+04	-1.88E+04	2.14E+05	-2.14E+05	84.38
30 0.	0.	0.	0.	1.350E+01	-7.740E+01	4.812E+00	-2.25E+04	2.25E+04	1.29E+05	-1.29E+05	143.59
31 0.	0.	0.	0.	4.775E+01	-8.823E+01	1.430E+01	-7.98E+02	7.98E+02	1.47E+05	-1.47E+05	84.38
32 0.	0.	0.	0.	6.187E+00	-5.337E+01	5.013E+00	-1.03E+04	1.03E+04	8.90E+04	-8.90E+04	135.97
33 0.	0.	0.	0.	-1.758E+01	1.980E+01	2.587E+01	2.93E+04	-2.93E+04	-3.30E+04	3.30E+04	16.88
34 0.	0.	0.	0.	-6.404E+00	9.018E+00	3.185E+01	1.07E+04	-1.07E+04	-1.50E+04	1.50E+04	28.13
35 0.	0.	0.	0.	5.852E+01	3.827E+01	5.430E+01	-9.75E+04	9.75E+04	-6.38E+04	6.38E+04	123.75
36 0.	0.	0.	0.	6.193E+01	5.783E+01	4.665E+01	-1.03E+05	1.03E+05	-9.64E+04	9.64E+04	39.38
37 0.	0.	0.	0.	1.798E+02	1.257E+02	9.473E+01	-3.00E+05	3.00E+05	-2.09E+05	2.09E+05	135.00
38 0.	0.	0.	0.	1.578E+01	-5.881E+01	-2.331E+01	-2.63E+04	2.63E+04	9.31E+04	-9.31E+04	39.38
39 0.	0.	0.	0.	-5.123E+01	1.023E+01	-2.978E+01	8.54E+04	-8.54E+04	-1.71E+04	1.71E+04	50.63
40 0.	0.	0.	0.	1.454E+02	1.333E+02	6.393E+01	-2.42E+05	2.42E+05	-2.22E+05	2.22E+05	50.63
41 0.	0.	0.	0.	1.872E+01	8.318E+01	5.873E+01	-3.12E+04	3.12E+04	-1.39E+05	1.39E+05	146.25
42 0.	0.	0.	0.	4.604E+01	6.437E+01	5.405E+01	-7.67E+04	7.67E+04	-1.07E+05	1.07E+05	38.84
43 0.	0.	0.	0.	1.759E+01	-2.079E+00	3.283E+01	-2.95E+04	2.95E+04	3.47E+03	-3.47E+03	61.88
44 0.	0.	0.	0.	2.559E+01	-1.787E+01	3.114E+01	-4.28E+04	4.28E+04	2.98E+04	-2.98E+04	73.13

VERSION 18 - RELEASED - JANUARY 1971

ENGINEERING ANALYSIS CORPORATION
1611 SOUTH PACIFIC COAST HIGHWAY

Appendix C - Structural Analyses
(Mortar Box/Pallet Structural
Attachment Analysis)

NO.	ATM 1064	REV. NO.
PAGE	122	OF
DATE	11/24/71	212

LOAD CASE NUMBER... 1

LOAD CASE 2 WITH .12 DOUBLER

JOINT DISPLACEMENTS (GLOBAL REFERENCE SYSTEM)

JOINT NUMBER	X-DISPLACEMENT	Y-DISPLACEMENT	Z-DISPLACEMENT	X-ROTATION	Y-ROTATION	Z-ROTATION
1	0.	0.	1.51846E-03	-1.38786E-03	2.27850E-29	0.
2	0.	0.	1.02174E-03	-1.06575E-03	2.64089E-29	0.
3	0.	0.	6.47942E-04	-8.13282E-04	8.31849E-30	0.
4	0.	0.	1.47978E-03	-1.33676E-03	6.25166E-04	0.
5	0.	0.	9.68477E-04	-1.01451E-03	5.58834E-04	0.
6	0.	0.	5.79872E-04	-7.71054E-04	5.10049E-04	0.
7	0.	0.	1.38268E-03	-1.19291E-03	1.13006E-03	0.
8	0.	0.	8.32290E-04	-8.80453E-04	1.00898E-03	0.
9	0.	0.	4.20537E-04	-6.14826E-04	8.04249E-04	0.
10	0.	0.	1.25571E-03	-1.02077E-03	1.47258E-03	0.
11	0.	0.	6.51438E-04	-7.10778E-04	1.30591E-03	0.
12	0.	0.	2.39825E-04	-3.56521E-04	8.46083E-04	0.
13	0.	0.	1.13402E-03	-8.80552E-04	1.64794E-03	0.
14	0.	0.	4.71705E-04	-6.14009E-04	1.45597E-03	0.
15	0.	0.	7.21074E-05	-4.71520E-05	6.77800E-04	0.
16	0.	0.	1.04964E-03	-7.89575E-04	1.69625E-03	0.
17	0.	0.	3.57526E-04	-6.78815E-04	1.41333E-03	0.
18	0.	0.	3.16199E-28	-2.81168E-29	1.39203E-28	0.
19	0.	0.	1.01698E-03	-6.58130E-04	1.71113E-03	0.
20	0.	0.	3.50915E-04	-5.77032E-04	1.26778E-03	0.
21	0.	0.	-4.49874E-05	-8.06177E-05	6.12245E-04	0.
22	0.	0.	1.01733E-03	-3.67322E-04	1.78153E-03	0.
23	0.	0.	3.61825E-04	-3.46077E-04	1.36711E-03	0.
24	0.	0.	-1.12776E-04	-7.77362E-05	1.01558E-03	0.
25	0.	0.	1.01993E-03	-1.20433E-29	1.82693E-03	0.
26	0.	0.	3.62868E-04	-1.69025E-29	1.45483E-03	0.
27	0.	0.	-1.53432E-04	4.55757E-31	1.21069E-03	0.
28	0.	0.	2.89377E-04	-5.78567E-04	7.22101E-04	0.
29	0.	0.	4.09257E-05	-3.56488E-04	4.76500E-04	0.
30	0.	0.	-6.41993E-29	-7.41260E-30	2.52067E-29	0.
31	0.	0.	-2.01110E-05	1.21549E-04	1.27312E-04	0.
32	0.	0.	-1.71690E-05	-1.22041E-04	-1.10167E-04	0.
33	0.	0.	-1.19109E-04	1.42366E-04	5.64485E-04	0.

Appendix C - Structural Analyses
(Mortar Box/Pallet Structural
Attachment Analysis)



Aerospace
Systems Division

TRIANGULAR ELEMENT STRESSES

LOAD CASE 1

- NOTE. 1. POSITIVE MEMBRANE RESULTANTS S(XX),S(YY) ARE TENSILE. THE UNITS ARE (F/L).
 2. POSITIVE BENDING RESULTANTS M(XX),M(YY) CAUSE COMPRESSION IN THE FIBERS OF THE POSITIVE FACE. THE UNITS ARE (FL/L).
 3. THE REFERENCE ANGLE IS THE ANGLE USED IN TRANSFORMING THE STRESS RESULTANTS TO THE COORDINATE SYSTEM DEFINED BY THE REFERENCE PLANE/TRIANGLE INTERSECTION.

ELEMENT NUMBER	MEMBRANE RESULTANTS			BENDING RESULTANTS		MAX/MIN STRESSES IN EXTREME FIBERS				REFERENCE ANGLE	
	S(XX)	S(YY)	S(XY)	M(XX)	M(YY)	TX+	TX-	TY+	TY-		
1 0.	0.	0.	0.	-1.117E+02	-1.066E+01	3.117E+00	2.07E+04	-2.07E+04	1.97E+03	-1.97E+03	5.63
2 0.	0.	0.	0.	-5.720E+01	8.519E+00	9.814E+00	1.06E+04	-1.06E+04	-1.58E+03	1.58E+03	64.84
3 0.	0.	0.	0.	-6.912E+01	1.018E-01	2.797E+00	1.28E+04	-1.28E+04	-1.88E+01	1.88E+01	5.63
4 0.	0.	0.	0.	-4.068E+01	5.222E+00	6.758E+00	7.53E+03	-7.53E+03	-9.67E+02	9.67E+02	57.22
5 0.	0.	0.	0.	-8.869E+01	-8.119E+00	1.970E+01	1.64E+04	-1.64E+04	1.50E+03	-1.50E+03	16.88
6 0.	0.	0.	0.	-3.999E+01	6.980E+00	1.919E+01	7.41E+03	-7.41E+03	-1.29E+03	1.29E+03	76.09
7 0.	0.	0.	0.	-5.453E+01	4.470E-01	1.413E+01	1.01E+04	-1.01E+04	-8.28E+01	8.28E+01	16.88
8 0.	0.	0.	0.	-1.393E+01	9.046E+00	1.648E+01	2.58E+03	-2.58E+03	-1.79E+03	1.79E+03	68.47
9 0.	0.	0.	0.	-5.539E+01	-6.864E+00	2.654E+01	1.03E+04	-1.03E+04	1.27E+03	-1.27E+03	28.13
10 0.	0.	0.	0.	-1.752E+01	6.865E+00	2.325E+01	3.24E+03	-3.24E+03	-1.27E+03	1.27E+03	87.34
11 0.	0.	0.	0.	-2.446E+01	4.749E+00	2.233E+01	4.53E+03	-4.53E+03	-8.79E+02	8.79E+02	28.13
12 0.	0.	0.	0.	1.980E+01	1.720E+01	2.457E+01	-3.67E+03	3.67E+03	-3.19E+03	3.19E+03	79.72
13 0.	0.	0.	0.	-2.185E+01	-2.715E+00	2.349E+01	4.05E+03	-4.05E+03	5.03E+02	-5.03E+02	39.38
14 0.	0.	0.	0.	3.889E+00	1.087E+01	1.887E+01	-7.20E+02	7.20E+02	-2.01E+03	2.01E+03	98.59
15 0.	0.	0.	0.	1.467E+01	2.180E+01	2.590E+01	-2.72E+03	2.72E+03	-4.05E+03	4.05E+03	39.38
16 0.	0.	0.	0.	6.326E+01	3.339E+01	3.285E+01	-1.17E+04	1.17E+04	-6.18E+03	6.18E+03	90.97
17 0.	0.	0.	0.	-6.475E-01	-7.339E-01	1.607E+01	1.20E+02	-1.20E+02	1.36E+02	-1.36E+02	50.63
18 0.	0.	0.	0.	2.964E+01	2.218E+01	6.252E+00	-5.49E+03	5.49E+03	-4.11E+03	4.11E+03	109.84
19 0.	0.	0.	0.	6.318E+01	5.360E+01	2.482E+01	-1.17E+04	1.17E+04	-9.94E+03	9.94E+03	50.63
20 0.	0.	0.	0.	1.607E+02	7.587E+01	2.833E+01	-2.98E+04	2.98E+04	-1.41E+04	1.41E+04	102.22
21 0.	0.	0.	0.	1.051E+01	-1.094E+01	1.092E+01	-1.95E+03	1.95E+03	2.03E+03	-2.03E+03	61.88
22 0.	0.	0.	0.	4.129E+01	-1.288E+00	9.174E+00	-7.65E+03	7.65E+03	2.38E+02	-2.38E+02	121.09
23 0.	0.	0.	0.	1.121E+02	5.697E+01	2.380E+01	-2.08E+04	2.08E+04	-1.06E+04	1.06E+04	61.88
24 0.	0.	0.	0.	3.543E+01	3.948E+01	4.121E+01	-6.56E+03	6.56E+03	-7.31E+03	7.31E+03	113.47
25 0.	0.	0.	0.	1.223E+01	-3.097E+01	1.345E+01	-2.26E+03	2.26E+03	5.74E+03	-5.74E+03	73.13
26 0.	0.	0.	0.	2.856E+01	-1.374E+01	1.058E+01	-5.29E+03	5.29E+03	2.54E+03	-2.54E+03	132.34
27 0.	0.	0.	0.	4.480E+01	-5.367E+00	2.914E+01	-8.30E+03	8.30E+03	9.94E+02	-9.94E+02	73.13
28 0.	0.	0.	0.	2.175E+01	1.675E+01	2.382E+01	-4.03E+03	4.03E+03	-3.10E+03	3.10E+03	124.72
29 0.	0.	0.	0.	1.170E+01	-5.096E+01	8.424E+00	-2.17E+03	2.17E+03	9.44E+03	-9.44E+03	84.38
30 0.	0.	0.	0.	2.108E+01	-2.040E+01	4.840E+00	-3.90E+03	3.90E+03	5.27E+03	-5.27E+03	143.59
31 0.	0.	0.	0.	1.794E+01	-4.024E+01	1.690E+01	-3.32E+03	3.32E+03	7.45E+03	-7.45E+03	84.38
32 0.	0.	0.	0.	1.494E+01	3.795E+00	7.563E+00	-2.77E+03	2.77E+03	-7.03E+02	7.03E+02	135.97
33 0.	0.	0.	0.	-1.211E+01	1.014E+01	1.670E+01	2.24E+03	-2.24E+03	-1.88E+03	1.88E+03	16.88
34 0.	0.	0.	0.	5.335E+00	4.171E+00	1.832E+01	-9.88E+02	9.88E+02	-7.72E+02	7.72E+02	28.13
35 0.	0.	0.	0.	2.348E+01	-3.979E+00	1.836E+01	-4.33E+03	4.33E+03	7.37E+02	-7.37E+02	123.75
36 0.	0.	0.	0.	3.765E+01	-2.608E+00	2.016E+01	-6.97E+03	6.97E+03	4.83E+02	-4.83E+02	39.38
37 0.	0.	0.	0.	7.212E+01	5.224E+00	1.662E+01	-1.34E+04	1.34E+04	-9.67E+02	9.67E+02	135.00
38 0.	0.	0.	0.	9.591E-01	-7.725E-01	-2.365E-01	-1.60E+03	1.60E+03	1.29E+03	-1.29E+03	39.38
39 0.	0.	0.	0.	-1.550E-01	-4.592E-01	-2.088E-02	2.58E+02	-2.58E+02	7.65E+02	-7.65E+02	50.63
40 0.	0.	0.	0.	1.115E+02	3.361E+01	5.663E+00	-2.06E+04	2.06E+04	-6.22E+03	6.22E+03	50.63
41 0.	0.	0.	0.	-1.487E+01	-4.143E+00	1.023E+01	2.75E+03	-2.75E+03	7.67E+02	-7.67E+02	146.25
42 0.	0.	0.	0.	-4.241E+01	-1.508E+01	1.732E+01	7.85E+03	-7.85E+03	2.90E+03	-2.90E+03	38.84
43 0.	0.	0.	0.	7.616E+00	3.741E+01	3.939E+01	-1.41E+03	1.41E+03	-6.93E+03	6.93E+03	61.88
44 0.	0.	0.	0.	1.881E+01	1.544E+01	3.741E+01	-3.48E+03	3.48E+03	-2.86E+03	2.86E+03	73.13

Appendix C - Structural Analyses
(Mortar Box/Pallet Structural
Attachment Analysis)



**Aerospace
Systems Division**

Appendix C - Structural Analyses
(Mortar Box/Pallet Structural
Attachment Analysis)

ATM 1064

PAGE 125 OF 212

DATE 11/24/71

2.2.3 Shear Pin Loads

Pin diameter = 0.094 in.

Pin Area = 0.00693 in.²

Pin shear load allow. = 154,000(.00693)

= 1067 lb (single shear)

Since the pin is in double shear,

$$P_{all} = 2134 \text{ lb.}$$

Hence,

$$MS = \frac{2134}{973} - 1 = 1.19$$

2.3 Locking Mechanism, Fwd. Mortar Box

The critical part of this mechanism is the Lug Carrier Frame (2339034). The Locking Mechanism, Front Mortar Box Lug (2369289), consisting of the Slide Bolt Mount (2369287) and the Slide Bolt (2369288) is much stronger than the lug carrier frame. Therefore, part no. 2339034 will be analyzed for structural integrity. The locking mechanism is shown on page 16 and 17.

Material: Mg Alloy AZ31B - H24

$$F_{tu} = 36,000 \text{ psi}$$

$$F_{ty} = 22,000 \text{ psi}$$

$$F_{cy} = 13,000 \text{ psi}$$

$$F_{su} = 18,000 \text{ psi}$$

$$E = 6.5 \times 10^6$$

2.3.1 Lug Analysis (Ref: Republic A/C Struct. Manual)

$r_{equiv.} = 0.16 \text{ in.}$ (see DETAIL A, p. 17)

$F_Z = 190 \text{ lb, } F_X = 130 \text{ lb}$



**Aerospace
Systems Division**

Appendix C - Structural Analyses
(Mortar Box/Pallet Structural
Attachment Analysis)

NO. ATM 1064	REV. NO.
PAGE 126	OF 212
DATE 11/24/71	

a. $\frac{e}{D} = \frac{0.39}{0.32} = 1.22$

$$\frac{W}{D} = \frac{0.50}{0.32} = 1.56$$

$$\frac{D}{t} = \frac{0.32}{0.15} = 2.13$$

$$A_t = 2(.15)(.15) = 0.045 \text{ in.}^2$$

$$A_{br} = .2(.15) = 0.030 \text{ in.}^2$$

b. Allow. shear brg. ult. load

$$K_{br} = 1.16 \text{ (Fig. 1.6200-8)}$$

$$F_{tu(g)} = 36,000 \text{ psi}$$

$$\begin{aligned} P_{bru} &= K_{br} F_{tu(g)} A_{br} \\ &= 1.16 (36,000)(.03) \\ &= 1250 \text{ lb} \end{aligned}$$

$$MS = \frac{1250}{190} - 1 = \text{High}$$

c. Allow. Tensile ult. load

$$K_t = 0.81 \text{ (Fig. 1.6200-7)}$$

$$\begin{aligned} P_{tu} &= K_t F_{tu(g)} A_t \\ &= 0.81(36,000)(.045) = 1312 \text{ lb, } MS = \frac{1312}{190} - 1 = \text{High} \end{aligned}$$



**Aerospace
Systems Division**

Appendix C - Structural Analyses
(Mortar Box/Pallet Structural
Attachment Analysis)

NO. ATM 1064	REV. NO.
PAGE 127	OF 212
DATE 11/24/71	

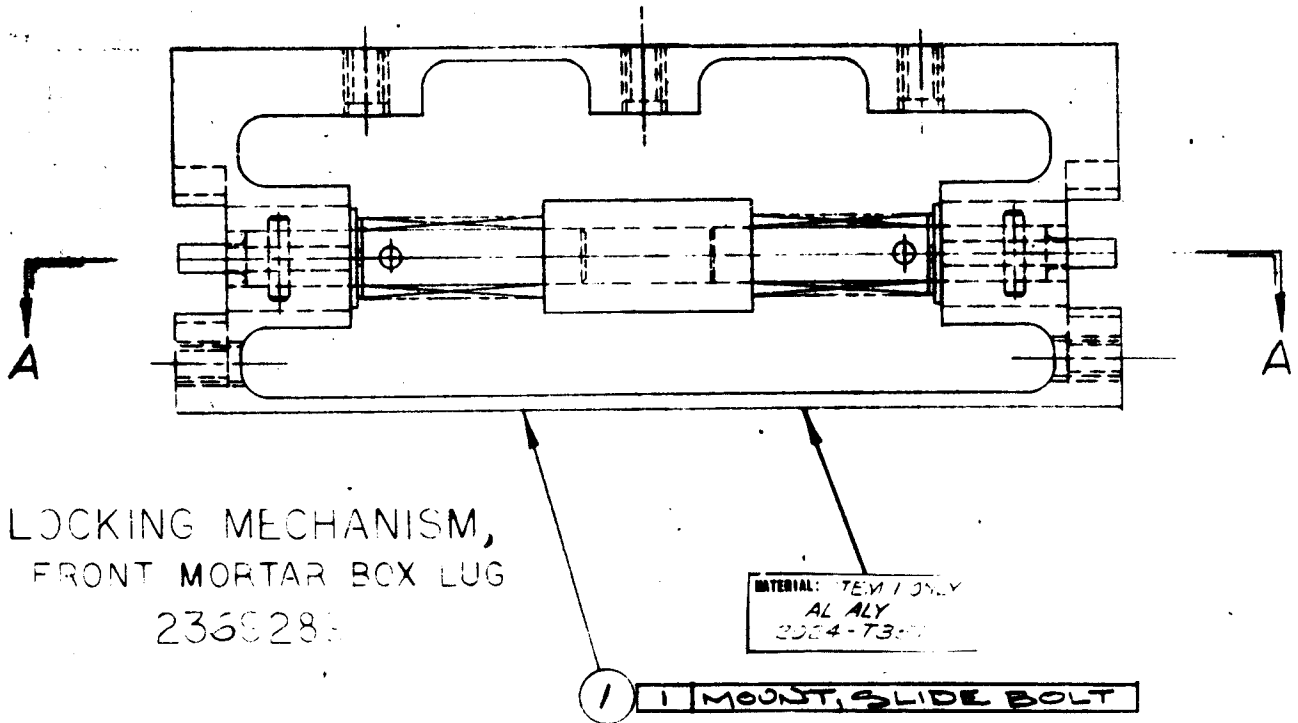


FIGURE C-7

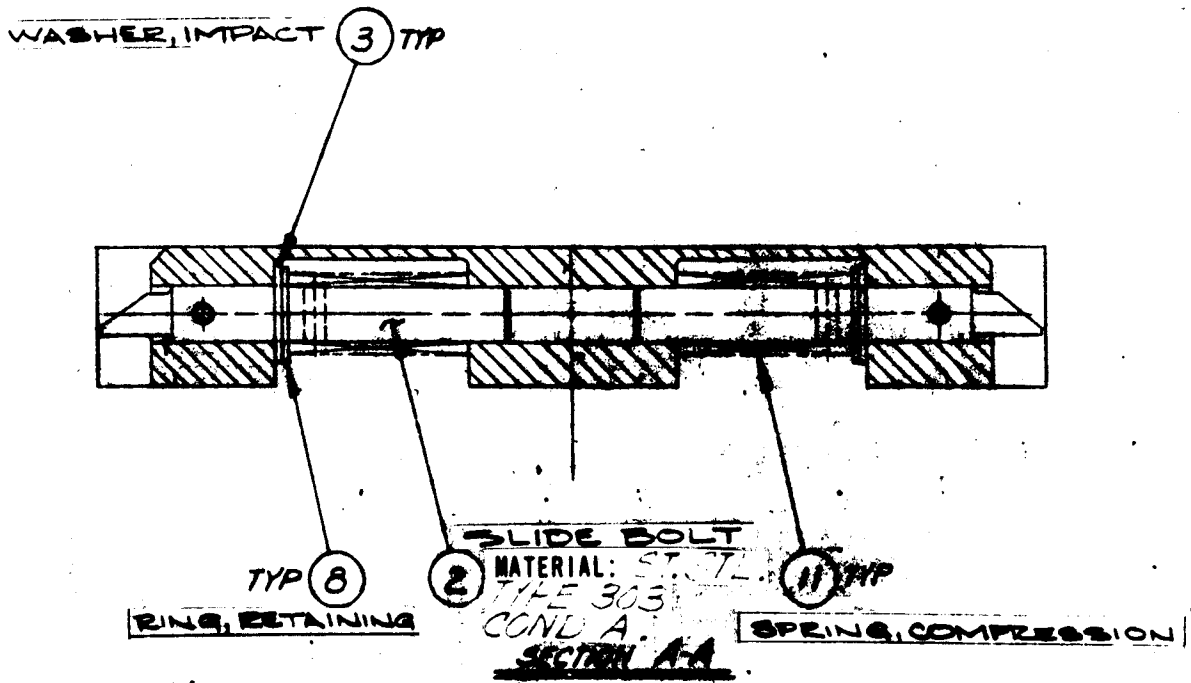


FIGURE C-8



**Aerospace
Systems Division**

Appendix C - Structural Analyses (Mortar Box/Pallet Structural Attachment Analysis)		NO. ATM 1064	REV. NO.
		PAGE 129	OF 212
		DATE 11/24/71	

d. Allow. yield load

$$K_{bry} = 1.17 \text{ (Fig. 1.6200-9)}$$

$$F_{ty(g)} = 22,000 \text{ psi}$$

$$P_{bry} = K_{bry} F_{ty(g)} A_{br}$$

$$= 1.17 (22,000)(.030)$$

$$= 772 \text{ lb.}$$

$$MS = \frac{772}{190} - 1 = \text{High}$$

e. Oblique loading correction

$$F_2 = \sqrt{F_z^2 + F_x^2}$$

$$= \sqrt{190^2 + 130^2}$$

$$= 230 \text{ lb @ } 55^\circ 36'$$

$$P_{tru} = K_{tru} F_{tu(g)} A_{br} \sim \text{Allow tensile ult load}$$

$$K_{tru} = 0.8 \text{ (Fig. 1.6200 - 13)}$$

$$= 0.8(36,000)(.03)$$

$$= 864 \text{ lb}$$

$$MS = \frac{864}{230} - 1 = 2.75$$

$$P_{try} = K_{try} F_{ty(g)} A_{br} \sim \text{Allow yield load}$$

$$K_{try} = 0.60 \text{ (Fig. 1.6200-4c)}$$



**Aerospace
Systems Division**

Appendix C - Structural Analyses
(Mortar Box/Pallet Structural
Attachment Analysis)

NO.	REV. NO.
ATM 1064	
PAGE <u>130</u>	OF <u>212</u>
DATE	11/24/71

$$P_{try} = 0.60(22,000)(.030)$$
$$= 396 \text{ lb}$$

$$MS = \frac{396}{230} - 1 = 0.72$$

The locking mechanism (2369289) is stronger than the lug carrier frame. Therefore this attachment is structurally adequate.

The plate section of this fitting is also stronger than the lug section. Hence, the plate section is adequate.

Rivet strength (holding the carrier frame to the mortar box frame) is greater than the lug strength. The tension capability of the rivets is 1125 lb.



**Aerospace
Systems Division**

ASE REDESIGN EVALUATION		NO.	REV. NO.
		ATM-1064	
PAGE <u>131</u>		OF <u>212</u>	
DATE		11/24/71	

APPENDIX D - LRC DATA

(Pressure, Accelerometer, and
Strain Gauge Data)



**Aerospace
Systems Division**

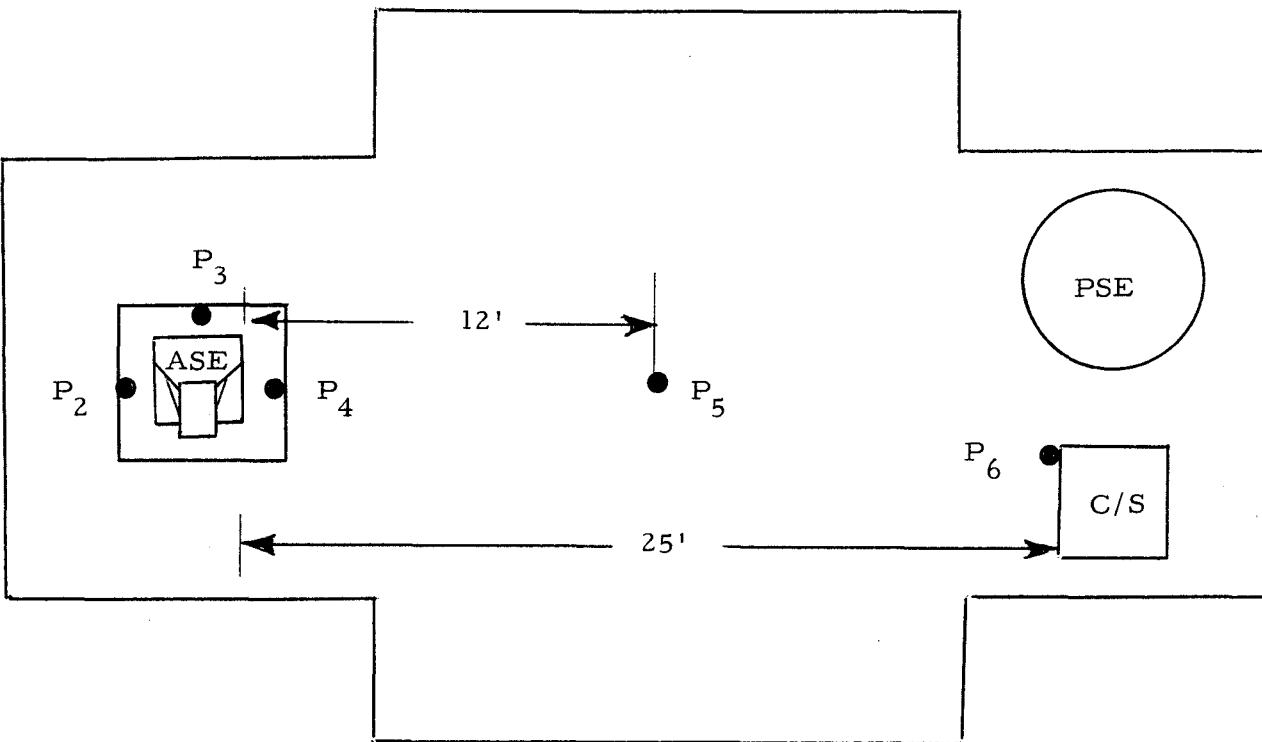


Figure D-1 Pressure Transducer Locations

ASE REDESIGN EVALUATION

NO.	ATM-1064	REV. NO.
PAGE	132	OF 212
DATE	11/24/71	



**Aerospace
Systems Division**

ASE REDESIGN EVALUATION

NO.	REV. NO.
ATM-1064	
PAGE <u>133</u>	OF <u>212</u>
DATE	11/24/71

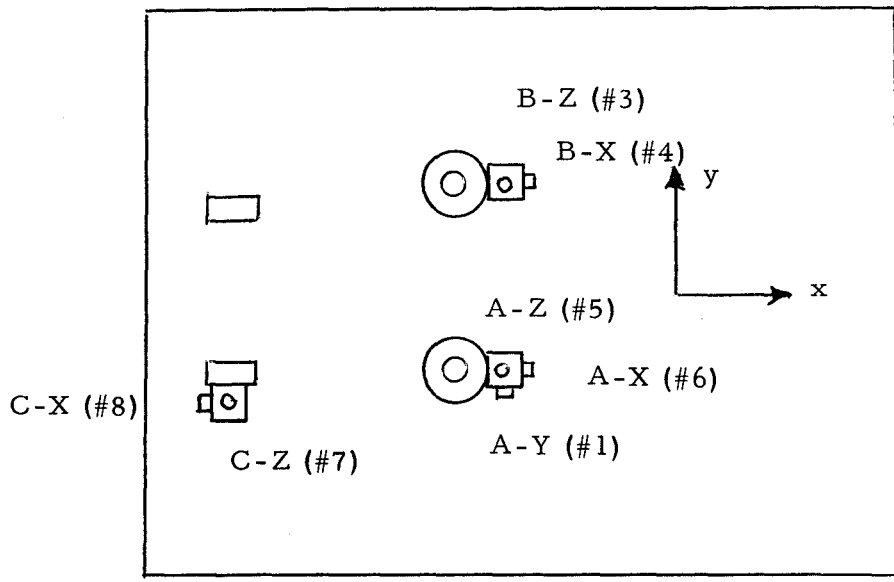
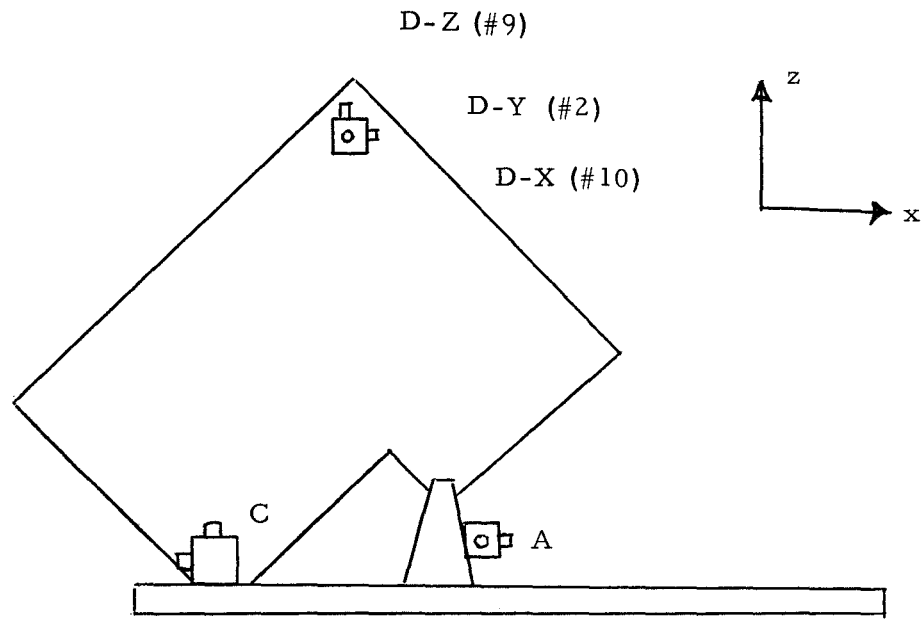


Figure D-2 Mortar Box/Pallet Accelerometer Locations



**Aerospace
Systems Division**

ASE REDESIGN EVALUATION

NO. ATM-1064

REV. NO.

PAGE 134 OF 212

DATE 11/24/71

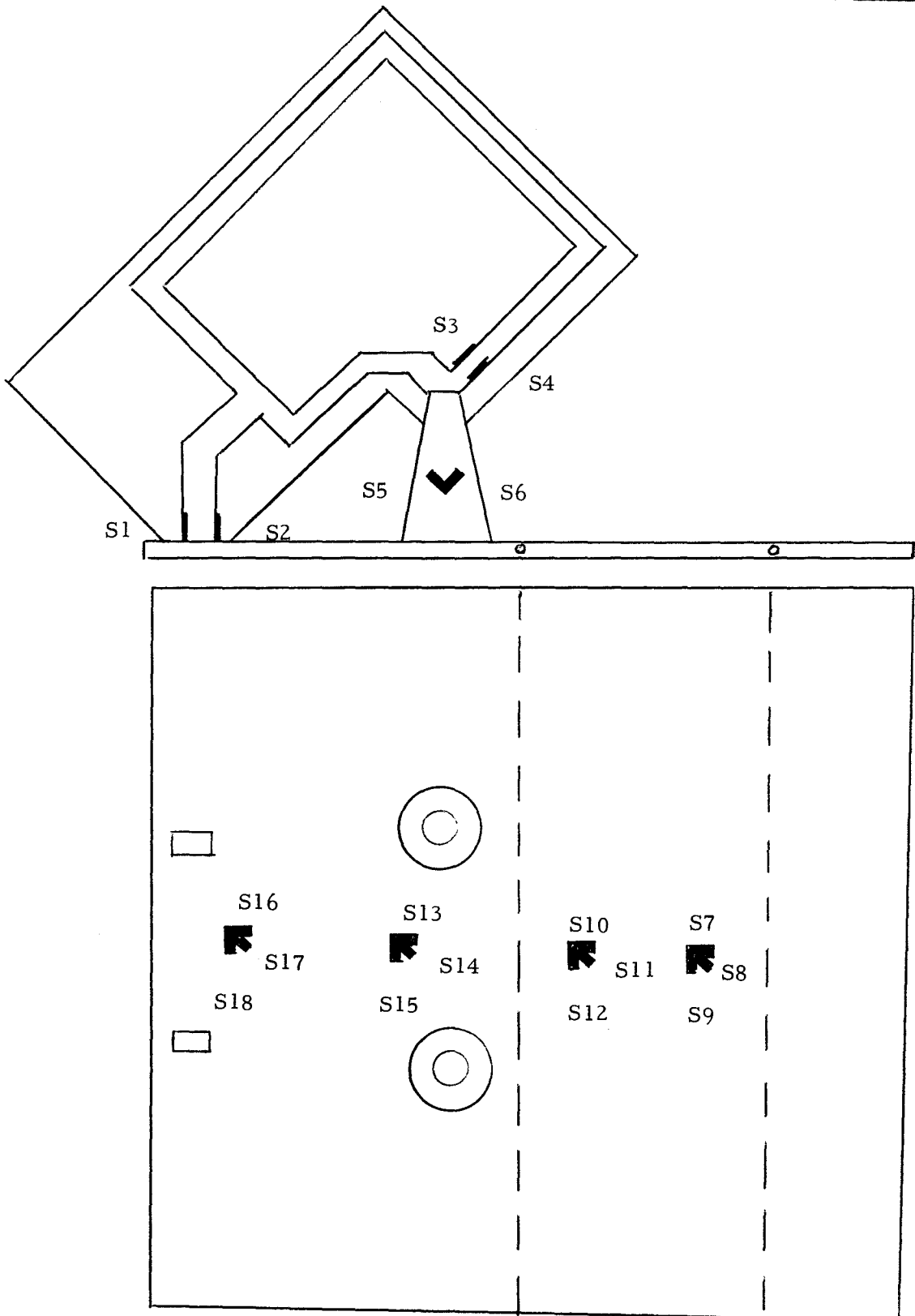


Figure D-3 Strain Gauge Locations

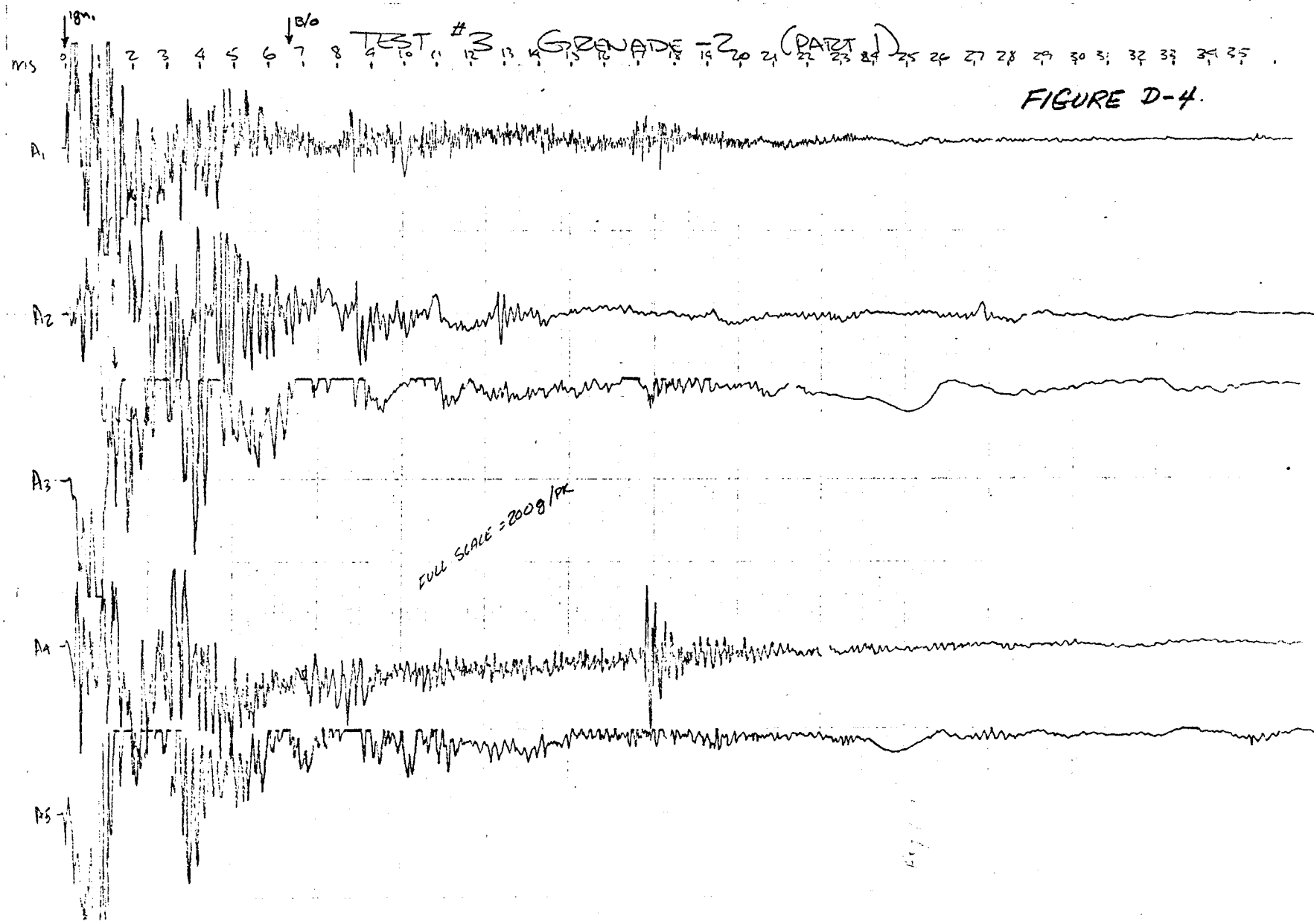


FIGURE D-4.

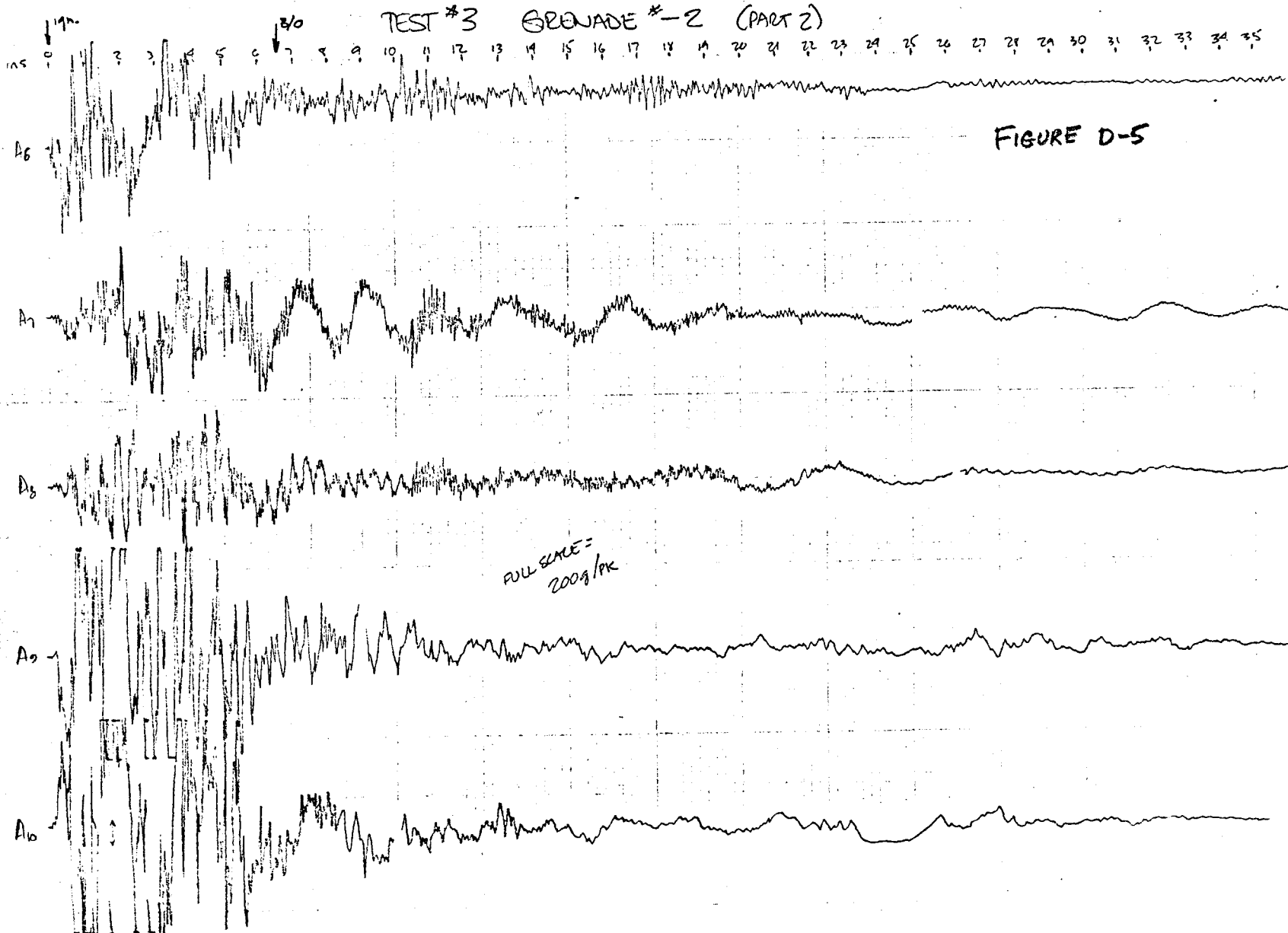
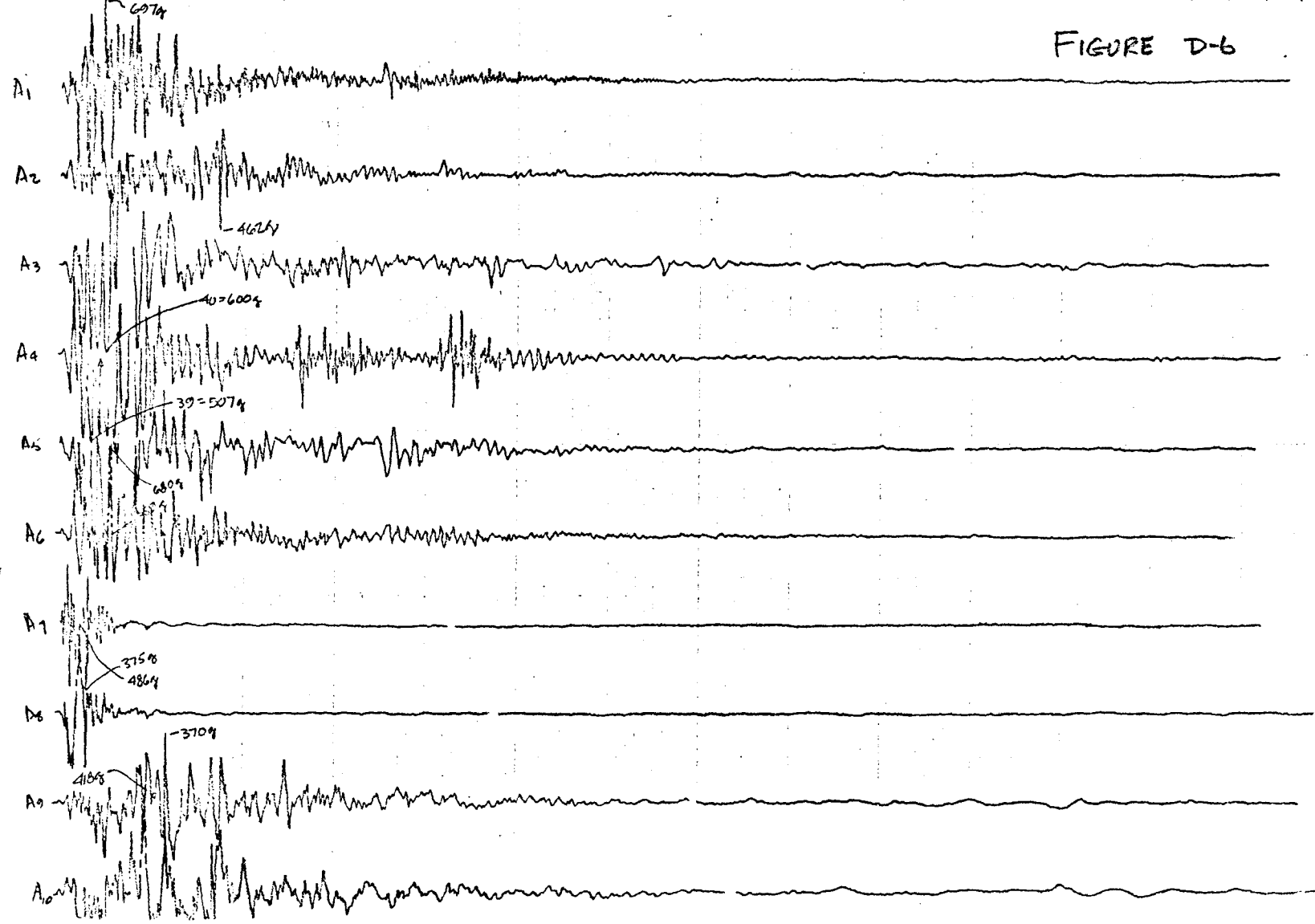


FIGURE D-5

↓ 18" 0 1 2 3 4 5 6 7 8 9 10 11 12 13 14 15 16 17 18 19 20 21 22 23 24 25 26 27 28 29 30 31 32 33 34

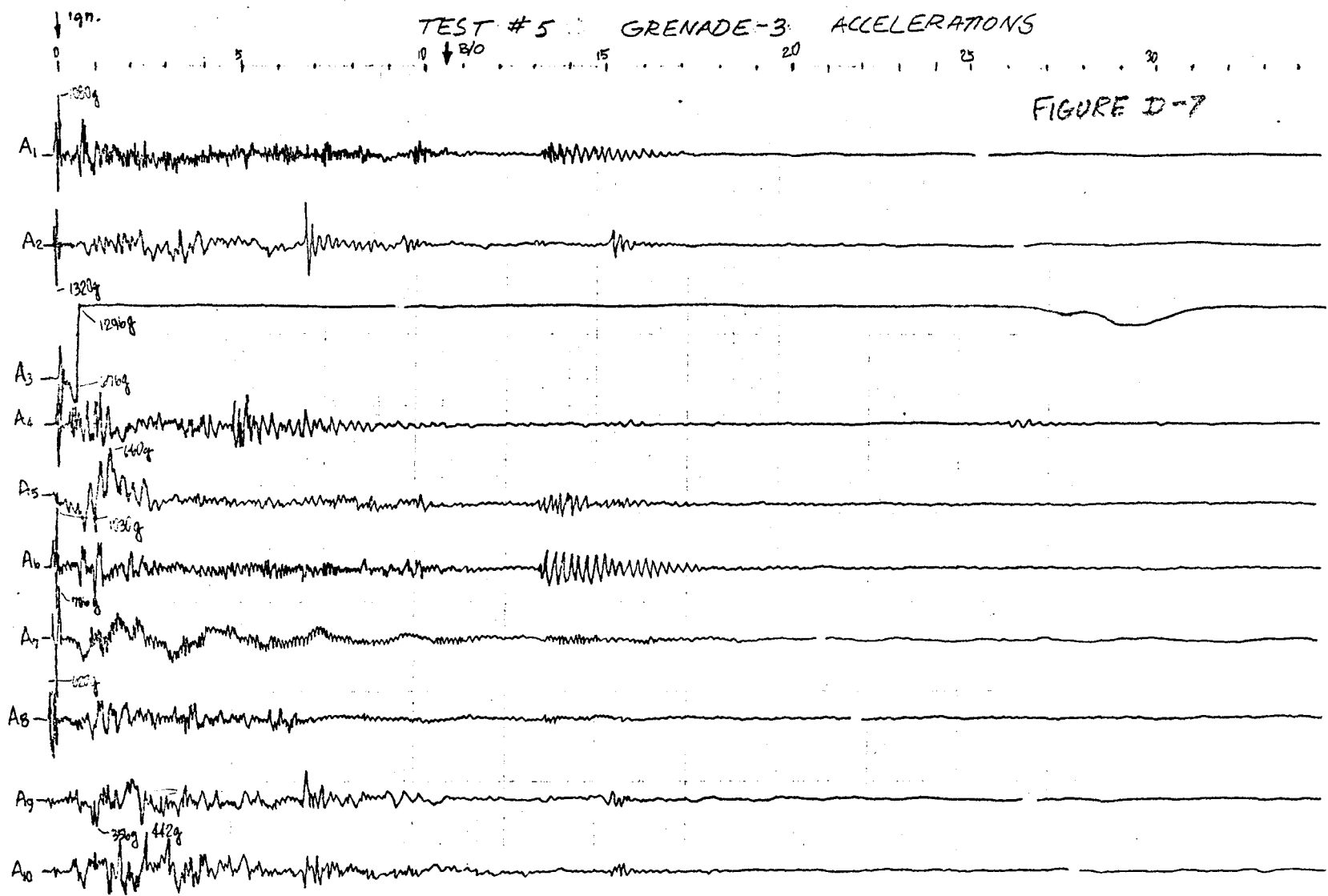
TEST #1 GRENADE - 9 ACCELERATIONS

FIGURE D-6



TEST #5 GRENADE-3 ACCELERATIONS

FIGURE D-7



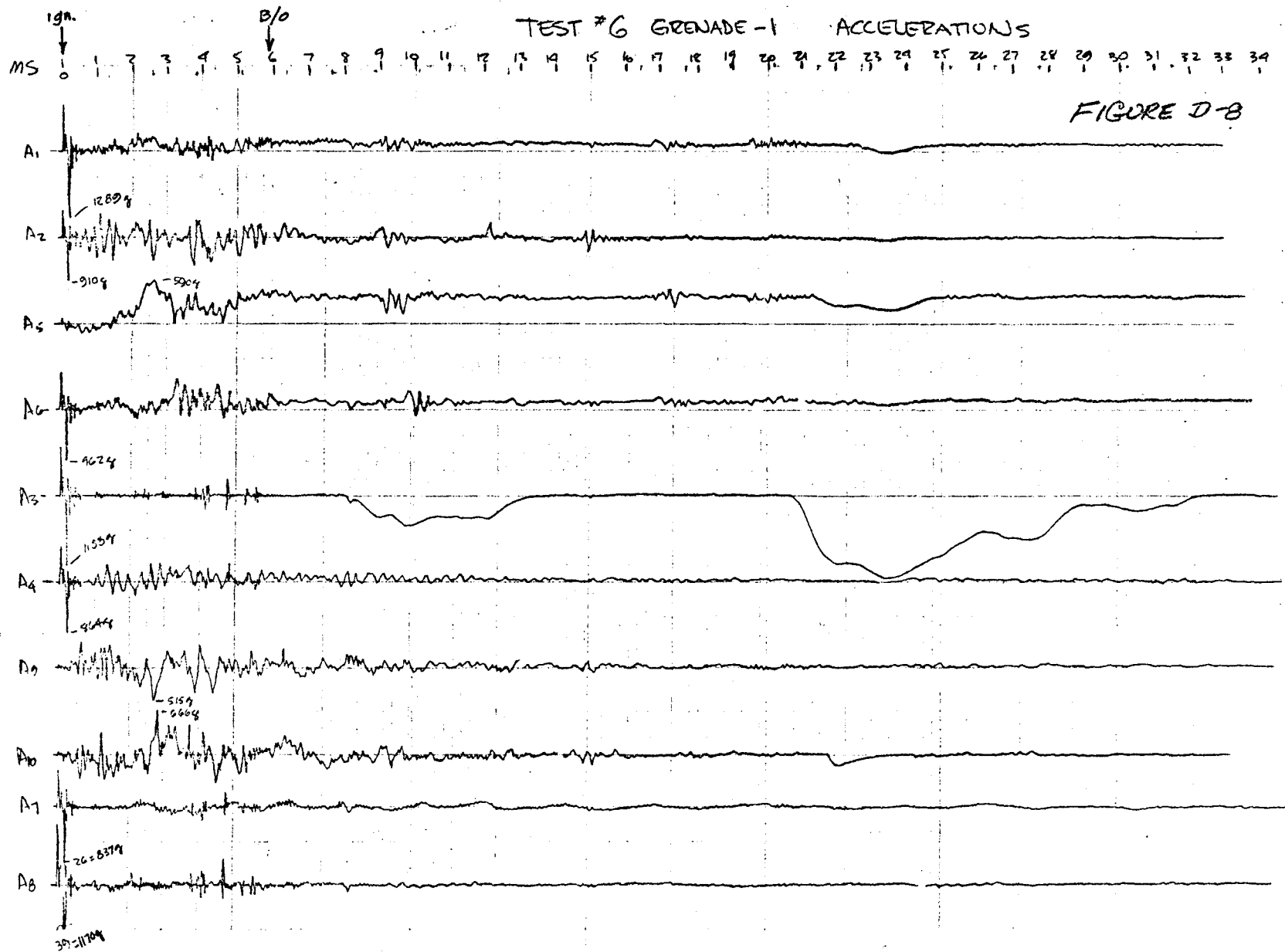


FIGURE D-8

TEST # 7 GRENADE - 2 ACCELERATIONS

0 5 10 15 20 25 30

milli-sec

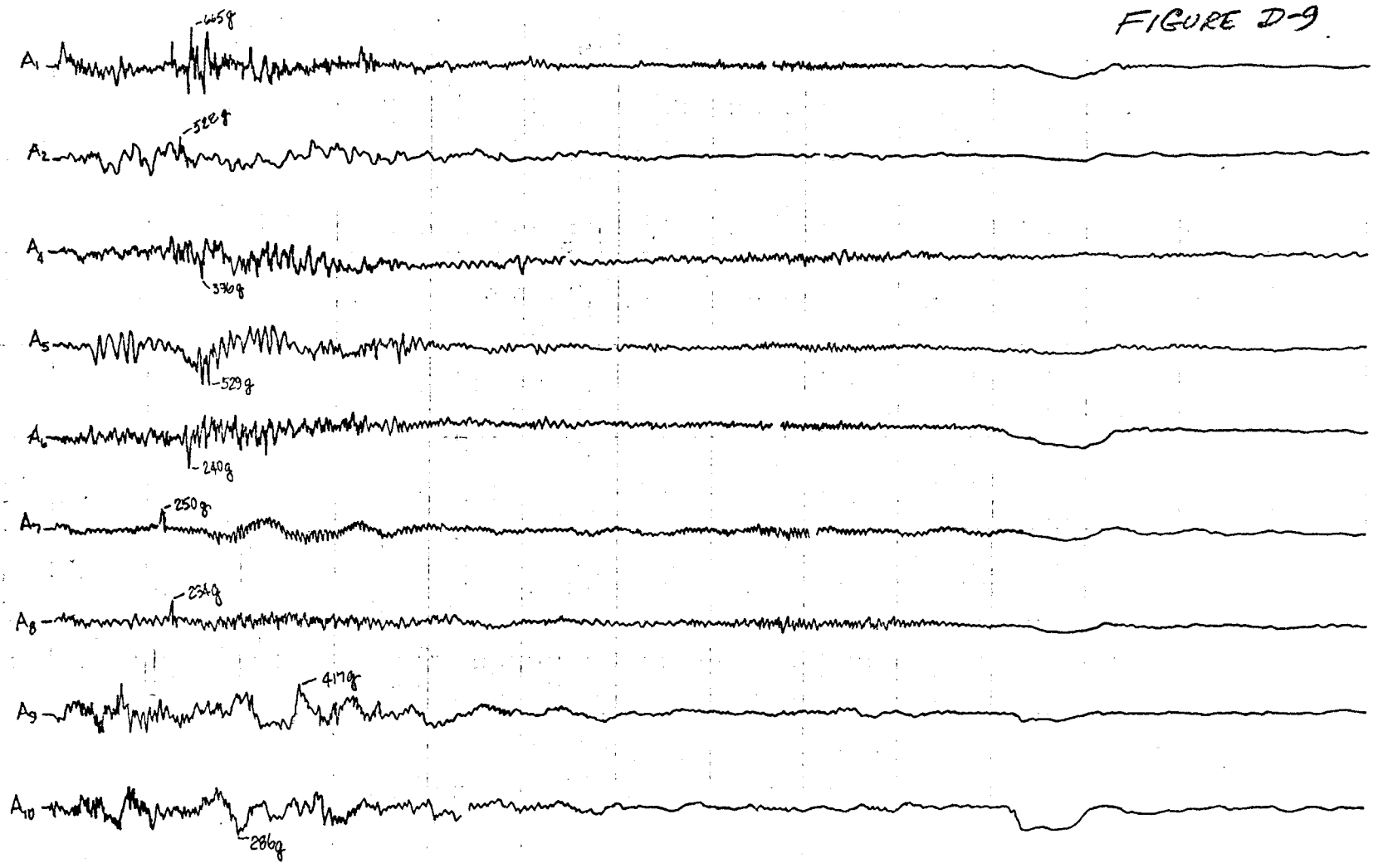


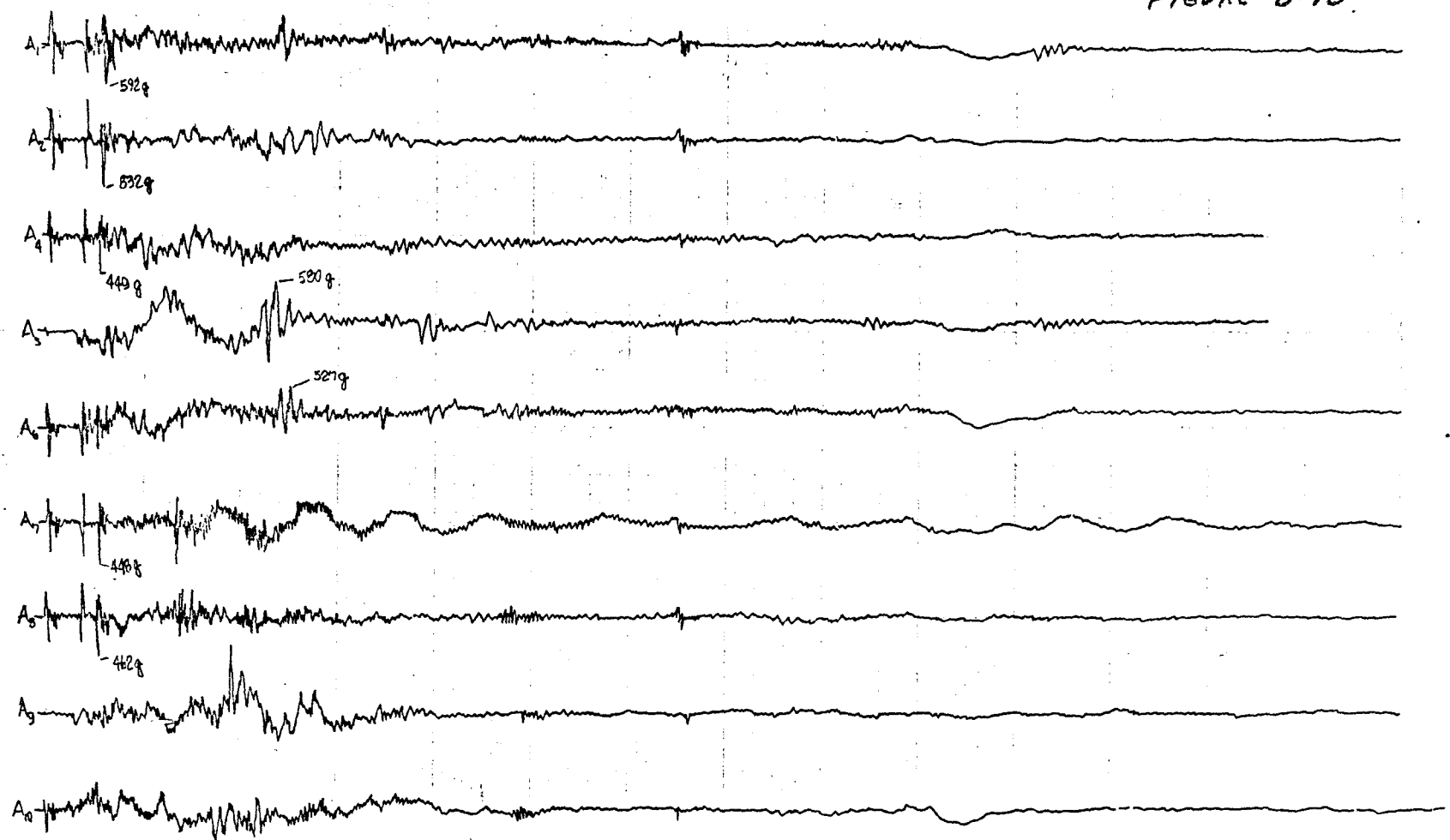
FIGURE D-9

ignition
0
MILLI-SEC

5 10 15 20 25 30

TEST # 3 GRENADE-1 ACCELERATIONS

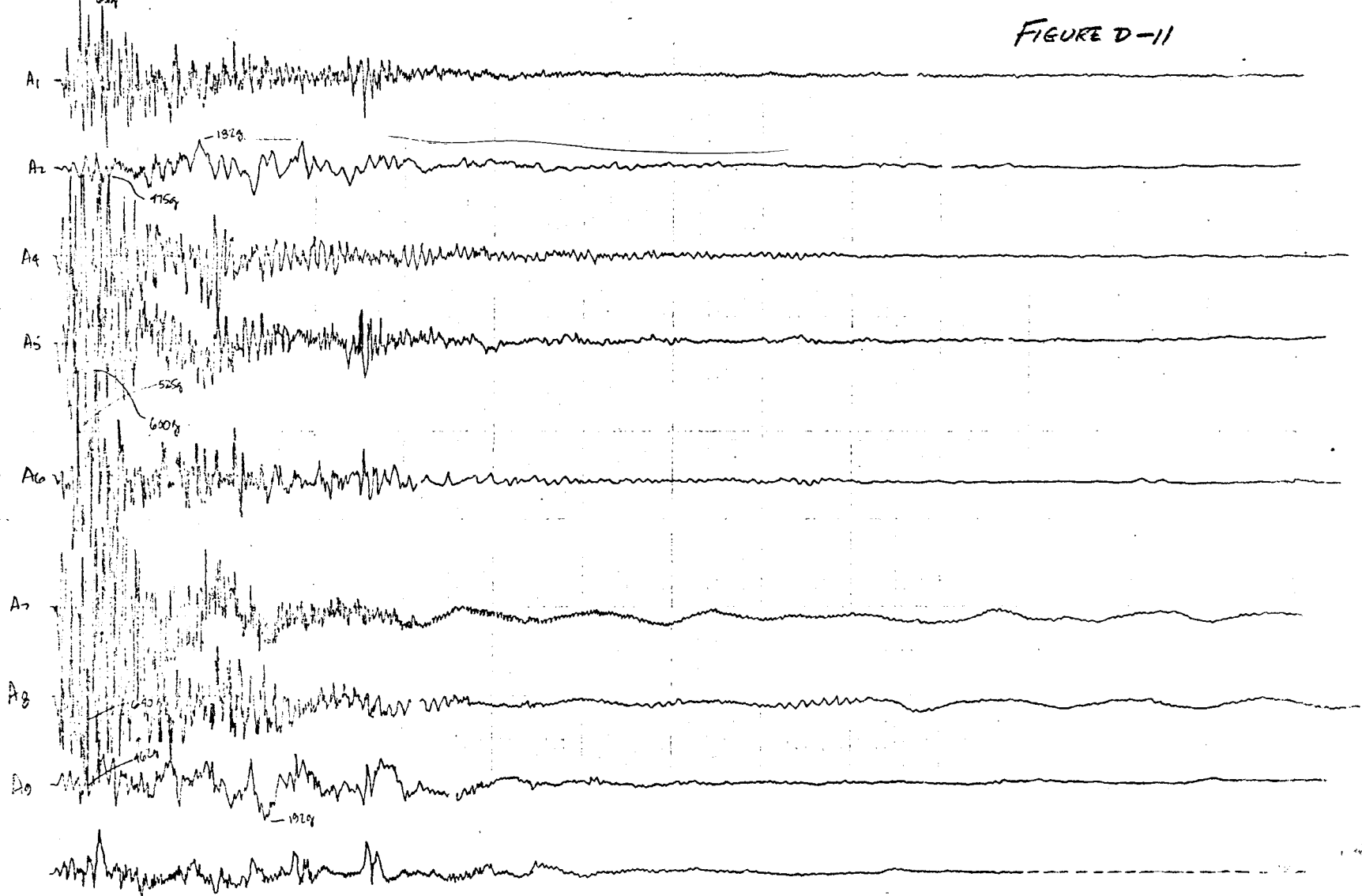
FIGURE D-10.



TEST #9 GRENADE - 4 ACCELERATIONS

ms 0 1 2 3 4 5 6 7 8 9 10 11 12 13 14 15 16 17 18 19 20 21 22 23 24 25 26 27 28 29 30 31 32 33 34 35

FIGURE D-11



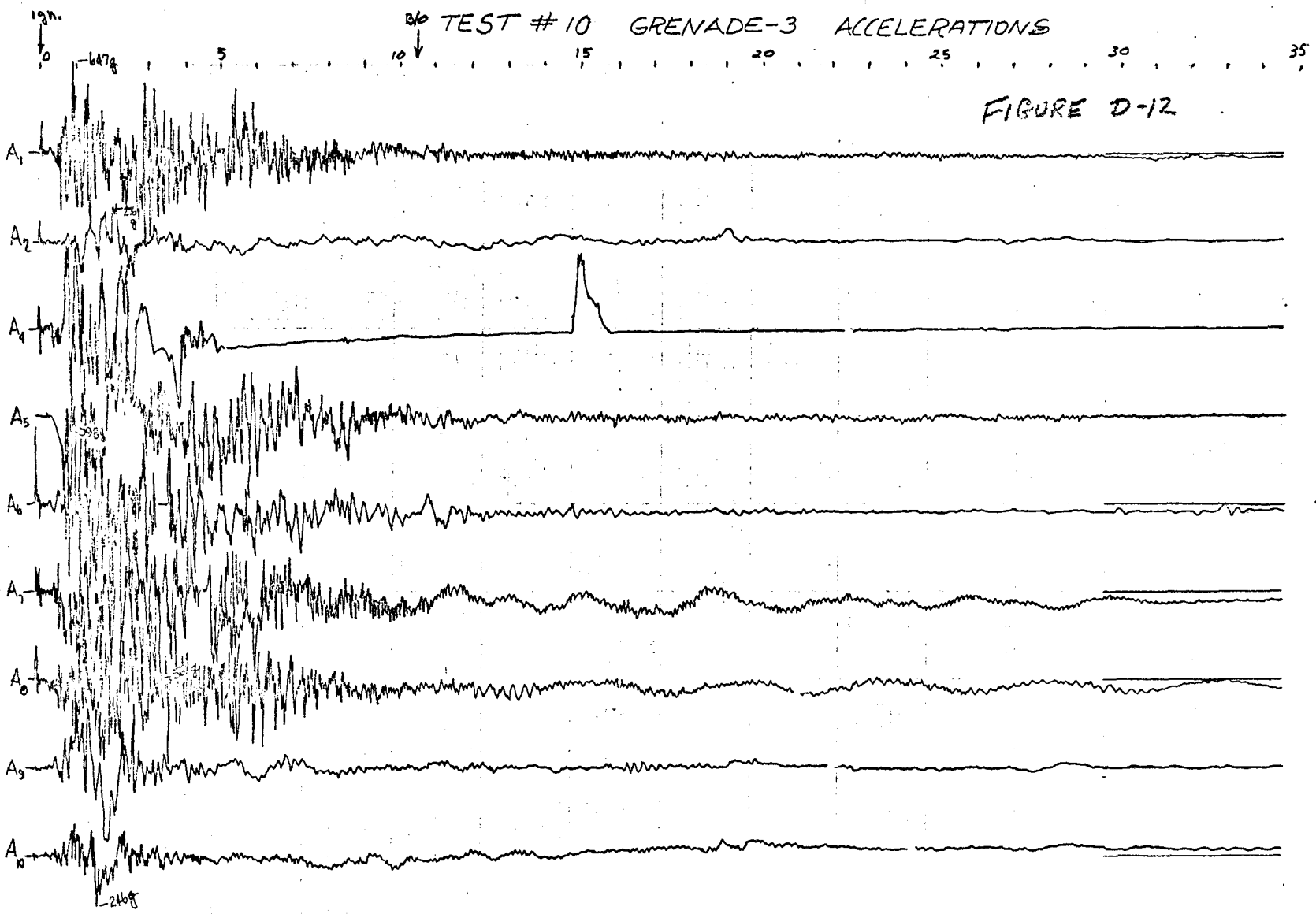


FIGURE D-12

TEST #3 GRENADE-2 ACCELERATIONS (VERTICAL)

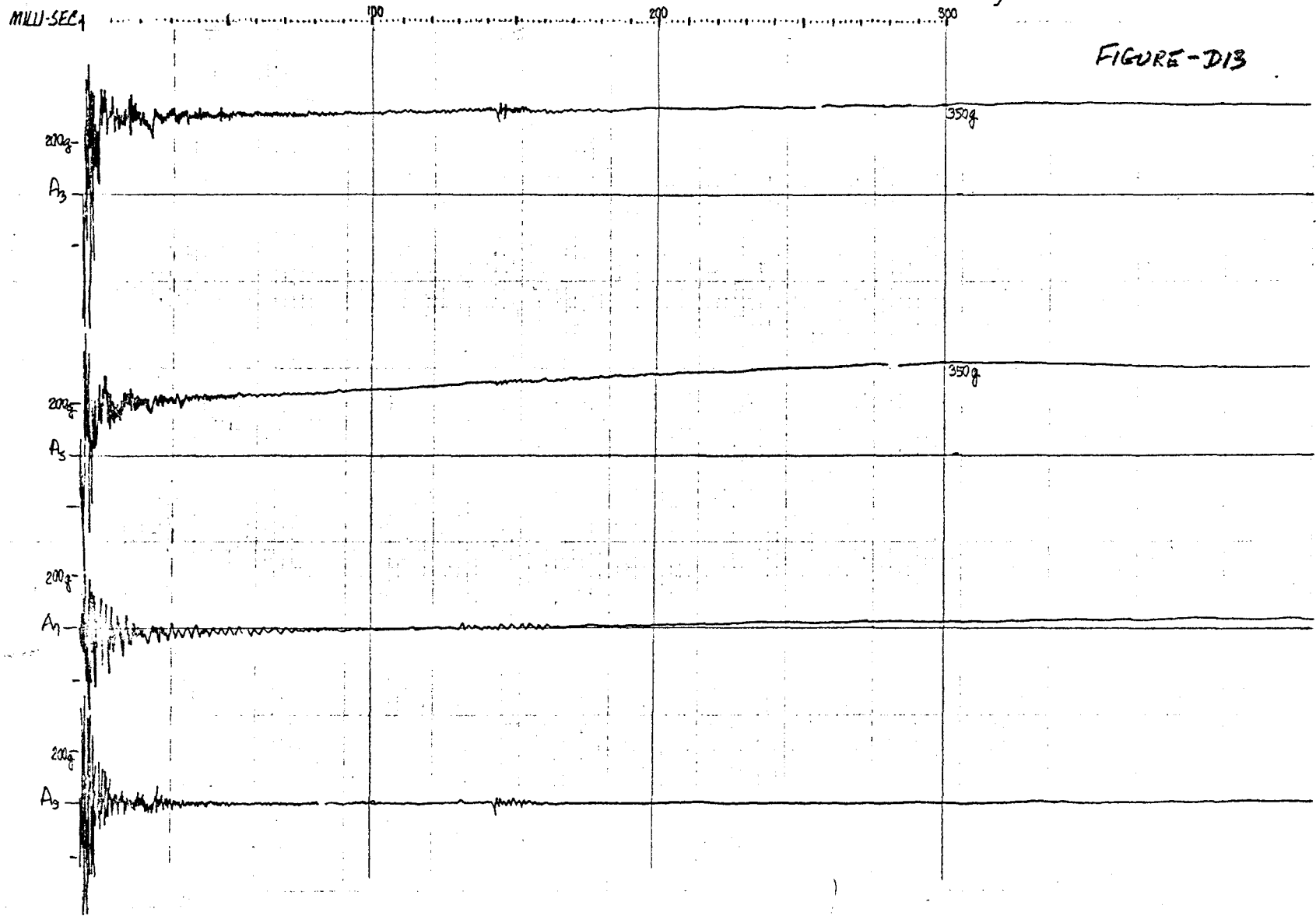
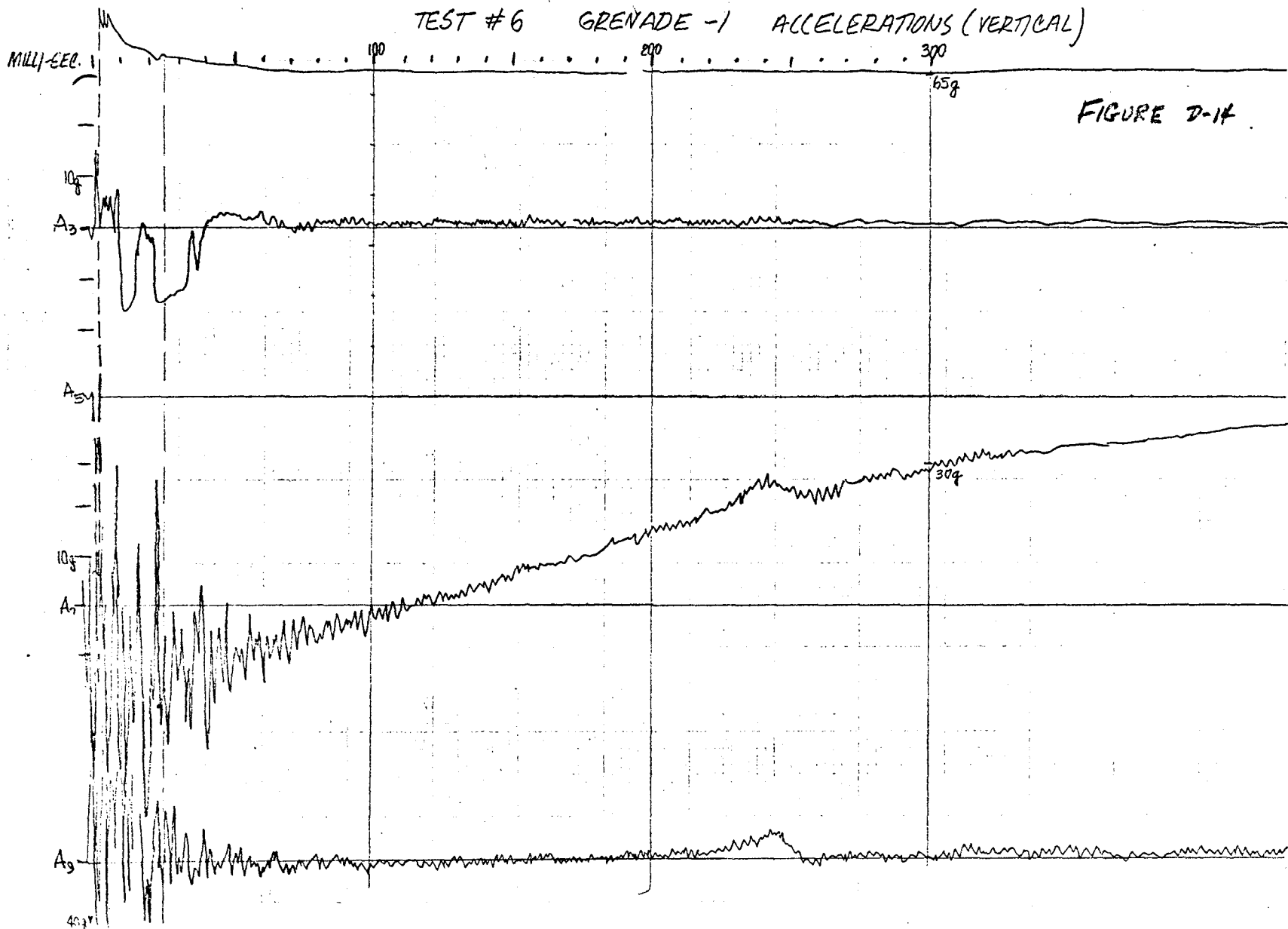


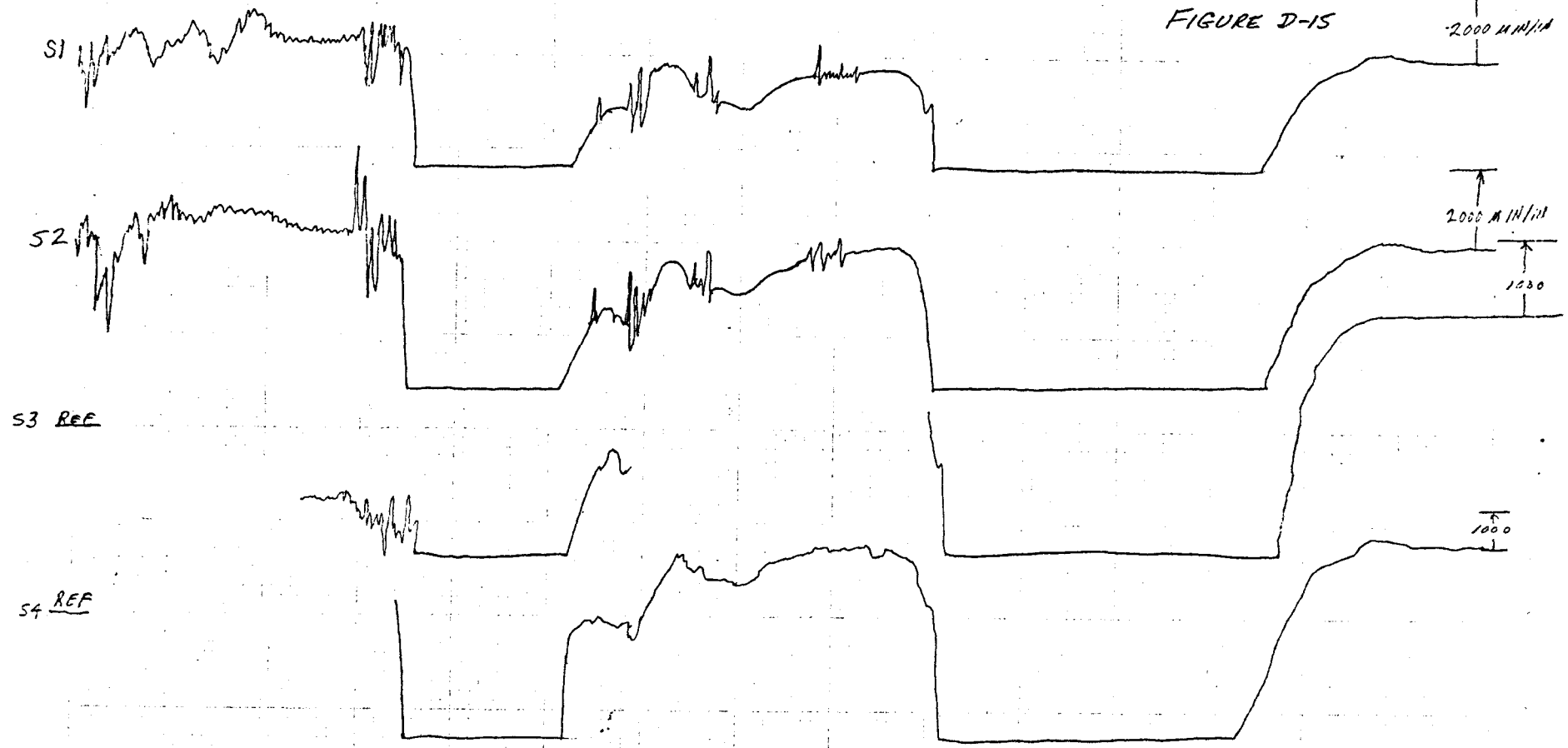
FIGURE-D13

TEST #6 GRENADE -1 ACCELERATIONS (VERTICAL)



BURN TIME = 6.7
TEST # 3 V GRENADE NO. 2
TIME 0 5 10 15 20 25 30 35 MS

FIGURE D-15

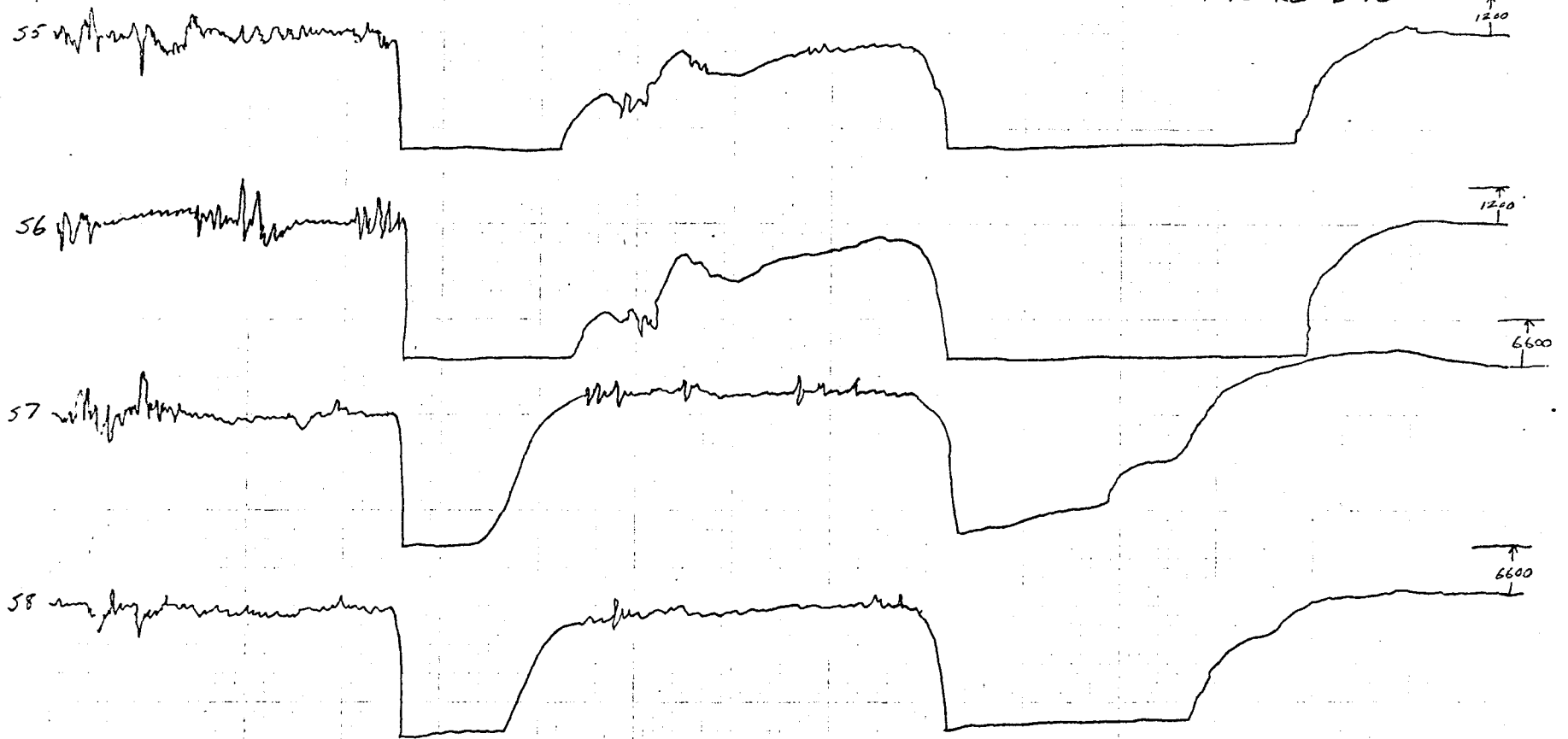


BURN TIME: 6.7

TEST # 3 ~ GRENADE No. 2

TIME 0 5 10 15 20 25 30 35

FIGURE D-16

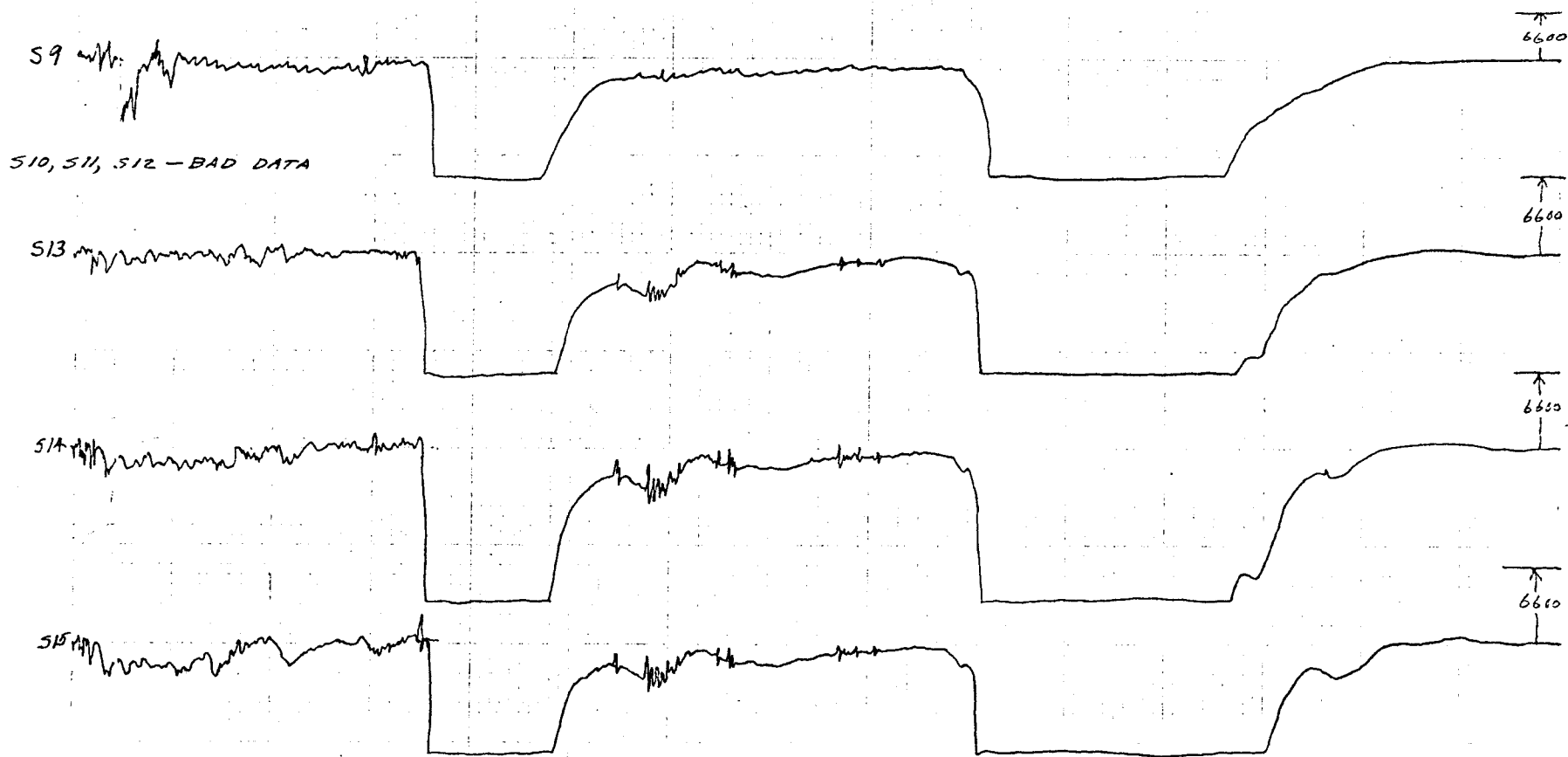


BURN TIME: 6.7

TEST NO. 3 ~ GRENADE NO. 2

TIME 0 5 10 15 20 25 30 35

FIGURE D-17



BURN TIME: 6.7

TEST NO. 3 W GRENADe No. 2

TIME 5 10 15 20 25 30 35

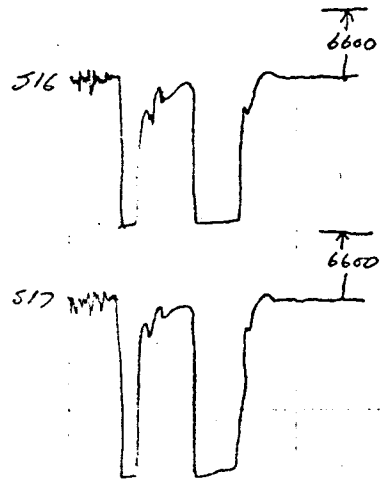


FIGURE D-18

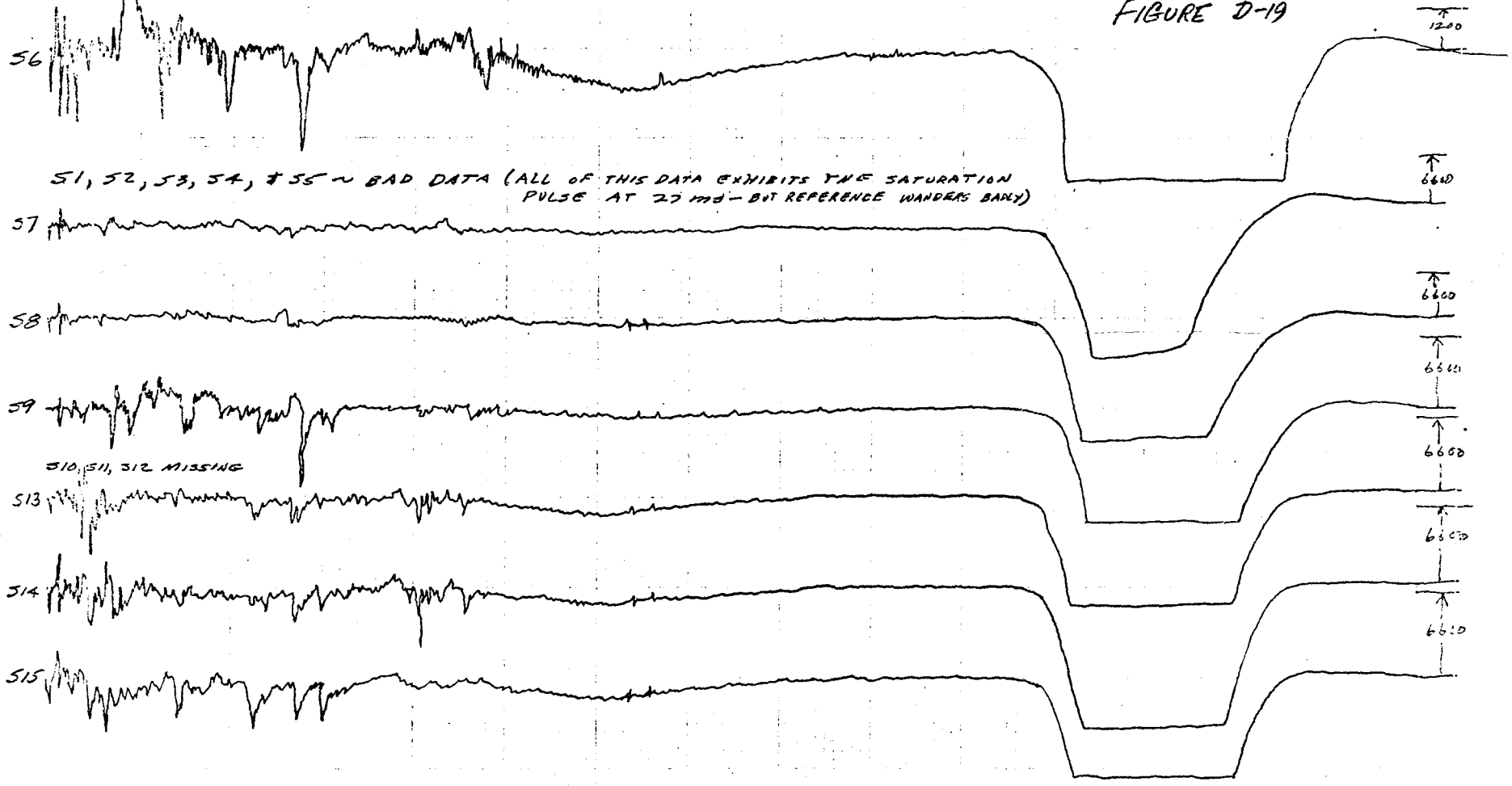
518 - BAD DATA

BURN TIME : 9.5

TEST NO. 4 ~ GRENADE No 4

TIME 0 5 10 15 20 25 30 35

FIGURE D-19



51, 52, 53, 54, & 55 ~ BAD DATA (ALL OF THIS DATA EXHIBITS THE SATURATION PULSE AT 22 MS - BUT REFERENCE WANDERS BAWY)

510, 511, 512 MISSING

1210

6610

6600

6610

6610

6610

6610

BURN TIME: 6.5

TEST NO. 4 - GRENADE NO. 4

TIME 0 5 10 15 20 25 30 35 40

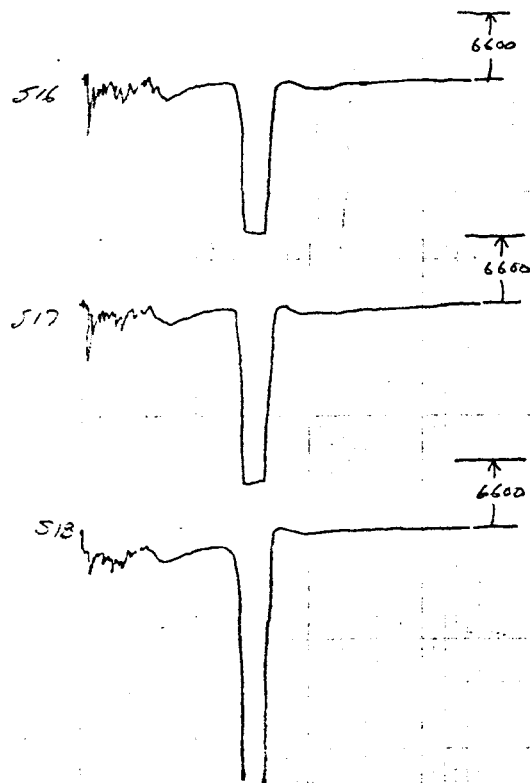
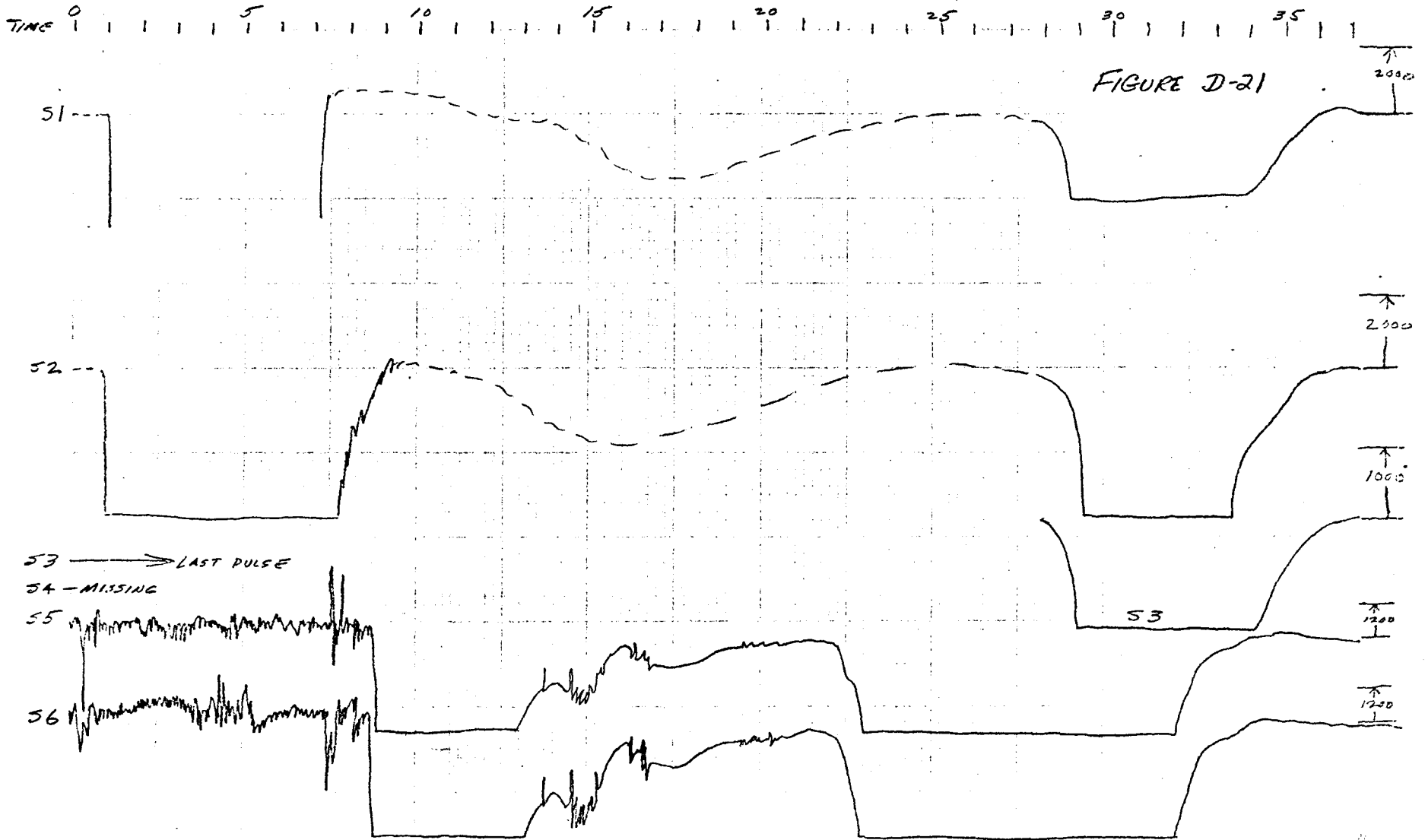


FIGURE D-20

BURN TIME: 10.5

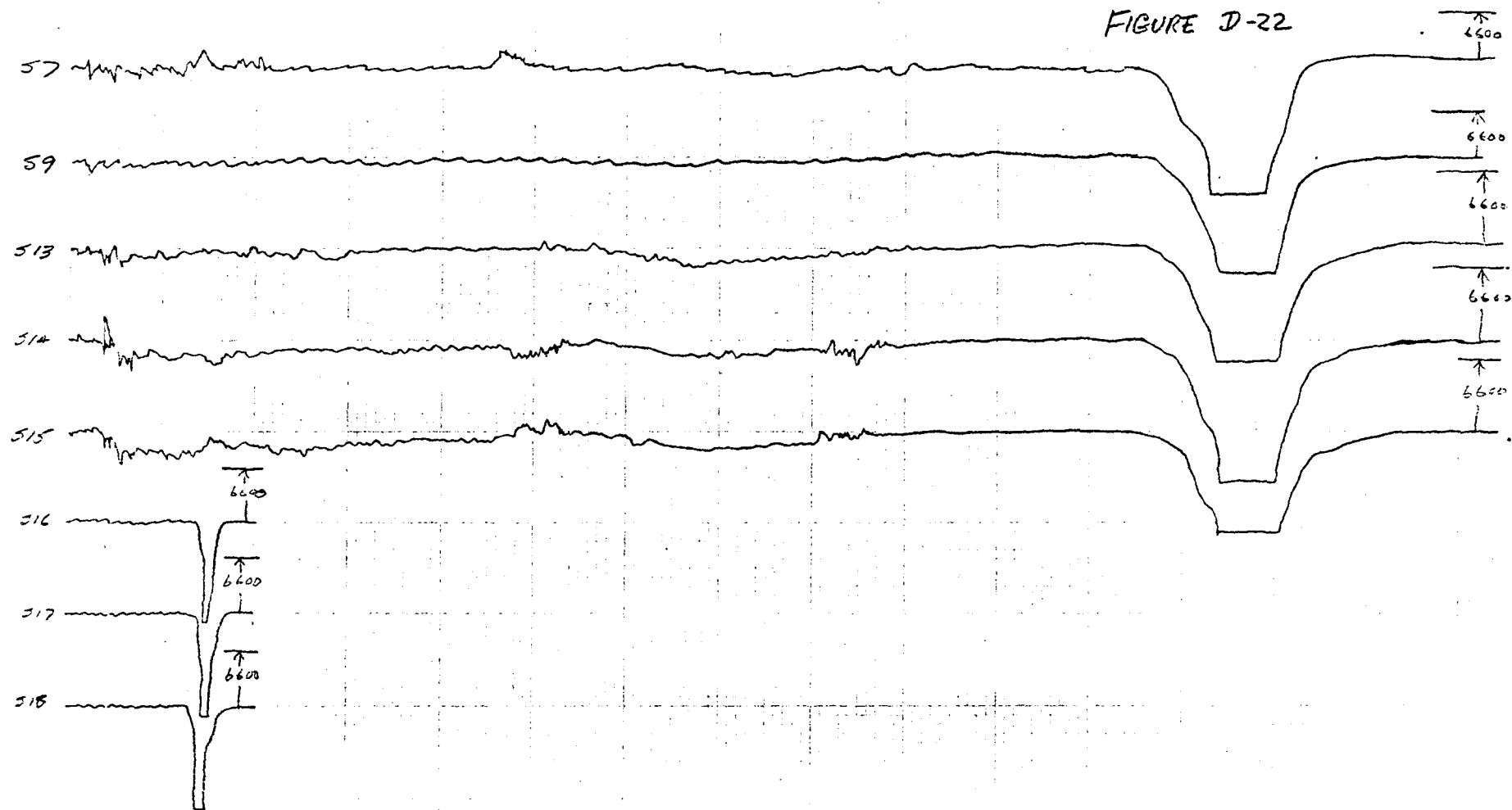
TEST NO. 5 ~ GRENADE NO. 3



BURN TIME: 10.5 TEST NO. 5 - GRENADE No. 3

TIME 0 5 10 15 20 25 30 35

FIGURE D-22



TIME 0 5 10 15 20 25 30 35 40
11, 12, 18

TEST #6 GRENADE-1 (SHEET 1)

(USE TIME SCALE ON SHT 2)

S₁ NO DATA

2000

S₂

1000

S₃

S_{4,5,6} NO DATA

S₇

1000

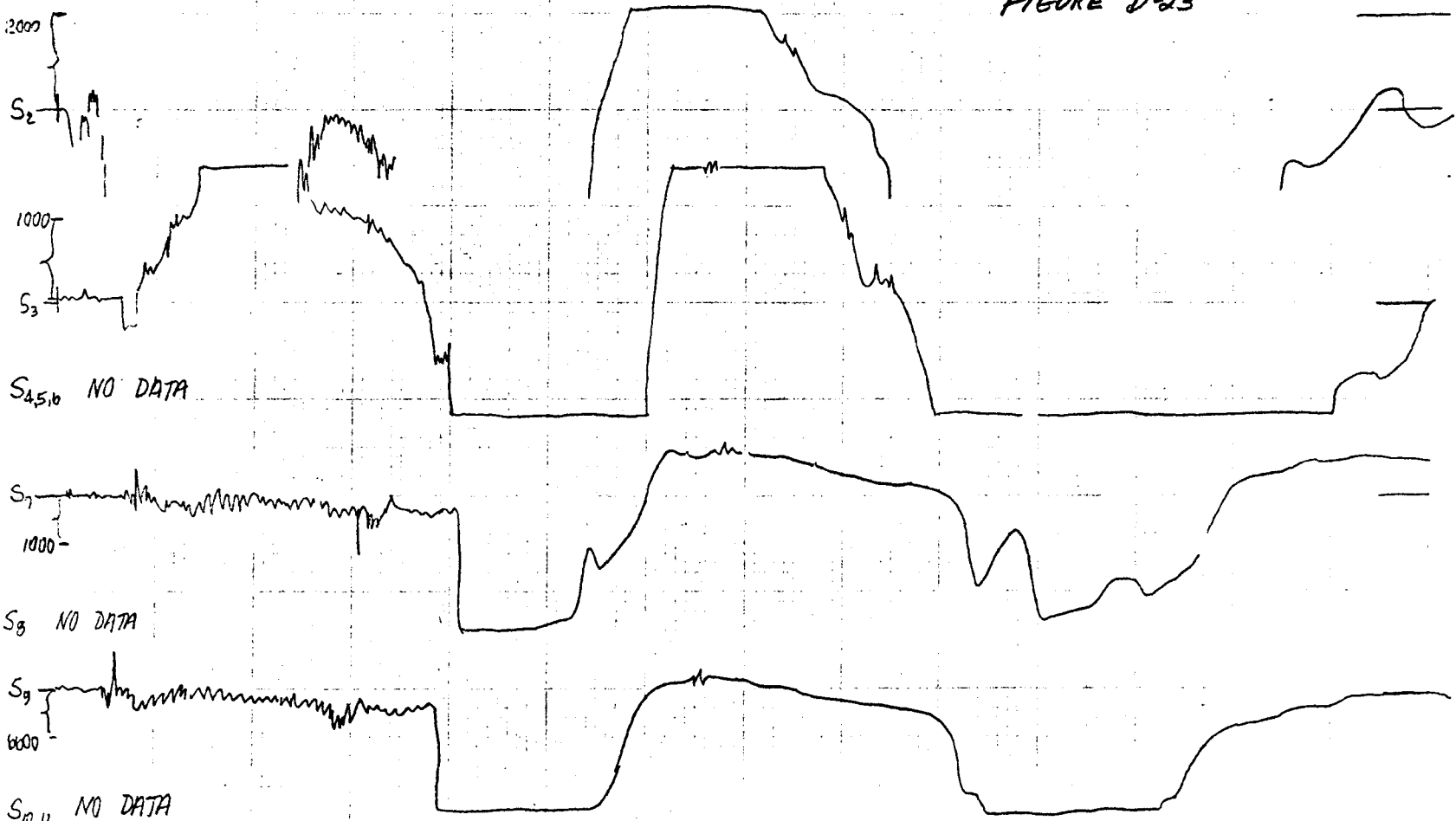
S₈ NO DATA

S₉

6000

S_{10,11} NO DATA

FIGURE D-23



TEST #6 GREYRDE -1 (SHEET 2)

MILLI-SECS 0 10 20 30

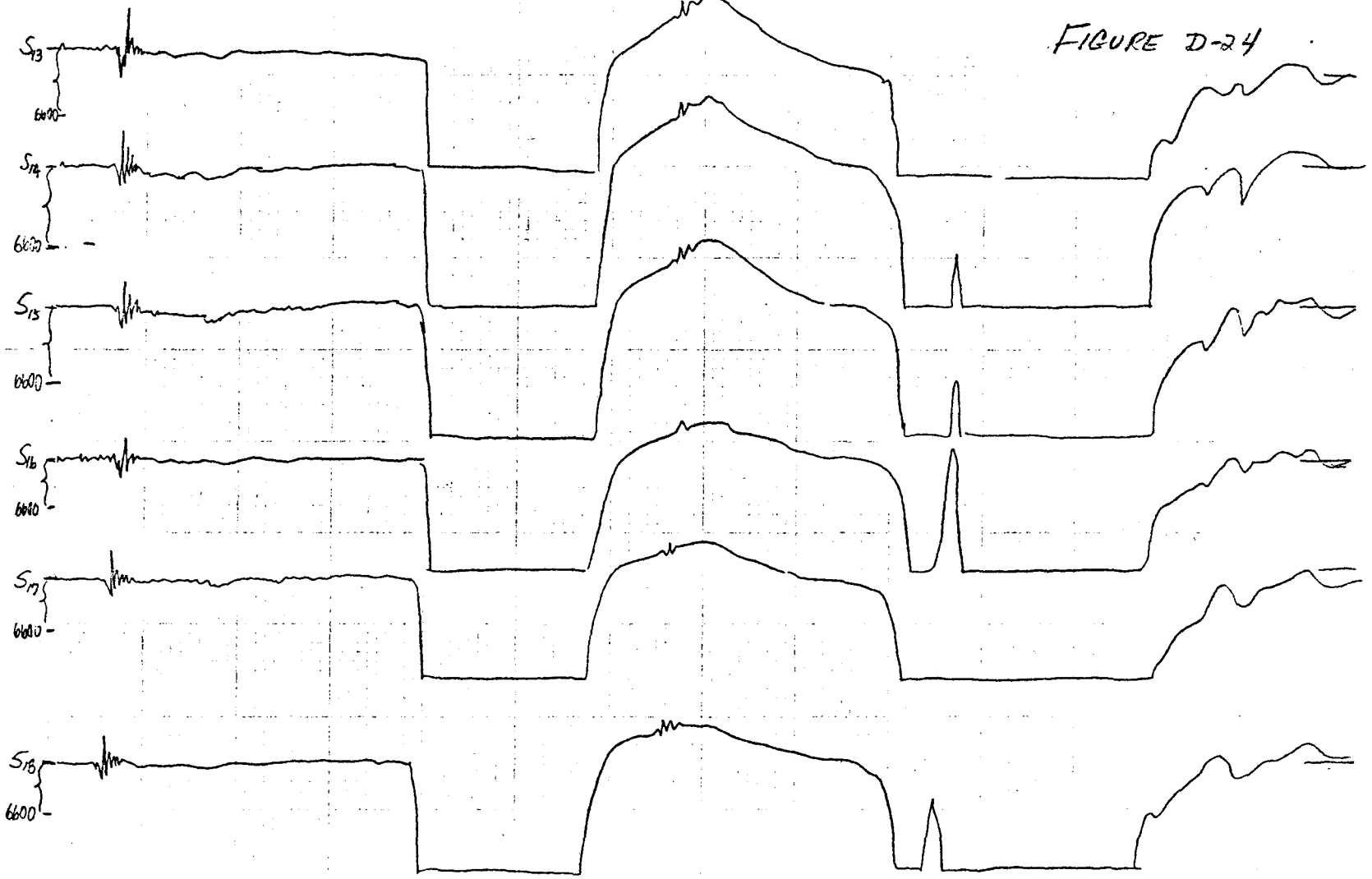
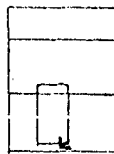


FIGURE D-24

0.002 b
0.002 9



LOCATION OF GAUGES

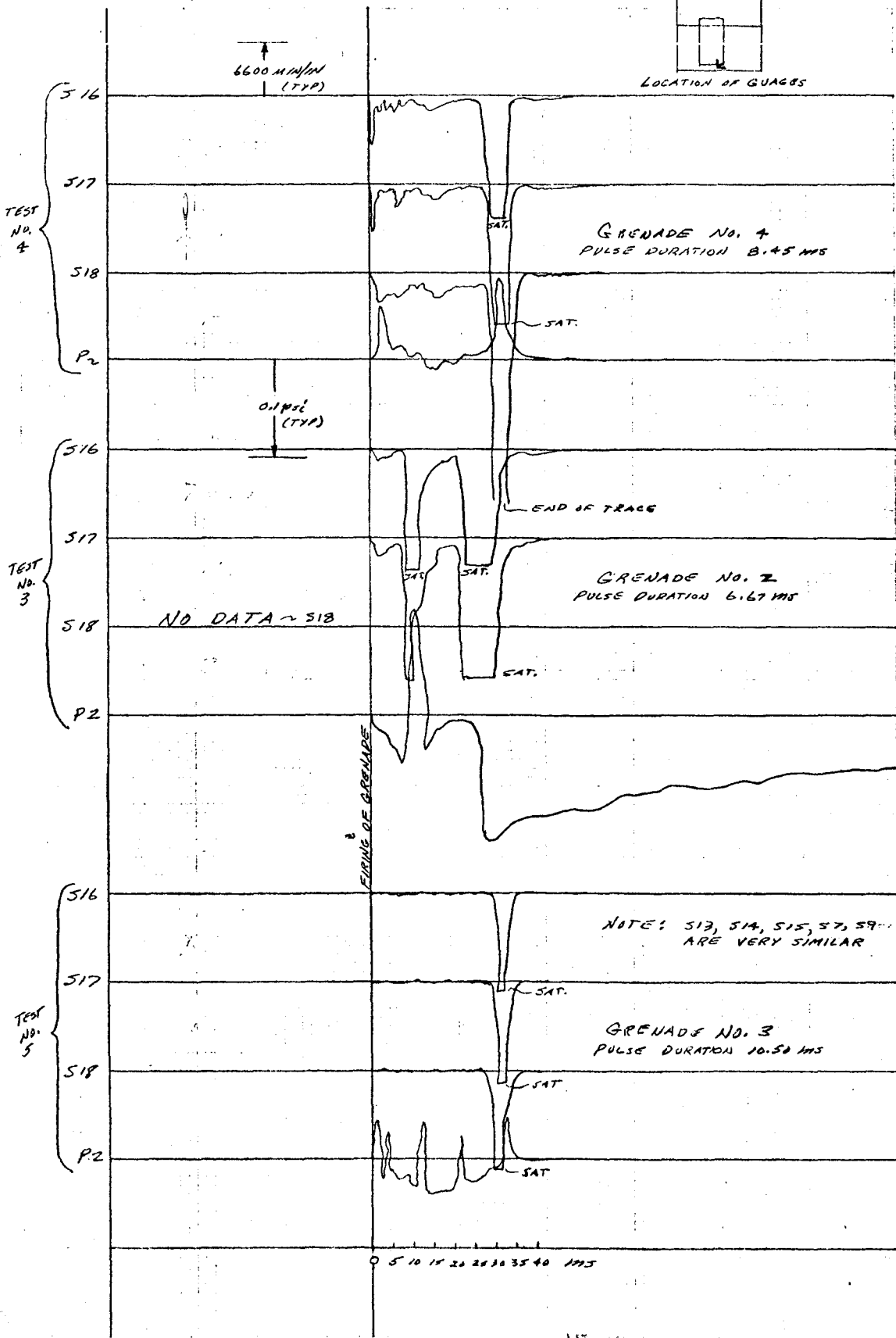


FIGURE D-25

17 1000 4001
 11 1000 200000
 11 1000 400000
 11 1000 200000

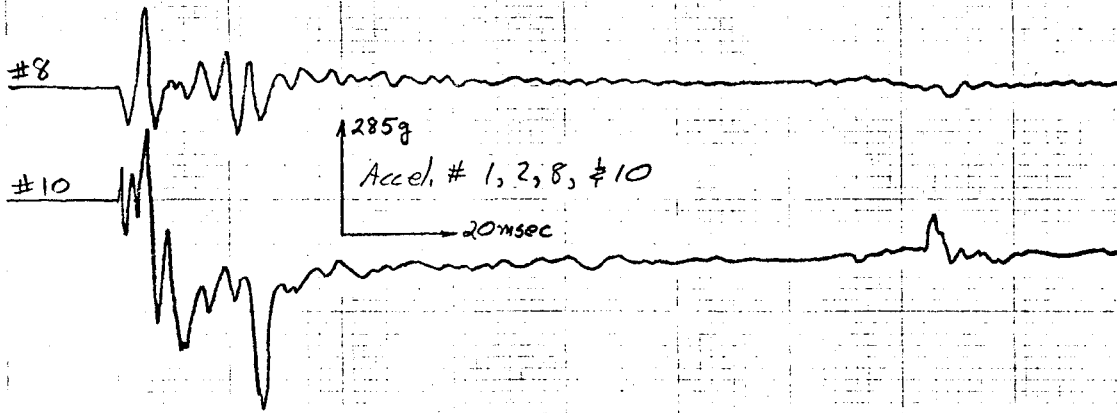
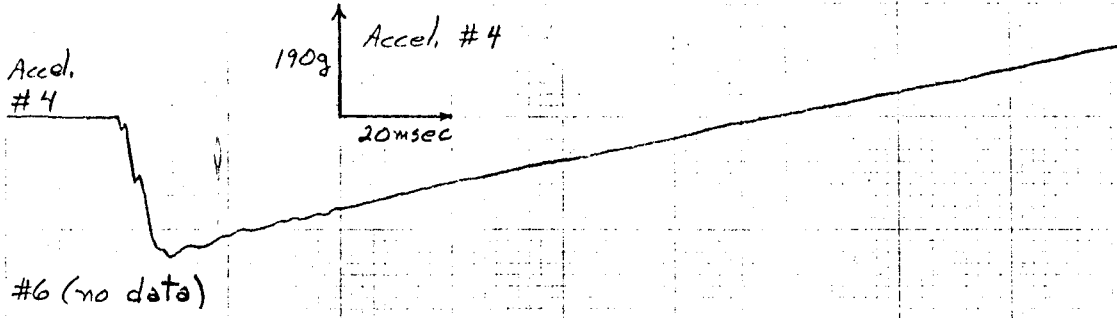
Filtered LRC Accelerometer Data

Accelerometer locations on MBA/Platform

<u>LOCATION</u>	<u>ACCEL. #</u>	<u>ACCEL. DIR.</u>
A-left pedestal	6, 1, 5	x, y, z respectively
B-rt. "	4, 3	x, z
C-fwd. support	8, 7	x, z
D-top MBA	10, 2, 9	x, y, z

FIGURE D-26

LRC-ASE ACCELEROMETER DATA (FILTERED ABOVE 100 Hz)
Test #3 (Eren. -2)
x-axis



y-axis

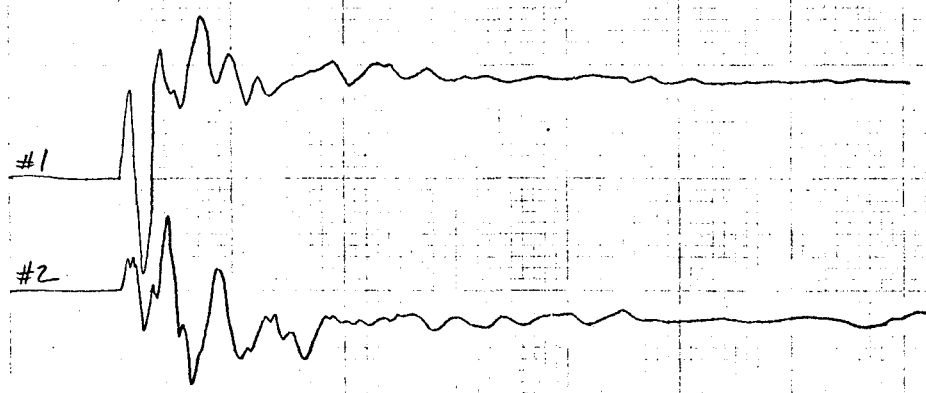


FIGURE D-27

LRC Filtered Accel. Data
Test #3 (Gren. -2)

Z-AXIS

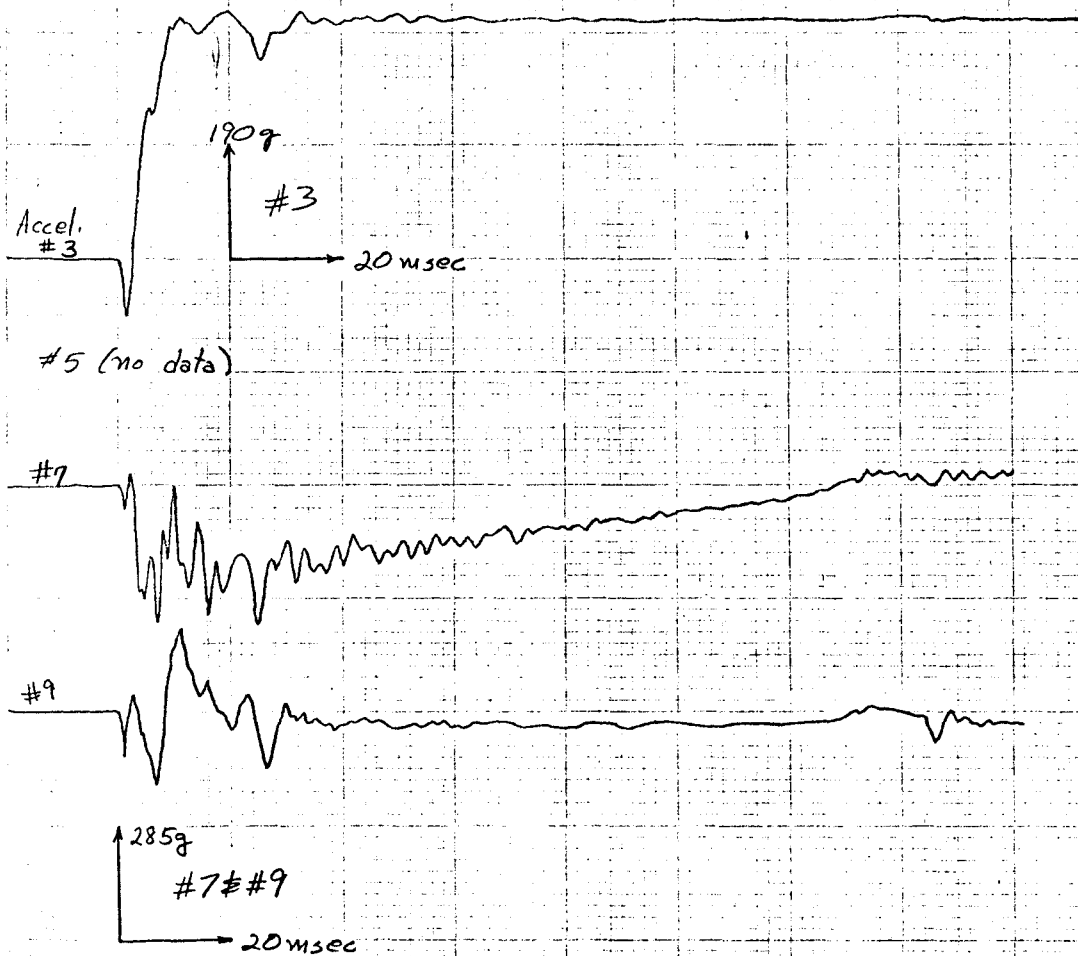
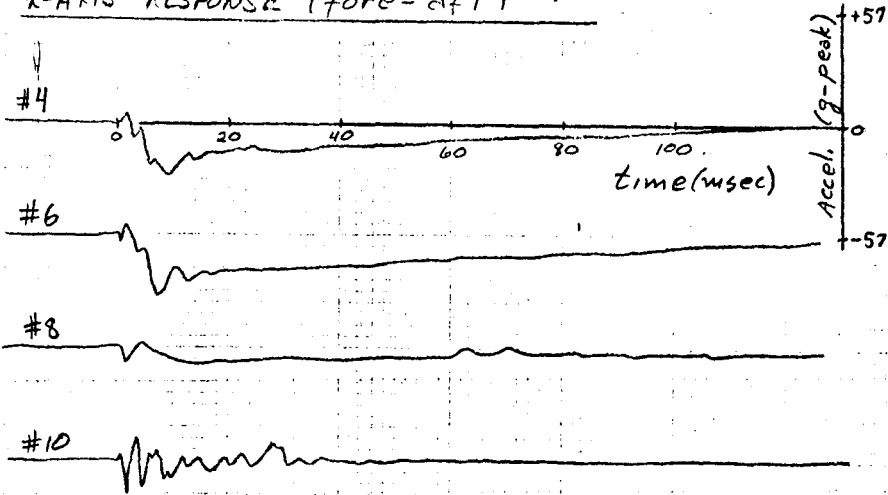


FIGURE D-28

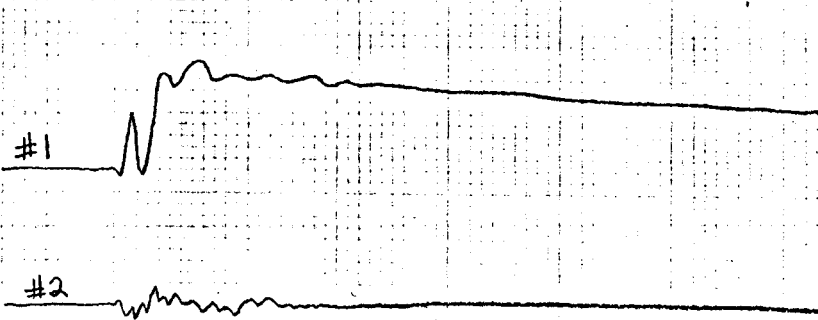
LRC-NSE ACCELEROMETER DATA (FILTERED ABOVE 100 Hz)

TEST #4 (GREN. -4)

X-AXIS RESPONSE (fore-aft)



Y-AXIS RESPONSE (lateral)



Z-AXIS RESPONSE (vertical)

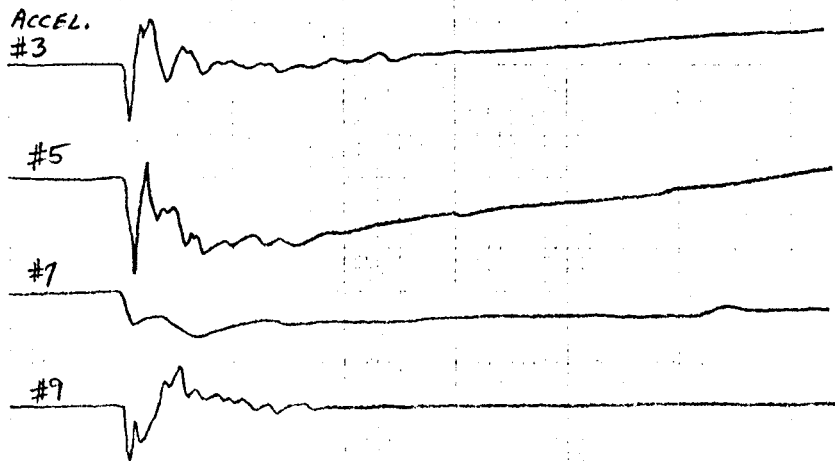
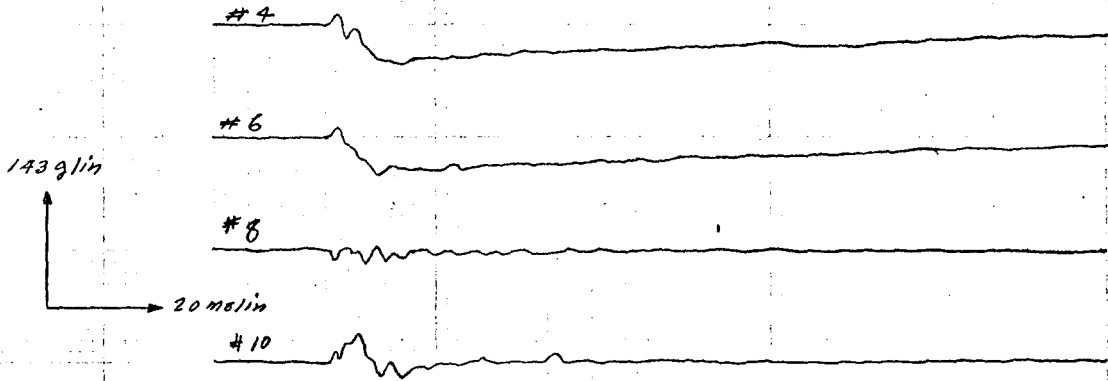


FIGURE D-29

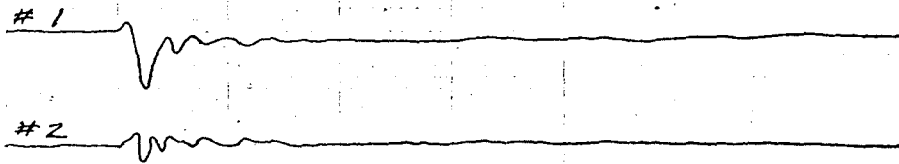
LRC-ASE FILTERED ACCELEROMETER DATA

TEST # 5 (BREN. -3)

X-AXIS



Y-AXIS



Z-AXIS

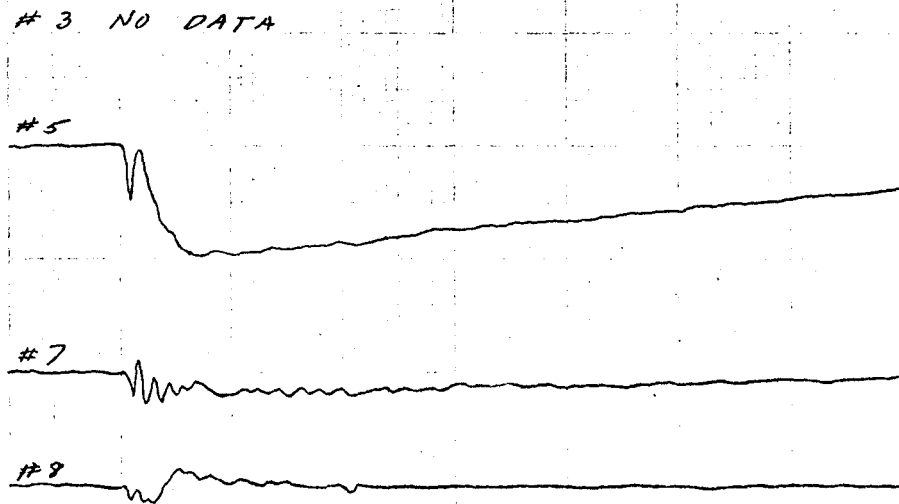


FIGURE D-30

LRC Filtered Accel. Data
Test #6 (Gren. -1)

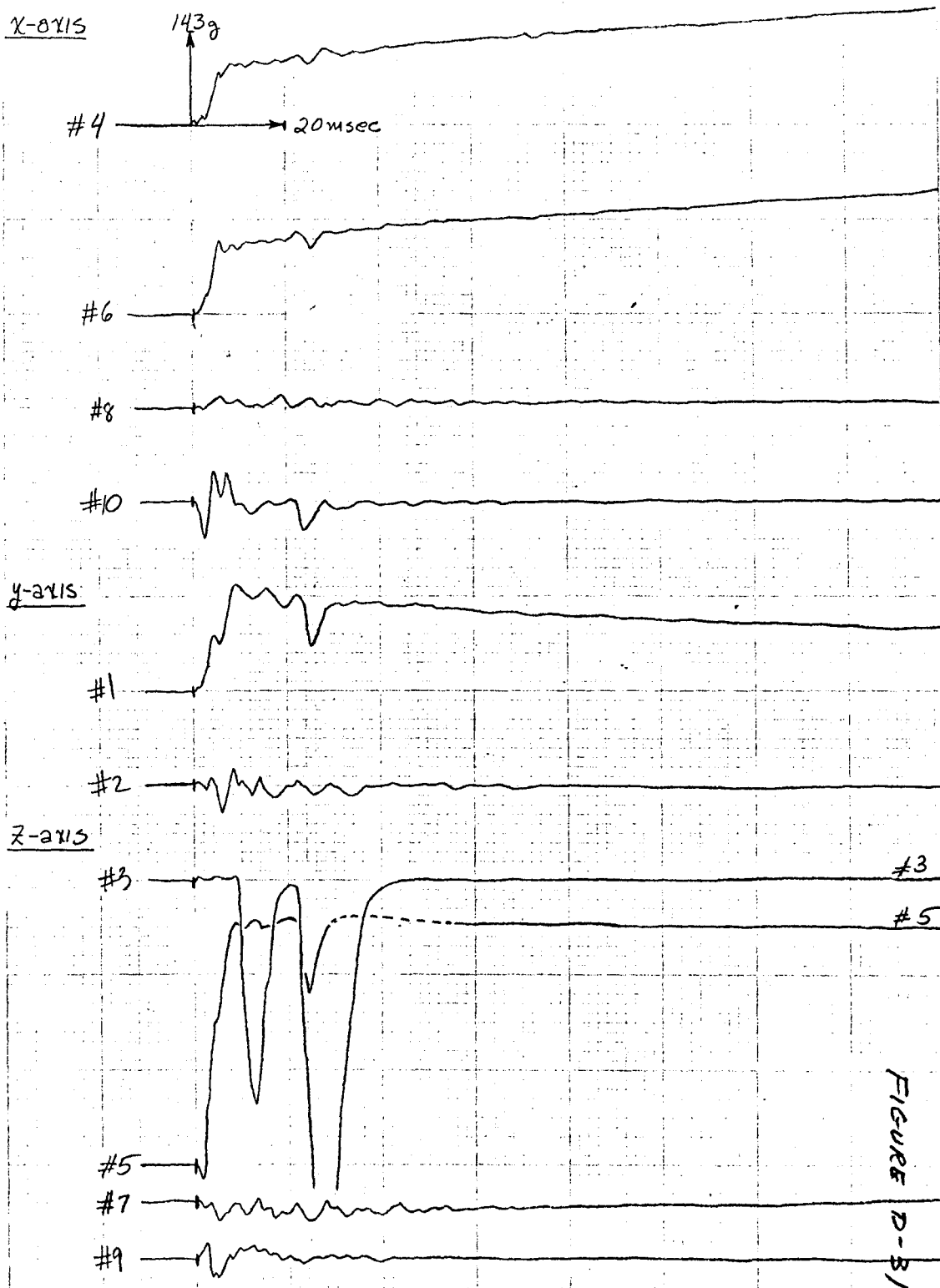


FIGURE D-31

LRC Filtered Accel. Data
Test #7 (Group -2)

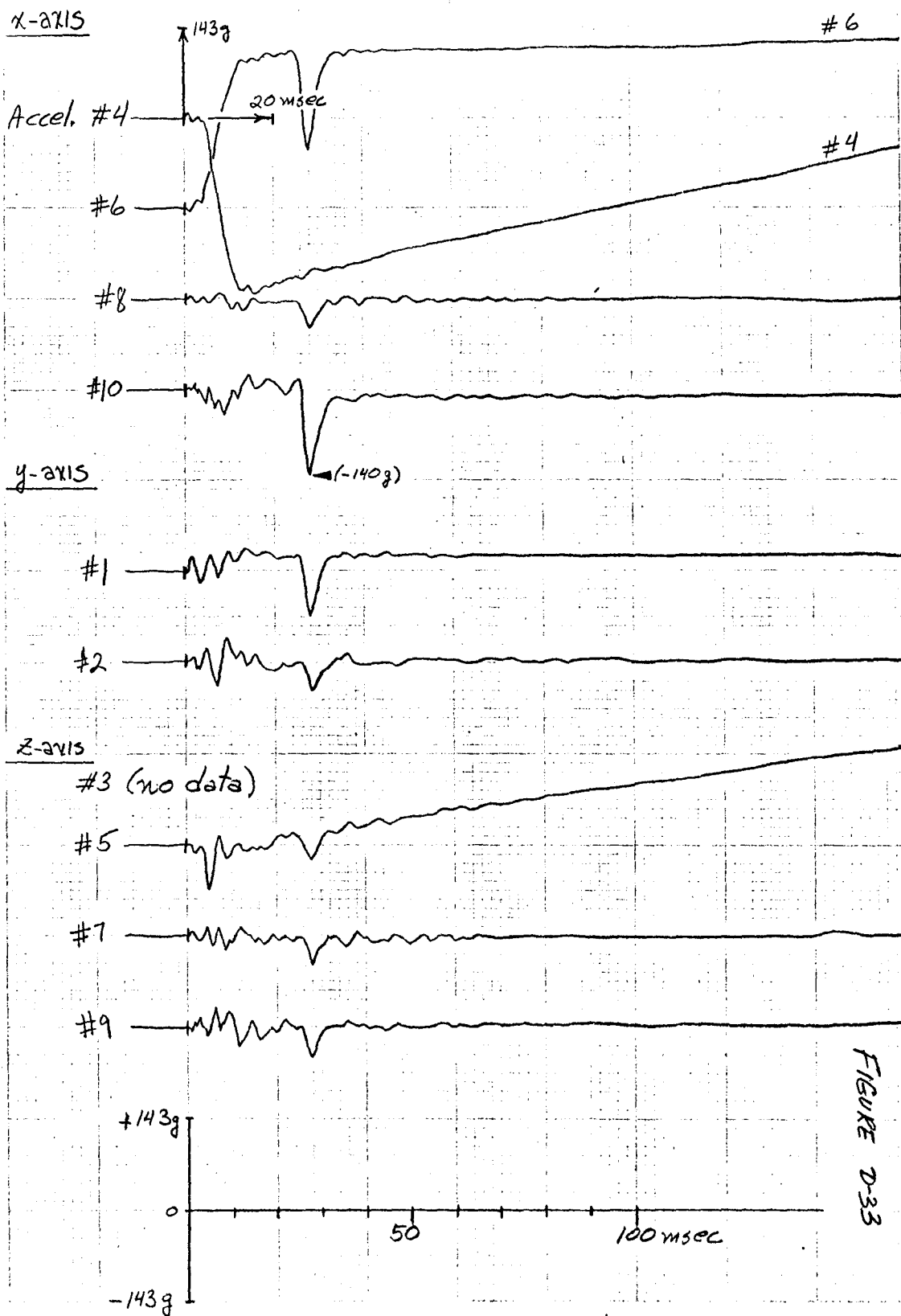
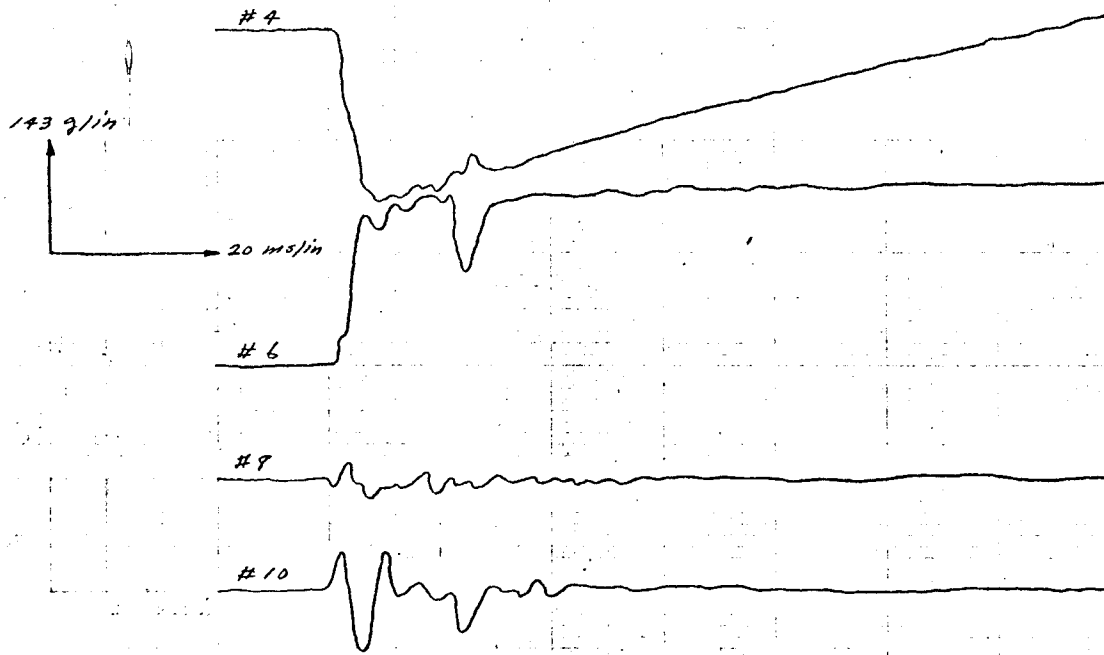


FIGURE D-33

LRC-ASE ACCELEROMETER DATA (FILTERED ABOVE 100HZ)

TEST # 8 (GREN. - 4)

X-AXIS



Y-AXIS

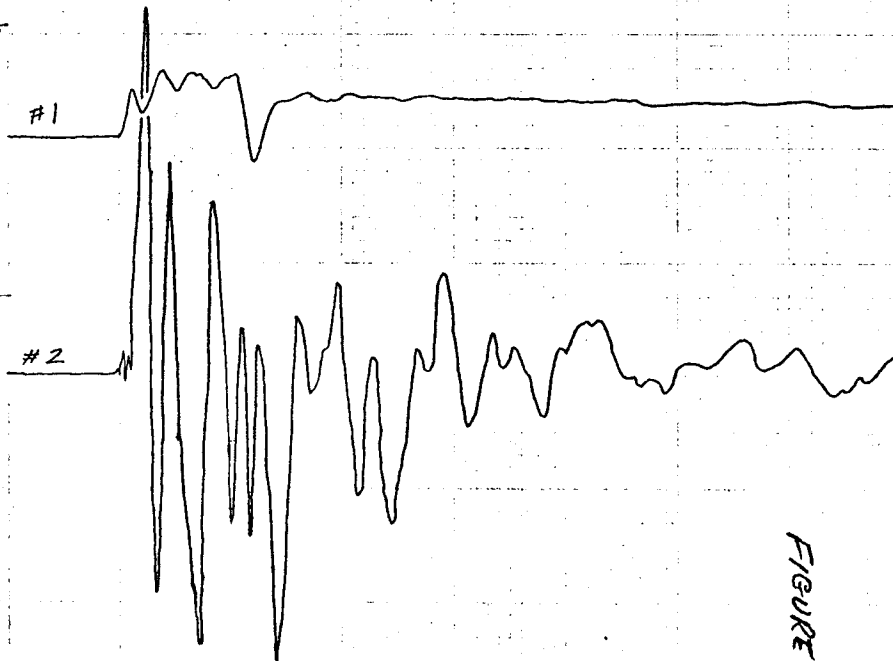


FIGURE D-33

TEST # 8 (GREN. -4), (CONT.)

Z-AXIS

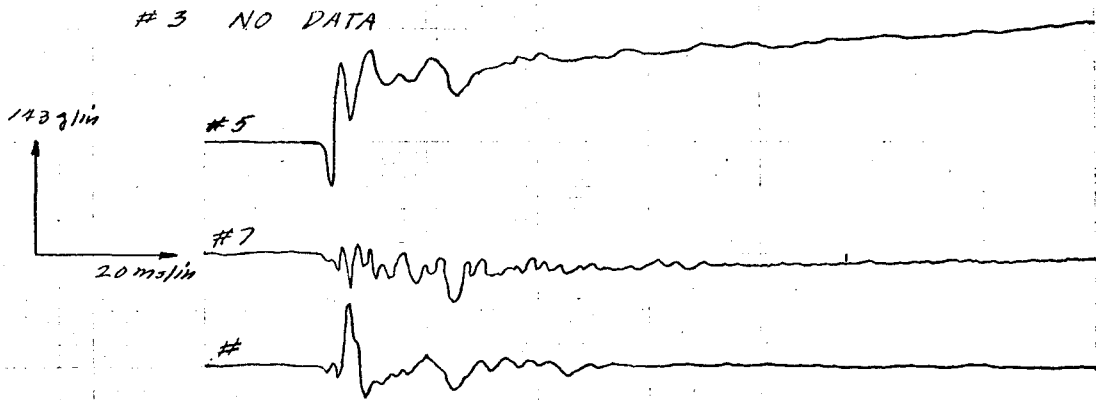
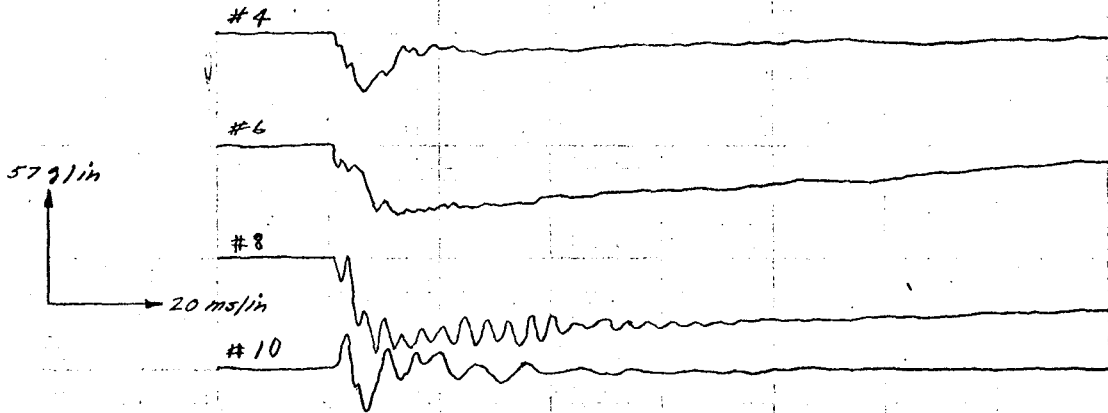


FIGURE D-34

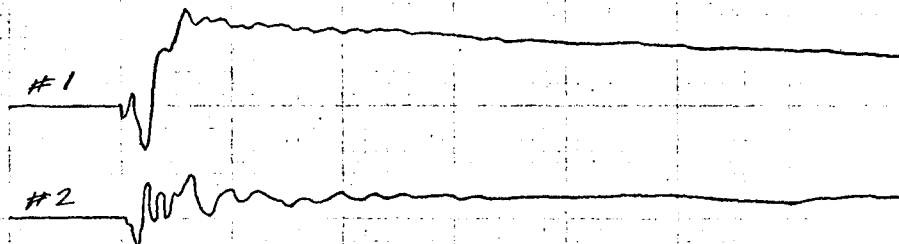
LRC-ASE FILTERED ACCELEROMETER DATA

TEST # 9 (GREN. -4)

X-AXIS



Y-AXIS



Z-AXIS

#3 NO DATA

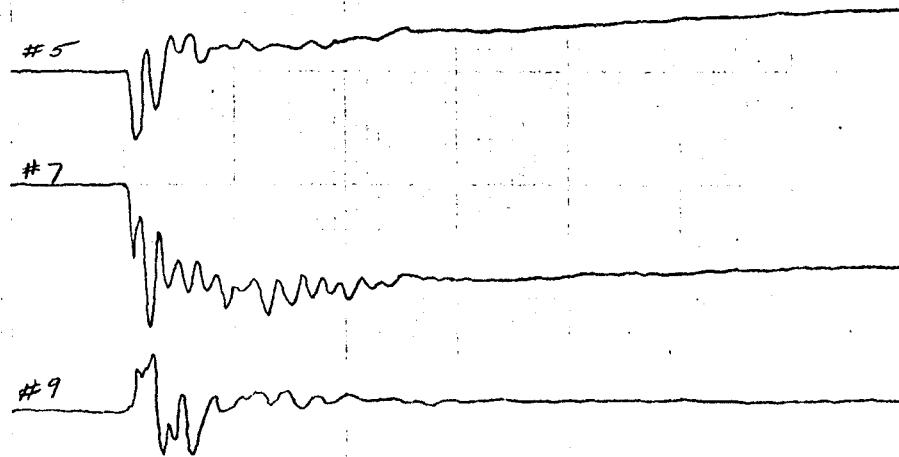
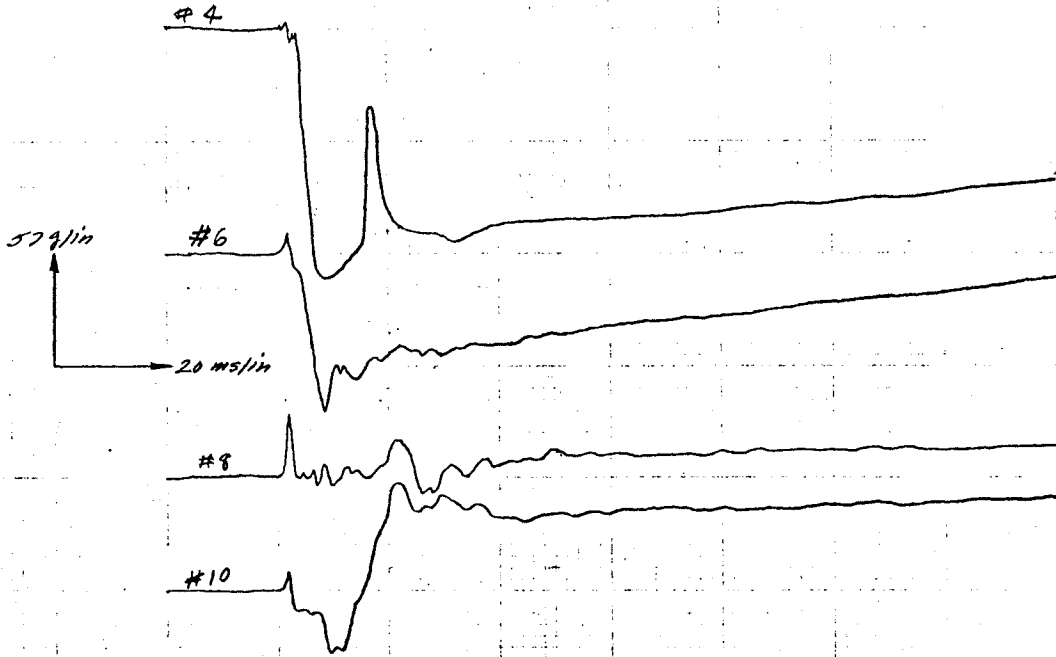


FIGURE D-35

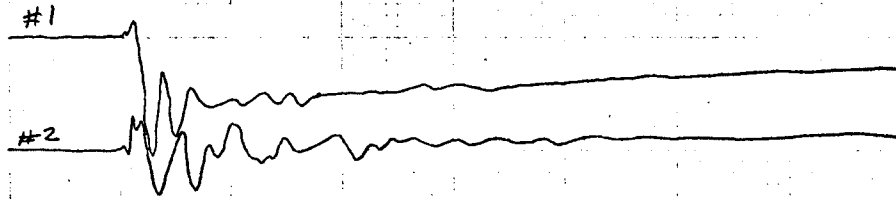
LRC-ASE FILTERED ACCELEROMETER DATA

TEST # 10 (GREN. - 3)

X-AXIS



Y-AXIS



Z-AXIS

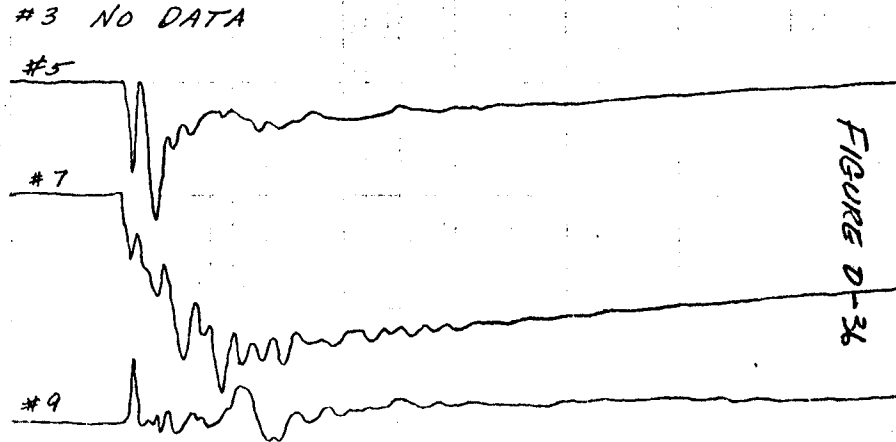
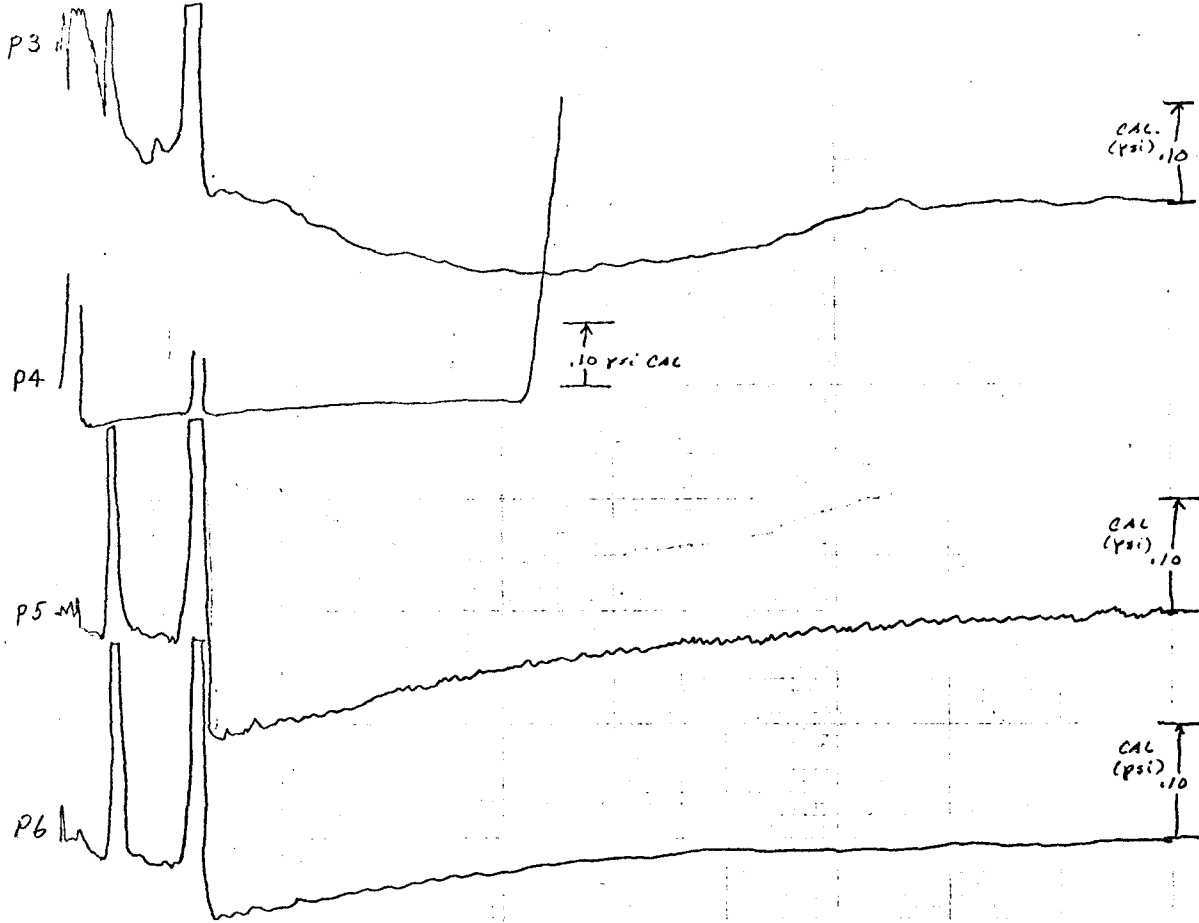


FIGURE D-36

TEST # 3, GRENADE # 2

TIME 0 10 20 30 40 50 60 70 80 90 100 MS



TEST # 4, GRENADE # 4

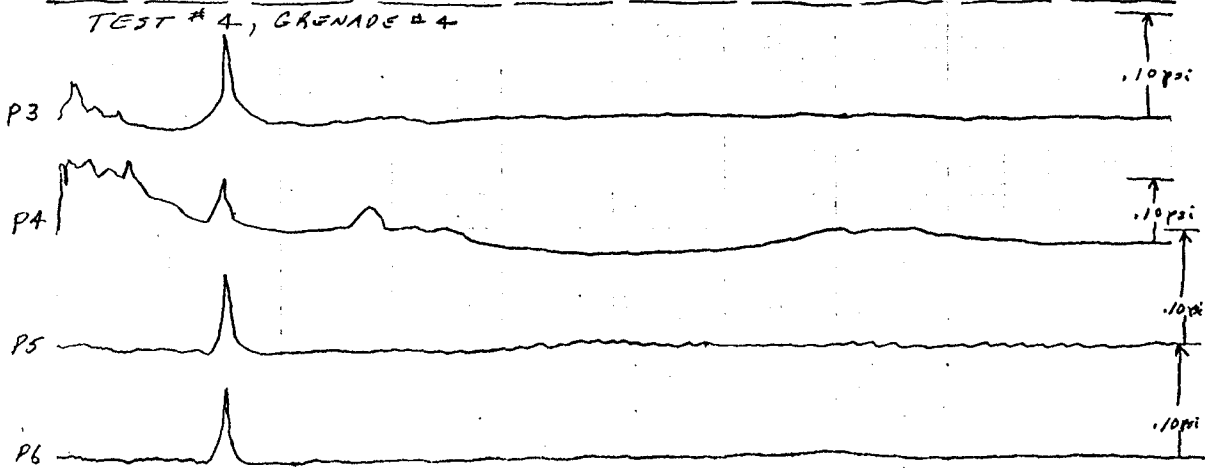
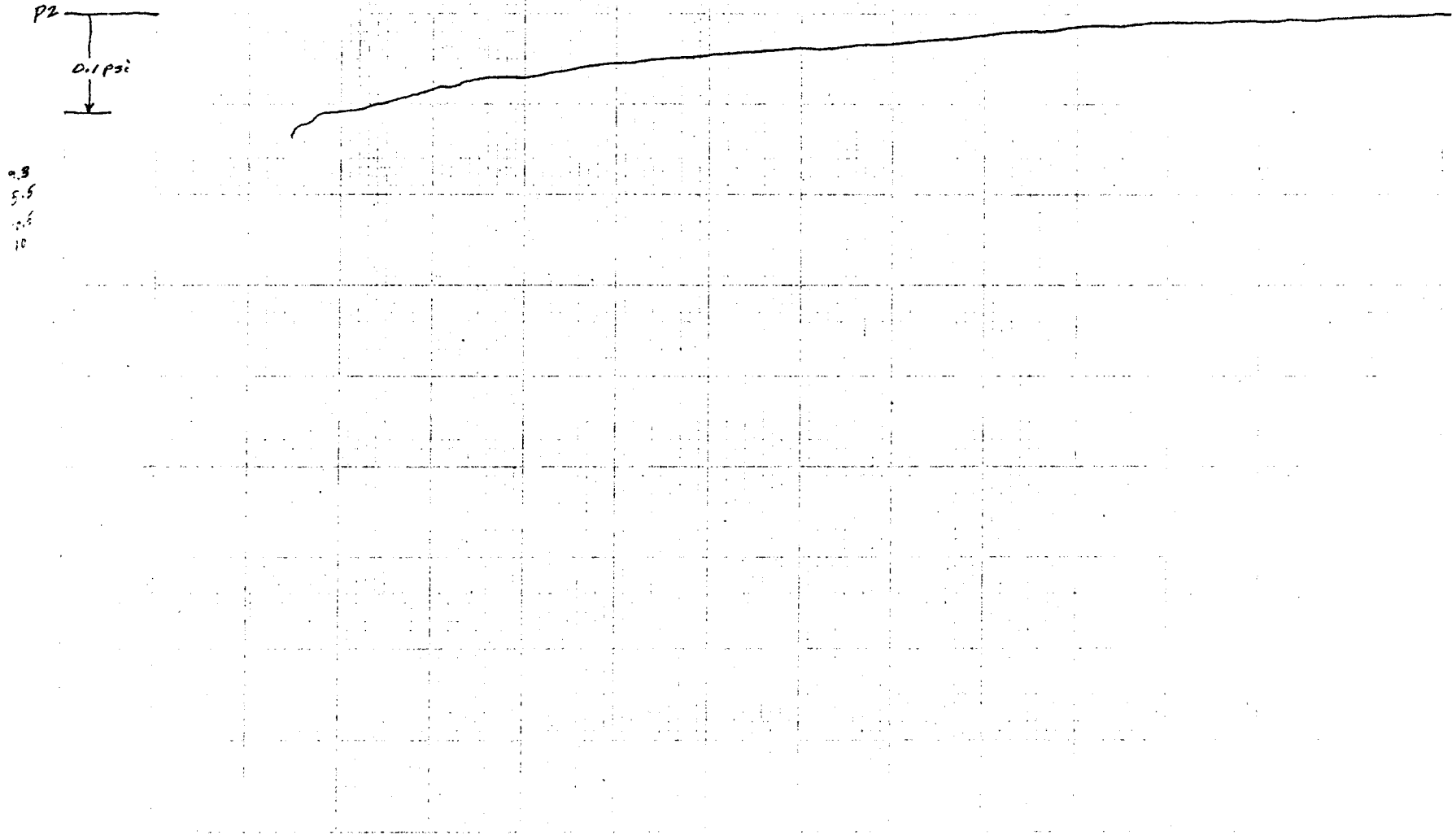


FIGURE D-37

TEST NO. 2. BURN TIME: 6.7 GRENADE # 2

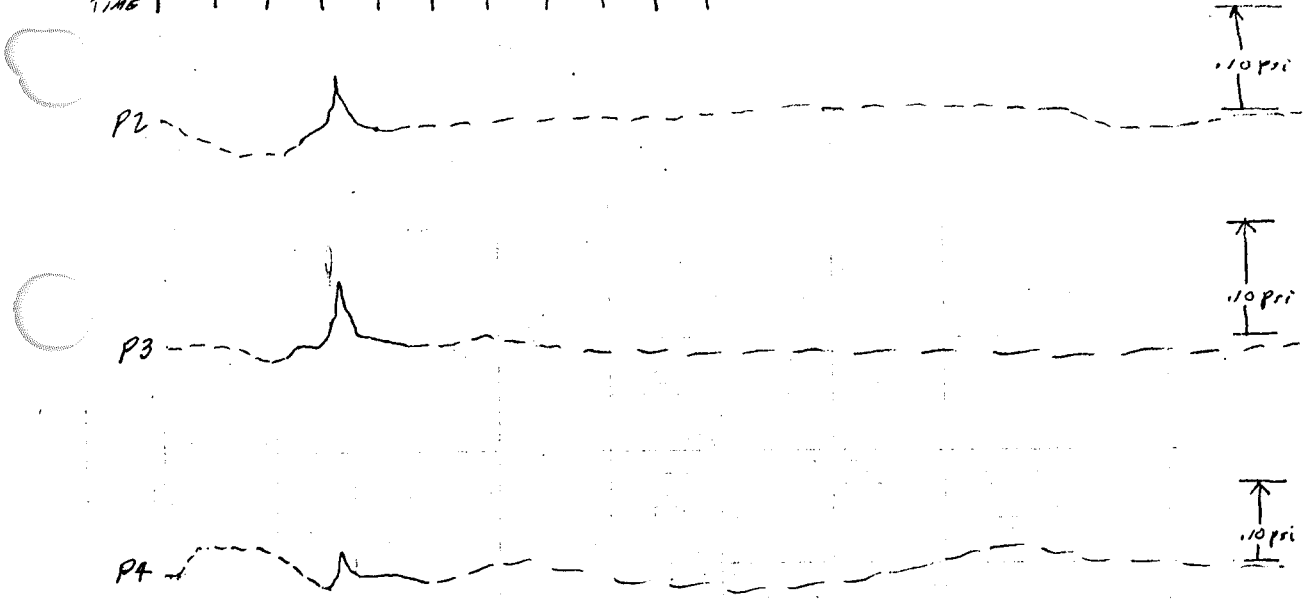
TIME 0 10 20 30 40 50 60 70 80 90 100 110 120 130 140 150 160 170 180 190 200 210 220 230 240 250 260 270 280 290 300

FIGURE D-38



TEST # 5, GRENADE # 3

TIME 0 10 20 30 40 50 60 70 80 90 100 MS



TEST NO. 6, GRENADE # 1

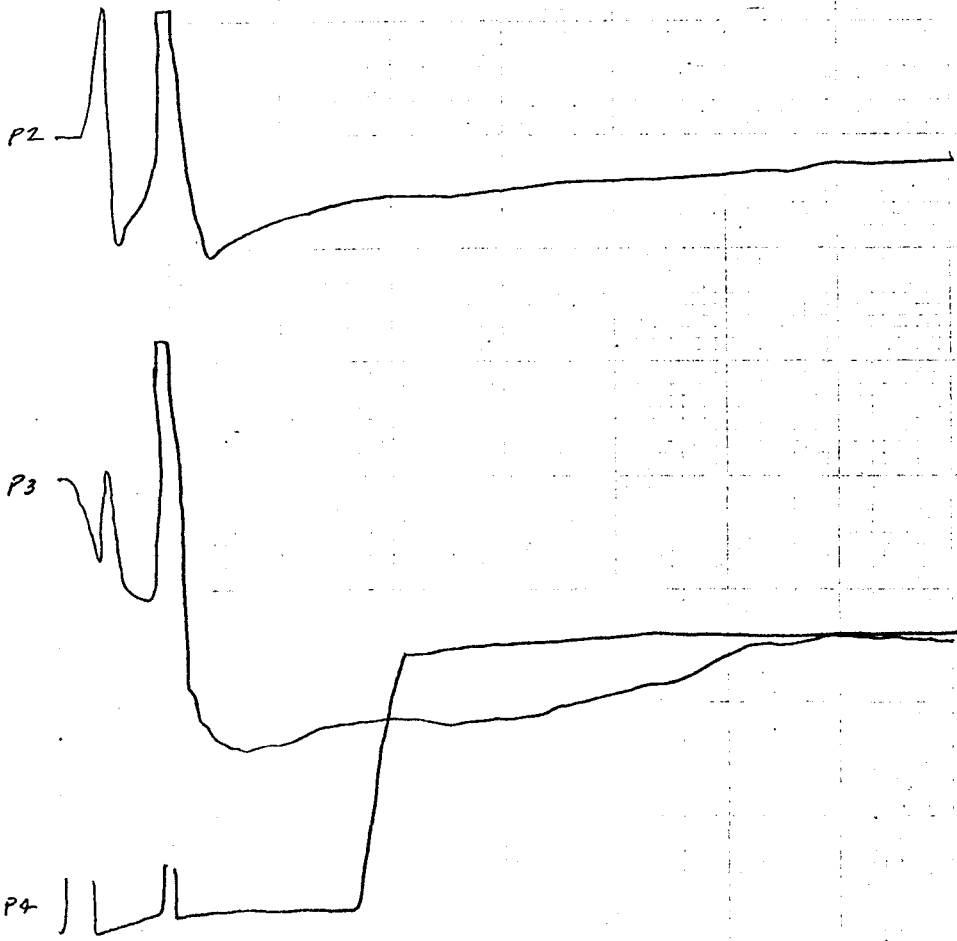
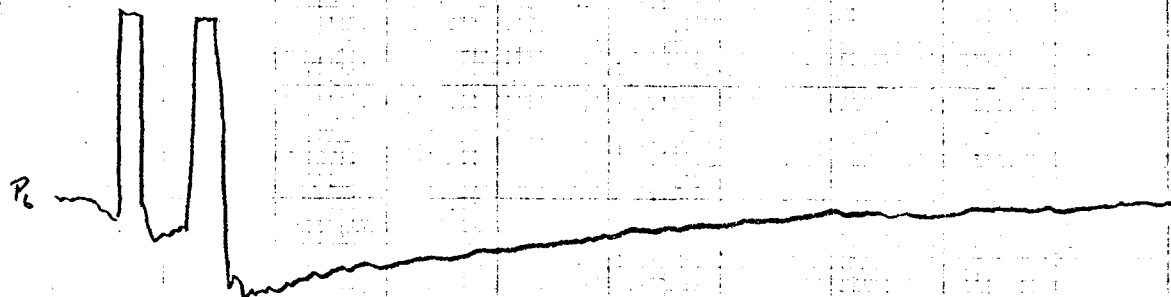
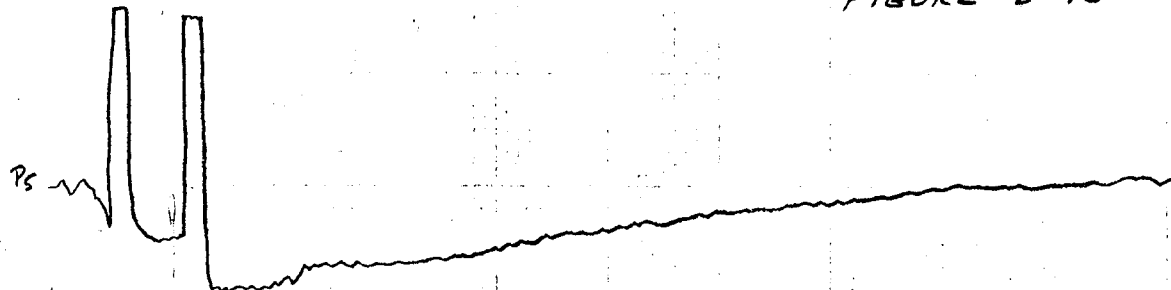


FIGURE T-39

TEST #6

TIME 0 10 20 30 40 50 60 70 80 90 100 MS

FIGURE D-40





**Aerospace
Systems Division**

ASE REDESIGN EVALUATION

NO.	REV. NO.
ATM-1064	
PAGE <u>172</u>	OF <u>212</u>
DATE	11/24/71

APPENDIX E

Grenade Launch Sequences



**Aerospace
Systems Division**

ASE REDESIGN EVALUATION

NO.	REV. NO.
ATM-1064	
PAGE <u>173</u> OF <u>212</u>	
DATE 11/24/71	

(- 2) Grenade
Launch Sequence

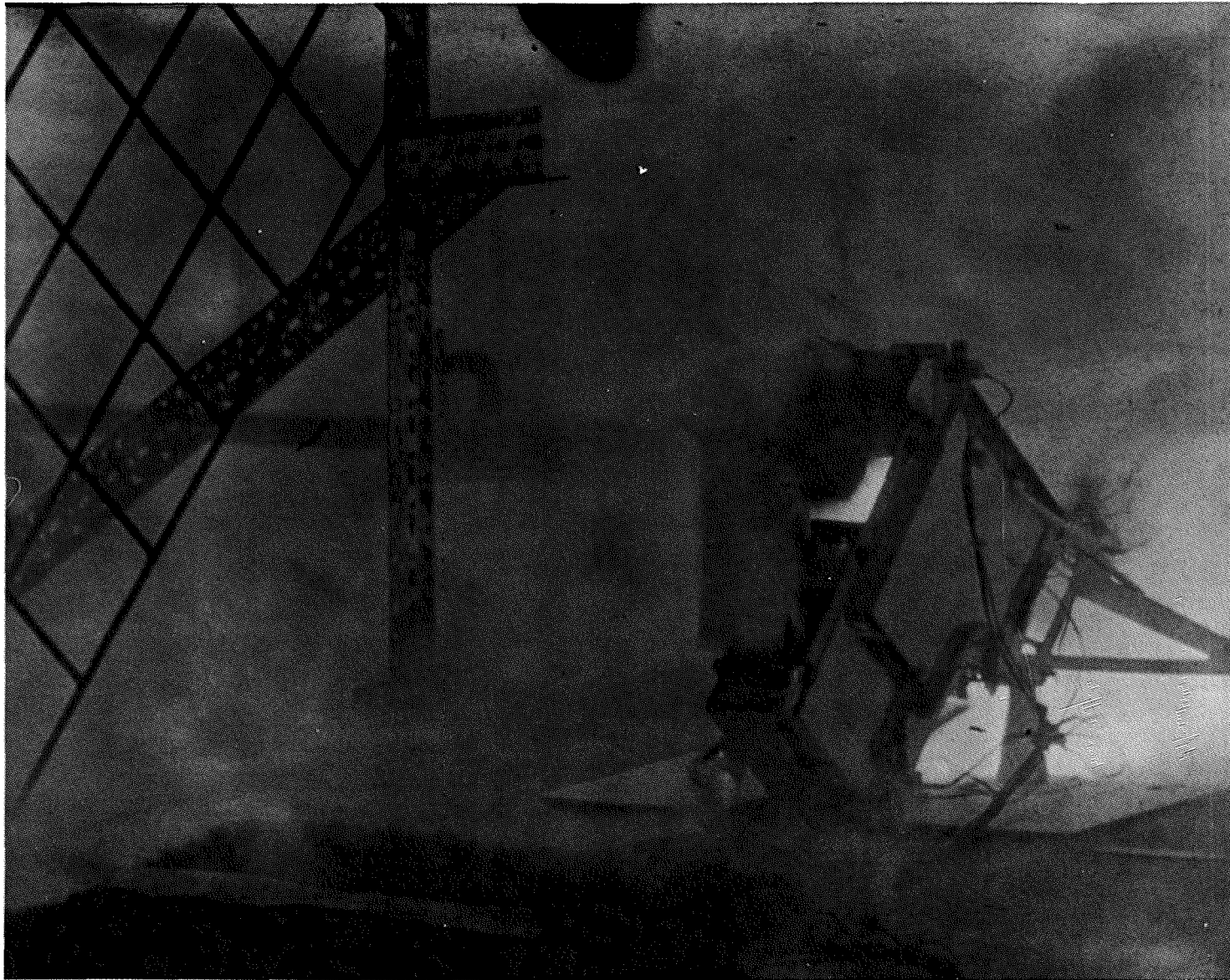


Figure E-(#2-1)

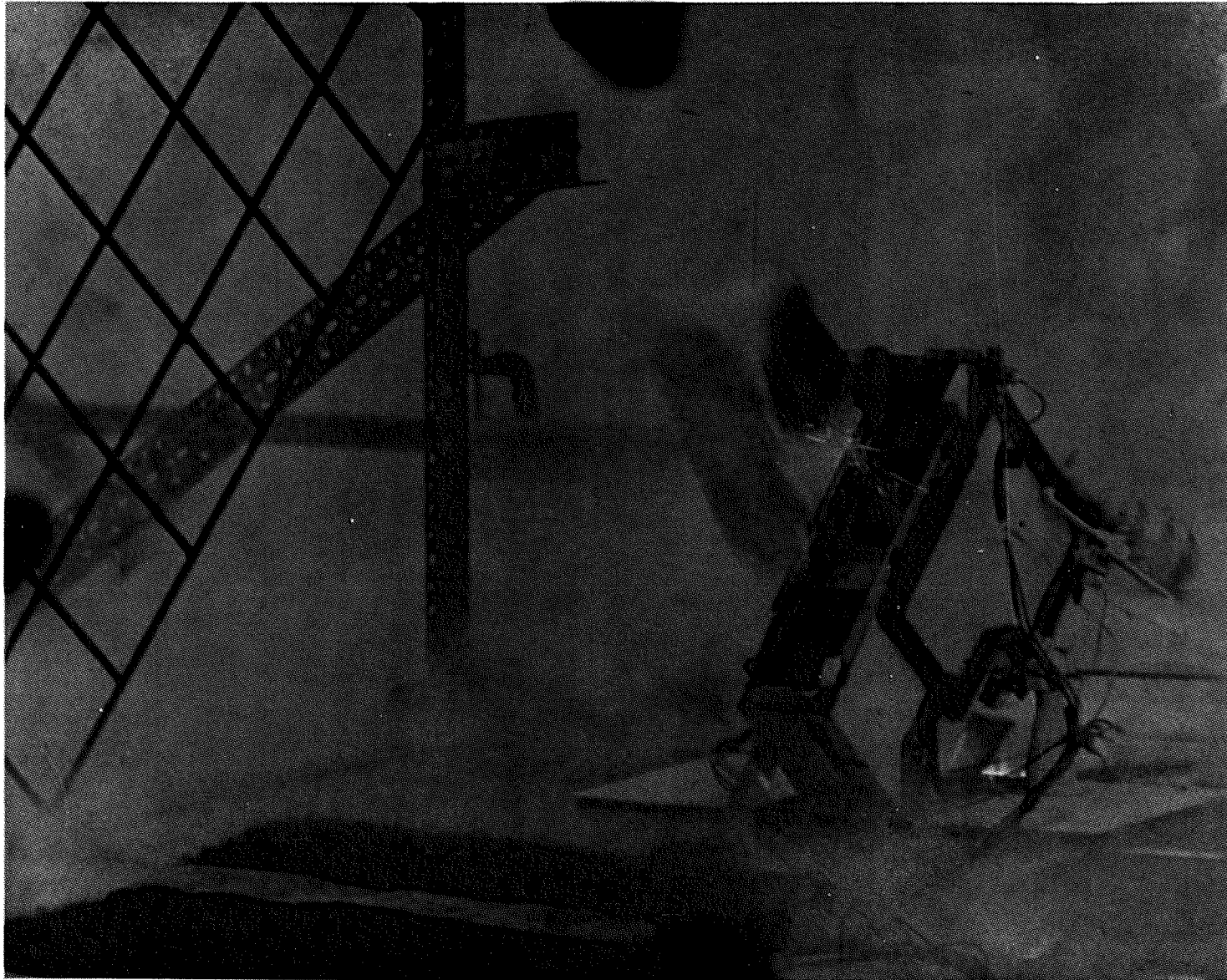


Figure E-(#2-2)

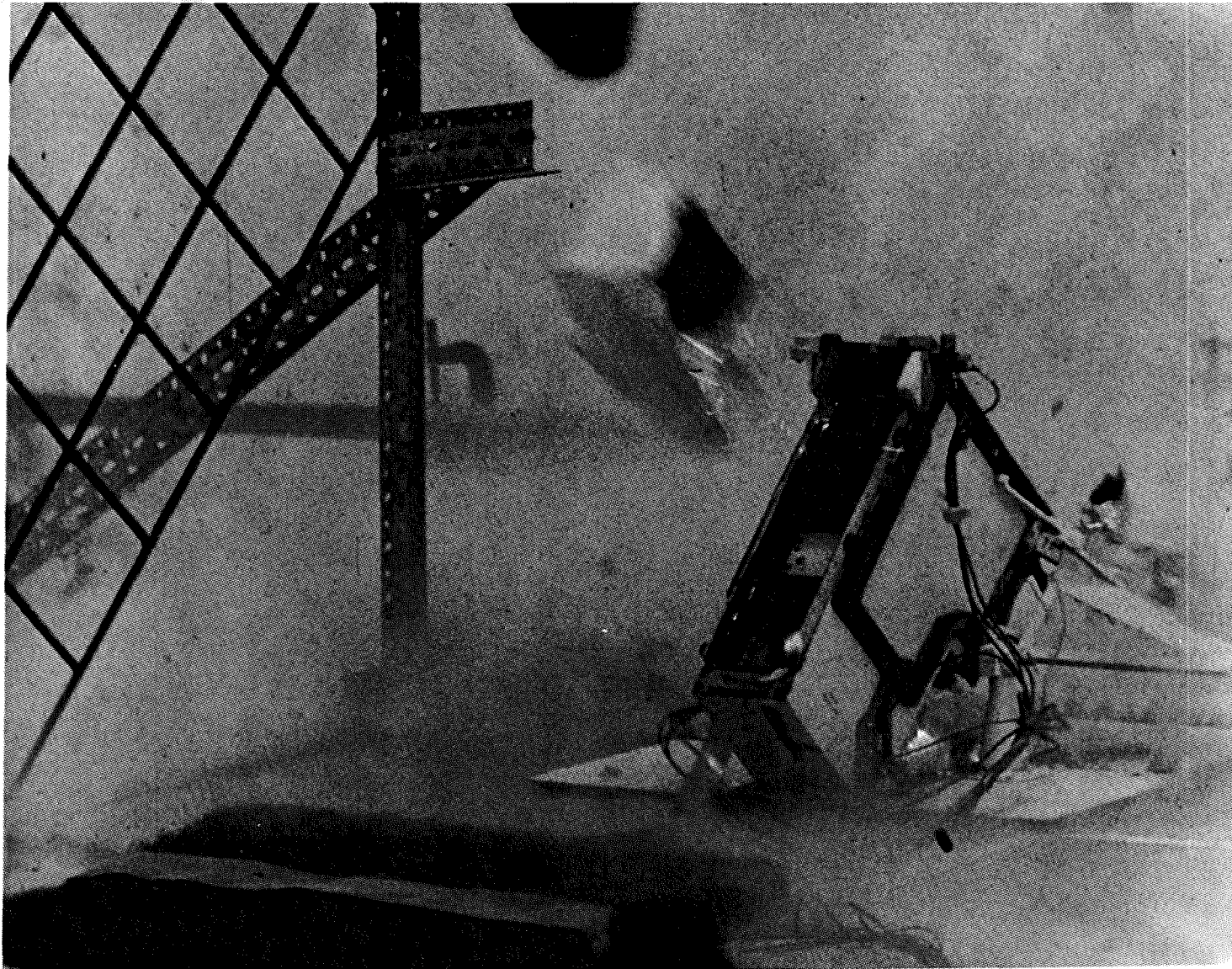


Figure E-(#2-3)

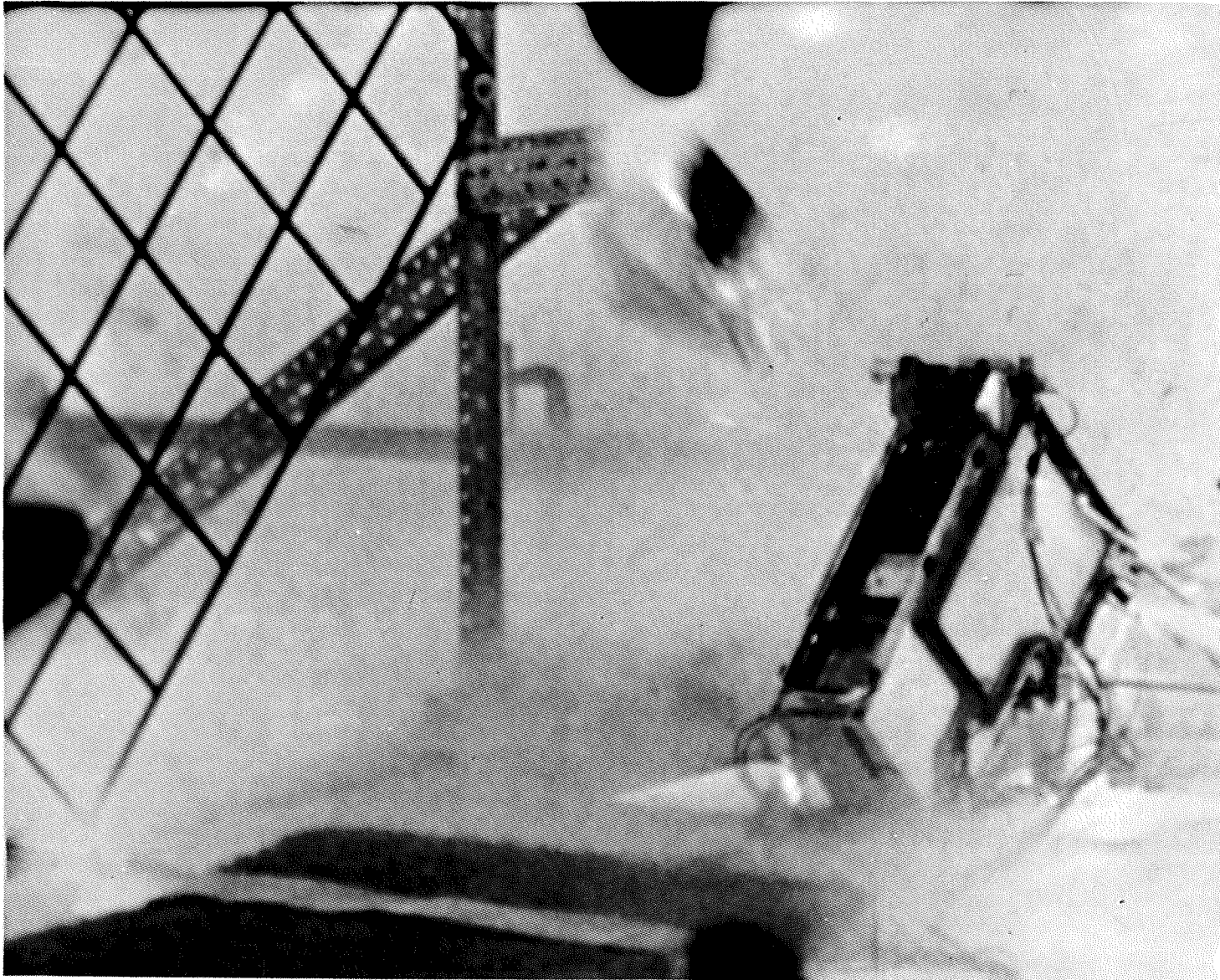


Figure E-(#2-4)

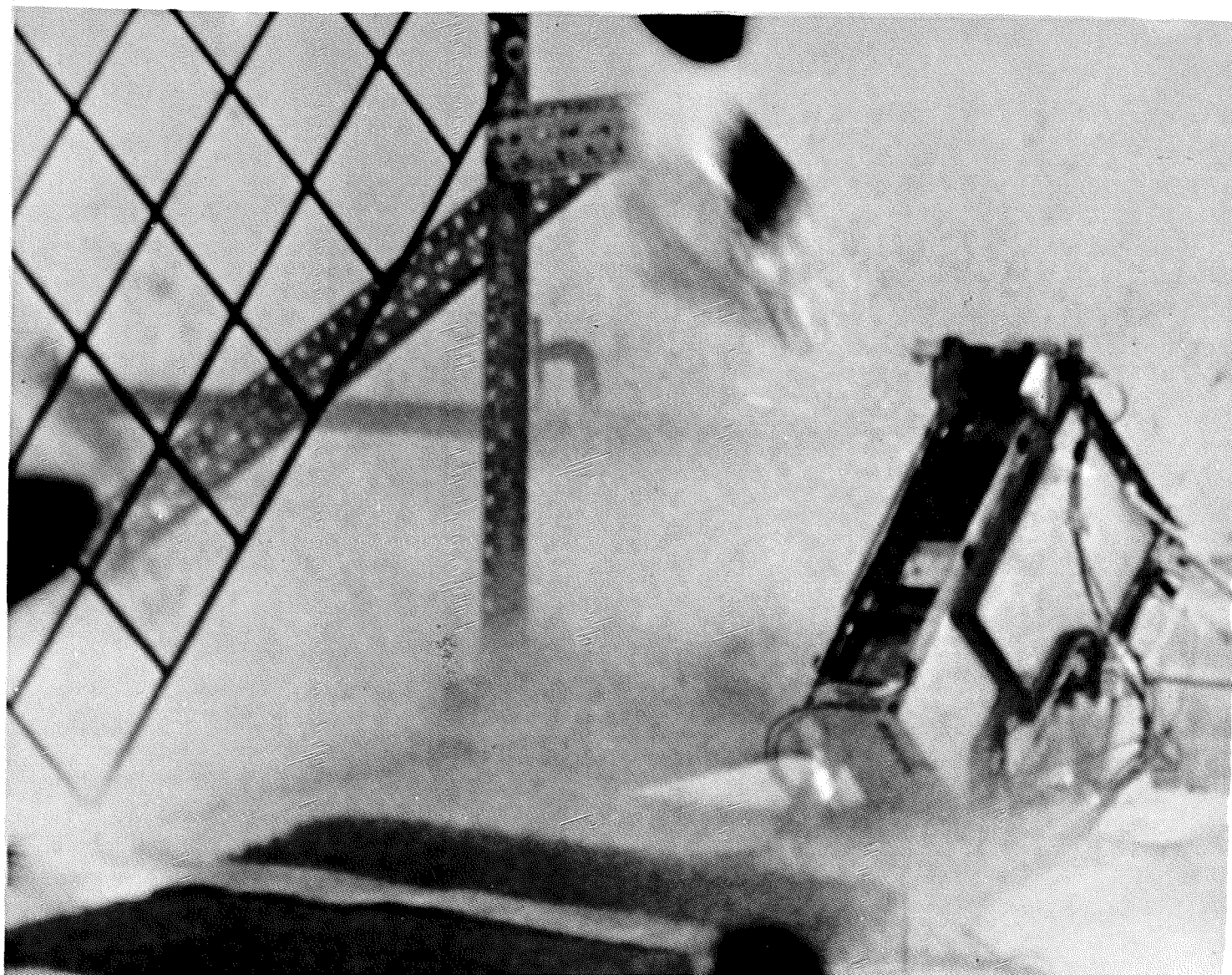


Figure E-(#2-5)



Figure E-(#2-6)

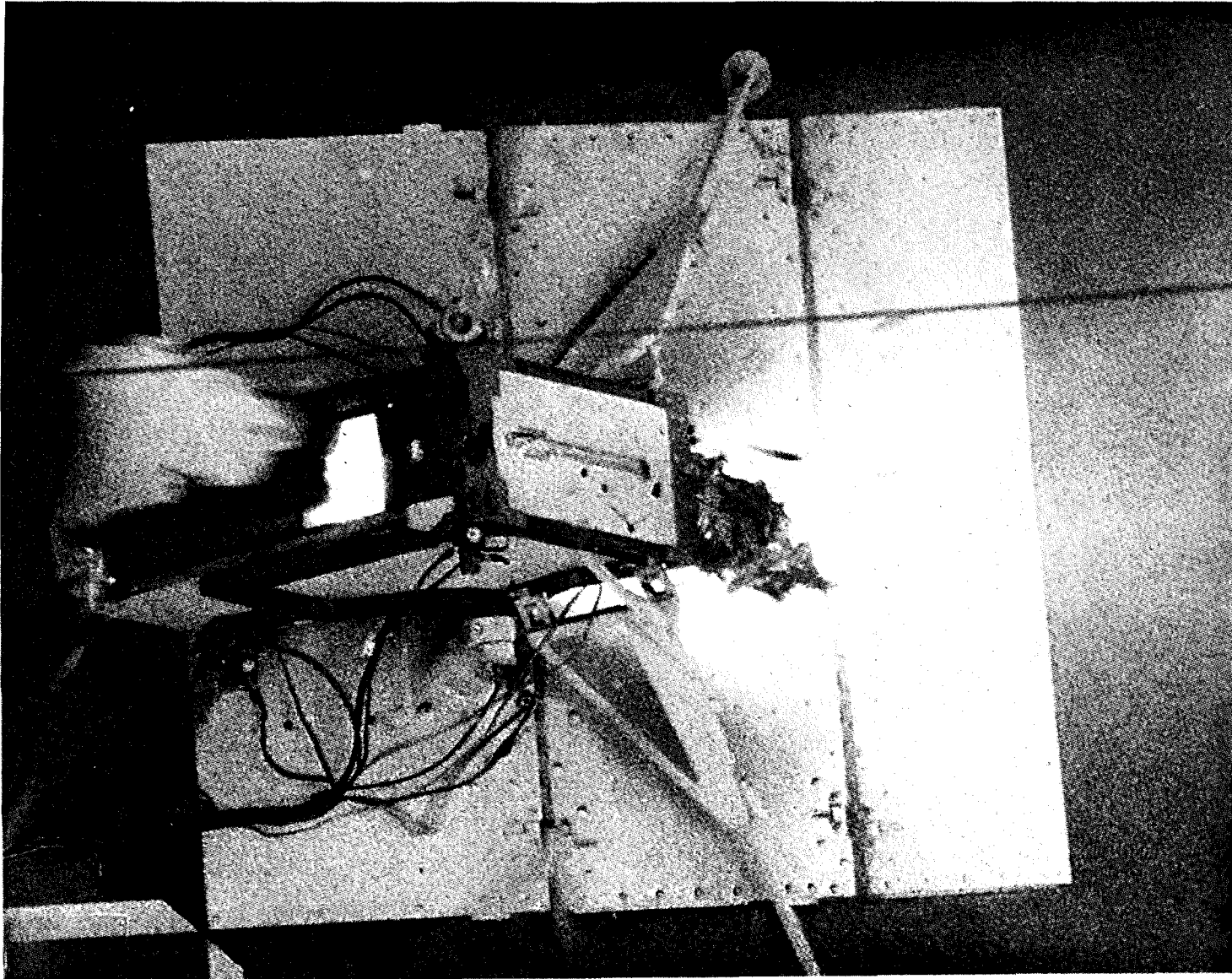


Figure E-(#2-7)

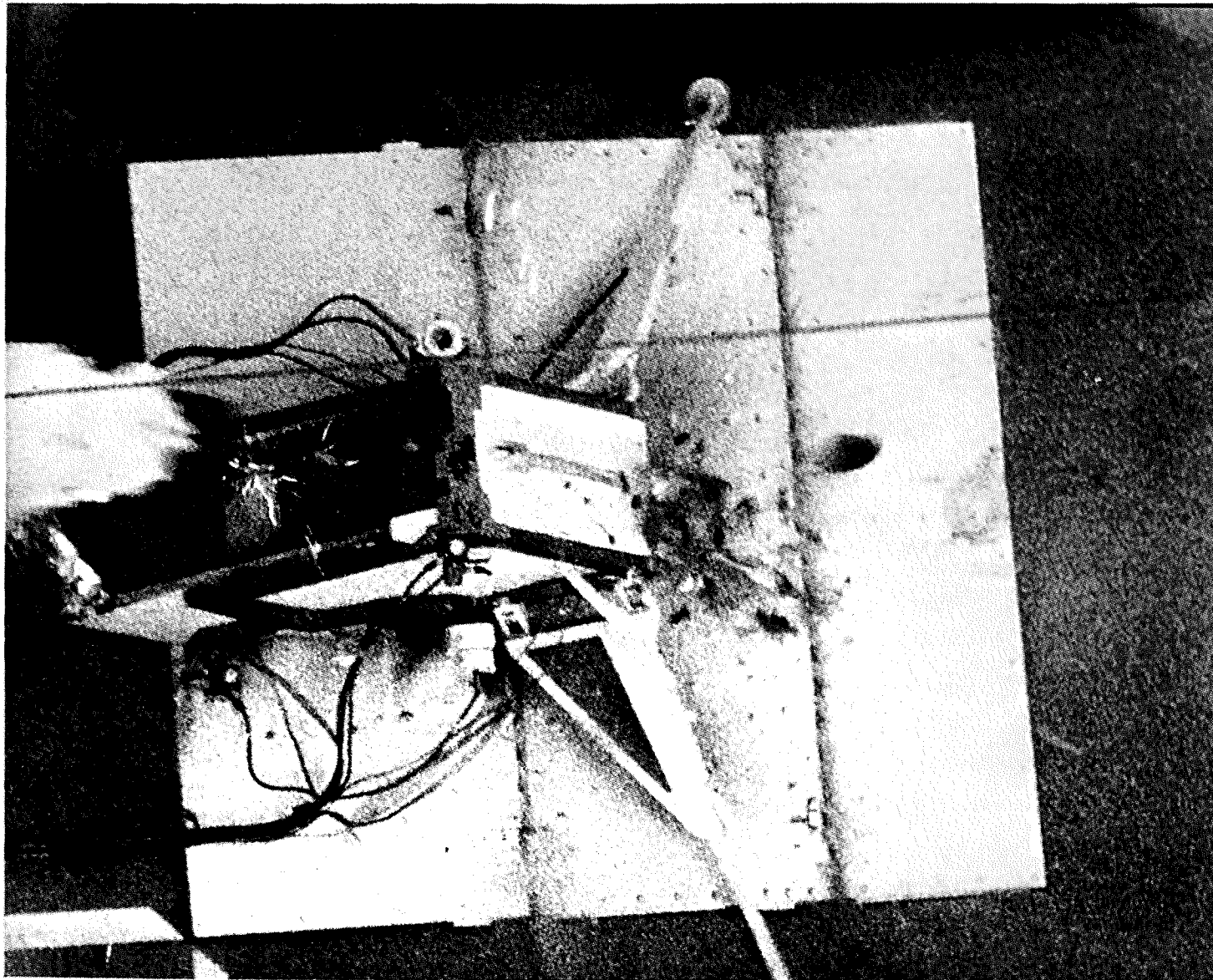


Figure E-(#2-8)

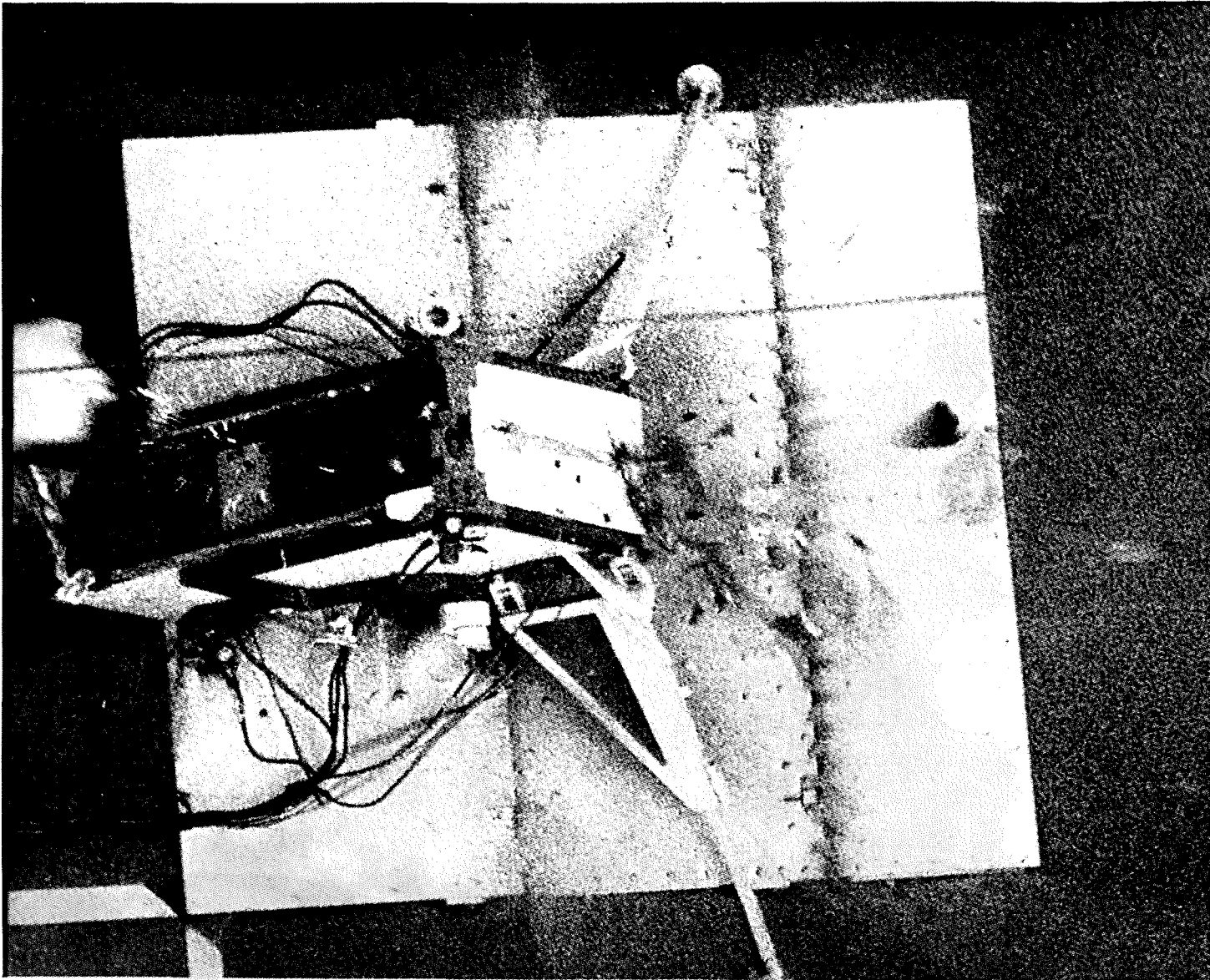


Figure E-(#2-9)

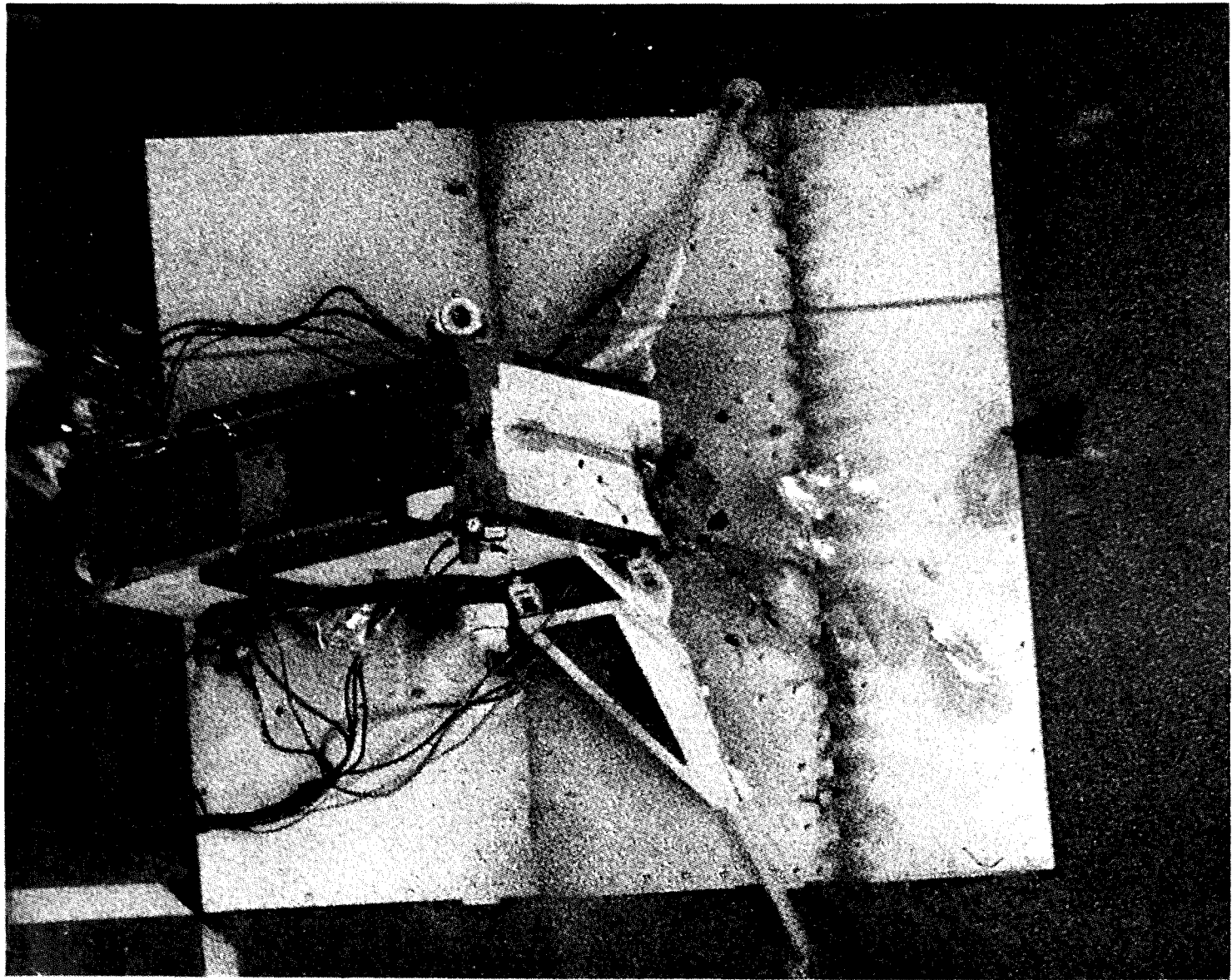


Figure E-(#2-10)

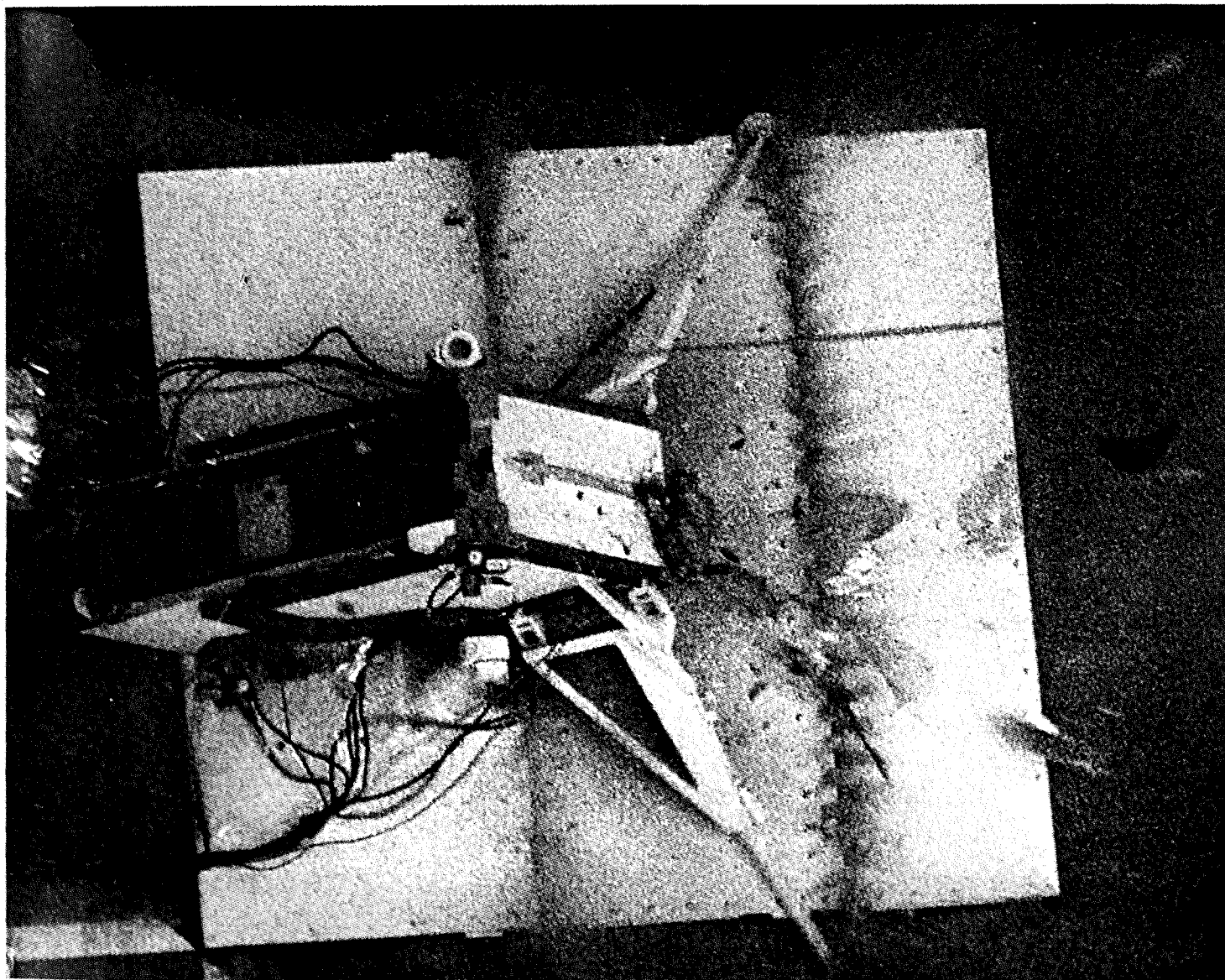


Figure E-(#2-11)



**Aerospace
Systems Division**

ASE REDESIGN EVALUATION

NO.	REV. NO.
ATM-1064	
PAGE <u>185</u> OF <u>212</u>	
DATE 11/24/71	

(-4) Grenade
Launch Sequence

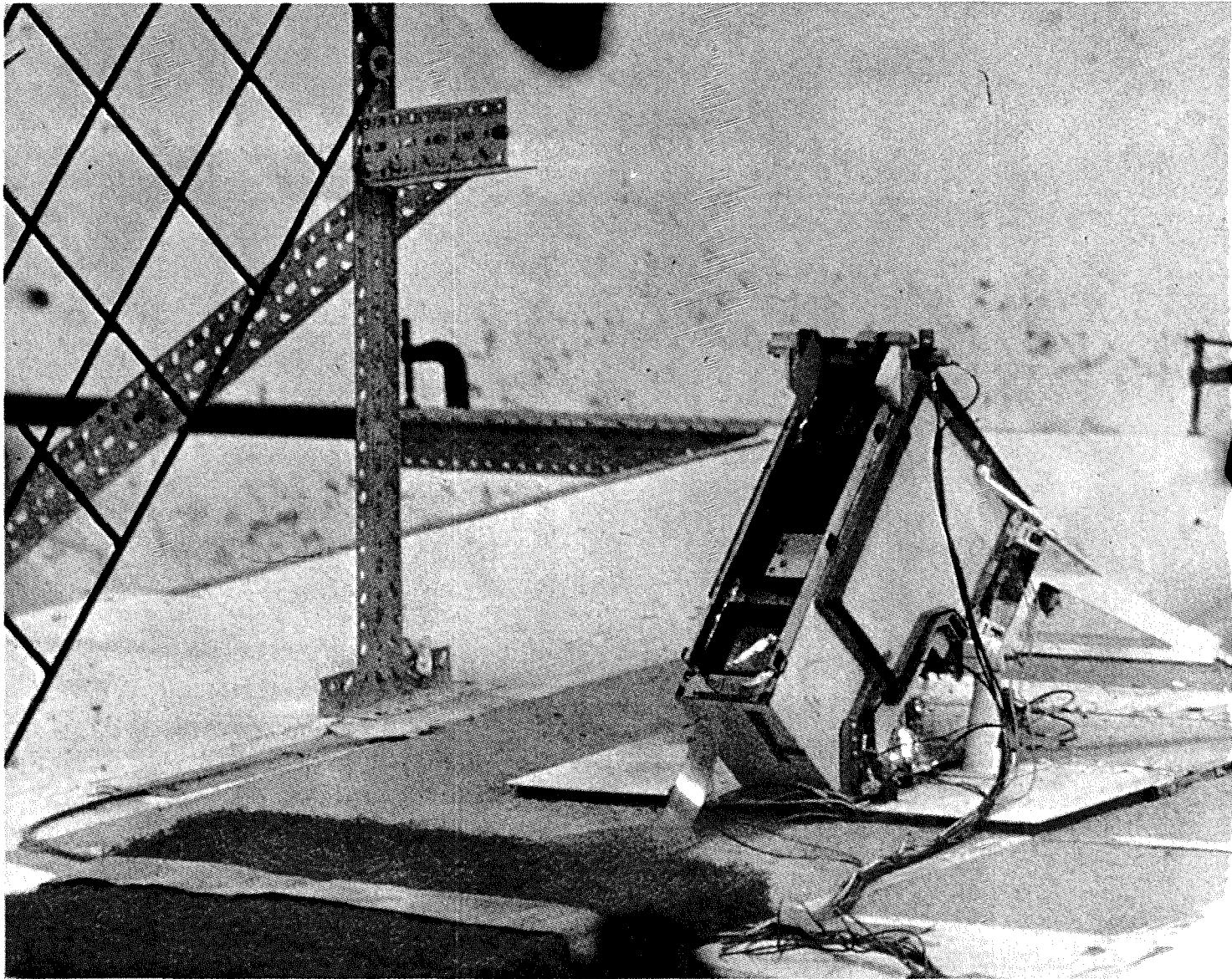


Figure E-(#4-1)

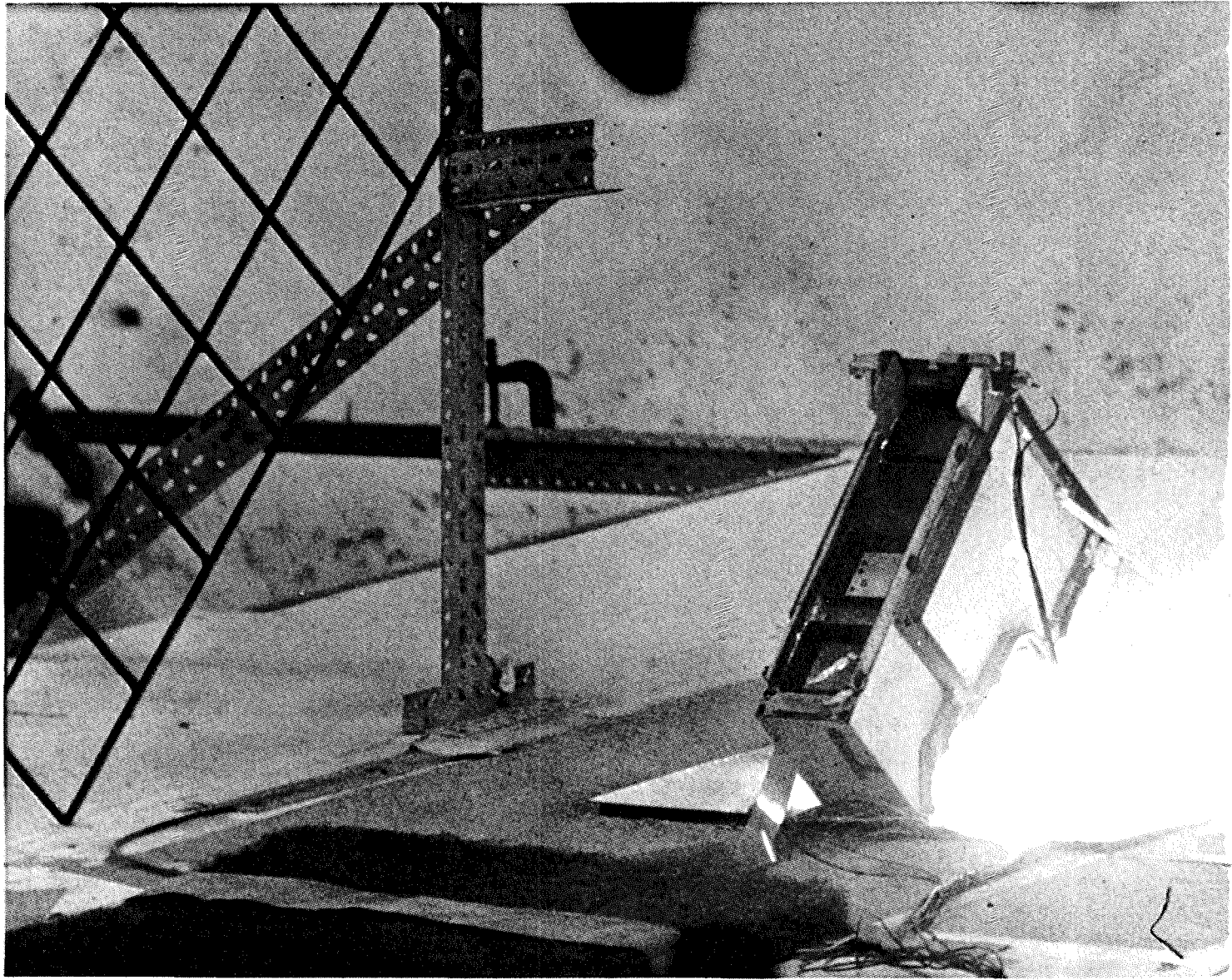


Figure E-(#4-2)



Figure E-(#4-3)



Figure E-(#4-4)

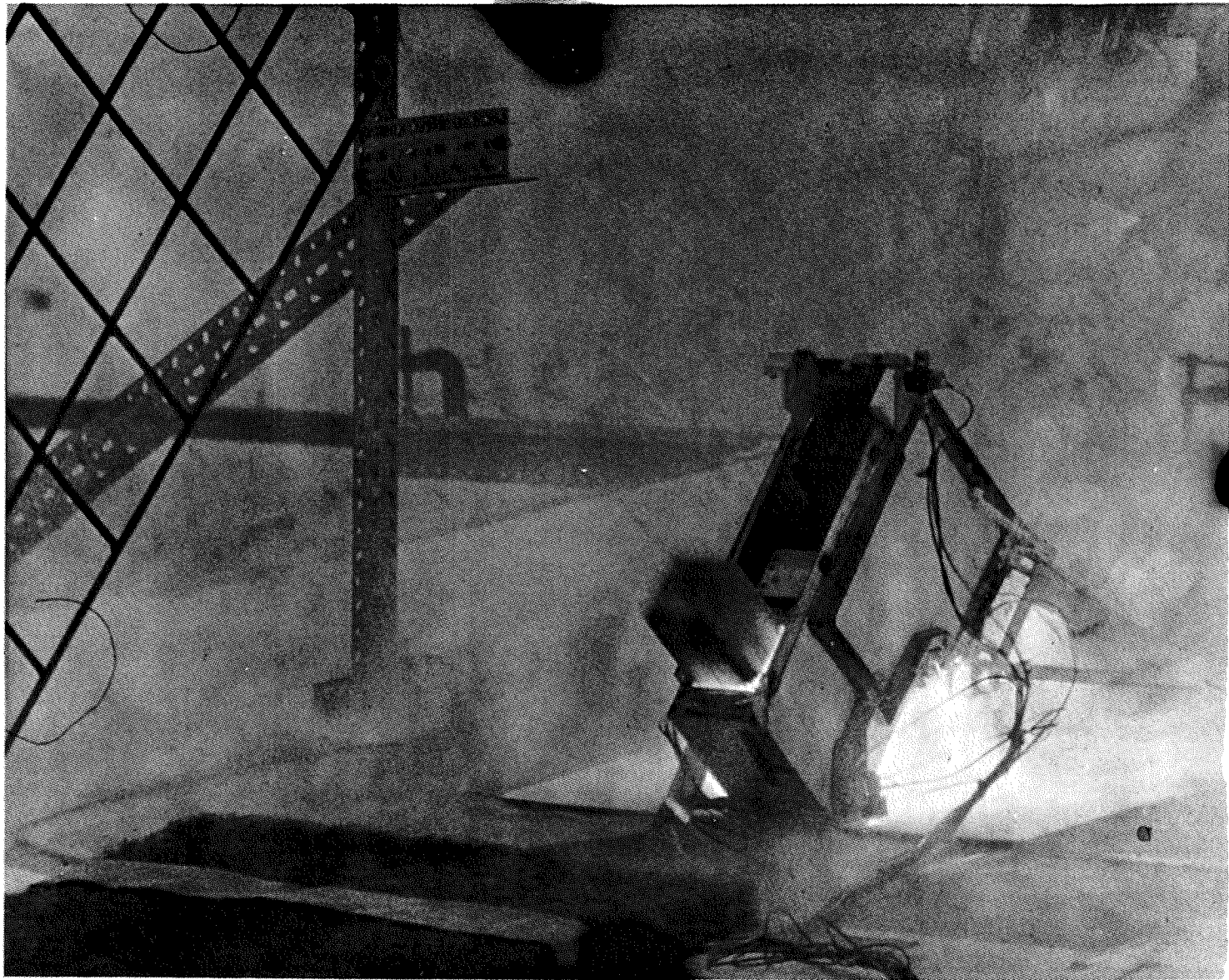


Figure E-(#4-5)

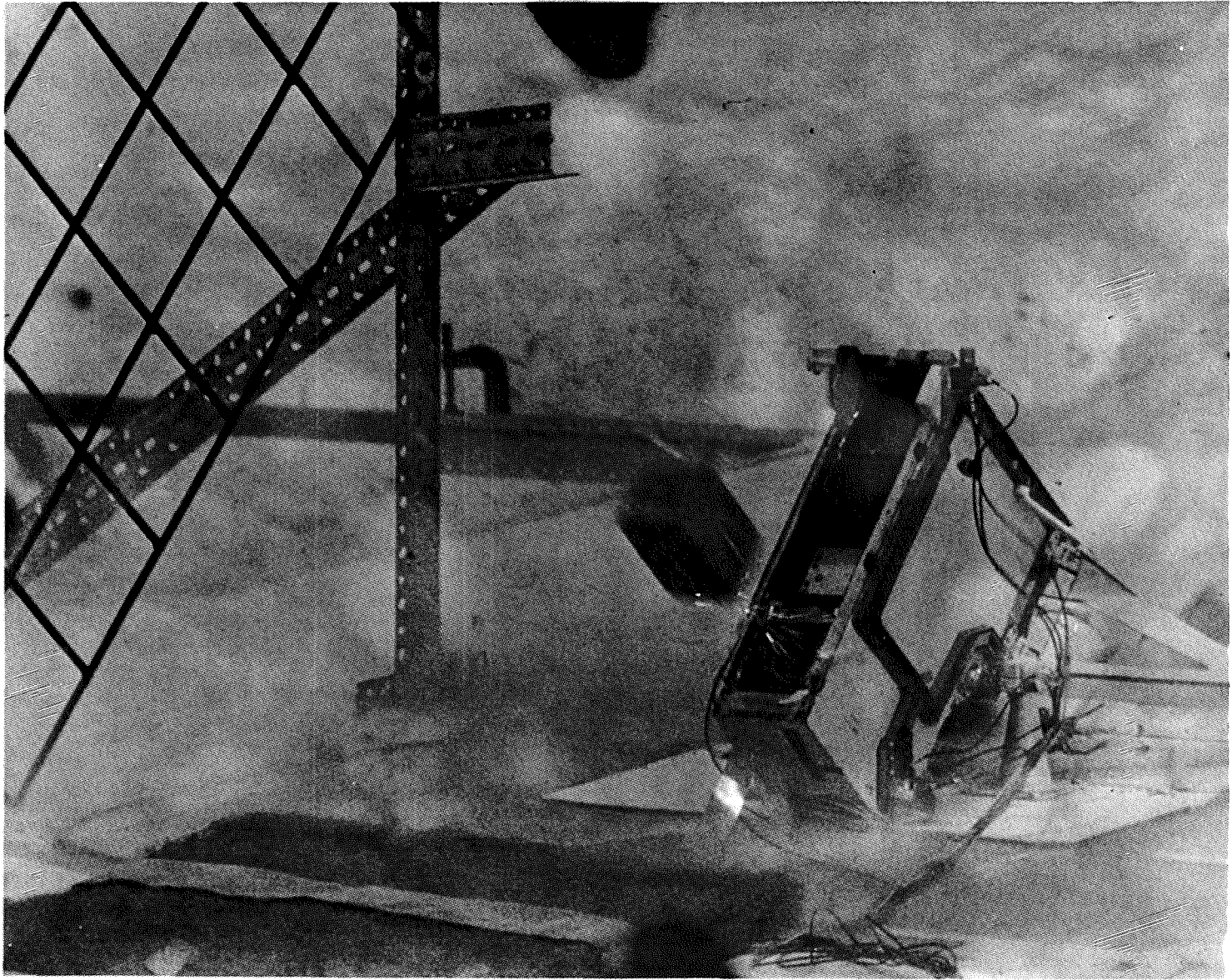


Figure E-(#4-6)

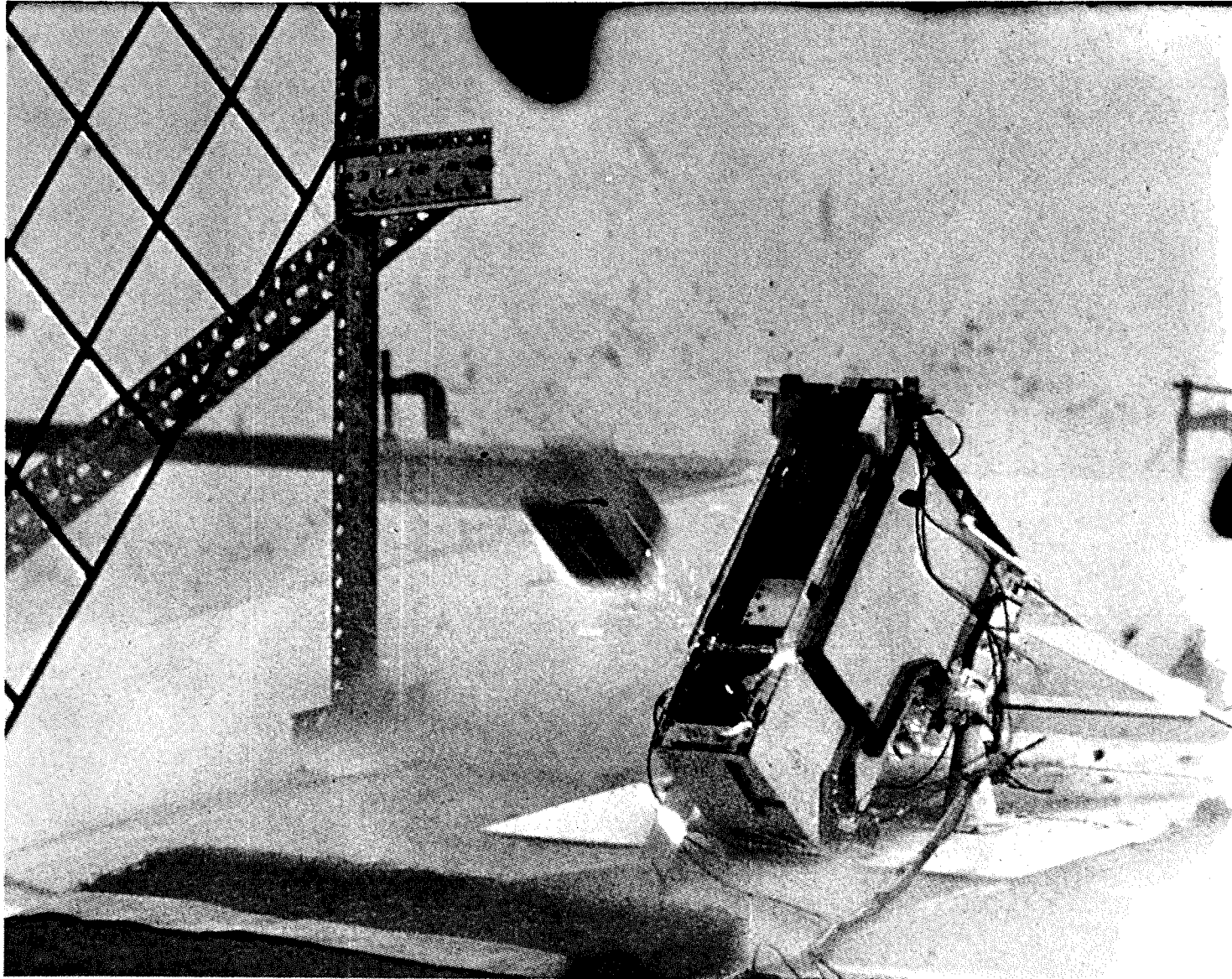


Figure E-(#4-7)

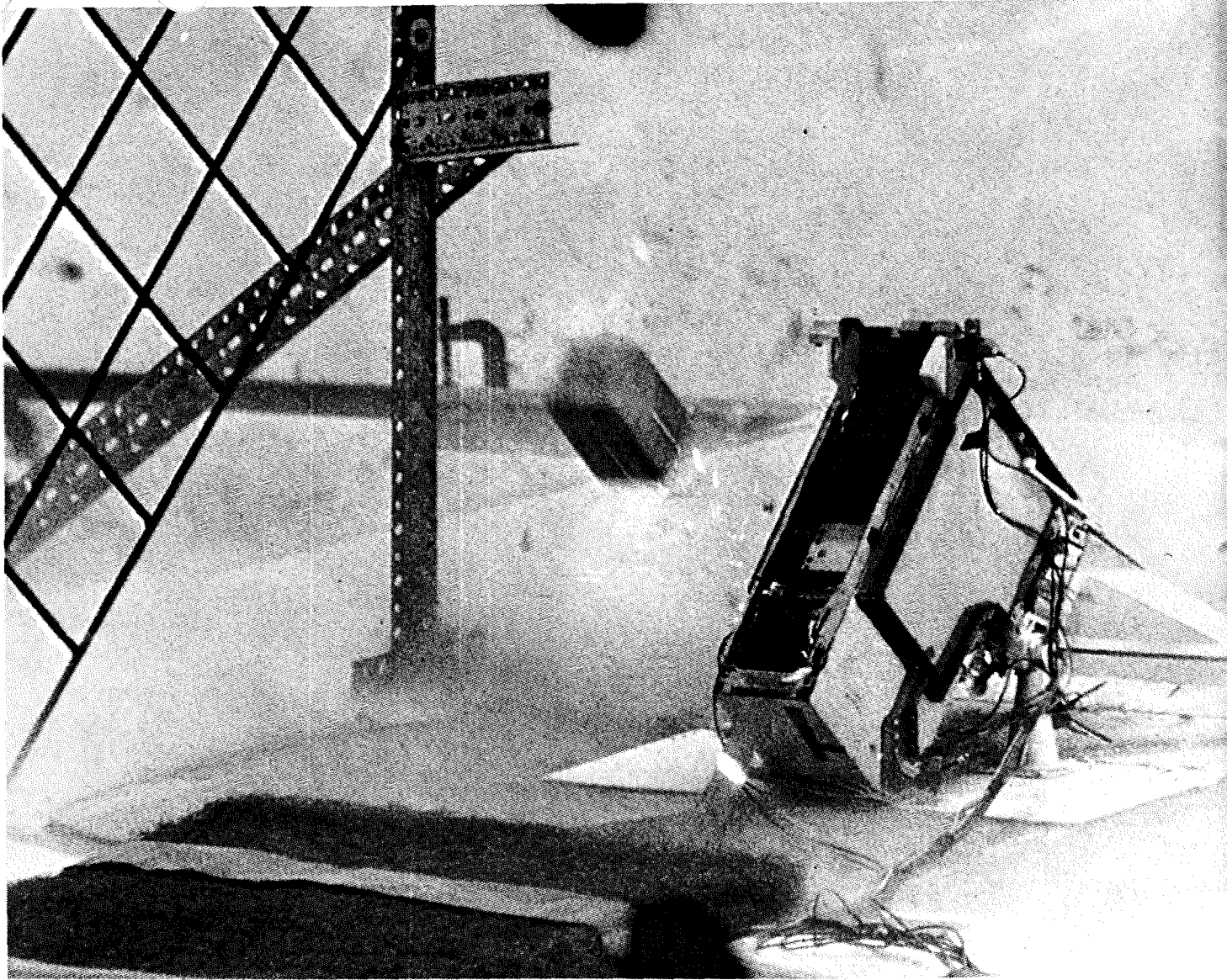


Figure E-(#4-8)

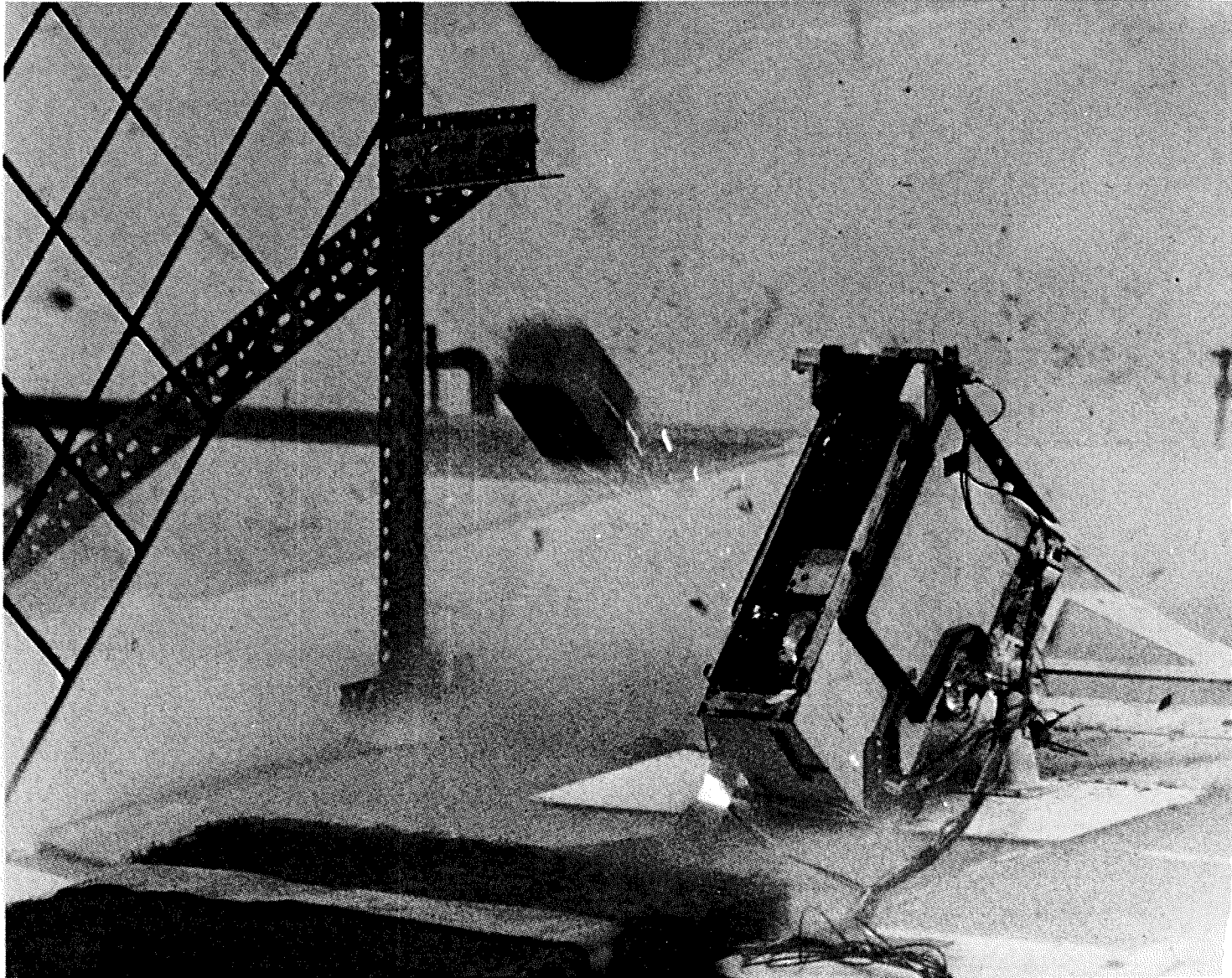


Figure E-(#4-9)

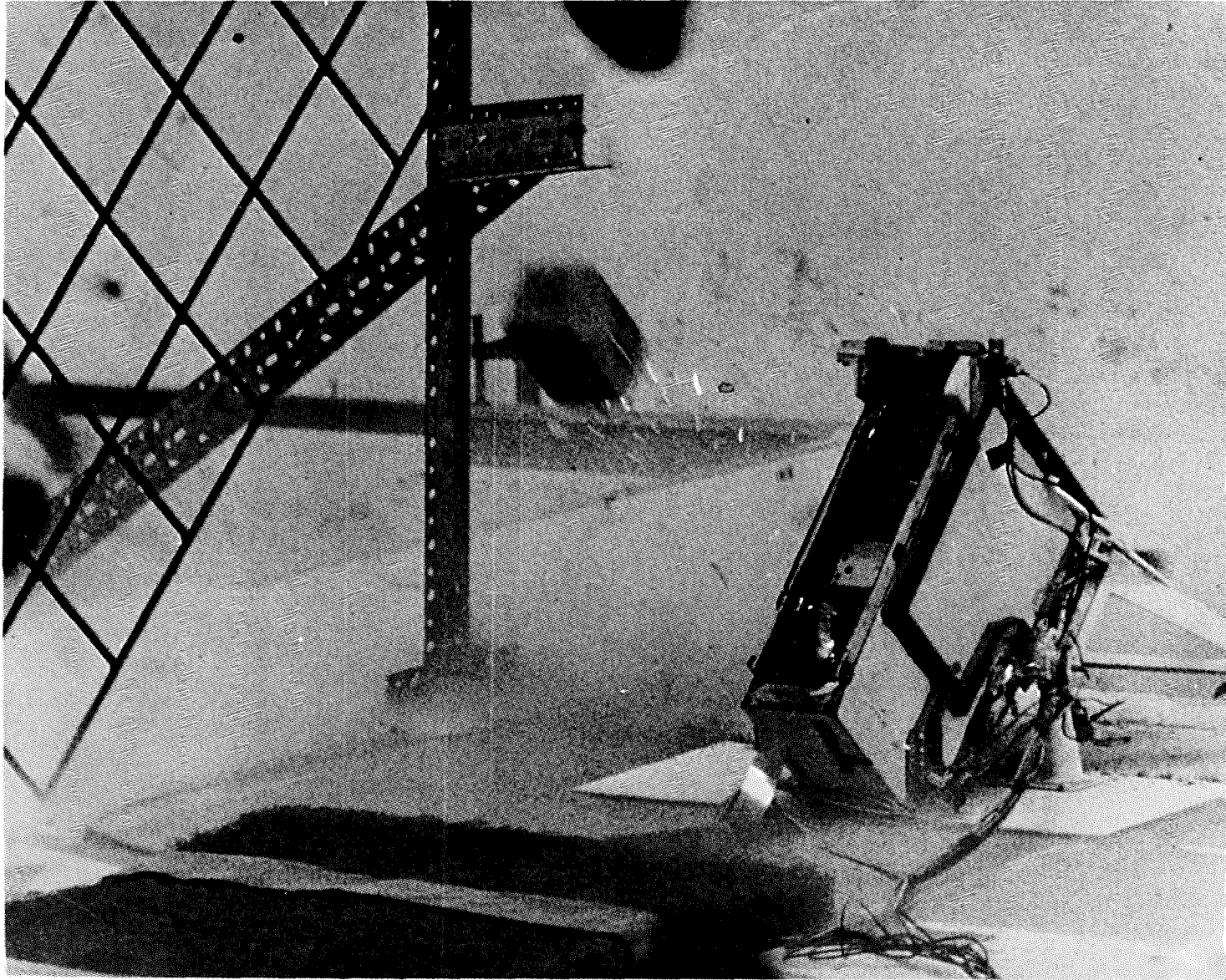


Figure E-(#4-10)

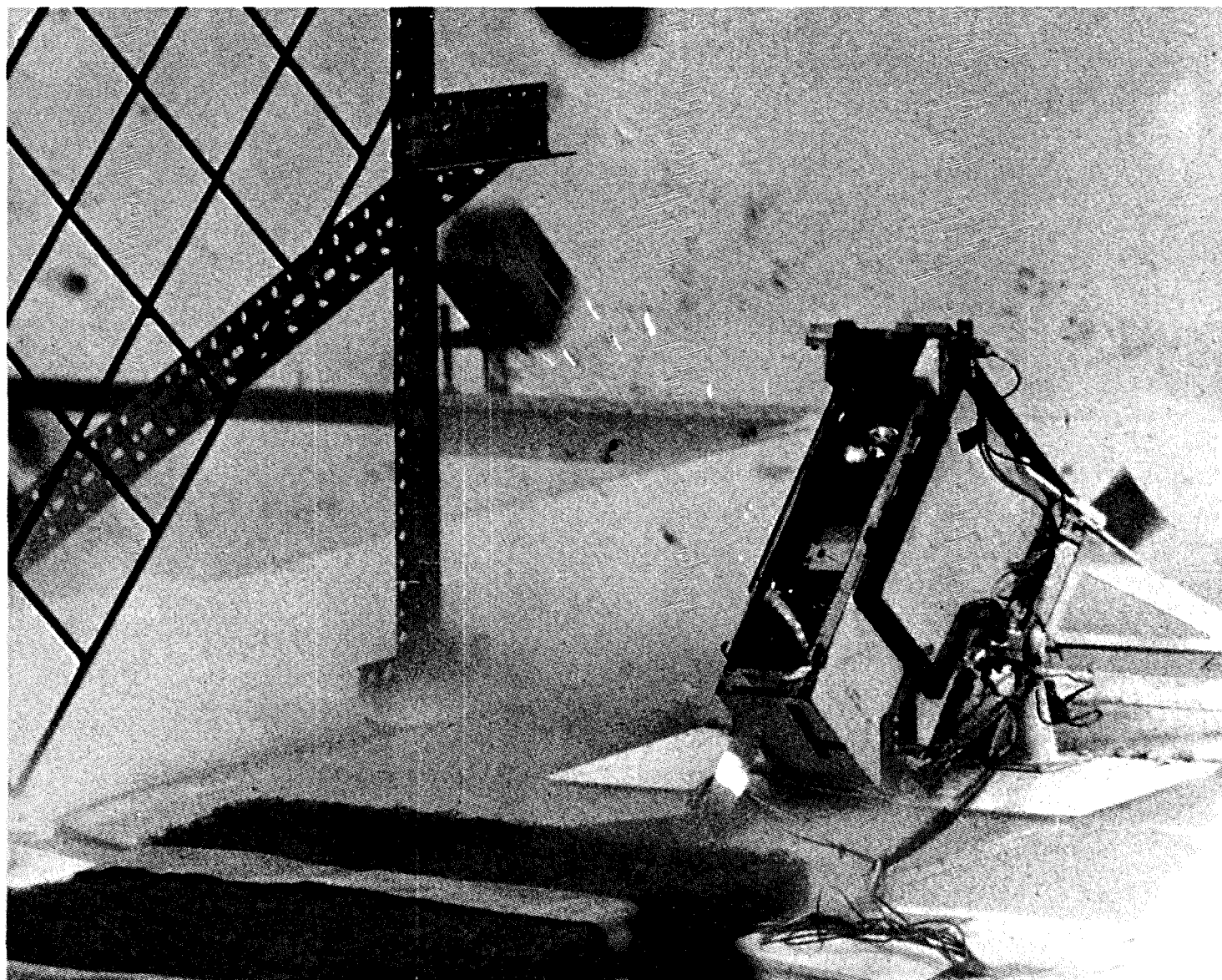


Figure E-(#4-11)

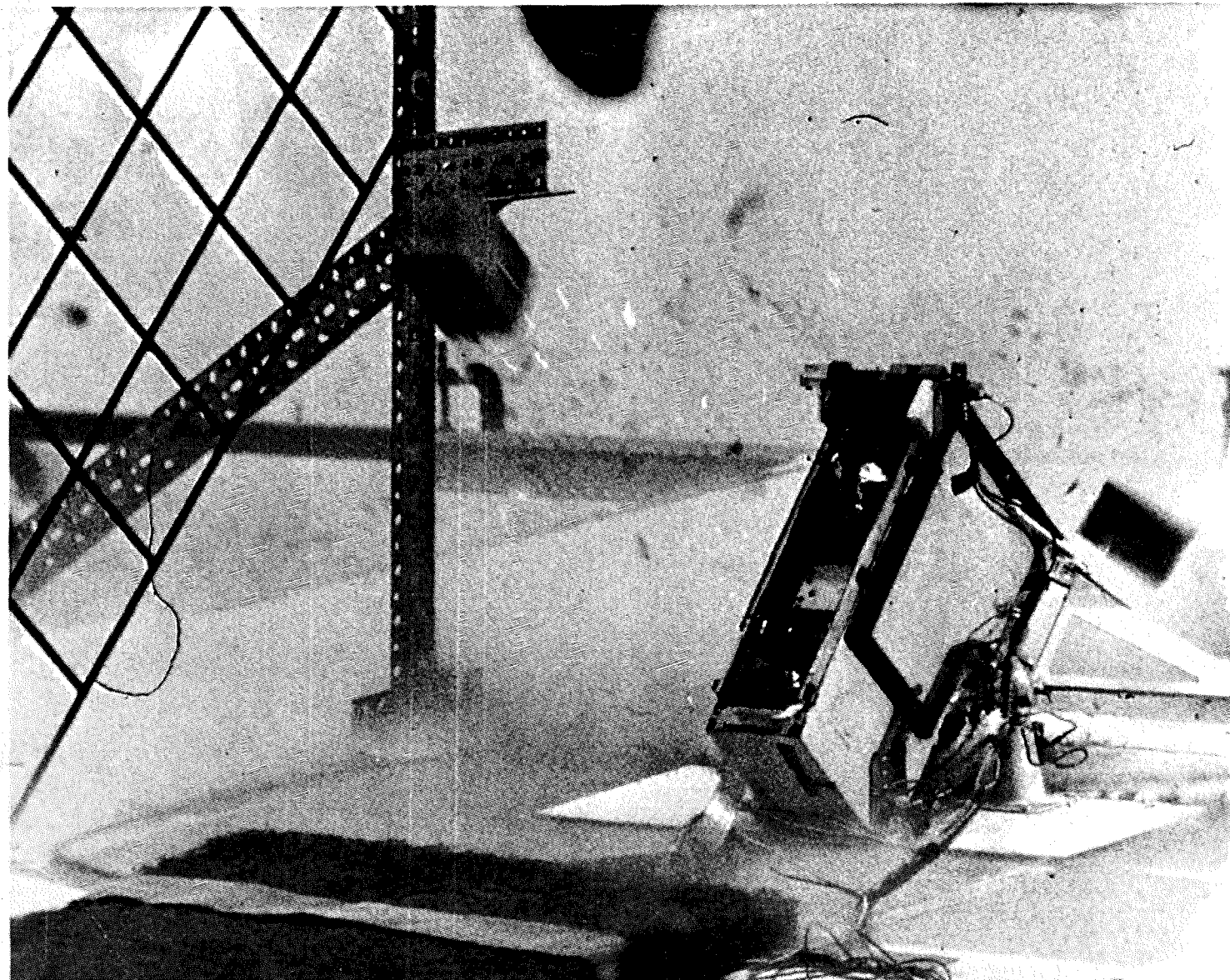


Figure E-(#4-12)



**Aerospace
Systems Division**

ASE REDESIGN EVALUATION

NO.	REV. NO.
ATM-1064	
PAGE 198	OF 212
DATE	11/24/71

(- 3) Grenade
Launch Sequence

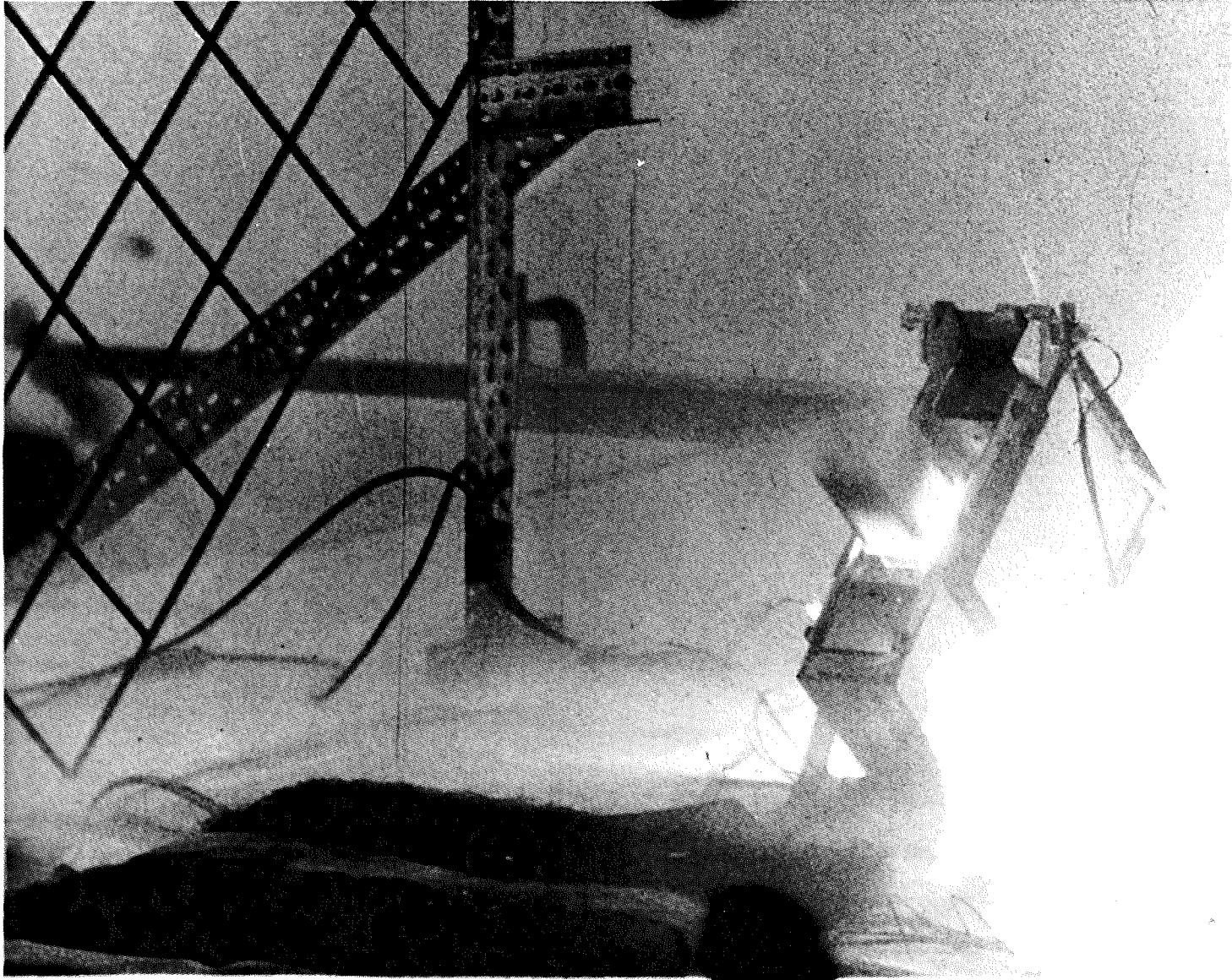


Figure E-(#3-1)

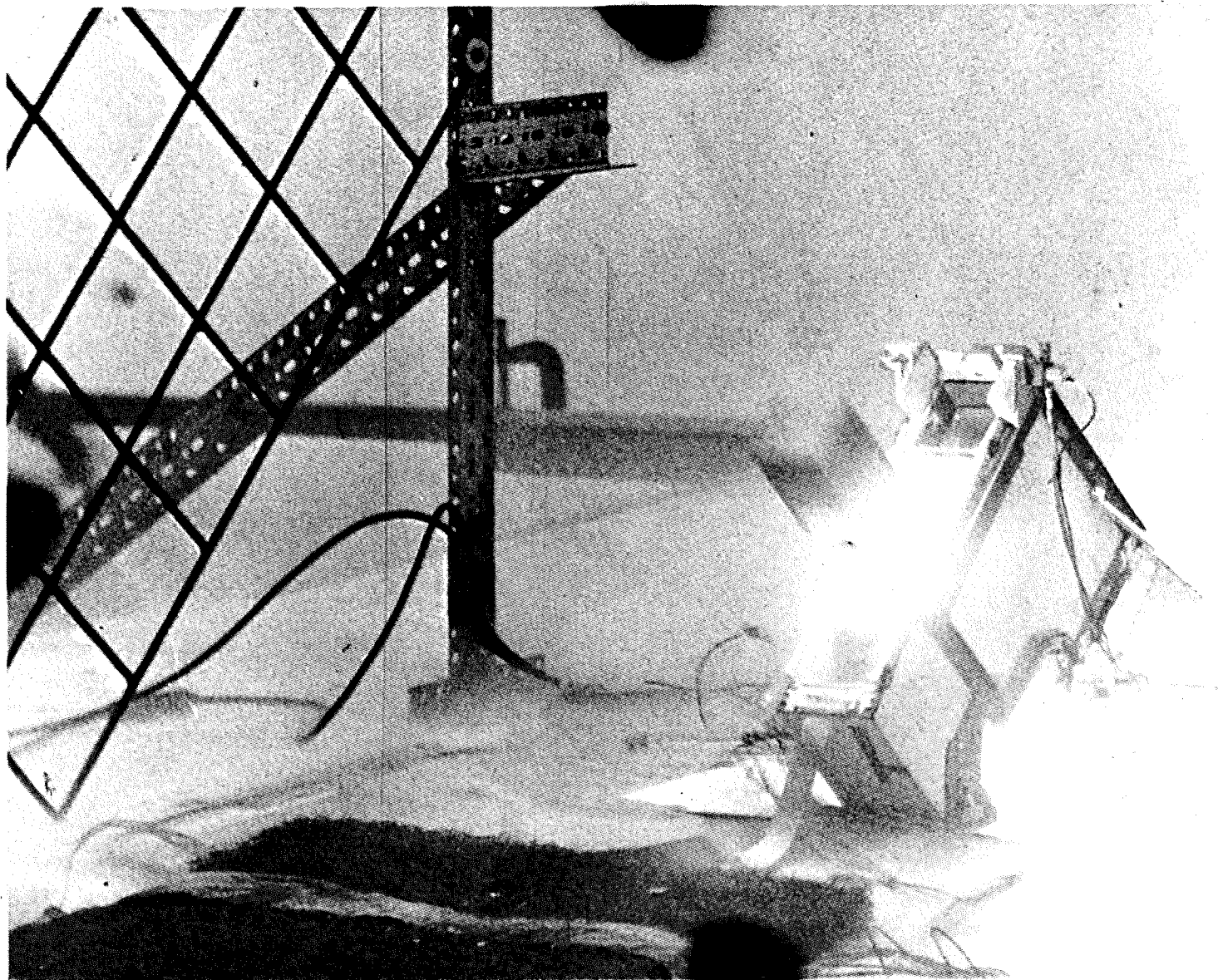


Figure E-(#3-2)

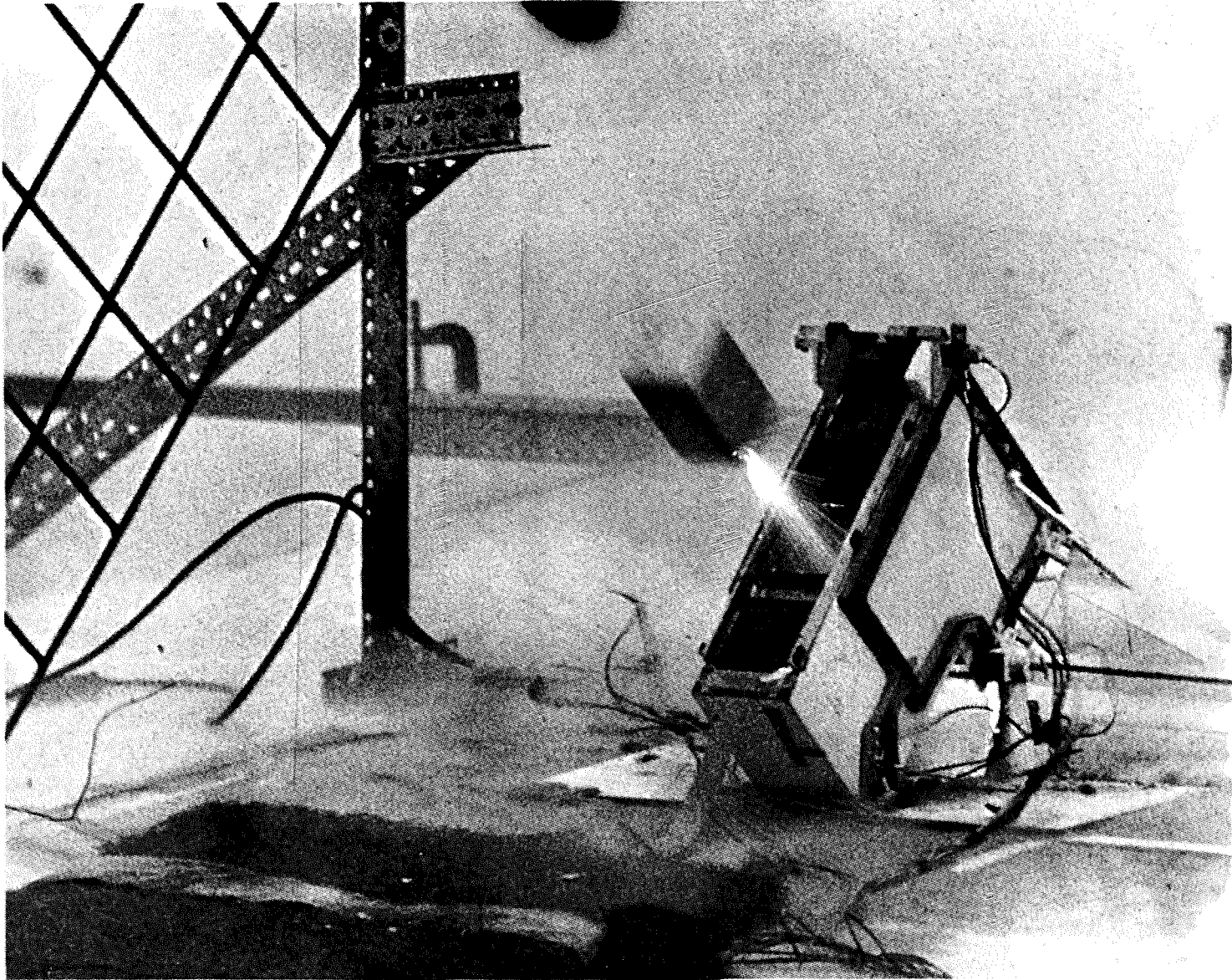


Figure E-(#3-3)

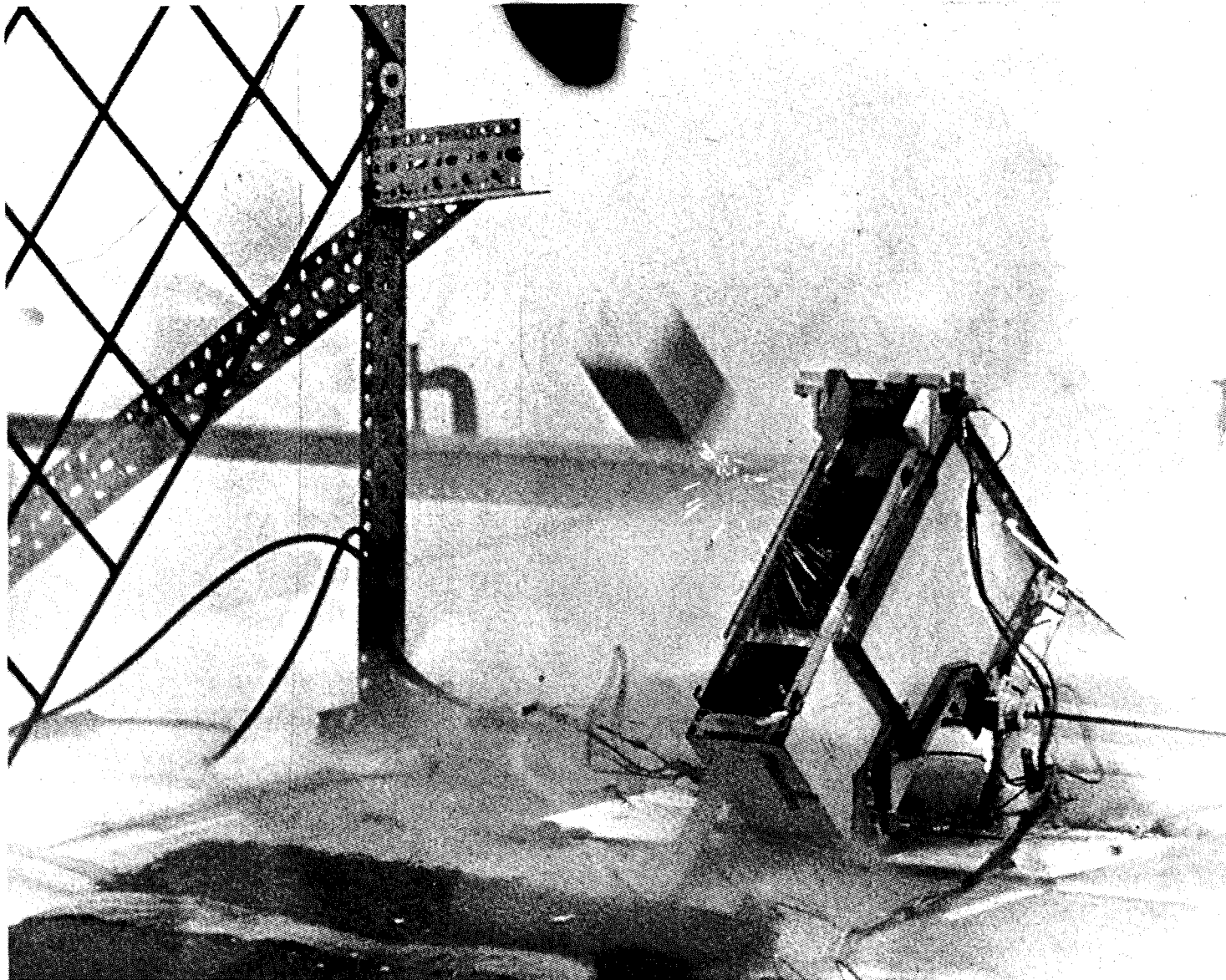


Figure E-(#3-4)

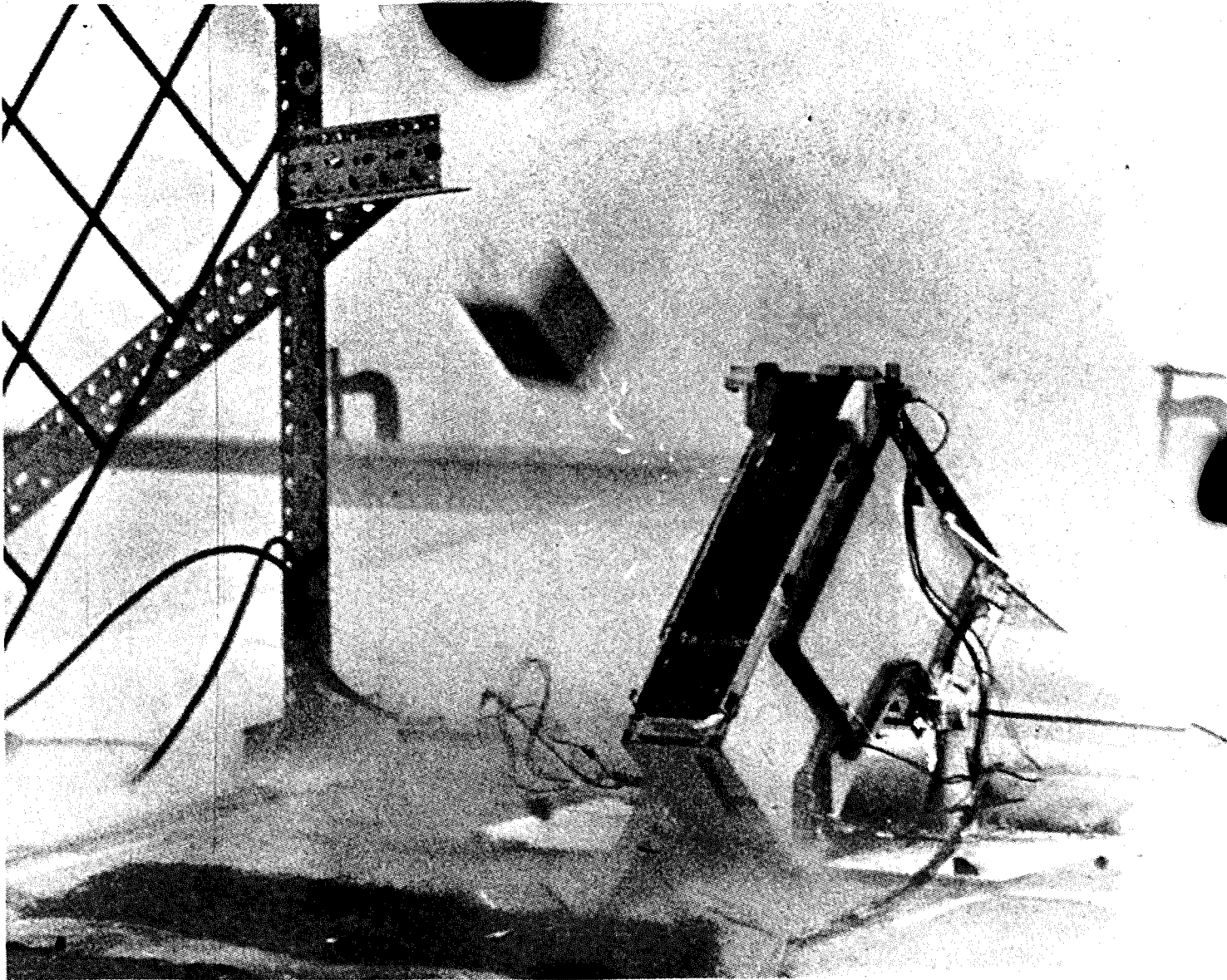


Figure E-(#3-5)

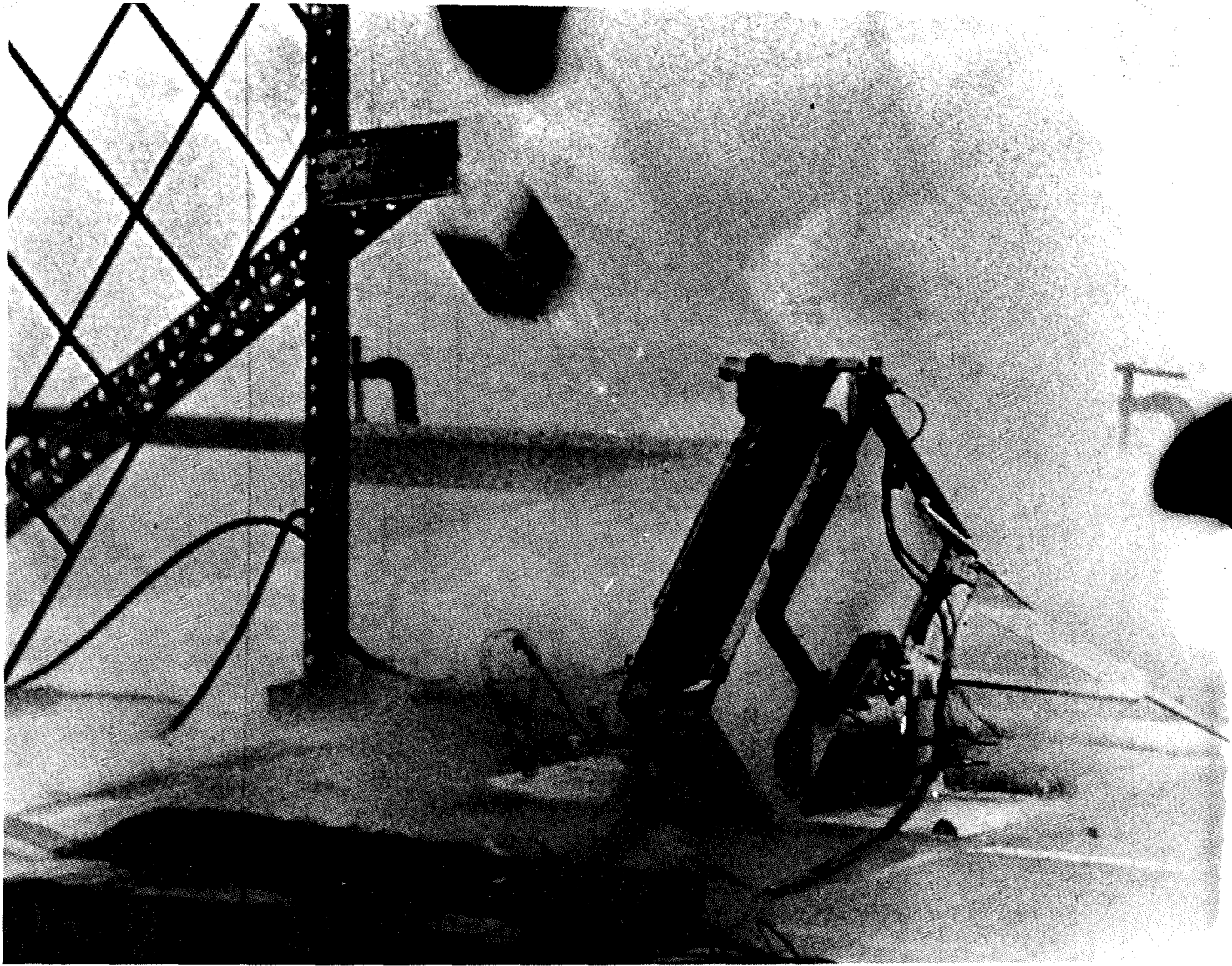


Figure E-(#3-6)

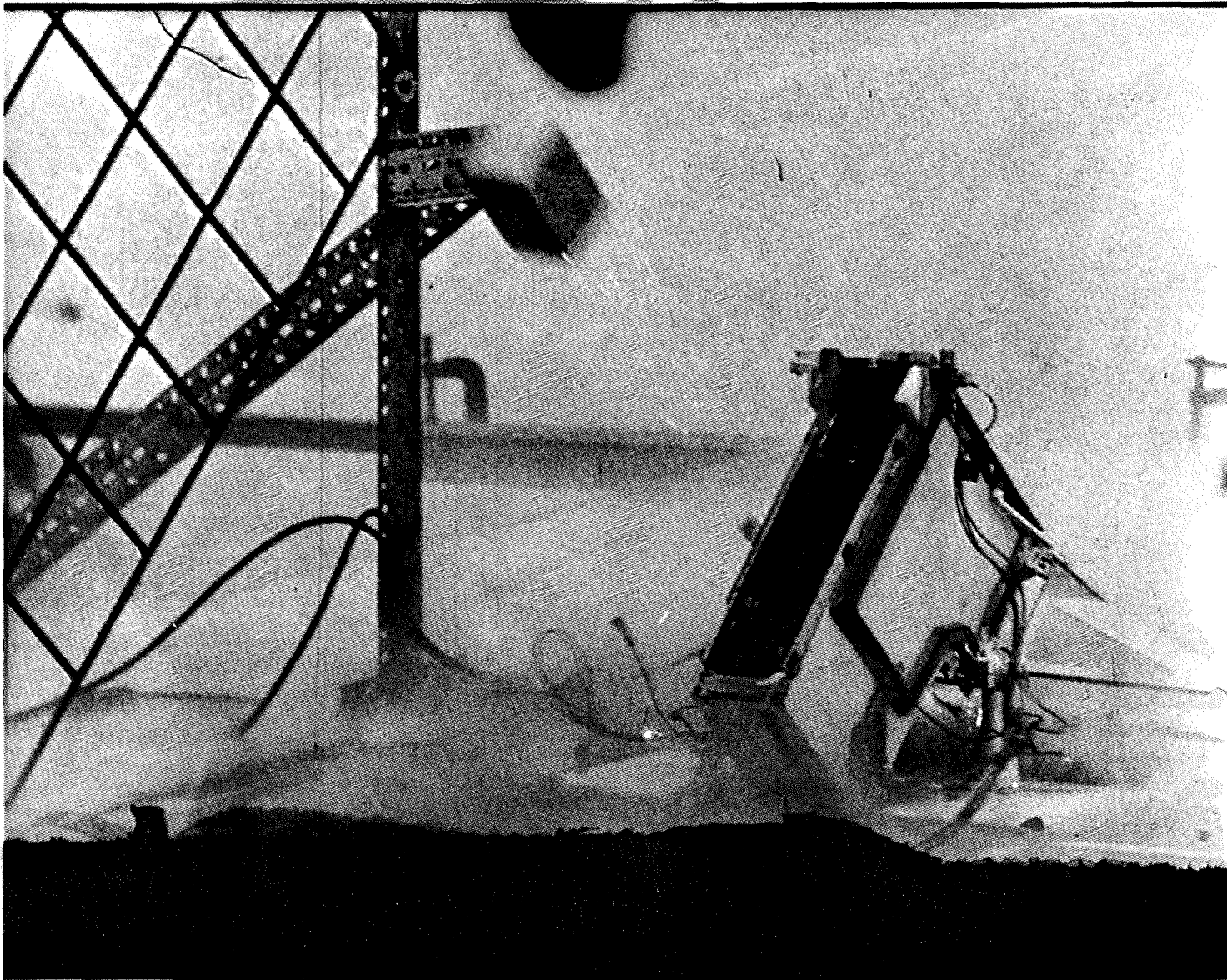


Figure E-(#3-7)



**Aerospace
Systems Division**

ASE REDESIGN EVALUATION

NO.	REV. NO.
ATM-1064	
PAGE <u>206</u>	OF <u>212</u>
DATE	11/24/71

(-1) Grenade
Launch Sequence

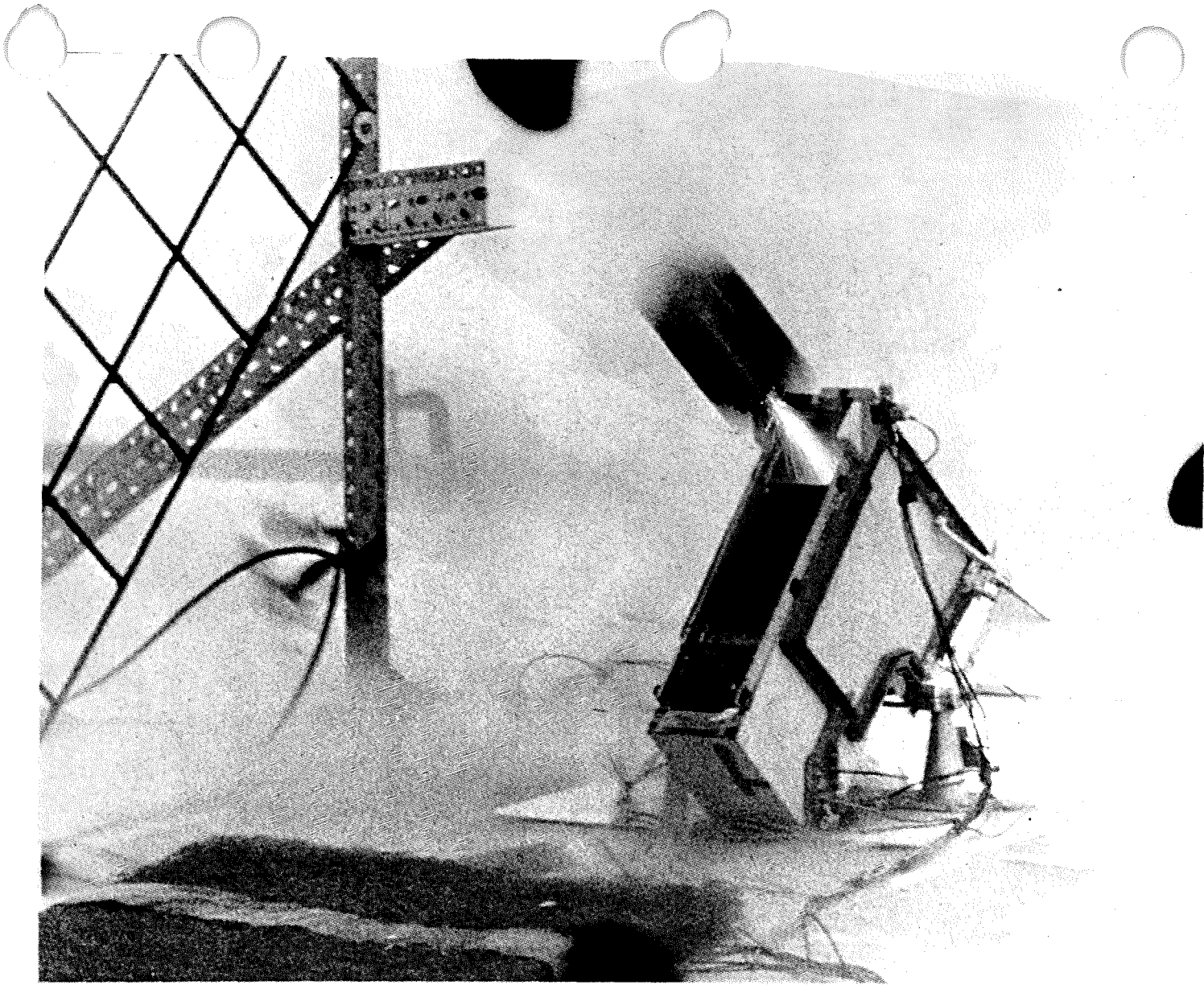


Figure E-(#1-1)

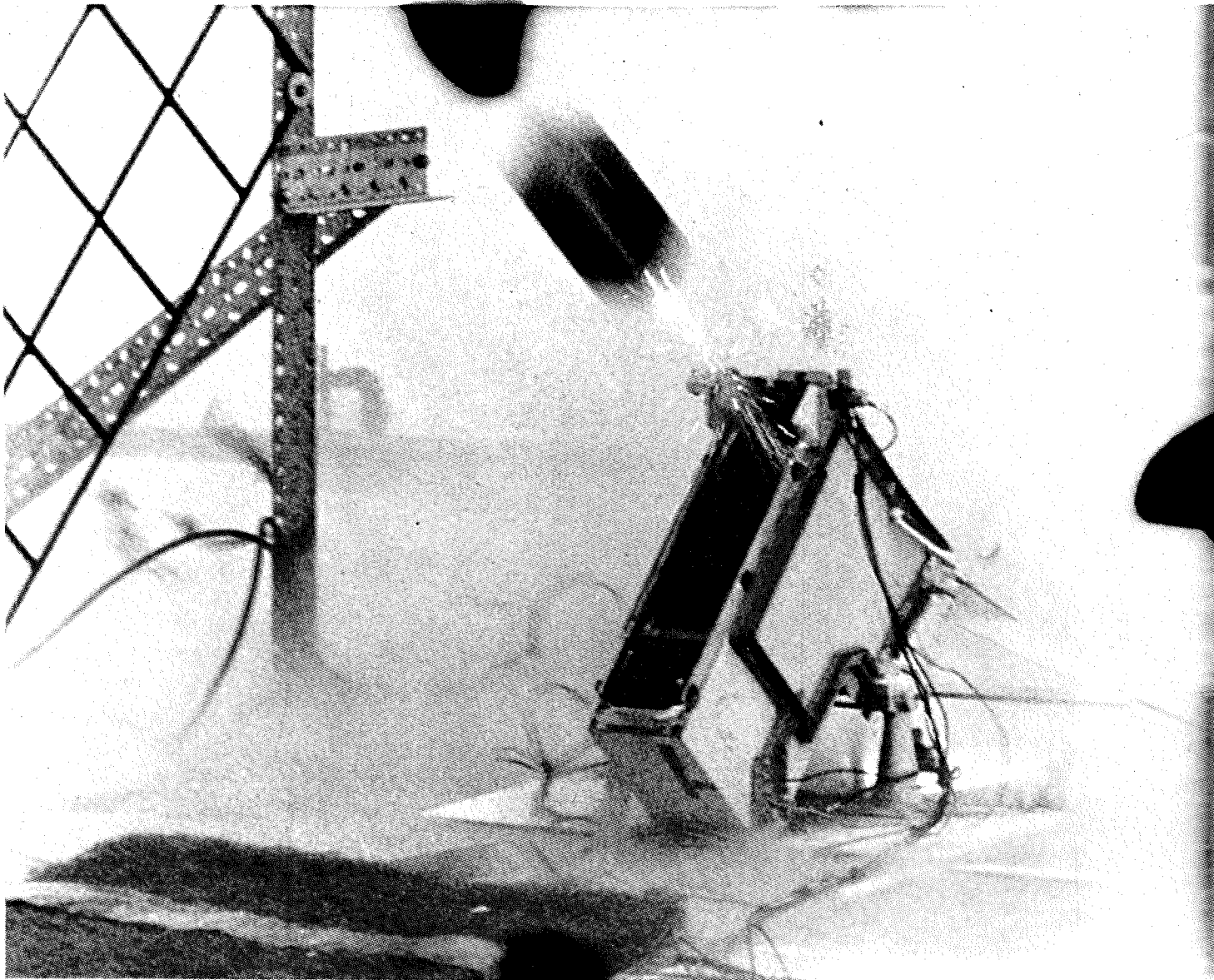


Figure E-(#1-2)

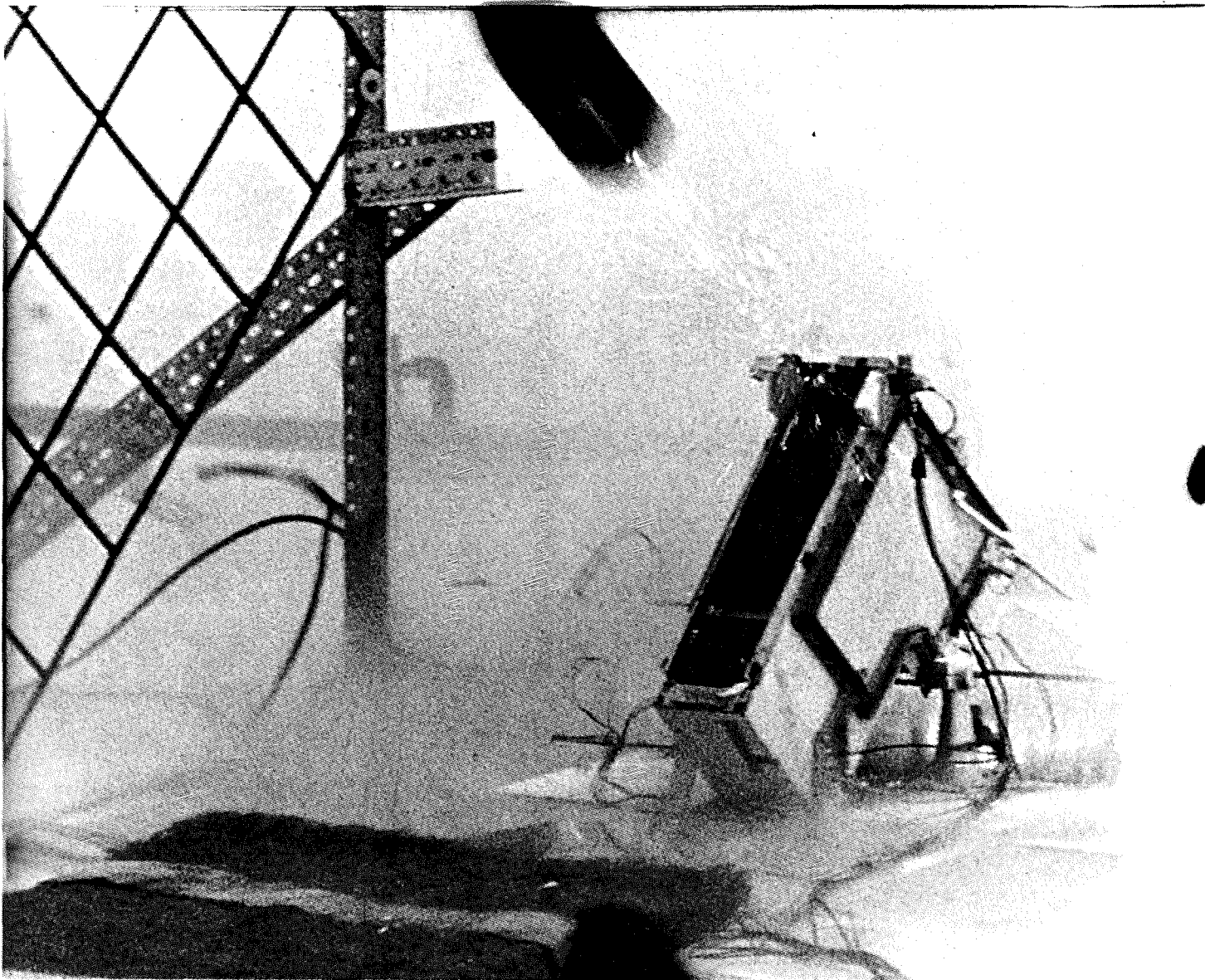


Figure E-(#1-3)



Figure E-(#1-4)

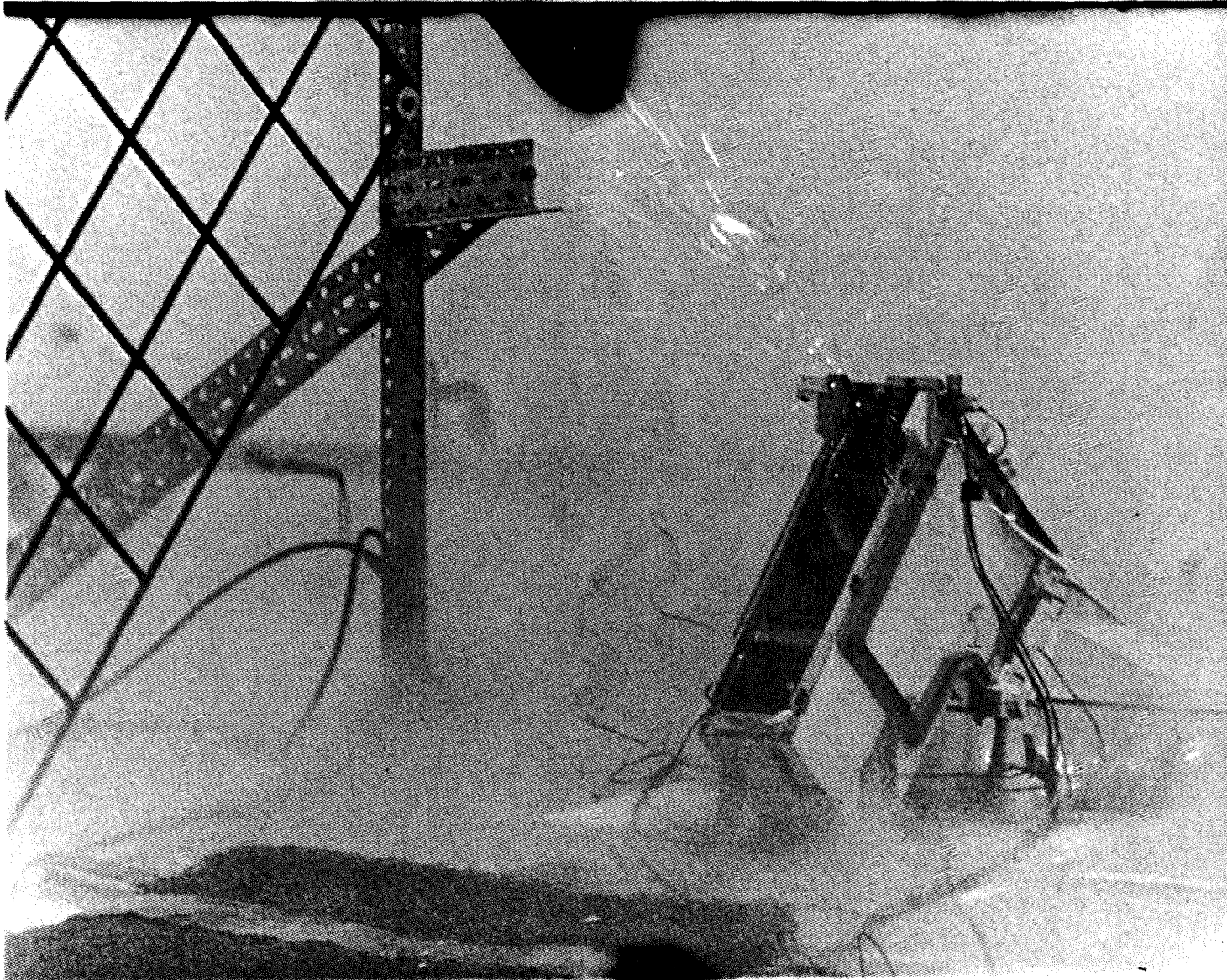


Figure E-(#1-5)

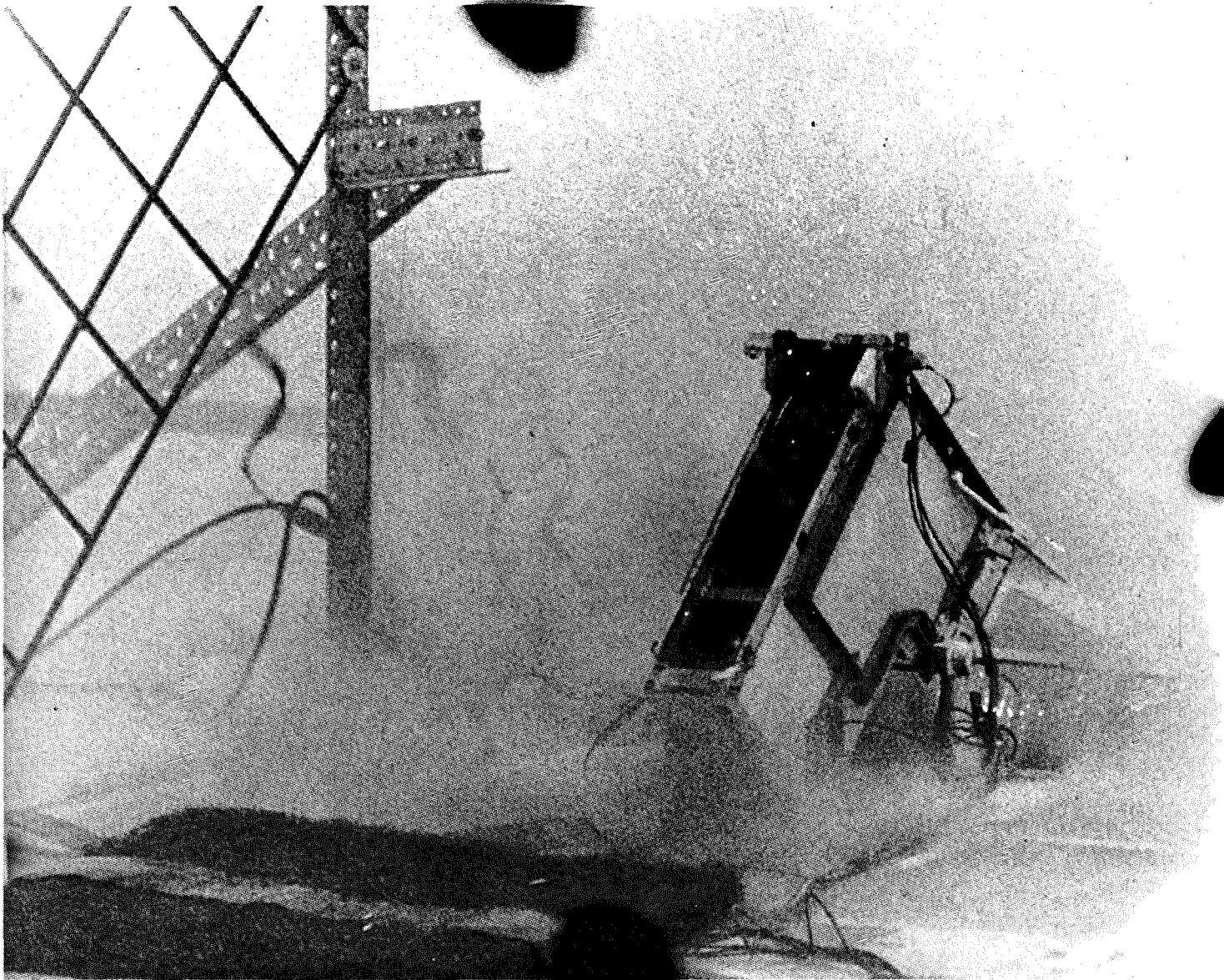


Figure E-(#1-6)